

A new rodent model of Parkinson's Disease based on neuron specific  
downregulation of glutathione production.

**PhD Thesis**

for the fulfilment of the requirements for the degree

“Doctor rerum naturalium”

at the Georg August University Göttingen,

Faculty of Biology

submitted by

**Manuel Joaquim Marques Garrido**

born in

Pardilhó (Portugal)

**Göttingen 2008**

Referent: Prof. Dr. Ralf Heinrich

Korreferentin: Prof. Dr. Frauke Melchior

Tag der mündlichen Prüfung: 19<sup>th</sup> of January 2009

*“Quem se dedica a problemas da Investigação científica anda alheado do mundo, preso à sua vida... Tudo se reduz a obter novas aquisições científicas a bem da Humanidade sofredora.”*<sup>1</sup>

António Caetano de Abreu Freire Egas Moniz,  
Nobel Prize in Physiology or Medicine (1949)

---

<sup>1</sup> “The one who devotes himself to scientific investigation walks apart from the world, trapped by his aims ... All gets reduced to obtain new scientific contributions for the sake of the suffering Humanity.”

## **Declaration**

I hereby declare that the thesis:

“A new rodent model of Parkinson’s Disease based on neuron specific downregulation of glutathione production.”

has been written independently and with no other sources and aids than quoted.

Göttingen, December 2008

Manuel Joaquim Marques Garrido

<b>1. Introduction:</b> .....	<b>- 1 -</b>
<b>1.1. Neurodegenerative disorders</b> .....	<b>- 1 -</b>
<b>1.2. Parkinson´s Disease</b> .....	<b>- 1 -</b>
1.2.1. PD prevalence and symptoms .....	- 1 -
1.2.2. PD pathology.....	- 2 -
1.2.3. PD etiology, genetic based models .....	- 3 -
1.2.3.1. $\alpha$ -synuclein .....	- 3 -
1.2.3.2. Parkin, UCH-L1 and synphilin-1 .....	- 4 -
1.2.3.3. DJ1 and PINK1 .....	- 4 -
1.2.3.4. HtrA2/ Omi .....	- 5 -
1.2.3.5. LRRK2 .....	- 5 -
1.2.4. PD etiology, environmental contributions .....	- 6 -
1.2.4.1. 6-Hydroxydopamine.....	- 6 -
1.2.4.2. MPTP .....	- 6 -
1.2.4.3. Rotenone.....	- 7 -
1.2.5. PD causative hypothesis.....	- 8 -
1.2.5.1. PD mitochondrial respiratory chain and ROS generation.....	- 8 -
1.2.5.2. PD and ROS generation hypothesis .....	- 9 -
1.2.5.3. Why dopaminergic cells?.....	- 9 -
<b>1.3. Cellular antioxidant defences</b> .....	<b>- 10 -</b>
1.3.1. Antioxidant properties of Glutathione.....	- 11 -
1.3.2. Glutathione synthesis .....	- 12 -
1.3.3. Fine tune regulation of Glutathione <i>de novo</i> synthesis .....	- 12 -
<b>1.4. RNAi basic mechanism of RNA mediated gene silencing</b> .....	<b>- 13 -</b>
1.4.1. RNAi is subdivided in two distinct phases: an initiation and an execution phase. -	14 -
1.4.2. shRNA, permanent way to bring RNAi into the cells.....	- 14 -
<b>1.5. Recombinant AAV vectors as tools for gene transfer and disease modelling</b> .....	<b>- 15 -</b>

<b>2. Materials and Methods</b> .....	<b>- 19 -</b>
<b>2.1. Materials</b> .....	<b>- 19 -</b>
2.1.1. Chemicals .....	- 19 -
2.1.2. Antibodies .....	- 21 -
2.1.3. Plasmids .....	- 22 -
2.1.4. Oligonucleotides for PCR amplification .....	- 22 -
2.1.5. Oligonucleotides for sequencing .....	- 23 -
2.1.6. Oligonucleotides for shRNAs .....	- 24 -
2.1.7. Cell lines and electrocompetent cells: .....	- 27 -
2.1.8. Buffers, solutions and medium: .....	- 28 -
2.1.9. Instruments .....	- 31 -
<b>2.2. Methods:</b> .....	<b>- 32 -</b>
2.2.1. Cloning procedures .....	- 32 -
2.2.1.1. PCR amplification .....	- 33 -
2.2.1.2. Sequencing of PCR amplified DNA .....	- 33 -
2.2.1.3. DNA precipitation .....	- 34 -
2.2.1.4. DNA restriction .....	- 34 -
2.2.1.5. Agarose gel electrophoresis .....	- 34 -
2.2.1.6. Gel extraction and determination of DNA concentration .....	- 35 -
2.2.1.7. DNA dephosphorylation .....	- 35 -
2.2.1.8. Remove or fill in DNA overhangs to create blunt ends .....	- 35 -
2.2.1.9. DNA ligation and E. coli electro-transformation .....	- 36 -
2.2.1.10. Production of electrocompetent E. coli cells .....	- 36 -
2.2.1.11. Plasmid Mini, Maxi and Mega Preps .....	- 37 -
2.2.1.12. Cloning into pGL3 for luciferase based test system .....	- 37 -
2.2.1.13. Cloning of shRNAs into pSuper vector .....	- 38 -
2.2.1.14. Transfer of hH1 promoter plus the shRNAs into pAAV vectors .....	- 39 -
2.2.1.15. Cloning of GCLc into AAV plasmids for protein expression .....	- 42 -
2.2.1.16. GCLc silent mutants in pAAV .....	- 42 -
2.2.1.17. GCLc non-targetable constructs .....	- 43 -
2.2.1.18. DJ1 cDNA in pAAV .....	- 44 -
2.2.1.19. $\alpha$ -synuclein A53T cDNA in pAAV .....	- 44 -
2.2.1.20. Cloning of GCLm cDNA into AAV plasmids for protein expression .....	- 44 -

2.2.2. Viral vectors production and purification .....	- 45 -
2.2.2.1. AAV packaging.....	- 45 -
2.2.2.2. AAV gradient centrifugation.....	- 46 -
2.2.2.3. AAV- Fast Protein Liquid Chromatography.....	- 47 -
2.2.2.4. Virus DNA preparation for qPCR:.....	- 48 -
2.2.2.5. Phenol/chloroform extraction:.....	- 48 -
2.2.2.6. AAV qPCR.....	- 49 -
2.2.2.7. Calculation of AAV viral genomes.....	- 49 -
2.2.3. Cell culturing.....	- 51 -
2.2.3.1. Continuous HEK-293 cell culture.....	- 51 -
2.2.3.2. Coating of culture plates for primary cortical cells culture.....	- 51 -
2.2.3.3. Primary cortical cells culture.....	- 52 -
2.2.4. Calcium phosphate transfection of HEK-293 cells.....	- 52 -
2.2.5. Luciferase assay .....	- 53 -
2.2.6. Primary culture treatment.....	- 54 -
2.2.6.1. AAV transduction .....	- 54 -
2.2.6.2. Ara-C treatment:.....	- 55 -
2.2.7. WST-1 assay .....	- 55 -
2.2.8. Glutathione assay .....	- 55 -
2.2.9. Protein analysis, overview: .....	- 57 -
2.2.9.1. Lysis for western blotting.....	- 58 -
2.2.9.2. SDS polyacrylamide gel electrophoresis (SDS-PAGE).....	- 58 -
2.2.9.3. Immunoblotting.....	- 59 -
2.2.9.4. Protein concentration determination .....	- 60 -
2.2.10. Immunofluorescence .....	- 60 -
2.2.10.1. Immunofluorescence on primary neurons.....	- 60 -
2.2.10.2. Immunofluorescence on brain slices.....	- 61 -
2.2.11. Animal procedures .....	- 61 -
2.2.11.1. Stereotaxic injection into the rat brain .....	- 62 -
2.2.11.2. Transcardial perfusion and brain tissue processing.....	- 62 -
2.2.12. Microscopy and image analysis .....	- 63 -
2.2.13. Quantification of neurodegeneration in shRNA rat model of PD.....	- 63 -
2.2.14. EGFP in live cortical neurons .....	- 64 -
2.2.15. Statistics .....	- 64 -

<b>3. Results</b> .....	<b>- 65 -</b>
<b>3.1. Downregulation of GSH production in cultured primary neurons</b> .....	<b>- 65 -</b>
3.1.1 Characterization of RNAi efficiency.....	- 65 -
3.1.1.1 Development of a test system for determination of RNAi efficacy.....	- 65 -
3.1.1.2. Quantification of protein down-regulation by shRNAs .....	- 68 -
3.1.1.2.1. Evaluation of GCLc shRNAs efficiency by western blot in HEK293 cells....	- 68 -
3.1.1.2.2. Non targeted GCLc design for “rescue experiments” .....	- 69 -
3.1.1.2.3. Evaluation of GCLm shRNAs efficiency by western blot in HEK293 cells ..	- 71 -
3.1.2. Construction of AAV vectors for transduction of primary cortical neurons.....	- 73 -
3.1.2.1. Targeting GCLc protein in primary cortical neuron culture .....	- 74 -
3.1.2.2. GCLc silencing induced cell viability loss in primary cortical culture.....	- 78 -
3.1.2.3. GCLc cell loss mechanism in primary cortical culture .....	- 80 -
3.1.2.4. Glutathione quantification upon GCLc silencing in primary cortical culture	- 80 -
3.1.2.5. Influence of GCLc-shRNA#2 and $\alpha$ -synucleinA53T expression on reduction of	
GSH levels in primary cortical culture.....	- 82 -
3.1.2.6. No prevention of neurotoxicity of GCLc targeting effects by expression of	
rescue constructs! .....	- 83 -
3.1.3. Targeting the modulatory subunit of the GCL holoenzyme.....	- 87 -
3.1.3.1. Targeting GCLm protein in primary cortical neuron culture.....	- 88 -
3.1.3.2. GCLm silencing results in cell viability loss in a primary cortical culture....	- 92 -
3.1.3.3. Glutathione levels upon GCLm silencing in primary cortical culture .....	- 93 -
3.1.3.4. Mechanism of cell loss in primary cortical culture upon GCLm silencing ...	- 94 -
3.1.4. GCLc or GCLm over-expression in primary cortical culture is not neurotoxic ...	- 96 -
3.1.5. Summary of <i>in vitro</i> results .....	- 98 -
<b>3.2. Targeting GSH metabolism in the SNpc <i>in vivo</i></b> .....	<b>- 99 -</b>
3.2.1 Transduction of SNpc by stereotaxic injection of AAV2 vector .....	- 99 -
3.2.1.1 Efficiency of AAV2 vectors injection in SNpc.....	- 99 -
3.2.1.2 AAV2 allowed for neuron specific transduction.....	- 101 -
3.2.2.1 <i>In vivo</i> neurotoxicity of control shRNAs .....	- 103 -
3.2.2.2. DA neuron degeneration mediated by targeting the catalytic subunit of GCL.....	- 105 -



3.2.2.3. $\alpha$ -synucleinA53T partially rescues DA neurons from degeneration induced by GCLc knock-down .....	- 110 -
3.2.2.4. FluoroJade C staining for degenerating neurons.....	- 111 -
3.2.2.5. shRNAs targeting the modulatory subunit of GCL in DA neurons .....	- 113 -
3.2.2.6. Overexpression of both subunits of GCL provoked degeneration of DA neurons -	117 -
3.2.2.7. NeuN loss in the SNpc upon GCLm or GCLc shRNAs expression. ....	- 121 -
<b>4. Discussion.....</b>	<b>- 125 -</b>
4.1. AAV2 as a gene transfer vehicle .....	- 125 -
4.2. shRNA silencing efficacy .....	- 126 -
4.3. <i>In vitro</i> experiments as proof of concept .....	- 127 -
4.4. <i>In vivo</i> targeting of GSH metabolism .....	- 127 -
4.5. Cell death mechanism .....	- 131 -
4.6. Perspectives.....	- 132 -
<b>5. Summary .....</b>	<b>- 133 -</b>
<b>6. References .....</b>	<b>- 135 -</b>
<b>7. Annexes.....</b>	<b>- 159 -</b>
7.1. Abbreviations.....	- 159 -
7.2. Acknowledgements.....	- 162 -
7.3. <i>Curriculum vitae</i> .....	- 163 -
7.4. Publications.....	- 164 -



## **1. Introduction:**

### **1.1. Neurodegenerative disorders**

Spontaneous or traumatic lesions in the central or peripheral nervous system are the major cause of disability in the western society; these disorders strongly impair quality of life in a degree rarely comparable with other diseases. Neurodegenerative diseases (NDD) are often associated with atrophy of the affected central or peripheral structures of the nervous system. They include diseases such as Alzheimer's Disease, Parkinson's Disease, Multiple Sclerosis, Amyotrophic Lateral Sclerosis, Prion Diseases, Huntington's Disease, Spinocerebellar ataxias, and many others. The majority of human neurodegenerative diseases is not related to inherited mutations of specific proteins but develops with aging as a multifactorial pathology. It is often characterized by features of oxidative stress, axonal degeneration, demyelination, protein aggregation with consequent impairment in cellular physiological functions, excitotoxicity, and inflammation, among others. Many neurodegenerative disorders have no cure nowadays, for some others the only available treatment is symptomatic. In addition, for most neurodegenerative diseases the cause has not been yet identified

In order to identify the possible causative disease mechanisms various experimental animal models of neurodegenerative diseases have been developed. They contribute to a better understanding of the complex mechanisms involved in neurodegeneration and to serve for the preclinical evaluation of prospective diagnostic tools and therapies. However, every model can reflect only certain aspects of the complex aetiology of respective diseases in humans. Thus, the evaluation of neuroprotective strategies aiming at generalized inhibition of neurodegeneration should be performed in more than one particular model system. Furthermore, considering the diversity of mechanisms leading to neurodegeneration, effective human therapy may necessitate targeting of more than one neurodegenerative pathway.

### **1.2. Parkinson's Disease**

#### **1.2.1. PD prevalence and symptoms**

Parkinson's disease (PD) was initially described by the British physician James Parkinson in "*An Essay on the Shaking Palsy*" in 1817 (Parkinson 2002 reprint). PD is the second most frequent neurodegenerative disorder of the central nervous system after Alzheimer's disease. Early onset of sporadic PD is rare, with about 4 % of patients developing clinical signs of the

disease before an age of 50 years (Van Den Eeden et al. 2003). PD affects approximately 1 to 2 % of the population over 65 years old and more than 3 to 5 % of those over 85 years of age (deRijk et al. 1997;Fahn 2003). PD typically begins around 60 years of age and the probability being affected by PD or other neurodegenerative disease increases with age. Therefore PD becomes more relevant in an aging society. The major clinical PD symptoms are poverty and slowness of voluntary movement without paralysis (bradykinesia), posture instability, muscle rigidity and resting tremor. In most cases these symptoms are sufficient for the disease diagnose (Hughes et al. 2001). Olfactory dysfunction, psychological symptoms, autonomic nervous system dysfunction (Radil et al. 1995;Herting et al. 2008) and adverse effects in the visual system (Bodiswollner 1990) typically develop as the disease progresses and often become a major cause of disability.

### **1.2.2. PD pathology**

PD is a typical neurodegenerative disorder in many aspects. Pathologically, the degeneration of the nigrostriatal system is selectively but not exclusively. In PD patients both the central, peripheral, and enteric nervous systems are affected. In CNS as examples the loss of dopaminergic neurons (DA) neurons in the *substantia nigra pars compacta* (SNpc), noradrenergic locus coeruleus, serotonergic raphe nuclei of reticular formation, cholinergic nuclei and anterior olfactory structures (Braak and Braak 2000;Braak et al. 2006a;Braak et al. 2006b). During the last years research major emphasis has been focused in the nigrostriatal pathway degeneration that has been consistently identified as the most severely damaged circuit. The degeneration of dopaminergic (DA) neurons in the SNpc and the loss of dopamine in the striatum are believed to induce the clinical motor deficits seen in PD patients. The SNpc is a structure located in the midbrain named substantia nigra from latin “black substance” because of the native content of the neuromelanin pigment (dark). In PD patients the SNpc was noted to show depigmentation, loss of nerve cells, gliosis and the presence of *Lewy bodies*. *Lewy bodies* are intraneuronal proteinaceous cytoplasmatic inclusions containing for example neurofilaments, ubiquitin and  $\alpha$ -synuclein (Goldman et al. 1983;Kuzuhara et al. 1988;Spillantini et al. 1997) and being recognized as one of the pathologic hallmarks of the disorder present in the remaining intact nigral neurons (Forno 1996;Braak and Braak 2000;Braak et al. 2003). Nevertheless, *Lewy bodies* may also occur in other anatomical regions even before they are found in the SNpc (Braak et al. 2003). It is believed that the first cardinal symptoms of the disease appear when 50-60% of DA neurons in SNpc and more than 70-80% of their projections in the striatum are lost (Deumens et al.

2002). Moreover, the severity and the stage of the disease are correlated with the neurodegeneration extent (Riederer and Wuketich 1976; Fearnley and Lees 1991). Normal aging induces neurodegeneration of DA neurons of SNpc at a rate of approximately 5% per decade, in PD patients the neurodegeneration ratio is about 10 fold faster (Fearnley and Lees 1991).

### **1.2.3. PD etiology, genetic based models**

Despite the description of clinical and pathological features of PD almost two centuries ago, the cause underlying the death of nigrostriatal DA neurons is incompletely understood. In the last decade the identification of rare genetic defects in families with autosomal-dominant or autosomal recessive PD has provided new insights into the pathogenesis of PD (Dauer and Przedborski 2003; Moore et al. 2005a). Although the minority of PD cases (~ 5%) are due to genetic defects, 10 different loci are responsible for rare Mendelian forms of PD and their identification opened new and exciting research opportunities to track the molecular pathways involved in the disease pathophysiology (Dawson and Dawson 2003). The typical and extremely consistent phenotype of both idiopathic and familial PD suggests that a common molecular mechanism may underlie PD (Thomas and Beal 2007). Understanding the pathogenesis of the sporadic form of PD will have the greatest impact on advancing novel therapies for this common and so far incurable neurodegenerative disorder.

Nine genes linked to rare familiar forms of PD have been identified, namely *α-synuclein*, *Parkin*, *UCH-L1*, *PINK1*, *DJ-1*, *LRRK2*, *ATP13A2*, *Synphilin-1* and *HtrA2/omi*.

#### **1.2.3.1. $\alpha$ -synuclein**

Normal  $\alpha$ -synuclein (*SNCA*) is an abundant soluble neuronal cytoplasmic protein, and is predominantly localized to pre-synaptic terminals in the CNS where it is associated with synaptic vesicles (Zhang et al. 2000). The  $\alpha$ -synuclein function is still unknown but the protein is known to be involved in other synucleinopathies (Bennett 2005). Three point mutations of  $\alpha$ -synuclein are causative for PD in a small number of families (Polymeropoulos et al. 1997; Kruger et al. 1998; Zarranz et al. 2004). Triplications in the  $\alpha$ -synuclein gene which result in increased gene dosage also cause PD (Singleton et al. 2003).  $\alpha$ -synuclein protein is the major proteinaceous component of the Lewy bodies (Spillantini et al. 1997; Spillantini et al. 1998; Goldberg and Lansbury 2000). Transgenic mouse models have been established for the expression of wild type and mutant forms of  $\alpha$ -synuclein (Masliah et al. 2000; Kahle et al.

2000;van der Putten et al. 2000;Lee et al. 2002;Stichel et al. 2007). Although abnormal accumulation of proteinase K resistant  $\alpha$ -synuclein in neuronal cell bodies and neurites, and severe mitochondrial pathology has been shown, none of these animal models showed convincing cell death (Neumann et al. 2002;Stichel et al. 2007).

In contrast with the lack of relevant neurodegeneration in transgenic mouse models of PD, studies in rats and primate using viral-mediated expression of human  $\alpha$ -synuclein variants in the SNpc have proved more successful with progressive and selective loss of dopaminergic neurons and their striatal nerve terminals (Kirik et al. 2002;Kirik et al. 2003;Lo Bianco et al. 2004).  $\alpha$ -synuclein deposited in Lewy bodies in brain tissue from patients with PD is extensively phosphorylated at Ser-129 (Okochi et al. 2000;Anderson et al. 2006). The expression of phosphorylated like or phosphorylation less  $\alpha$ -synuclein mediated by AAV in the SNpc revealed that phosphorylation may eliminate the  $\alpha$ -synuclein induced toxicity in the nigrostriatal system (Gorbatyuk et al. 2008).

### **1.2.3.2. Parkin, UCH-L1 and synphilin-1**

Parkin functions as an E3 ubiquitin protein ligase (Shimura et al. 2000;Zhang et al. 2000) and loss of function mutations in the Parkin gene have been identified in patients with a young disease onset (Kitada et al. 1998). The loss of Parkin function or mutations in the ubiquitin C-terminal hydrolase L1 gene (UCH-L1) (Leroy et al. 1998) indicates the dysfunction in the ubiquitin proteasome system (UPS) as a primary cause of the pathology (Kruger et al. 2002). Parkin interacts with and ubiquitinates the  $\alpha$ -synuclein interacting protein, synphilin-1. Co-expression of  $\alpha$ -synuclein, synphilin-1 and parkin results in the formation of Lewy body like ubiquitin positive cytosolic inclusions (Chung et al. 2001). The recently identified R621C mutation in synphilin-1 is the first genetic evidence for either a direct contribution or a susceptibility factor of synphilin-1 in the pathogenesis of PD (Marx et al. 2003).

### **1.2.3.3. DJ1 and PINK1**

Mutations on DJ-1 and PTEN induced kinase 1 (PINK1) are autosomal recessive genes causative of PD (Bonifati et al. 2003;Valente et al. 2004;Ibanez et al. 2006). Data obtained from studies on DJ-1 and PINK1 mutations may serve as an indirect evidence of the seminal role of mitochondrial dysfunction and oxidative stress in PD pathogenesis. Endogenous DJ-1 is localised in the mitochondrial matrix, the mitochondrial intermembrane space and in the cytoplasm (Zhang et al. 2005). DJ-1 is thought to function both as chaperone and as

antioxidant since it can be oxidized at the cysteine residue C106 (Taira et al. 2004;Canet-Aviles et al. 2004;Shendelman et al. 2004). The L166P mutation destabilizes the protein, inhibits DJ1 dimerization, facilitates degradation by the ubiquitin-proteasome system provoking a reduction of neuroprotective properties (Miller et al. 2003;Olzmann 2004).

PINK1 contains a conserved serine/threonine kinase domain (Unoki and Nakamura 2001;Nakajima et al. 2003) and a mitochondrial targeting motif at the N terminus (Valente et al. 2004). Overexpression of PINK1 protected from mitochondrial dysfunction and apoptosis induced by proteasomal inhibition, suggesting that PINK1 may act as a protein protecting from oxidative stress (Valente et al. 2004). A mutation on PINK1, e.g. the G309D mutation, leads to the reduction in protein kinase activity and protein stability (Beilina et al. 2005).

#### **1.2.3.4. HtrA2/ Omi**

Mutation and polymorphism in mitochondrial protease HtrA2/Omi encoding gene have been associated with PD. Disruption of HtrA2/Omi cause neurodegeneration and a parkinsonian phenotype in mice. Novel heterozygous G399S mutation and the A141S polymorphism found in PD patients is associated with PD (Strauss et al. 2005). HtrA2/Omi is a nuclear encoded protein with a mitochondrial targeting sequence at the N-terminus and serine protease activity. Both mutations of HtrA2/Omi resulted in defective activation of the protease activity, induced mitochondrial dysfunction and increased susceptibility to apoptosis (Hegde et al. 2002;Martins et al. 2002). HtrA2/Omi was identified to interact with PINK1 (Plun-Favreau et al. 2007).

#### **1.2.3.5. LRRK2**

Mutations in the leucine-rich repeat kinase 2 (LRRK2) or dardarin gene cause autosomal dominant Parkinson's disease (Zimprich et al. 2004;Paisan-Ruiz et al. 2004). Mutations in LRRK2 are the most common monogenetic form of PD, affecting up to 6% of all PD patients in Europe and up to 40% in specific ethnic groups (Zimprich et al. 2004;Paisan-Ruiz et al. 2004;Lesage et al. 2006;Ozelius et al. 2006;Healy et al. 2008). Mutations in the MAPKKK domain and in other domains appear to increase the kinase activity (Brice 2005;West et al. 2007) with reduction of neurite length and branching both in primary neuronal cultures and in rat substantia nigra (MacLeod et al. 2006). These mutations induce a typical Parkinsonian syndrome with disease onset between 35 and 78 years of age.

#### **1.2.4. PD etiology, environmental contributions**

Many different toxins are used to generate DA degeneration. Most are able to potently inhibit complex I or enhance the production of reactive oxygen species (ROS) through their effect on mitochondria. Some toxins specifically target the DA neurons through preferential uptake by transporters. An emphasis of recent research has been on the creation of models where exposure is chronic and damage occurs slowly and progressively to mimic human PD (Meredith et al. 2008).

##### **1.2.4.1. 6-Hydroxydopamine**

The neurotoxin 6-hydroxydopamine (6-OHDA) is structurally similar to dopamine and norepinephrine (NE) entering the cells by the catecholamines plasma membrane transporters (Breese and Traylor 1971). Once inside the neurons, it is oxidized and produces hydrogen peroxide and paraquinone, both of which are highly toxic (Saner and Thoenen 1971). 6-OHDA is administered directly in the brain where it specifically kills DA and NE neurons (Javoy et al. 1976;Jonsson 1980). The degree of loss of DA neurons and their striatal terminals is dependent upon the location, dose of the toxin, and the survival time following the lesion. 6-OHDA is generally administered unilaterally to the SNpc, medial forebrain bundle (MFB) or striatum. Following delivery of 6-OHDA to the SNpc, the DA cells are destroyed within a few hours or days, and before the striatal terminals completely disappear (Jeon et al. 1995), but when injected into the MFB, striatal terminals degenerate first, followed by DA cell death (Zahm 1991). Several 6-HODA toxicity models are reported, differing in the 6-HODA dosage, number of injections, the injection place and the time course of injection, resulting in models of pre clinical, early or late stage PD (Meredith et al. 2008).

Overall, the 6-OHDA treated rat models are unsatisfactory because DA neurons die rapidly, with little progressive loss of the nigrostriatal DA pathway and without the presence of Lewy body like inclusions (Dauer and Przedborski 2003;Lane and Dunnett 2008).

##### **1.2.4.2. MPTP**

MPTP was found as a chemical contaminant of synthetic heroin that induced Parkinson disease in drug abusers (Davis et al. 1979;Langston et al. 1983). MPTP application leads specifically to DA neurons death and has become the most widely used toxins to mimic the hallmarks of PD (Fornai et al. 1997). Lipophilic MPTP rapidly passes the blood brain barrier



(BBB) and cellular membranes. In astrocytes, monoamine oxidase B converts MPTP into 1-methyl-4-phenyl-pyridinium ion (MPP<sup>+</sup>), the active toxic metabolite (Ransom et al. 1987). MPP<sup>+</sup> is taken up into DA neurons by the dopamine transporters (Mayer et al. 1986), inhibiting mitochondrial complex I in DA neurons (Tipton and Singer 1993). MPTP models have been most useful in studies of the molecular changes that underlie mitochondrial dysfunction by complex I inhibition promoting ATP depletion and generation of ROS in DA neurons (Rossetti et al. 1988; Dawson and Dawson 2003; Dauer and Przedborski 2003). With some variation the acute, subacute (Petroske et al. 2001; Karunakaran et al. 2007) and chronic (Lau et al. 1990; Petroske et al. 2001) MPTP protocols are widely used. For all these protocols, TH immunoreactivity disappears in DA neurons at different rates depending on the administration protocol. If neurons are estimated shortly after MPTP treatment the TH immunoreactivity loss may not reflect the actual DA cell death, since MPP<sup>+</sup> down-regulates TH gene expression (Xu et al. 2005). Small granular inclusions that contain alpha-synuclein, have been seen in DA SN neurons and limbic cortical cells between 3 and 24 weeks post MPTP treatment (Meredith et al. 2002; Meredith et al. 2004).

The MPTP-treated mouse models are also disappointing in that DA neurons die quickly and there is little progressive loss of the nigrostriatal DA pathway. Nevertheless, the pattern of DA terminal loss in the striatum replicates that of PD.

### **1.2.4.3. Rotenone**

Epidemiological studies link pesticide exposure to PD (Ascherio et al. 2006; Dick et al. 2007). Rotenone is a naturally occurring pesticide which inhibits mitochondrial complex I and has been used to generate the first chronic PD model (Betarbet et al. 2000; Hoglinger et al. 2003; Sherer et al. 2003). Rotenone is lipophilic, crosses cell membranes and penetrates the BBB. It produces a loss of striatal DA terminals followed by progressive degeneration of SN DA neurons. Degenerating DA neurons contain cytoplasmic inclusions like Lewy bodies which are immunopositive for  $\alpha$ -synuclein and ubiquitin (Betarbet et al. 2000). Elevations in oxidative damage, gliosis and increased iron deposits have been reported (Fleming et al. 2004).

The progressive nature of degeneration and presence of neuronal inclusions are advantages of the rotenone model over more acute administration of other toxins. However, even with

identical experimental conditions, rotenone causes either selective damage to DA neurons or more widespread cell loss (Betarbet et al. 2000;Sherer et al. 2003).

### **1.2.5. PD causative hypothesis**

Overall the causative hypothesis leading to PD indicates that deficits in mitochondrial function, oxidative and nitrosative stress, the accumulation of aberrant or misfolded proteins, protein phosphorylation, alterations in protein ubiquitination and protein degradation by the 26S proteasome (McNaught and Jenner 2001;McNaught et al. 2001) represent the principal molecular pathways or events that commonly underlie the pathogenesis of sporadic and familial forms of PD (Thomas and Beal 2007).

#### **1.2.5.1. PD mitochondrial respiratory chain and ROS generation**

Mitochondria are key intracellular organelles that play a crucial role in various cellular processes including energy production via pyrimidine biosynthesis, fatty acid oxidation, calcium homeostasis and cell survival (Wang et al. 1991;Elston et al. 1998;Wang and Oster 1998;Thress et al. 1999;Newmeyer and Ferguson-Miller 2003;Melov 2004). Some components of the oxidative phosphorylation system in mitochondria are encoded by its own genome (mitochondrial DNA; mtDNA). The mitochondrial oxidative phosphorylation machinery is composed of five multisubunit complexes (complex I–V). From Krebs cycle intermediates (NADH and FADH<sub>2</sub>), electrons feed into complex I or II, and are transferred to complex III, then to complex IV, and finally to O<sub>2</sub>. Energy released during the electron transfer process in complexes I, III and IV is utilized to actively pump out protons (H<sup>+</sup>) from the mitochondrial matrix to the intermembrane space, generating the electrochemical gradient ( $\Delta\psi$ ) of H<sup>+</sup> across the inner membrane which is ultimately utilized by complex V (F<sub>0</sub>F<sub>1</sub>-ATPase) to produce ATP or used directly for transmembrane transport. (Wallace 2005;Fukui and Moraes 2008). This energy production system is not perfect where up to 2% of electrons passing through the electron transport chain, mostly at complex I and complex III, react with molecular oxygen and yield superoxide anion production (O<sub>2</sub><sup>-</sup>) which can be converted into other ROS such as hydrogen peroxide and the highly reactive hydroxyl radical through enzymatic and non-enzymatic reactions (Balaban et al. 2005). In pathological cases the blocking the electron transport system or the reduced availability of final acceptors like cytochrome *c* or oxygen can lead to excessive reduction of ubiquinone and ubisemiquinone (Staniek et al. 2002). These free oxygen radicals may induce intracellular modification of lipids, proteins and nucleosides.

Beside ROS generation, mitochondria are also important regulators of  $\text{Ca}^{2+}$  signalling. Mitochondria actively and sensitively respond to the local increase  $\text{Ca}^{2+}$  concentration by a transient and massive uptake of the ion into the organelle (Rizzuto et al. 1999). Ultimately, this may lead to the loss of mitochondrial membrane potential, energy deprivation and cell death. The fluctuations of intracellular  $\text{Ca}^{2+}$  are observed in glutamate excitotoxic damage, which was suggested as one of the factors involved in DA cell death in PD, and may serve as an additional link between mitochondrial dysfunction and SNpc pathology.

### **1.2.5.2. PD and ROS generation hypothesis**

The occurrence of oxidative stress in PD is supported by both *post-mortem* studies and by studies demonstrating the capacity of oxidative stress and oxidizing toxins to induce nigral cell degeneration. There is evidence to support high levels of basal oxidative stress in the SNpc in the normal brain and that this is increased in PD. Furthermore, symptomatic treatment with L-dopa may add to the oxidative load and play a role in disease progression (Fahn 1997;Shulman 2000).

### **1.2.5.3. Why dopaminergic cells?**

Dopaminergic neurons of SNpc are more likely to be susceptible to the oxidative stress due to the highly oxidative intracellular environment (Lotharius and Brundin 2002a;Lotharius and Brundin 2002b). The neurotransmitter dopamine is degraded in the DA cells of SNpc either by monoamine oxidase A (MAO) (Adams et al. 1972;Gotz et al. 1994) or by autooxidation. Oxidation of dopamine by MAO-A results in the production of hydrogen peroxide, which after conversion to the hydroxyl radical, leads to oxidation of cellular compounds including the formation of oxidized glutathione (GSSG), suggesting the occurrence of oxidative stress and impairment of a major antioxidant system (Spina and Cohen 1988). Autooxidation of dopamine generates both dopamine quinones and hydrogen peroxide inside the cell (Graham et al. 1978;Sulzer et al. 2000). Dopamine quinones can directly modify proteins by reacting with their sulfhydryl groups and reduce the level of intracellular antioxidant glutathione (Graham et al. 1978;Sofic et al. 1992;Stokes et al. 1999). The conversion of hydrogen peroxide to highly reactive hydroxyl radical (Fenton reaction) requires  $\text{Fe}^{2+}$  ions (Riederer et al. 1989). Interestingly, the  $\text{Fe}^{2+}$  level in the SNpc is natively higher than in the other areas of the brain and, moreover, was found to be increased in PD (Sofic et al. 1988;Dexter et al. 1989b). Excess of dopamine was reported to inhibit the complex I function in the brain

(Benshachar et al. 1995). The reduced activity of the complex I of the respiratory chain was also found in PD (Schapira 1994). The vulnerability of DA neurons to inhibition of the complex I activity (Cohen and Heikkila 1974), suggests that these neurons are intrinsically more sensitive to the oxidative damage and mitochondrial dysfunction which may result from the DA catabolism.

Abundant evidences of the major role of oxidative stress in the pathogenesis of PD have accumulated over the recent decades. Additionally to increased iron level (Cohen and Heikkila 1974; Sofic et al. 1988; Dexter et al. 1989b; Hirsch et al. 1991), reduced levels of glutathione (GSH) (Perry et al. 1982; Sofic et al. 1992; Sian et al. 1994a; Fitzmaurice et al. 2003), and reduced GSH peroxidase expression (Kish et al. 1985; Marttila et al. 1988; Saggu et al. 1989; Johannsen et al. 1991; Sofic et al. 1992; Damier et al. 1993; Sian et al. 1994b) were found in the SN of PD affected brains. Moreover, decreased immunoreactivity of the reduced form of complex I (Mizuno et al. 1989; Schapira et al. 1990), and multiple signs of protein, lipid and DNA oxidation (Dexter et al. 1989a; Floor and Wetzell 1998; Zhang et al. 1999) were observed in the SN of PD brains in comparison to unaffected age matching controls. There is still no agreement over whether changes occur in proteins such as ferritin that are important in the regulation of iron levels (Riederer et al. 1989; Dexter et al. 1990; Jellinger et al. 1990; Mann et al. 1994; Kuiper et al. 1994; Cabreravaldivia et al. 1994; Connor et al. 1995; Logroscino et al. 1997). However, overall there is sufficient evidence to support the concept that oxidative stress occurs in substantia nigra in PD and that it contributes to nigral cell degeneration (Fahn and Cohen 1992).

The major difficulty in understanding the pathogenesis of PD is the separation of the oxidative stress role from other components of the cascade that themselves can play a primary role and, in turn, can initiate the formation of reactive oxygen and nitrogen species (Jenner 2003).

### **1.3. Cellular antioxidant defences**

The cells of the human brain utilize 20% of the oxygen consumed by the body and have a higher metabolic rate although it constitutes only 2% of the body weight (Clarke and Sokoloff 1999; Pelicano et al. 2004). This indicates the potential generation of a high quantity of ROS during oxidative phosphorylation in the brain. Cells are endowed with robust endogenous antioxidant systems to counteract excessive ROS and enable a long human life. The primary enzymatic defence against toxic oxygen oxidation metabolites includes the copper zinc

superoxide dismutase, manganese superoxide dismutase (SOD), catalase, glutathione S-transferases (GST), glutathione reductase (GSR) and glutathione peroxidases (GPx). SOD is in the first line of defence against oxygen-derived free radicals, and catalyzes the dismutation of the superoxide anion ( $O_2^-$ ) into hydrogen peroxide ( $H_2O_2$ ).  $H_2O_2$  can be transformed into  $H_2O$  and  $O_2$  by catalase. Glutathione peroxidase reduces lipidic or nonlipidic hydroperoxides as well as  $H_2O_2$  while oxidizing glutathione (Marklund et al. 1982;Taysi et al. 2002). In the normal human brain glutathione peroxidase activity is sevenfold greater than that of catalase. Further, while glutathione peroxidase is present in the cytosol, catalase is localized mainly in peroxisomes. As a result, the more ubiquitous presence of glutathione peroxidase predicts it to be the more important enzyme in responding to increased hydrogen peroxide (Marklund et al. 1982) resulting in higher GSH oxidation.

### **1.3.1. Antioxidant properties of Glutathione**

Glutathione has an essential cellular antioxidant role in the defence of brain cells against oxidative stress (Cooper and Schapira 1997;Dringen et al. 2000;Dringen and Hirrlinger 2003). Glutathione is a ubiquitous molecule produced intracellularly in all organs and cell types. It is a linear tripeptide formed from the amino acids glycine, cysteine and glutamate. It is present in concentrations of 0.5 to 10 mM in many different cell types and at 0.01 mM concentrations in extracellular space and plasma mainly because of its rapid catabolism (Meister and Anderson 1983). Inside cells glutathione can exist as a monomer in its reduced form (GSH), or as a disulfide dimer formed due to its oxidation (GSSG) which usually accounts for less than 1% (Franco et al. 2007). GSR is 85 to 90% freely distributed in the cytosol, although it can be compartmentalized in different organelles including mitochondria, peroxisomes, nuclear matrix and endoplasmic reticulum after its cytosolic synthesis (Jefferies et al. 2003;Wu et al. 2004;Circu and Aw 2008). GSH is not only in the first line response to redox changes and detoxification of drugs metabolites but it also regulates gene expression and apoptosis (Nicole et al. 1998;Circu and Aw 2008). GSH is also involved in the transmembrane transport of organic solutes, and in the modulation of ionotropic receptor function (Janaky et al. 1993;Bains and Shaw 1997;Janaky et al. 1999;Sies 1999;Dickinson and Forman 2002b;Grima et al. 2003;Ghezzi et al. 2005;Meyer 2008).

### 1.3.2. Glutathione synthesis

Glutathione synthesis starts by the formation  $\gamma$ -glutamylcysteine ( $\gamma$ -GC), a dipeptide formed by the combination of glutamate and cysteine catalyzed by the  $\gamma$ -glutamylcysteine ligase ( $\gamma$ -GCS), also known as glutamate cysteine ligase (GCL). GCL catalyzes the rate limiting step in GSH *de novo* production and cysteine is the rate limiting factor in GSH *de novo* synthesis (Sies 1999; Dickinson and Forman 2002a; Wu et al. 2004; Estrela et al. 2006). The unusual peptide  $\gamma$ -linkage formed by GCL is thought to protect GSH from degradation by aminopeptidases (Sies 1999). In a second step, glycine is added to  $\gamma$ -glutamylcysteine by the activity of GSH synthetase (GS). Both enzymatic steps consume one molecule of ATP per catalytic cycle. GSH acts as a feedback inhibitor of its synthesis since it can competitively inhibit the GCL activity. In the cell, GSH is recycled after oxidation by the GSR enzyme with consumption of NADPH reduction equivalents produced in the pentose phosphate pathway. The  $\gamma$ -glutamyl transpeptidase ( $\gamma$ -GT) is expressed mainly on the apical surface of cells and initiates the catabolism of glutathione and glutathione complexes.  $\gamma$ -GT removes the  $\gamma$ -glutamyl moiety from GSH, GSSG and GSH conjugated compounds by transferring it to other acceptors producing  $\gamma$ -glutamyl-derivatives and cysteinylglycine or cysteinylglycine complexes. These products are further hydrolyzed by ectoprotein dipeptidases which remove the peptide bond between cysteine and glycine. Cysteine and with the  $\gamma$ -glutamyl-derivatives are then uptaken by the activity of specific transporters. The  $\gamma$ -glutamyl-derivatives are further processed resulting in the production of glutamate (Meister and Anderson 1983; Paolicchi et al. 2002; Estrela et al. 2006). Since this pathway provides a means of recycling GSH precursors from glutathione and glutathione complexes that have been lost from cells, its up-regulation can provide an additional mechanism for increase GSH content in cells.

### 1.3.3. Fine tune regulation of Glutathione *de novo* synthesis

GSH synthesizing enzymes which include GCLm, GCLc and GS are regulated at transcription level by oxidative stress sensors regulators of gene expression. The key transcription factors identified thus far include Nrf2/Nrf1 via the antioxidant response element (ARE), the activator protein-1 (AP-1) and the nuclear factor kappa B (NFkappaB) (Huang et al. 2000; Yang et al. 2002; Dickinson and Forman 2002b; Lee et al. 2005). High oxidative environment in the cell leads to increased expression of these enzymes.

GCL catalyzes the rate limiting step in GSH *de novo* production and the catalytic activity of enzyme is tightly modulated. GCL is a heterodimer which can be dissociated under non-denaturing conditions into a modulatory, or light, subunit (GCLm), and a catalytic, or heavy, subunit (GCLc) (Seelig and Meister 1985). GCLc is 73 kDa in size protein, possesses all of the catalytic activity of GCL and the site of GSH feedback inhibition. The lighter 31 kDa GCLm subunit, which as a monomer has no catalytic function, exhibits a modulatory or regulatory effect, on the GCLc subunit when associated. This association is probably essential for GSH biosynthesis under normal physiological concentrations of glutamate and GSH. Studies performed *in vitro* using purified rat (Huang et al. 1993) or recombinant human enzymes (Tu and Anders 1998;Griffith 1999), and *in vivo* observations from transgenic mice (Choi et al. 2000) suggest that the major effect of the light subunit is the elevation of the inhibition constant ( $K_i$ ) for GSH decreasing the negative feedback inhibition, and decreasing the Michaelis constant ( $K_m$ ) for glutamate and adenosine triphosphate [ATP] (Griffith 1999;Chen et al. 2005). The activity of the GCL holoenzyme can further be regulated either positively or negatively by S-nitrosation (Griffith 1999), phosphorylation (Sun et al. 1996) and oxidation (Ochi 1995), although increased GCL activity in most cases involves a transcriptional component leading to increased production. The second enzyme required for *de novo* GSH biosynthesis is glutathione synthetase (GS), a homodimer of 118 kDa, which appears to not be catalytically regulated.

#### **1.4. RNAi basic mechanism of RNA mediated gene silencing**

RNA interference (RNAi) was formally discovered in 1998. RNAi revolution started with the observations that microinjected dsRNA was very effective in gene silencing in *Caenorhabditis elegans* (Fire et al. 1998). This finding, together with the discovery that genes of *C. elegans* feeding on bacteria expressing double-stranded RNA (dsRNA) were silenced in the whole organism (Timmons and Fire 1998), were fundamental for an increase RNAi application (Mello and Conte 2004). RNAi is nowadays one of the most widely applied technologies in molecular and cellular research. The RNAi mechanism was first elucidated biochemically using *Drosophila* embryo or cell extracts (Tuschl et al. 1999;Hammond et al. 2000;Zamore et al. 2000) which led to the identification of the dsRNA processing enzyme Dicer (Bernstein et al. 2001) as well as the RNA induced silencing complex (RISC) (Hammond et al. 2000). RISC executes RNAi by using the small dsRNA species generated by Dicer as guidance molecules to target the homologous, endogenous mRNA for degradation (Zamore et al. 2000;Elbashir et al. 2001a;Elbashir et al. 2001b).

#### **1.4.1. RNAi is subdivided in two distinct phases: an initiation and an execution phase.**

The initiation phase involves processing of dsRNA into small RNA molecules, called small interfering RNAs (siRNA). siRNAs are generated from stretches of double stranded RNA (Tuschl et al. 1999;Hammond et al. 2000;Zamore et al. 2000) by Dicer, a member of the RNase III gene family (Bernstein et al. 2001). Sources of the dsRNA molecules are experimentally expressed dsRNAs, aberrantly expressed transgenes, viral RNA, transposons, or short hairpin RNAs (shRNAs) (Hannon 2002). Dicer contains a dsRNA binding domain, an RNA helicase as well as two RNaseIII like domains (Bernstein et al. 2001). Dicer cuts dsRNA generating a 21 to 23 nt long siRNA molecules with overhanging 3' ends (Blaszczyk et al. 2001). Dicer is present in many organisms including yeast (Volpe et al. 2002), plants (Golden et al. 2002;Park et al. 2002), *C. elegans* (Knight and Bass 2001), *Drosophila* (Bernstein et al. 2001), mice (Bernstein et al. 2003) and humans (Provost et al. 2002;Zhang et al. 2002), suggesting that all these organisms use the same basic mechanism to initiate the RNAi pathway.

In the execution phase, dicer generated siRNAs are incorporated into a large multiprotein complex, which is involved in various gene-silencing modes, the RNA induced silencing complex, or RISC (Hammond et al. 2000;Nykanen et al. 2001). Processing of dsRNA and assembly of a functional RISC occurs in the cytoplasm, as Dicer is a cytosolic enzyme and RISC activity can be purified from cytosol (Billy et al. 2001). After unwinding of the siRNA duplex, a single RNA strand is incorporated into the RISC (Martinez et al. 2002). In the siRNA mediated mRNA degradation pathway, the antisense strand of the siRNA molecule is used to recognize the mRNA for degradation (Schwarz et al. 2002). This process involves specific base pairing between the antisense strand of the siRNA and the target mRNA, which results in endonucleolytic cleavage of the mRNA strand across the middle of the siRNA strand which finally results in mRNA degradation (Elbashir et al. 2001a;Martinez et al. 2002).

#### **1.4.2. shRNA, permanent way to bring RNAi into the cells**

In order to overcome the poor transfection efficiency and transient RNAi limitations, several *in vitro* and *in vivo* siRNA expression systems have been engineered. The majority of these systems employ RNA polymerase III promoters (Paule and White 2000), such as the U6 or H1 RNA gene promoters (Miyagishi and Taira 2002;Paul et al. 2002;Brummelkamp et al. 2002a;Paddison et al. 2002a). The transcription from these small and compact promoters



starts at a defined site and can be precisely terminated by using a stretch of 5 consecutive T's (thymine). In contrast to the U6 promoter, where the first nucleotide has to be a G, the H1 promoter tolerates any nucleotide at the +1 position. The two strands of the siRNAs can be expressed individually (Miyagishi and Taira 2002) or as a short hairpin RNA (shRNA) molecule (Paul et al. 2002; Brummelkamp et al. 2002a; Paddison et al. 2002a)

shRNA expression plasmids are a powerful means to induce stable and even inducible RNAi in mammalian cells. The hairpin RNAs are usually designed as sense-loop-antisense (19 to 29 nt) molecules followed by 5 T's. These RNAs fold up as hairpins and are processed by Dicer into mature siRNAs. As with siRNAs, the efficacy of shRNAs is not fully predictable (Jia et al. 2006; Li and Cha 2007) and has to be determined experimentally. Due to their small size the shRNA expression cassettes have been incorporated into many different vector systems, including retro (Barton and Medzhitov 2002; Brummelkamp et al. 2002b; Paddison et al. 2002b), lentivirus (Rubinson et al. 2003; Yamamoto et al. 2006; Chen et al. 2007a; Kim et al. 2008), adenoviral (Zhu et al. 2007; Rauschhuber et al. 2008; Yoo et al. 2008; Witting et al. 2008; Sakamoto et al. 2008) or AAV constructs (Michel et al. 2005; Moore et al. 2005a; Paskowitz et al. 2007; Fechner et al. 2008; Garza et al. 2008; Franich et al. 2008) for efficient and long term expression. Recently AAV mediated shRNA expression has been shown to result in dramatic knockdown of mutant huntingtin exon 1 (htt containing 70 CAG repeats) preventing striatal neurodegeneration and concomitant motor behavioural impairment in adult rats (Franich et al. 2008). Our group has shown efficient silencing of EGFP expression in retinal ganglion cells over a period of 12 weeks after transduction with an AAV EGFP-shRNA vector (Michel et al. 2005). These results demonstrate the power of RNAi and its potential use as a therapeutic agent over a long period of time.

### **1.5. Recombinant AAV vectors as tools for gene transfer and disease modelling**

Viral vectors are ideal gene delivery vehicles to the CNS due to their ability to infect both dividing and non-dividing cells (Flotte et al. 1992; Flotte et al. 1994; Shevtsova et al. 2006; Kugler et al. 2007). They allow for the expression (Kirik et al. 2002; Kirik et al. 2003; Gorbatyuk et al. 2008) or silencing (Michel et al. 2005; Moore et al. 2005b; Paskowitz et al. 2007; Fechner et al. 2008; Garza et al. 2008; Franich et al. 2008) of proteins related with cell death or survival, aiming for therapeutical neuroprotective gene transfer into the lesioned CNS (Bjorklund et al. 1997; McBride et al. 2003; Shevtsova et al. 2006; Leaver et al.

2006;Shen et al. 2006), or the establishment of new models of disease, aiming to dissect individual gene contributions to human diseases.

Adeno-associated virus (AAV) is a small dependovirus from the *Parvoviridae* family, which is replication deficient in the absence of a helper virus such as adenovirus, herpes virus or vaccinia virus (Atchison et al. 1965;Buller et al. 1981). Wild type AAV is not known to be associated with any disease in humans or mammals, which makes it an attractive tool for human gene therapy. Wild-type AAV contains a linear single-stranded genome of approximately 4.700 nucleotides in length and is flanked by two inverted terminal repeats (ITRs) of 145 nucleotides, the first 125 nucleotides of which form a palindromic sequence (Srivastava et al. 1983;Gao et al. 2005). Wild type AAV genome possesses two non overlapping large open reading frames (ORF). The *cap* ORF encodes for virus coat proteins (capsid proteins), the *rep* ORF, for the proteins necessary for virus replication and transcription of the viral genes. At least ten different AAV serotypes (AAV-1 to AAV-9, and AAV-Rh10) have been identified (Cearley and Wolfe 2006;Cearley et al. 2008;Zincarelli et al. 2008) most of them share certain sequence homology in *cap* genes (Bantel-Schaal et al. 1999). Recombinant AAV (rAAV) vectors used for gene transfer have only 4% of wild-type AAV genome consisting of ITRs sequence, the only *cis* elements which are required for packaging. Methods used nowadays allow for the production of helper free rAAV stocks with high purity (Samulski et al. 1989;Grimm et al. 1998). Therefore, recombinant AAV vectors are considered to be one of the most bio safe viral vectors. Numerous pre-clinical and clinical experiments have been performed using rAAV vectors in gene therapy strategies to treat neurological disorders including Parkinson's disease (Muramatsu et al. 2002;Mandel and Burger 2004;Feigin et al. 2007;Kaplitt et al. 2007), and Alzheimer's disease (Fukuchi et al. 2006).

Natural rAAV serotypes exhibit different transduction properties which have been explored using “pseudotyping”, the generation of hybrid AAV vectors which contain the genome of one serotype (typically AAV2) packaged into the capsid of another serotype (Duan et al. 2001;Auricchio et al. 2001;Hildinger et al. 2001). Other technique exploring the different serotype properties of capsid proteins has led to the generation of chimeric rAAV vectors by means of mixing the capsid proteins resulting in the generation of “new virions” (Hauck et al. 2003;Rabinowitz et al. 2004). Except for variations in cellular tropism, the capsid proteins of different serotypes may also influence the onset and the intensity of gene expression (Chao et al. 2000;Auricchio et al. 2001;Rabinowitz et al. 2004). The recombinant AAV vectors lack

the wild-type *rep* gene, which is responsible for the site-specific integration in the chromosomal DNA, and thus persist mainly in an episomal form (Duan et al. 1998). They can, nevertheless, mediate stable transgene expression for more than 7 years in a primate model of Parkinson disease (PD) (Bankiewicz et al. 2006). rAAV vectors have been reported to be non-toxic, non-inflammatory and inducing only a very limited immune response without any noticeable decrease in transgene expression after injection into the brain (Mastakov et al. 2002).



## 2. Materials and Methods

### 2.1. Materials

#### 2.1.1. Chemicals

**Applichem BioChemica:** 2-Propanol, Acetone, Agarose, Ampicillin (Sodium salt), Boric acid, chloroform, DAPI, DMEM, D(+)-Glucose, Ethanol absolute, Glycine, HEPES, LB medium (powder), LB agar (powder), Magnesium chloride (MgCl<sub>2</sub>), Methanol, milk powder, NADPH (nicotinamide adenine dinucleotide phosphate), Paraformaldehyde, PBS (1x Dulbecco's powder), Phenol equilibrated stabilized, Potassium chloride (KCl), Sodium chloride (NaCl), Sodium dodecylsulfate (SDS), Sodium hydroxide pellets, D(+)-Sucrose, Tris.

**Applied Biosystems:** BigDye Terminator v3.1 cycle sequencing kit

**BIO-RAD:** 0.2 ml RT-PCR tubes with domed caps, Precision Plus Protein Standards, fluorescein

**Beckman Coulter:** Quick-Seal Polyallomer ultracentrifuge tubes (cat# 342414)

**Calbiochem:** Moviol, Sodium citrate.

**Carl Roth:** Milk powder, Rothiphorese.

**GE Healthcare:** HiTrap™ Heparin HP Columns (1ml)

**Gibco:** B27 Supplement, DMEM:F12 (1:1), HBSS 10x, Neurobasal medium (NBM), PS-N.

**Fluka:** Chloral hydrate, Coumaric acid, Sodium acetate, L-Buthione-sulfoximine, Tween 20.

**Fresenius Kabi:** Opti Prep™ (iodixanol)

**Invitrogen:** Platinum SYBR Green qPCR SuperMix UDG

**Merck:** Agar, Ammonium peroxide, Coomassie Brilliant Blue, Formaldehyde, Hydrogen peroxide (H<sub>2</sub>O<sub>2</sub>).

***Macherey-Nagel:*** NucleoBond PC2000 Mega Kit.

***New England Biolabs:*** all restriction endonucleases for molecular biology, dATP, dCTP, dGTP, dTTP, DNase I, Phusion high-fidelity DNA Polymerase.

***PAA the cell culture company:*** NGS, FCS, penicillin/streptomycin (PS), Trypsin for HEK 293 cells.

***PIERCE:*** BCA protein assay reagent, Slide-A-Lyzer 10K MWCO Dialysis Cassett

***QIAGEN:*** QIAGEN Plasmid Maxi Kit, QIAquick Gel Extraction Kit, QIAquick PCR Purification Kit, QIAprep Spin MiniPrep Kit

***Roche:*** Alkaline Phosphatase shrimp, DNase I (for primary cell culture), glycogen for molecular biology, Glycerol, cell proliferation reagent WST-1, Glutathione Reductase.

***Seromed:*** L-glutamine.

***Serva:*** Bromophenol blue sodium salt (BPB), tetramethylethylenediamine (TEMED).

***Sigma:*** 2-mercaptoethanol, 2VP (2-Vinylpyridine), 6-hydroxydopamine hydrochloride,  $\alpha$ -chymotrypsin, Bactotryptone, Benzonase, BSA, D(+)- glucose, DTNB (5,5'-Dithio-bis(2-nitrobenzoic acid)), Dithiothreitol (DTT), EDTA, Ethidium bromide, GSSG (oxidized Glutathione), Laminin, L-ascorbic acid, Luminol, MOPS, Poly-L-Ornithine, Sodium azide, Sodium bicarbonate ( $\text{Na}_2\text{CO}_3$ ), SSA (5-sulfosalicylic acid dehydrate), Transferrin, Triton X-100, Trypsin for primary cell culture, Yeast extract.

***Sigma-Genosys:*** all oligonucleotides

**2.1.2. Antibodies**

Table 2.1.1. List of primary antibodies used in this study

<b>Antigen</b>	<b>Species</b>	<b>Supplier</b>
Anti-AU1	mouse monoclonal	Covance, #MMS-130R
Anti- $\beta$ -tubulin	mouse monoclonal	Sigma, #T 4026
Anti-cleaved caspase-3 (Asp175)	rabbit polyclonal	Cell Signalling Technologies, #9661
Anti- Cleaved caspase-9	rabbit polyclonal	Cell Signalling Technologies, #9507
Anti-CD11b	mouse monoclonal	AbD serotec, #MCA275R
Anti-DJ1	goat polyclonal	IMGENEX, #IMG-3038
Anti-GCLc	rabbit polyclonal	abcam, #ab17926
Anti-GCLm	rabbit polyclonal	Santa Cruz Biotechnology, #sc-22754
Anti-GFP	rabbit polyclonal	Clontech, # 632376
Anti-GFAP	rabbit polyclonal	DAKO A/S, #Z0334
Anti-Glutathione-protein complexes	mouse monoclonal	abcam, #ab19534
Anti-Glutathione Reductase	rabbit polyclonal	abcam, #ab16801
Anti-MAP LC3	goat polyclonal	Santa Cruz Biotechnology, #sc-16756
Anti-NeuN	mouse monoclonal	Chemicon, #MAB377
Anti-NT	mouse monoclonal	abcam, #ab7048
Anti-TH	mouse monoclonal	Sigma, #T 1299
Anti-TH	rabbit polyclonal	Advanced Immunochemicals, #R-Th1
Anti-VMAT2	rabbit polyclonal	Chemicon, #AB1767

Table 2.1.2. List of secondary antibodies used in this study

<b>Conjugation</b>	<b>Species</b>	<b>Supplier</b>
Cy2 conjugated IgG	goat anti-mouse	dianova, # 115-225-072
Cy2 conjugated IgG	goat anti-rabbit	dianova, # 111-227-003
Cy3 conjugated IgG	goat anti-mouse	dianova, # 115-165-164
Cy3 conjugated IgG	goat anti-rabbit	dianova, # 111-165-006
Cy3 conjugated IgG	mouse anti-goat	dianova, # 205-165-108
Cy5 conjugated IgG	donkey anti-goat	dianova, # 705-176-147
Cy5.5 conjugated IgG	goat anti-mouse	Rockland, #610-113-121
HRP-conjugated IgG	goat anti-mouse	Santa Cruz Biotechnology, #sc-2005
HRP-conjugated IgG	goat anti-rabbit	Santa Cruz Biotechnology, #sc-2004
HRP-conjugated IgG	donkey anti-goat	Santa Cruz Biotechnology, #sc-2020

### 2.1.3. Plasmids

**pAAV-6P-SEWB**, kindly provided by Dr. Sebastian Kügler, University Hospital Göttingen, Göttingen, Germany

**pAAV-hSyn1-DsRed2N1-CytbAS**, **pGL3-SV40-fluc-short-RhoA-test1**, and **pSuper-hSyn1-DsRed2N1-CytbAS** were kindly provided by Prof. Dr Uwe Michel, University Hospital Göttingen, Göttingen, Germany

**pBluescriptR-GCLm** Homo sapiens, RZPD (German resource center for genome research, clone # IRATp970A0262D)

**pDG**, kindly provided by Dr Jürgen Kleinschmidt, German Cancer Research Center, Heidelberg, Germany

**pExpress-1-GCLc** Rattus norvegicus, RZPD (German resource center for genome research, clone # IRAKp961B11182Q2)

**pExpress-1-GCLm** Rattus norvegicus, RZPD (German resource center for genome research, clone # IRBPp993C098D)

**pExpress-1-GSR** Rattus norvegicus, RZPD (German resource center for genome research, clone # IMAGp998M1215338Q1)

**pSuper neoGFP fluc-shRNA#2**, kindly provided by Prof. Dr. Juan P. Bolanos, University of Salamanca, Spain.

### 2.1.4. Oligonucleotides for PCR amplification

#### **5'-Spe1-Apa1-PspOM1- shortGCLc:**

TTTTTTACTAGTAAGGGCCCGTCCAGTTGTTACTGAATGGCGGGCGAT

#### **3'-EcoR1-Age1-shortGCLc:**

TTTTTTGAATTCAAACCGGTCCCGTGTTCTATCATCTACAGATGCAGA

#### **5'-Spe1-shorGSR:**

TTTACTAGTAAGGGATGCTTACGTGAGCCGCCTGAA

#### **3'-EcoR1-shortGSR:**

TTTGAATTCAAACCCTTAGAATTTGGGTCCCGTCCAA

#### **5'-Mlu1-hH1promoter:**

AAAAAAACGCGTTGCAGGAATTCGAACGCTGACGTCATCAACC



**3'-Mlu1-9(5)-stuffer:**

AAAAAAACGCGTAACACCGGATCCTGGACCCACTGAGCAAG

**5'-Age1-GCLc:**

AAAAAACCGGTCGCCACCATGGGGCTGCTGTCCCAAGGC

**3'-Not1-GCLc:**

AAAAAGCGGCCGCCTAGTCTGAAGGGTCGCTTTTACC

**5'-blunt-GCLc-shRNA#2-bp-exch#2:**

P-CGT ATA TGA TCG AAG GGA CAC CTG GCC AGC CGT AC

**3'-blunt-GCLc-shRNA#2-bp-exch#2:**

P-AAC CGT ATT CTG GTC TCC AGA GGG TTG GGT GG

**5'-blunt-GCLc-shRNA#3-bp-exch#3:**

P-CCA TTA CCT CAT TTC CCA GGC TAG GCT GCC

**3'-blunt-GCLc-shRNA#3-bp-exch#3:**

P-TAC ACA GTG CCT GAT GTT CTC CTA ATA CAG

**5'-Age1-GCLm:**

AAA AAA CCG GTC GCC ACC ATG GGC ACC GAC AGC CG

**3'-Not1-GCLm-Rattus-norvegicus:**

AAA AAG CGG CCG CTT AAG AAC CCT TTC TTT TGG CTT GC

**3'-Not1-GCLm-Homo-sapiens:**

AAA AAG CGG CCG CTT AAG AAC CCC TTC TTT TAG CTT G

**2.1.5. Oligonucleotides for sequencing**

**T7:**

TAATACGACTCACTATAGGG

**T3:**

ATTAACCCTCACTAAAGGGA

**SP6:**

GATTTAGGTGACACTATAG

**hSyn1-promoter-forward:**

CAGCGGAGGAGTCGTGTCG

**H1-promoter-forward:**

CCCTGCAATATTTGCATGTCGCTA

**9(5)-stuffer-reverse:**

GAAATTCATGCATGAATC

**GCLc-forward1:**

TAGAAACATTTCTGAGGATGAGGAG

**GCLc-reverse2:**

TACACAGCAGAGGAGACTCAAGA

**GCLc-forward3:**

TGACCATTTTGAGAATATTCA

**GCLc-reverse4:**

ATTGCATTTCAAATGAGGCTA

**SVpA-reverse:**

GTGGTTTGTCCAAACTCATCAA

**fluc-forward:**

GACGAAGTACCGAAAGGTCTTA

**GSR-forward:**

GGCCATTGGACGGGACCCAAA

**GSR-reverse:**

CGTAGCCGTGGATGACTTCGA

**WPRE-reverse:**

TACCAGTCAATCTTTCAC

**2.1.6. Oligonucleotides for shRNAs**

**Dharmacon shRNA#1 sense:**

P-GATCCCCTAGCGACTAAACACATCAACTTCCTGTCATTGATGTGTTTAGTCGCT  
ATTTTTGGAAA

**Dharmacon shRNA#1 antisense:**

P-AGCTTTTCCAAAAATAGCGACTAAACACATCAATGACAGGAAGTTGATGTGTT  
TAGTCGCTAGGG

**Dharmacon shRNA#2 sense:**

P-GATCCCCTAAGGCTATGAAGAGATACCTTCCTGTCAGTATCTCTTCATAGCCTT  
ATTTTTGGAAA

**Dharmacon shRNA#2 antisense:**

P-AGCTTTTCCAAAAATAAGGCTATGAAGAGATACTGACAGGAAGGTATCTCTTC  
ATAGCCTTAGGG

**EGFP-shRNA sense:**

P-GATCCCCAAGCTGACCCTGAAGTTCATTCAAGAGATGAACTTCAGGGTCAGCTT  
TTTTTGAAA

**EGFP-shRNA antisense:**

P-AGCTTTTCCAAAAAAGCTGACCCTGAAGTTCATCTCTTGAATGAACTTCAGGG  
TCAGCTT GGG

**fluc-shRNA#1 sense:**

P-GATCCCCGTGCGCTGCTGGTGCCAACCCCTTCCTGTCAGGGTTGGCACCAGCAG  
CGCACTTTTTTGAAA

**fluc-shRNA#1 antisense:**

P-AGCTTTTCCAAAAGTGCGCTGCTGGTGCCAACCCCTGACAGGAAGGGGTTGGC  
ACCAGC A GCGCACGGG

**fluc-shRNA#2 sense:**

P-GATCCCCCTGACGCGGAATACTTCGATTCAAGAGATCGAAGTATTCCGCGTCAG  
TTTTTGAAA

**fluc-shRNA#2 antisense:**

P-AGCTTTTCCAAAAGCTGACGCGGAATACTTCGATCTCTTGAATCGAAGTATTCC  
GCGTCAGGGG

**GCLc shRNA#1 sense:**

P-GATCCCCAAGGAGGCTACTTCTGTATTACTTCCTGTCATAATACAGAAGTAGC  
CTCCTTTTTTTTGAAA

**GCLc shRNA#1 antisense:**

P-AGCTTTTCCAAAAAAGGAGGCTACTTCTGTATTATGACAGGAAGTAATACAG  
AAGTAGCCTCCTTGGG

**GCLc shRNA#2 sense:**

P-GATCCCCGAGTATGGGAGTTACATGATTCTTCCTGTCAAATCATGTAACTCCCA  
TACTCTTTTTTGAAA

**GCLc shRNA#2 antisense:**

P-AGCTTTTCCAAAAGAGTATGGGAGTTACATGATTTGACAGGAAGAATCATGT  
AACTCCCACTCGGG

**GCLc shRNA#3 sense:**

P-GATCCCCGGCTCTTTGCACGATAACTTCCTTCCTGTCAGAAGTTATCGTGCAA  
GAGCCTTTTTGGAAA

**GCLc shRNA#3 antisense:**

P-AGCTTTTCCAAAAAGGCTCTTTGCACGATAACTTCTGACAGGAAGGAAGTTAT  
CGTGCAAAGAGCCGGG

**GSR shRNA#1 sense:**

P-GATCCCCATCCACGGCTACGCAACATTTCTTCCTGTCTAAATGTTGCGTAGCCG  
TGGATTTTTTGGAAA

**GSR shRNA#1 antisense:**

P-AGCTTTTCCAAAAATCCACGGCTACGCAACATTTAGACAGGAAGAAATGTTG  
CGTAGCCGTGGATGGG

**GSR shRNA#2 sense:**

P-GATCCCCAACCAGTGATGGGTTCTTTCCTTCCTGTCATGAAAGAACCCATCA  
CTGGTTTTTTTGGAAA

**GSR shRNA#2 antisense:**

P-AGCTTTTCCAAAAAACCAGTGATGGGTTCTTTCATGACAGGAAGTGAAAGAA  
CCCATCACTGGTTGGG

**GSR shRNA#3 sense:**

P-GATCCCCTTGCCCAGCCGCAGCGTTATTCTTCCTGTCAAATAACGCTGCGGCT  
GGGCAATTTTTTGGAAA

**GSR shRNA#3 antisense:**

P-AGCTTTTCCAAAAATTGCCAGCCGCAGCGTTATTTGACAGGAAGAATAACGC  
TGCGGCTGGGCAAGGG

**GCLm shRNA#1 sense:**

P-GATCCCCGGAATGTACCATGTCCCATGCCTTCCTGTCAGCATGGGACATGGTAC  
ATTCCTTTTTTGGAAA

**GCLm shRNA#1 antisense:**

P-AGCTTTTCCAAAAAGGAATGTACCATGTCCCATGCTGACAGGAAGGCATGGGA  
CATGGTACATTCCGGG

**GCLm shRNA#2 sense:**

P-GATCCCCGCAAGAAGATTGTTGCTATAGCTTCCTGTCACTATAGCAACAATCTT  
CTTGCTTTTTTGGAAA

**GCLm shRNA#2 antisense:**

P-AGCTTTTCCAAAAAGCAAGAAGATTGTTGCTATAGTGACAGGAAGCTATAGCA  
ACAATCTTCTTGCGGG

**GCLm shRNA#3 sense:**

P-GATCCCCGCAGTTGACATGGCATGCTCACTTCCTGTCATGAGCATGCCATGTCA  
ACTGCTTTTTGGAAA

**GCLm shRNA#3 antisense:**

P-AGCTTTTCCAAAAAGCAGTTGACATGGCATGCTCATGACAGGAAGTGAGCATG  
CCATGTCAACTGCGGG

Table 2.1.3. List of shRNAs sequences used in this study

Name	Sense sequence	Antisense sequence
Dhar-shRNA#1	TAGCGACTAAACACATCAA	TTGATGTGTTTAGTCGCTA
Dhar-shRNA#2	TAAGGCTATGAAGAGATAC	GTATCTCTTCATAGCCTTA
EGFP-shRNA	AAGCTGACCCTGAAGTTCA	TGAACTTCAGGGTCAGCTT
fluc-shRNA#1	GTGCGCTGCTGGTGCCAACCC	GGGTTGGCACCAGCAGCGCAC
fluc-shRNA#2	CTGACGCGGAATACTTCGA	TCGAAGTATTCCGCGTCAG
GSR-shRNA#1	ATCCACGGCTACGCAACATTT	AAATGTTGCGTAGCCGTGGAT
GSR-shRNA#2	AACCAGTGATGGGTTCTTTCA	TGAAAGAACCCATCACTGGTT
GSR-shRNA#3	TTGCCAGCCGCAGCGTTATT	AATAACGCTGCGGCTGGGCAA
GCLc-shRNA#1	AAGGAGGCTACTTCTGTATTA	TAATACAGAAGTAGC CTCCTT
GCLc-shRNA#2	GAGTATGGGAGTTACATGATT	AATCATGTAACCTCCATACTC
GCLc-shRNA#3	GGCTCTTTGCACGATAACTTC	GAAGTTATCGTGCAAAGAGCC
GCLm-shRNA#1	GGAATGTACCATGTCCCATGC	GCATGGGACATGGTACATTCC
GCLm-shRNA#2	GCAAGAAGATTGTTGCTATAG	CTATAGCAACAATCTTCTTGC
GCLm-shRNA#3	GCAGTTGACATGGCATGCTCA	TGAGCATGCCATGTCAACTGC

**2.1.7. Cell lines and electrocompetent cells:**

**HEK 293/ AAV 293:** Stratagene

**DH5 $\alpha$**  E. coli strain: ElectroMAX<sup>TM</sup>DH5 $\alpha$ -E<sup>TM</sup>Cells, Invitrogen

**SURE** E. coli strain: SURE<sup>®</sup>Electroporation-Competent Cells (Stop Unwanted Rearrangement Events) Stratagene

### 2.1.8. Buffers, solutions and medium:

**Annealing buffer (for oligonucleotides, 2x):** 20 mM Tris, pH 7.8, 100 mM NaCl, and 0.2 mM EDTA

**Blocking solution for IHC and ICC:** 10% NGS, 0.3% Triton X-100 in PBS.

**Blocking solution for WB:** 5% non fat dry Milk in TBS-T (see below).

**Borate buffer:** 150 mM Boric Acid in H<sub>2</sub>O, pH 8.4 (sterile filtered).

**Ca<sup>2+</sup>/Mg<sup>2+</sup> Free (CMF) medium:** 50 ml 10x Hanks Balanced Salt Solution (HBSS), 450 ml Ampuwa H<sub>2</sub>O, pH 7.3 adjusted with sterile Na bicarbonate.

**Chloral hydrate 7%:** 7 g chloral hydrate in 100 ml of H<sub>2</sub>O (sterile filtered).

**Citric saline (1x):** 135 mM potassium chloride, 15 mM sodium citrate.

**Calcium Chloride:** 2.5 M CaCl<sub>2</sub>·2H<sub>2</sub>O H<sub>2</sub>O (sterile filtered, stored at -20° C)

**Coomassie-fixing solution:** 50% methanol, 10% acetic acid, 40% H<sub>2</sub>O.

**Coomassie-staining solution:** 0,05% Coomassie Brilliant Blue G-250, 10% acetic acid, 50% methanol, 40% H<sub>2</sub>O.

**Coomassie-destaining solution:** 5% methanol, 7% acetic acid, 88% H<sub>2</sub>O.

**Dephosphorylation buffer:** 50 mM Tris-HCl, 50 mM MgCl<sub>2</sub>, pH 8.5

**DMEM:** Dulbecco's modified Eagle's medium, used as supplied by manufacturer.

**DNA loading buffer (6x):** 15% Ficoll 400 DL, 100 mM LiCl, 2% glycerol, 100 mM EDTA, pH 8.0; 0.6% SDS, 0.03% BPB in H<sub>2</sub>O.

**DNase for primary cell culture:** 5 mg of DNase were dissolved in 1 ml of Ca<sup>2+</sup>/Mg<sup>2+</sup> free medium (CMF) and stored at -20°C. Final concentration 5 mg/ml.

**DNase I buffer (10x):** DNase I buffer: 100 mM Tris-HCl pH 7.6, 25 mM MgCl<sub>2</sub>, 5 mM CaCl<sub>2</sub>

**ECL-1:** 2.5 mM Luminol, 0.4 mM p-Coumar acid, 0.1 M Tris-HCl, pH 8.5.

**ECL-2:** 18% H<sub>2</sub>O<sub>2</sub>, 0.1 M Tris-HCl, pH 8.5.

**Electrophoresis buffer:** 192 mM Glycine, 0.1% SDS, 25 mM Tris-HCl, pH 8.3.

**FCS (inactivated):** FCS was thawed, pre-warmed at 37°C and incubated for 30 min at 56°C (heat inactivation). Aliquots were stored at -20°C.

**HBS (2x):** 280 mM NaCl, 10 mM KCl, 1.5 mM Na<sub>2</sub>HPO<sub>4</sub>, 12 mM glucose, 50 mM HEPES, in H<sub>2</sub>O, pH 7.04/7.05 sterile filtered and stored in aliquots at - 20° C.

**HCN medium:** 5µg/ml transferrin, PSN (Penicillin 50 µg/ml, Streptomycin 50 µg/ml, Neomycin 100 µg/ml), 2 mM L-Glutamin, 2% B-27 supplement in Neurobasal medium (NBM).

**Incubation solution for primary antibody for immunofluorescence (IF):** 2% NGS, 0.3% Triton X-100 in PBS.

**Incubation solution for secondary antibody for immunofluorescence (IF):** 2% NGS in PBS.

**Laminin:** Laminin was diluted 1:1000 in DMEM-F12 before use.

**LB medium:** 25 g of LB powder in 1000 ml H<sub>2</sub>O, autoclaved and stored at 4° C.

**LB agar:** 40 g of LB agar in 1000 ml H<sub>2</sub>O, autoclaved. The solution was cooled to 60°C and the appropriate resistance antibiotic (10 mg/ml) was added shortly before distribute in Petri dishes and let dry overnight. Plates were stored at 4°C.

**Ligation buffer (1x):** 10 mM MgCl<sub>2</sub>, 1 mM ATP, 10 mM DTT, 25 µg/ml BSA, 50 mM Tris-HCl, pH 7.5)

**Lysis buffer for cell culture:** 0.5% SDS, 1 mM DTT, 50 mM Tris-HCl pH 8.0; 1x P1c.

**Mowiol:** 4.8 g MOWIOL<sup>®</sup> 4-88 in 12 g glycerol and mix. Add 6 ml of water and stir for several hours at RT. Add 12 ml of 0.2 M Tris (pH 8.5) and heat to 50°C for 10 min with occasional mixing. After the MOWIOL<sup>®</sup> 4-88 dissolves, clarify the solution by centrifugation at 5000 x g for 15 min. After reconstitution mowiol was aliquoted and frozen (-20°C) for long-term storage or kept at 4° C for short-term storage.

**Paraformaldehyde (PFA) 4%:** 40 g PFA in 1000 ml PBS and dissolved at 60° C for 4-6 h. Solution was paper filtered.

**PBS:** 9.55 g of PBS powder in 1 L Millipore ddH<sub>2</sub>O, autoclaved.

**PBS-MK:** 2.5 mM KCl, 1 mM MgCl<sub>2</sub>, in PBS

**PBS-MK 1M NaCl:** 2.5 mM KCl, 1 mM MgCl<sub>2</sub>, 1 M NaCl in PBS

**Poly-D-ornithine:** 50 mg of poly-D-ornithine was dissolved in 50 ml of sterile borate buffer to produce a 10 fold concentrated stock solution (1 mg/ml).

**Protease inhibitor cocktail (P1c):** Two protease inhibitor cocktail tablets dissolved in 800 µl H<sub>2</sub>O to produce a 25 fold concentrated working solution.

**Proteinase K buffer (10x):** 100 mM Tris-HCl pH 8.0, 100 mM EDTA, 10% SDS

**qPCR hot-start 2x mix:** hot-start Platinum<sup>®</sup> Taq DNA polymerase (60U/ml), SYBR<sup>®</sup> Green I fluorescent dye, 40 mM Tris-HCl pH 8.4, 100 mM KCl, 6 mM MgCl<sub>2</sub>, 400 µM dGTP, 400 µM dATP, 400 µM dCTP, 400 µM dUTP, uracil DNA glycosylase (40 U/ml, UDG), and stabilizers.

**SDS-Sample buffer (6x):** 350 mM Tris-HCl, pH 6.8; 10% SDS, 0.6 M DTT, 30% Glycerol, 0.03% BPB

**SOC<sup>++</sup> medium:** 2% bacto-tryptone, 0.5% yeast extract, 10 mM NaCl, 2.5 mM KCl, 10 mM MgCl<sub>2</sub>, 10 mM MgSO<sub>4</sub>, 20 mM glucose pH 7.0) Add Glucose after autoclaving the solution with the remaining ingredients.



**TE:** 10 mM Tris-HCl, 1mM EDTA, pH 8.0.

**TBE:** 42 mM Boric Acid, 10 mM EDTA, 50 mM Tris-HCl, pH 8.0 (autoclaved).

**TBS:** 150 mM NaCl, 10 mM Tris-HCl, pH 9.0 (for antigen retrieval).

**TBS-T:** 150 mM NaCl, 10 mM Tris-HCl, 0.1% Tween 20, pH 7.6.

**Transfer buffer:** 192 mM Glycine, 20% Methanol, 25 mM Tris-HCl, pH 8.3.

**Trypsin 0.25% for primary culture:** 25 mg Trypsin in 10 ml CMF, sterile filtered

**Tris/SDS pH 6.8 4x:** 0.5 M Tris-HCl, 0.4% SDS, 100 ml H<sub>2</sub>O, pH 6.8.

**Tris/SDS pH 8.8 4x:** 1.5 M Tris-HCl, 0.4% SDS, 100 ml H<sub>2</sub>O, pH 8.8.

### 2.1.9. Instruments

Table 2.1.4. List of instruments used in this study

<b>Instrument</b>	<b>Supplier</b>
ABI PRISM 310 Genetic Analyzer	Applied Biosystems, California, USA
ÄKTA fast protein liquid chromatography	Amersham Biosciences, Freiburg, Germany
Apotome <sup>TM</sup>	Zeiss, Göttingen, Germany
Autoclave	Systec, Greiz, Germany
Axioplan fluorescence microscope	Zeiss, Göttingen, Germany
Axiovert 25, light microscope	Zeiss, Göttingen, Germany
Axiovert fluorescence microscope	Zeiss, Göttingen, Germany
Binocular microscope	Zeiss, Göttingen, Germany
Biophotometer	Eppendorf, Hamburg, Germany
CCD camera AxioCam	Zeiss, Göttingen, Germany
Cell culture hood, HeraSafe HS18	Heraeus, Hanau, Germany
CO <sub>2</sub> chamber (for live microphotographs)	Zeiss, Göttingen, Germany
Cryostat	Leica, Nussloch, Germany
CTI-controller (for live microphotographs)	Zeiss, Göttingen, Germany
DNA electrophoresis chambers	BioRad, Munich, Germany
Electrophoresis power supply	BioRad, Munich, Germany
ELISA spectrophotometer, Tecan RainBow	Tecan, Crailsheim, Germany
Fluor-S <sup>TM</sup> MultiImager	Bio-Rad, Munich, Germany
Freezers (-80° C)	Heraeus, Hanau, Germany
Gene Pulser II	BioRad, Munich, Germany
Heat block, ThermoStat Plus	Eppendorf, Hamburg, Germany

Ice machine	Scotman® Frimont, Milan, Italy
Incubator, for bacterial culture	Heraeus, Hanau, Germany
Incubator, for cell culture	B. Braun, Melsungen, Germany
Instruments for dissection/surgery	Fine Science Tools, Heidelberg, Germany
Liquid scintillation and luminescence counter	Wallac, Freiburg, Germany)
Micro4 smart controller	World Precision Instruments, Florida, USA
Microwave oven	Bosch, Stuttgart, Germany
Mini-Sub Cell GT and Wide Mini-Sub Cell GT	BioRad, Munich, Germany
Nanoliter2000 injector	World Precision Instruments, Florida, USA
PCR machine	MJ Research Biozym, Hessisch Oldendorf, Germany
Peristaltic pump, IP4	Ismatec, Glattbrugg, Switzerland
pH-meter	Sartorius, Göttingen, Germany
Pipettes	Gilson, Villiers le Bel, France
Pipetboy, accu-jet pro	Brand, Wethiem, Germany
Refrigerators (4° C and -20° C)	Liebherr, Biberach, Germany
Scales	Sartorius, Göttingen, Germany
Sonicator	Bandelin, Berlin, Germany
Stereotaxic frame	David Kopf Instruments, California, USA
Surgery microscope	Zeiss, Göttingen, Germany
Table centrifuges	Eppendorf, Hamburg, Germany
Transluminator, gel documentation	Bio-Rad, Munich, Germany
Temperature-controller (for live imaging)	Zeiss, Göttingen, Germany
Ultracentrifuge Sorvall	DuPont Instruments, Bag Homburg, Germany
Vortex mixer	NeoLab, Heidelberg, Germany
Waterbath	GFL, Burgwedel, Germany
Water purifier, PureLab Plus	Elga Labwaters, Ransbach-Baumbach, Germany
Western blot Electrophoresis chambers	BioRad, Munich, Germany

## 2.2. Methods:

### 2.2.1. Cloning procedures

Primer design and all cloning steps were first virtually done using the SECentral (Scientific & Educational Software, NC, US). Necessary restriction sites for cloning of DNA fragments into respective plasmids were added to the DNA fragments by PCR using appropriated primers. The Kozak sequence (CCACCATG, (Kozak 1984;Kozak 1986;Kozak 1987)) was added in between the restriction endonuclease recognition sequence and the cDNA start codon of interest. All restriction nucleases used in this work were purchased from New England Biolabs. ShRNAs inserts were chemically synthesised as single stranded DNA and complementary annealed. All the DNA procedures were essentially performed according to

the described protocols in *Molecular Cloning: A Laboratory Manual* (Sambrook J. et al. 1989).

#### **2.2.1.1. PCR amplification**

The PCR amplification of the cDNA sequences of interest was preceded by small scale optimization PCR in order to determine the best working conditions. Thus, different concentrations (1.5 mM, 2 mM and 2.5 mM) of magnesium chloride (MgCl<sub>2</sub>) in the buffer and annealing temperatures (usually between 60°C and 72°C) were used for amplification. Those conditions that resulted in the best yield and specificity of PCR-product were chosen for further amplification or further optimization. The PCR reaction mix contained: the Phusion HF (High Fidelity) Reaction Buffer, 1.5-2.5 mM of MgCl<sub>2</sub>, 400 nM of sense and antisense primers, 200 μM of dATP, dCTP, dGTP, dTTP (BioLabs), 5-10 ng of the template DNA, 0.6 unit of the Phusion High-Fidelity DNA Polymerase (2 units/μl; BioLabs), and millipore H<sub>2</sub>O to achieve a final volume of 50 μl. Amplification started with 1 min incubation at 98°C followed by 25 cycles of amplification (annealing 15 sec between 60°C and 72°C, elongation for 20 sec/kb at 72°C and separation of DNA strands for 15 sec at 98°C). The amplified fragments were purified from contaminants using the PCR purification kit as described in the manufacturer's instruction manual with the exception that DNA was eluted in 30 μl H<sub>2</sub>O instead of the elution buffer provided in the kit.

#### **2.2.1.2. Sequencing of PCR amplified DNA**

The sequencing reactions were carried out using the ABI PRISM BigDye Terminator v3.1 cycle sequencing kit according to the manufacturer's protocol. The Terminator Ready Reaction Mix contained the four dNTPs with different fluorescence labels (BigDyeTerminators), unlabeled dNTPs, AmpliTaq DNA Polymerase FS, MgCl<sub>2</sub>, Tris-HCl buffer (pH 9.0). Template DNA (450 ng), 8 pmol of the sequencing primer, 3 μl of the Terminator Ready Reaction Mix and reaction buffer were used in a 20 μl sequencing reaction. The sequencing reaction mixes were subjected to 25 amplification cycles. Each cycle consisted of 30 sec at 95°C, 45 sec at 50°C and 1 min at 60°C. The amplified probes were then precipitated in the following way: 80μl of 75% isopropanol were added to 20 μl of amplified probe, mixed shortly and incubated at RT (between 15 min and 24 hours). The probes were then centrifuged for 20 min at maximum speed in a microcentrifuge at RT. The supernatant was carefully removed and 250 μl 75 % isopropanol were added to the

precipitate. The mix was further centrifuged at maximum speed in a microcentrifuge for 5 min at RT. The supernatant was removed and the precipitate dried for 1 min at 90°C in a heated block (Eppendorf). The precipitate was resuspended in 20 µl of template suppression reagent (Applied Biosystems) and subjected to DNA capillary electrophoresis on the ABI PRISM 310 Genetic Analyzer. Sequence analysis and alignment with reference cDNA were performed using ABI PRISM 3100 and SECentral software.

#### **2.2.1.3. DNA precipitation**

Ethanol precipitation is used routinely to concentrate and purify DNA. One tenth volume of 3 M Sodium Acetate (pH = 5.0-5.3) was added to the DNA solution to neutralize the charge on the sugar-phosphate backbone of the DNA. After mixing, two volumes of cold 100 % ethanol (-20° C) were added to the mix, the mix was briefly swirled incubated at -20° C for 5 to 10 min and then centrifuged for 30 min at highest speed in a 4°C microcentrifuge. The supernatant was removed and 2 volumes of cold 70 % ethanol were added to the precipitate. The mix was centrifuged again for 20 minutes in a 4°C centrifuge. The supernatant was carefully removed and the precipitate dried at room temperature for 5 min. The DNA pellet was resuspended in the desired volume of TE buffer or 10 mM Tris pH 8.5.

#### **2.2.1.4. DNA restriction**

Restriction enzymes and DNA were mixed in the appropriate buffers and incubated for 80 min at the temperature specified for each enzyme according to the manufacturer's instruction manual. The amounts of plasmid DNA and enzyme units were matched in order to achieve optimal digestion, 5-10 µg of plasmid DNA and 0.5-3 µg of PCR product were used. In brief, the restriction digests were done in a total volume of 50 µl with 5 µl of appropriate 10x buffer, Y µg of plasmid DNA (5-10 µg) and Y units of endonuclease (1.5x the µg of DNA) for approximately 80 min in a water bath at optimal temperature. When the activity of two enzymes was maximal in the same buffer and temperature, double digest was performed, when it was not the case, the restriction digest were performed in sequence with DNA purification step in between (PCR Purification Kit).

#### **2.2.1.5. Agarose gel electrophoresis**

Agarose gel electrophoresis was performed to analyse the DNA qualitatively (size and purity) or quantitatively (amount). Depending on the DNA fragment size to be analysed, gels with

different agarose percentage were prepared, e.g. for ~300 bp 2% agarose, for ~700 bp 1.5% agarose, for >1000 bp 1% agarose. Agarose was dissolved in TBE buffer in a microwave oven and 1µl of ethidium bromide per 50 ml solution was then added. The agarose was polymerized in the electrophoresis tray at RT. DNA samples were mixed with DNA loading buffer and TE to reach the desired final loading volume for the gel. The gel was run in 1x TBE buffer, usually at 70 V or overnight at low voltage. DNA bands were visualized by UV-light in Gel Documentation 2000 UV-transilluminator using the Quantity One software (BioRad).

#### **2.2.1.6. Gel extraction and determination of DNA concentration**

DNA extraction after gel electrophoresis was performed with QIAquick Gel Extraction Kit protocol as described in the manufacturer's instruction manual with the exception that DNA was eluted in 30 µl of TE buffer instead of the elution buffer provided in the kit. For low yield or low concentrations of DNA (e.g. after restriction digest, gel extraction, PCR amplification) the concentration was estimated by gel electrophoresis. Using a marker with known concentration ( $\lambda$  Hind III digest) as reference, bands of identical density and size were compared. With high DNA concentrations and quantity (e.g. after plasmid mini- maxi- or mega-preps) the DNA concentration in the final solution was measured by optical density with the Biophotometer at a wavelength of 260 nm. Additionally, the ratio OD260nm /OD280nm was also recorded as an indicator of protein contamination in the sample.

#### **2.2.1.7. DNA dephosphorylation**

Dephosphorylation consists in the removal of the 5' phosphate present in the DNA cohesive or blunt ends. This avoids unimolecular ligation in case the vector DNA monomolecular ligation is possible (e.g. same compatible sticky ends or blunt ends). Approximately 200 ng of DNA vector to be dephosphorylated were incubated in dephosphorylation buffer with 1.5 units of shrimp Alkaline Phosphatase during 25 min at 37°C. The enzyme was then inactivated for 15 min at 65°C.

#### **2.2.1.8. Remove or fill in DNA overhangs to create blunt ends**

When compatible sticky ends are difficult to achieve or a restriction site has to be deleted, the DNA Polymerase I, Large (Klenow) fragment can be used to fill in 5' overhangs or remove 3' overhangs to form blunt ends. After the restriction digest to create the overhangs, the

restriction enzyme was heat inactivated accordingly with the manufacturer instructions and incubated with 0.9  $\mu$ l of 2 mM dNTPs (2 mM each dATP, dCTP, dGTP, dTTP, final concentration 33  $\mu$ M) and 1.3  $\mu$ l of Large (Klenow) fragment (5 units/ $\mu$ l, total of 6.5 units) for 15 min at 25° C (the indicated volumes refer to a final volume of 50  $\mu$ l in Klenow buffer). After Klenow reaction, the obtained DNA was purified by ethanol precipitation.

#### **2.2.1.9. DNA ligation and E. coli electro-transformation**

Before ligation the concentration of the vector DNA and DNA fragment (insert) was estimated by gel electrophoresis. BB DNA and insert were mixed in a molar ratio of 1:3 (total of ~200 ng of BB and insert) in the presence of ligation buffer, sterile water and T4 DNA ligase (2 000 units) in a total volume of 20  $\mu$ l. The ligation reaction was performed for 20 min for compatible sticky ends and during 1 h for blunt ends at room temperature. Four  $\mu$ l of DNA ligation product (~40 ng DNA) was added to 70  $\mu$ l of de-frozen and kept on ice electrocompetent E.coli cells. For all plasmids were used DH5 $\alpha$  E.coli cells (ElectroMAX™DH5 $\alpha$ -E™Cells), with the exception of all pAAV vectors were SURE E. coli cells (SURE®Electroporation-Competent Cells, “Stop Unwanted Rearrangement Events”) were used. The mixture was transferred to a pre-cooled on ice electroporation cuvette and subjected to the electroporation pulse procedure at Bio-Rad Gene Pulser II (Voltage = 1.8 kV, pulse controller- low resistance = 200 Ohm, capacitance = 25  $\mu$ F). Immediately after the pulse 700  $\mu$ l of warm SOC<sup>++</sup> medium was added and the cells transferred to a sterile culture tube. The transformed cells were incubated for approximately 60 min with moderate shaking at 37°C to allow the bacteria to recover and express the antibiotic resistance protein encoded by the plasmid. Bacteria was plated on LB agar plates containing the corresponding antibiotic (e.g. ampicillin 100 $\mu$ g/ml) for selection of clones.

#### **2.2.1.10. Production of electrocompetent E. coli cells**

One litter of pre-warmed LB medium was inoculated with 10 ml of a fresh overnight culture of E. coli (DH5 $\alpha$  or SURE electrocompetent strains). The cultures were grown at 37 °C with shaking to reach an optic density at 600 nm of 0.8 to 1.0 and chilled on ice water bath for 2 h with slow mixture every 2 min during 15 min. Cells were transferred to a pre-chilled centrifuge bottles and harvested by centrifugation (10 minutes, 5,000 g, 4°C). Pellets were resuspended in the original culture volume of ice-cold water. After a second centrifugation step (15 minutes, 5,000 g, 4°C) the pellets were resuspended in a 10 ml of ice-cold water and

washed with an original culture half-volume of ice-cold water. The cells were centrifuged again (15 minutes, 5,000 g, 4°C). Bacterial pellets now were re-suspended in 2 fold the pellet volume of ice-cold 10% Glycerol in water and transferred to 30 ml centrifugation tubes (Beckmann). Following the last centrifugation (15 minutes, 5,000 x g, 4°C), the pellets were now re-suspended in 2 fold the pellet volume of ice-cold 10% Glycerol in water, aliquoted (70 µl/tube) and quickly frozen in dry ice-ethanol bath and stored at -80 °C. The cells were kept ice-cold during the entire procedure. Cell efficiency was checked with control transformation with 10 pg of pUC control plasmid (Stratagene).

#### **2.2.1.11. Plasmid Mini, Maxi and Mega Preps**

Mini- maxi- and mega-preps allow DNA plasmid extraction on a smaller, medium or large-scale. The extractions were performed using the QIAprep Spin Miniprep Kit, QIAGEN Plasmid Maxi Kit, NucleoBond® PC 2000 (Macherey-Nagel), mini- maxi- and mega-preps respectively, according to the manufacturer's instructions. Mentioned buffers refers to the Mega Prep kit (NucleoBond® PC 2000), but the principle is the same for all kits with minor buffer differences. In brief, the procedure consists of alkaline lysis of the bacterial cell wall (solution constituted of 1% SDS, 10 mM EDTA, 200 mM NaOH) and RNA degradation with RNase A (100 µg/ml). The next step removal of cell debris while keeping the supernatant containing the nucleic acids (addition of 2.8 M KAc, pH 5.1 to neutralise NaOH and precipitate the SDS, proteins and genomic DNA associated to proteins). The plasmid DNA is bound to a anion-exchange resin column (under appropriate low-salt and pH conditions), washed with high-salt solution to remove the chromosomal DNA and proteins (100 mM Tris-HCl, 15% ethanol, 1.15 M KCl pH 6.3) and eluted in low-salt solution with pH 8.5 (100 mM Tris-HCl, 15% ethanol, 1 M KCl pH 8.5). Plasmid DNA is then concentrated and desalted by isopropanol precipitation, followed by ethanol precipitation.

#### **2.2.1.12. Cloning into pGL3 for luciferase based test system**

Incomplete cDNA of the glutamate cysteine ligase (GCLc) (shortGCLc, 737 bp fragment , base pair 255-991 from accession number NM\_012815) and glutathione reductase (GSR) (shortGSR, 594 bp fragment, base pair 286 to 880 from accession number NM\_053906) were inserted into the pGL3-SV40-fluc-short-RhoA-test1 vector described elsewhere (Malik et al. 2006). The shortGCLc was PCR amplified with 5'-Spe1-Apa1-PspOM1-shortGCLc and 3'-EcoR1-Age1-shortGCLc primers from pExpress-1-GCLc template. The short-GSR was PCR

amplified with 5'-SpeI-shortGSR and 3'-EcoRI-shortGSR primers from pExpress-1-GSR. The vector pExpress-1-GCLc and pExpress-1-GSR were sequence verified before serving as template for PCR amplification with the primers T7, SP6, GCLc-forward1, GCLc-reverse2, GCLc-forward3, GCLc-reverse4 for pExpress-1-GCLc and the primers T7, SP6, GSR-forward, GSR-reverse for pExpress-1-GSR.

The pGL3-SV40-fluc-short-RhoA-test1 vector (Fig.2.2.1.A) was digested with SpeI and EcoRI to remove short-RhoA. ShortGCLc and shortGSR were cut with SpeI and EcoRI to allow the insertion of the PCR products into the vector backbone. The resultant pGL3-SV40-fluc-shortGSR-test1 (Fig. 2.2.1.B) and pGL3-SV40-fluc-shortGCLc-test1 (Fig. 2.2.1.C) were subjected to sequencing procedure to verify the absence of any mutations generated through PCR amplification. The primers used were fluc-forward (binds 3' of firefly luciferase cDNA, complementary strand) and SVpA-reverse (binds 5' of simian virus 40 polyadenylation region, sense strand).

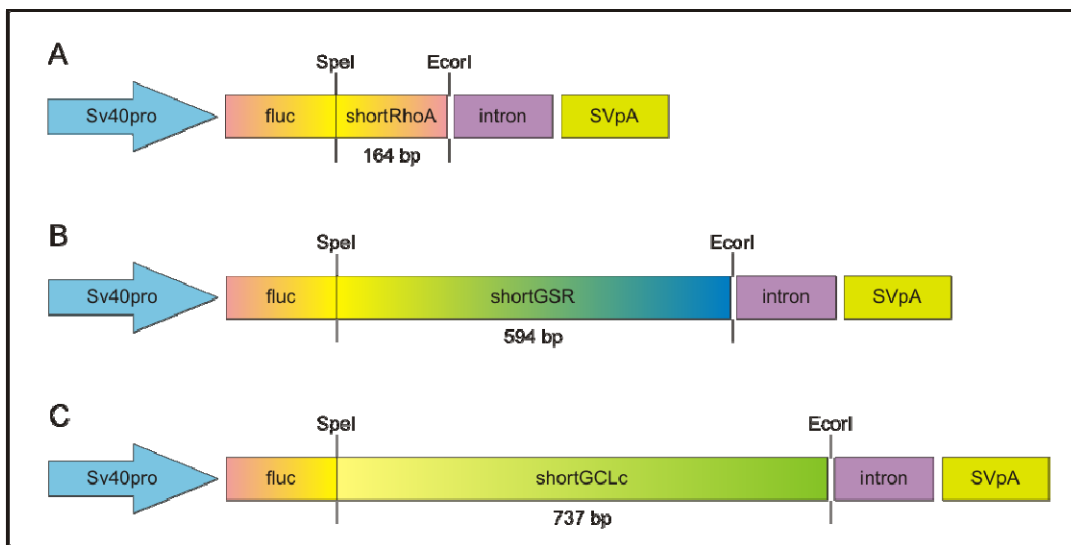


Fig. 2.2.1. Schematic description of A: pGL3-SV40-fluc-short-RhoA-test1 (shortRhoA flanked by SpeI/EcoRI sites); B: pGL3-SV40-fluc-shortGSR-test1 (shortGSR flanked by SpeI/EcoRI sites) and C: pGL3-SV40-fluc-shortGCLc-test1 (shortGCLc flanked by SpeI/EcoRI sites) plasmid genomes. These vectors contain the simian virus40 promoter (Sv40pro), a reporter protein luciferase firefly (fluc) fused with the target sequence that was either the short RhoA (164 bp fragment), the shortGCLc (737 bp fragment) or the shortGSR (594 bp fragment), the chimeric intron (intron from the pCI-Neo vector, Promega) and the polyadenylation site from simian virus-40 (SVpA). The short target sequences are drawn accordingly with their size.

### 2.2.1.13. Cloning of shRNAs into pSuper vector

Construction of pSuper-hSyn1-DsRed2N1-CytbAS (Accession No. AY640628) vector has been described previously (Michel et al. 2005). The shRNA-containing pSuper vectors were



constructed as described (Brummelkamp et al. 2002c). In brief, 200 pmol of the sense and antisense oligonucleotides (section 2.1.6.) containing the shRNA sequence were dissolved in 25 µl water plus 25 µl of 2x annealing buffer. The solution was boiled for 5 min in 1000 ml water and then cooled to room temperature. Annealed oligonucleotides (200 fmol) were ligated to 22.5 fmol BglII/HindIII digested pSuper-hSyn1-DsRed2N1-CytbAS derived vector to produce pSuper-hSyn1-DsRed2N1-X-shRNA (X indicates all shRNA's, Table 2.1.3.). For schematic plasmids map see Figure 2.2.2. At this stage, in positive clones the shRNA sequence was checked for correctness using the primer H1 promoter forward.

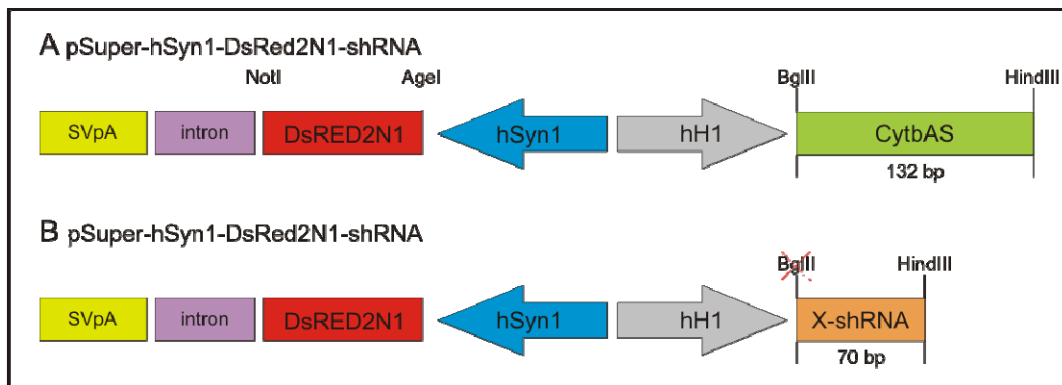


Fig. 2.2.2. Schematic description of pSuper-hSyn1-DsRed2N1-CytbAS (A, CytbAS fragment flanked by BglII/HindIII) and pSuper-hSyn1-DsRed2N1-X-shRNA (B, X-shRNA with HindIII side and BglII destroyed site with the shRNA insertion). These vectors contain the human polymerase III H1 RNA promoter (hH1) followed by the human cytochrome b antisense sequence (CytbAS) or the shRNAs sequence (X-shRNA). The CytbAS and shRNAs sequence contains 5 consecutive thymidine residues as stop signal for hH1 promoter directed transcription. The vector also contains the human synapsin 1 gene promoter (hSyn1), a reporter protein red fluorescent protein (DsRED2N1, *Discosoma sp.*, Clontech), the chimeric intron (intron from the pCI-Neo vector, Promega) and the polyadenylation site from simian virus-40 (SVpA). The CytbAS and X-shRNA sequences are drawn accordingly with their size.

#### 2.2.1.14. Transfer of hH1 promoter plus the shRNAs into pAAV vectors

The adeno-associated virus (AAV) vectors pAAV-6P-SEWB was provided by Dr. Kügler and has been described previously (Kügler et al. 2003), this vector expresses EGFP driven by the human synapsin 1 gene promoter (hSyn1). In order to insert the shRNA cassette into pAAV-6P-SEWB, one HindIII restriction site present between EGFP and WPRE in pAAV-6P-SEWB was deleted. For this purpose, Hind III restriction endonuclease was used and the plasmid ends were filled-in using the Klenow polymerase creating blunt ends (see 2.2.1.8.). Thus, after re-ligation we obtained a subcloning vector lacking the HindIII restriction site (pAAV-6P-SEWB-no-HindIII, Fig. 2.2.3. A).

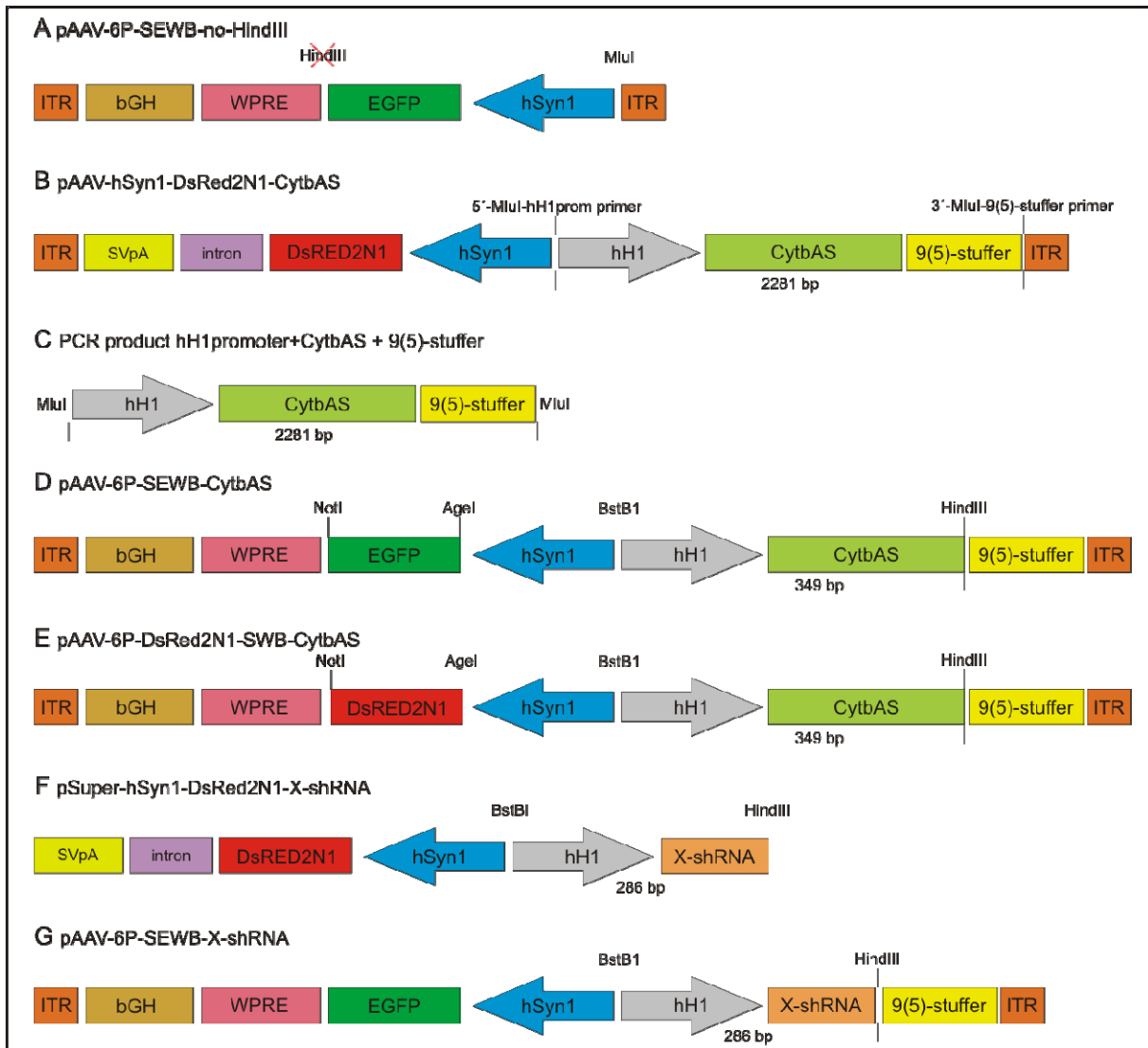


Fig. 2.2.3. Schematic description of pAAV-6P-SEWB-no-HindIII (A), pAAV-hSyn1-DsRed2N1-CytbAS (B), PCR product hH1promoter + CytbAS + 9(5)-stuffer (C), pAAV-6P-SEWB-CytbAS (D), pAAV-6P-DsRed2N1-SWB-CytbAS (E), pSuper-hSyn1-DsRed2N1-X-shRNA (F) and pAAV-6P-SEWB-X-shRNA (G). All important restriction sites and the size of the obtained fragments are indicated. bGH- bovine growth hormone derived polyadenylation site; CytbAS- human cytochrome b antisense sequence; DsRED2N1- red fluorescent protein (reporter protein); EGFP- enhanced green fluorescent protein; hH1- human polymerase III H1 promoter; hSyn1- human synapsin 1 gene promoter; intron- chimeric intron from the pCI-Neo vector (Promega); ITR-inverted terminal repeat; SVpA- polyadenylation site from simian virus-40; WPRE- woodchuck hepatitis virus posttranscriptional regulatory element; X-shRNA- shRNA's sequence; 9(5)-stuffer- untranscribed 2281 bp fragment of the porcine gene UM 9(5)p.

The 9(5)-stuffer plus the hH1 promoter and the CytbAS were PCR amplified with the primers 5'-MluI-hH1promoter and 3'-MluI-9(5)-stuffer from pAAV-hSyn1-DsRed2N1-CytbAS vector previously described (Michel et al. 2005) (Fig. 2.2.3.B). Part of 9(5)-stuffer was used (1972 bp) of the total 2281 bp untranscribed fragment of the porcine gene UM 9(5)p (Accession No. AY072606) necessary in the pAAV-hSyn1-DsRed2N1-CytbAS, pAAV-6P-

SEWB-CytbAS and pAAV-6P-DsRed2N1-SWB-CytbAS to obtain the optimal packaging size of the AAV-2 vectors (Dong et al. 1996).

PCR product digested with MluI (Fig. 2.2.3. C) was ligated into pAAV-6P-SEWB-no-HindIII (Fig. 2.2.3.A) digested with MluI restriction endonuclease and dephosphorylated. Two possible products were obtained, and the hSyn1 promoter head to head with the H1 promoter was selected (pAAV-6P-SEWB-CytbAS, Fig. 2.2.3.D).

One plasmid with DsRED2N1 reporter gene was also produced, for that the EGFP cDNA contained in the pAAV-6P-SEWB-CytbAS was replaced by DsRed2N1 cDNA from pSuper-hSyn1-DsRed2N1-CytbAS (Fig. 2.2.3.F). DsRed2N1 cDNA was excised by AgeI and NotI restriction endonuclease and the EGFP cDNA removed from pAAV-6P-SEWB-CytbAS using the same endonuclease. The vector BB was ligated to the DsRed2N1 cDNA insert to produce pAAV-6P-DsRed2N1-SWB-CytbAS (Fig. 2.2.3.E.).

Each shRNA was transferred from the pSuper-hSyn1-DsRed2N1-X-shRNA (Fig. 2.2.3.F) or the pSuper-neo/GFP vector (OligoEngine, Seattle, WA) for fluc-shRNA#2 (Diaz-Hernandez et al. 2005). All pSuper vectors were digested with BstBI and Hind III endonuclease producing a 286 base pair fragment (containing the hH1 RNA promoter and the shRNA sequence). This fragment was ligated with the vector BB resultant from the pAAV-6P-SEWB-CytbAS digestion with BstBI and Hind III or pAAV-6P-DsRed2N1-SWB-CytbAS for the ligation of EGFP-shRNA. Final vectors were pAAV-6P-SEWB-X-shRNA (Fig. 2.2.3.G) and pAAV-6P-DsRed2N1-SWB-X-shRNA. The final constructs were sequence verified using the hH1-promoter forward and 9(5)-stuffer reverse primers.

AAV vectors are characterized by inherent high recombination probability due to the presence of ITRs. The recombination possibility was increased with the insertion of the shRNAs, sequences with high probability of forming DNA secondary and tertiary structures. Therefore all AAV plasmids were propagated in the *E. coli* strain SURE<sup>®</sup> Electroporation-Competent Cells (“Stop Unwanted Rearrangement Events”, Stratagene), and the integrity of AAV vector genome ITR region was confirmed with a SmaI digest before proceeding to AAV vector production.

### **2.2.1.15. Cloning of GCLc into AAV plasmids for protein expression**

Rattus norvegicus glutamate cysteine ligase cDNA (GCL) was PCR amplified from the pExpress-1-GCLc vector (RZPD, clone IRAKp961B11182Q2) with the primers 5'-Age1-GCLc and 3'-Not1-GCLc. The pAAV-6P-SEWB vector and the GCLc PCR product were cut with Age1 and Not1 endonuclease. The purified products were ligated to produce pAAV-6P-GCLc-SWB (Fig. 2.2.4.C).

### **2.2.1.16. GCLc silent mutants in pAAV**

In order to perform rescue experiments, the sequence targeted by GCLc-shRNA#2 and GCLc-shRNA#3 were individually changed. The nucleotide sequence was changed without altering the aminoacid sequence (Fig.3.1.5 section 3.1.1.2.2.). The silent mutants were produced by two PCR amplification reactions ligated into the pAAV-6P-SEWB backbone digested with Age1 and Not1 endonuclease (EGFP was removed). The template for the mutagenesis PCR amplification was pExpress-1-GCLc. PCR1 (Fig. 2.2.4. D, E) was performed with primer 5'-Age1-GCLc and primer 3'-blunt-GCLc-shRNA#2-bp-exch#2. This PCR1 produced the GCLc cDNA from the 5' start codon until the GCLc shRNA#2 binding place (the 5' primer introduced an Age1 restriction site and the 3' primer a blunt end, the 3' primer was 5' phosphorylated). The PCR2 (Fig. 2.2.4. D, F) using the primer 5'-blunt-GCLc-shRNA#2-bp-exch#2 (5' phosphorylated) and the 3'-Not1-GCLc primer produced a 5' blunt end and a 3' end with Not1 restriction site. The GCLc cDNA sequence in PCR1 ends exactly where the sequence of GCLc cDNA from PCR2 starts. Both PCRs and the backbone were ligated in a 3 molecular ligation reaction producing pAAV-6P-GCLc-bp-exch#2-SWB (Fig. 2.2.4. G). Proper sequence was verified by sequencing reactions covering the complete GCLc cDNA. This strategy was also applied to produce silent mutations in the GCLc gene in the base pairs where the GCLc-shRNA#3 binds. In PCR1 the used primers were 5'-Age1-GCLc and 3'-blunt-GCLc-shRNA#3-bp-exch#3 (5' phosphorylated), and in PCR2 were 5'-blunt-GCLc-shRNA#3-bp-exch#3 (5' phosphorylated) and 3'-Not1-GCLc. The produced rescue construct was named pAAV-6P-GCLc-bp-exch#3-SWB.

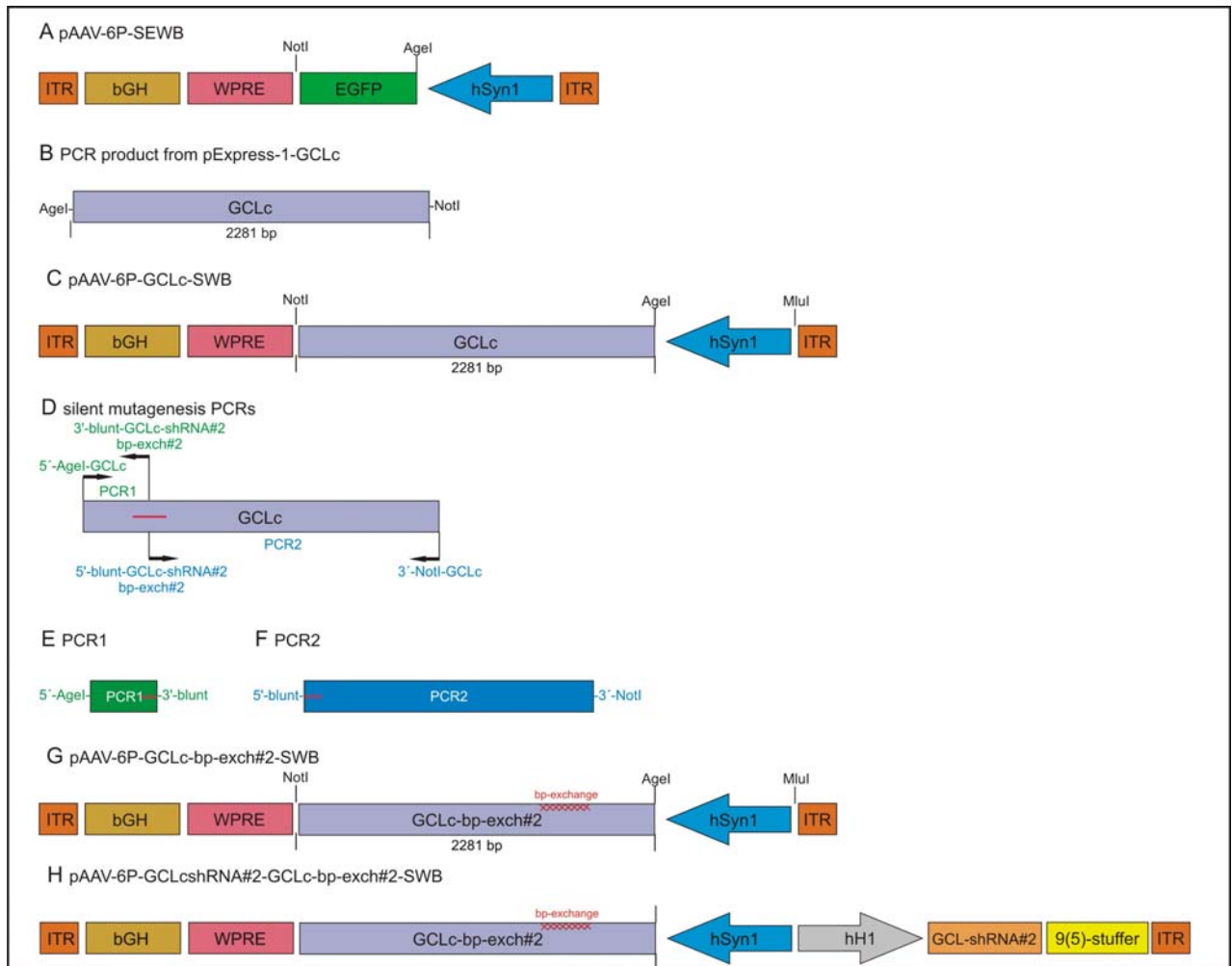


Fig. 2.2.4. Schematic description of pAAV-6P-SEWB (A), the GCLc PCR product from pExpress-1-GCLc (B), pAAV-6P-GCLc-SWB (C), the silent mutagenesis PCRs strategy with indication of the primers for GCLc-bp-exch#2 construction (D), PCR1 for silent mutagenesis (E), PCR2 for silent mutagenesis (F), pAAV-6P-GCLc-bp-exch#2-SWB (G), and pAAV-6P-GCLc-shRNA#2-GCLc-bp-exch#2-SWB (H). All important restriction sites and the size of the obtained fragments are indicated. bGH- bovine growth hormone derived polyadenylation site; EGFP- enhanced green fluorescent protein; GCLc- rat catalytic subunit of glutamate cysteine ligase; GCLc-bp-exch#2- rat catalytic subunit of glutamate cysteine ligase resistant to GCLc-shRNA#2; GCLc-shRNA#2- shRNA#2 targeting the rat catalytic subunit of glutamate glutamate cysteine ligase; hH1- human polymerase III H1 promoter; hSyn1- human synapsin 1 gene promoter; ITR-inverted terminal repeat; WPRE- woodchuck hepatitis virus posttranscriptional regulatory element; 9(5)-stuffer- untranscribed 2281 bp fragment of the porcine gene UM 9(5)p.

### 2.2.1.17. GCLc non-targetable constructs

In order to ensure that each cell expressing the GCLc shRNA#2 would express as well the correspondent rescue mutant mRNA (GCLc-bp-exch #2) or hDJ1, both expression constructs were combined into a single vector (Fig. 2.2.4. H). For this, the 9(5)-stuffer plus the hH1-promoter and the GCLc-shRNA#2 were excised from pAAV-6P-SEWB-GCLc-shRNA#2 with MluI, then this insert was introduced in pAAV-6P-GCLc-bp-exch#2-SWB (Fig. 2.2.4.

G) and pAAV-6P-hDJ1-SWB both linearized with MluI and dephosphorylated producing the pAAV-6P-GCLc-shRNA#2-GCLc-bp-exch#2-SWB and pAAV-6P-GCLc-shRNA#2-hDJ1-SWB respectively.

#### **2.2.1.18. DJ1 cDNA in pAAV**

The vector encoding human wild type DJ1 (hDJ1) was a generous gift from Dr. Sebastian Deeg (pCI-neo-vector-flag-DJ1). Both pAAV-6P-SEWB vector and pCI-neo-vector-flag-DJ1 were cut with NheI and NotI endonuclease. The purified products were then ligated to produce pAAV-6P-hDJ1-SWB.

#### **2.2.1.19. $\alpha$ -synuclein A53T cDNA in pAAV**

$\alpha$ -synuclein A53T cDNA expression vector was provided by Dr. Zinayida Shevtsova (pBS-hSyn1-koz-AU1- $\alpha$ -synucleinA53T-Int-SVpA). pBS-hSyn1-koz-AU1- $\alpha$ -synucleinA53T-Int-SVpA and pAAV-6P-SEWB were restriction digested with NheI and NotI producing AU1- $\alpha$ -synucleinA53T insert and pAAV-6P-SWB back bone respectively. The ligation the back bone with the AU1- $\alpha$ -synucleinA53T insert produced the pAAV-6P-AU1- $\alpha$ -synucleinA53T-SWB vector. This vector was further used to insert the 9(5)-stuffer plus the H1-promoter and the GCLc-shRNA#2 or the EGFP-shRNA with the MluI digestion strategy reported above. Using this method, the pAAV-6P-GCLc-shRNA#2-AU1- $\alpha$ -synucleinA53T-SWB and pAAV-6P-EGFP-shRNA-AU1- $\alpha$ -synucleinA53T-SWB were constructed.

#### **2.2.1.20. Cloning of GCLm cDNA into AAV plasmids for protein expression**

GCLm subunit cDNA from *Rattus norvegicus* or *Homo sapiens* were PCR amplified from pExpress-1-GCLm (RZPD clone IRBPp993C098D), using primers 5'-AgeI-GCLm and 3'-NotI-GCLm-*Rattus-norvegicus*, or pBluescriptR-GCLm (RZPD clone IRATp970A0262D), using primer 5'-AgeI-GCLm and 3'-NotI-GCLm-*Homo-sapiens*, respectively. The derived PCR products were cut with AgeI and NotI restriction endonuclease and ligated into pAAV-6P-SEWB cut with the same enzymes. The products pAAV-6P-GCLm-rat-SWB and pAAV-6P-GCLm-hum-SWB were sequence verified.

## 2.2.2. Viral vectors production and purification

### 2.2.2.1. AAV packaging

AAV are small dependovirus which are replication deficient, they need the presence of adenovirus, herpesvirus or vaccinia virus to replicate. In order to exclude any other virus contamination, viral vectors were propagated in AAV-293 cells using the pDG2 helper, a plasmid encoding the proteins necessary for AAV replication (e.g. capsid and replication proteins) (Grimm et al. 1998). The AAV-293 cells produce adenovirus E1 in trans, allowing the production of infectious virus particles only when cells are co-transfected with the two AAV production plasmids (an ITR-containing plasmid, and pDG2). Viral particles were purified according to established protocols (Zolotukhin et al. 1999) by iodixanol step gradient centrifugation. In brief, AAV-293 (HEK-293) cells were grown in 10% FCS 1% PS DMEM in 4 layers cell factories (CF, Nunc), when reaching approximately 50% confluence cells were washed with 400 ml PBS, trypsinized (50 ml PBS + 50 ml trypsin/EDTA - PAA) for 5 min at 37°C incubator. Trypsin was inactivated by addition of 100 ml of 10% FCS 1% PS DMEM to the CF and cells were then centrifuged for 5 min at 800 rpm. The CF was washed with 200 ml of DMEM to remove remnant cells. Usually 2 CF were seeded for each virus plus 1 CF for further cell amplification with  $5.5 \times 10^7$  cells per factory in 500 ml of 10% FCS DMEM 1% PS. When the cells reached 50-60% confluence (ca. 48 h), they were subjected to calcium-phosphate transfection. Cells were first washed with ca. 400 ml of DMEM without supplements. The transfection mix contained 265 µg of AAV-plasmid, 1 mg of helper plasmid (pDG for AAV-2), 1650 µl 2.5 M CaCl<sub>2</sub> in 16.5 ml of deionised sterile water. Afterwards 16.5 ml of 2 x HBS (pH 7.05) were added to 16.5 ml of transfection mix and incubated for exactly 1 min at 25°C. The transfection mix was added to 315 ml of 2% FCS DMEM (without antibiotics) and the obtained transfection medium was equally distributed through the four layers of the cell factory. For the transfection the cell factories were incubated between 10 and 16 h at 37°C, 5% CO<sub>2</sub>, 95% humidity. The medium was changed to 10% FCS 1% PS DMEM (ca. 750 ml/ cell factory). At ca. 36-40 h after transfection the cells were checked for reporter fluorescence at the microscope. Cells were harvested ca. 50 h after transfection, after removing the medium from the cell factory, the cells were briefly washed 300 ml with citric saline (CS). For cell detachment 200 ml of CS were added and the cells incubated at 37°C for 5-8 min, the CF was tapped and cells were collected to a sterile bottle. Collected cells were centrifuged for 5 to 10 min at 1,300 rpm at RT. The cell pellets were resuspended in total

volume of 20 ml of Tris-buffered saline (150 mM NaCl, 50 mM Tris, pH 8.5) and stored at -80°C until further processing.

#### **2.2.2.2. AAV gradient centrifugation**

Before virus gradient centrifugation, the virus-containing cells were thawed and frozen 3 times in an ethanol/dry ice bath. 1.6 µl of Bezonase (12,5 U/ml) was added to the cells and incubated for 30 min at 37°C water bath. The cell mix was slightly shaken every 5 to 10 min during incubation. Following incubation, the cell mix was centrifuged at 4,000 rpm at 18°C for 30 min. The supernatants were carefully transferred to new 50 ml falcon tube and adjusted to a 30 ml volume by addition of Tris-buffered saline.

Using a pump catheter connected to a spinal needle (20G x 2<sup>3/4</sup>) the iodixanol (Opti Prep™) step gradient was performed. The following stock solutions were prepared (E solution freshly prepared):

**B** - 10 x PBS-MK (80g NaCl, 2 g KCl, 14.4 g Na<sub>2</sub>HPO<sub>4</sub>, 2.4 g KH<sub>2</sub>PO<sub>4</sub> dissolved in 990 ml millipore sterile water, pH 7.4; plus 5 ml 2.5 M KCl and 5 ml 1 M MgCl<sub>2</sub>, solution was sterile filtered).

**C** - 1x PBS-MK (500 µl 2.5 M KCl, 500 µl 1M MgCl<sub>2</sub> in 499 ml PBS)

**D** - 2 M NaCl in 1x PBS-MK

**E** - 54 % working solution: (45 ml iodixanol and 5 ml B).

For obtaining different iodixanol gradient solutions the solutions C, D, E, iodixanol and phenol red were intermixed as follow (volumes for 4 step gradient tubes):

15% gradient: 15.0 ml E, 27.0 D, 12.0 ml C

25% gradient: 12.2 ml E, 14.5 ml C, 150 µl phenol red (0.05 % in water)

40% gradient: 20.0 ml E, 7.0 ml C

60% gradient: 25.0 ml iodixanol, 150 µl phenol red (0.05 % in water)

15 ml of diluted supernatant containing the virus particles was transferred to each "Quick Seal Tubes" (Beckmann; 1x 3.5 inch [25x 89 mm]), by using a 20 ml a syringe connected to the spinal needle (20G x 2<sup>3/4</sup>).



Using the pump, the iodixanol gradient solutions were added consecutively (10 ml of the 15% gradient, 6 ml of the 25% gradient, 4 ml of the 40% gradient, and 6 ml or more of the 60% gradient to fill up the tube) into the Beckmann tubes underneath the virus solution. Every next gradient solution was placed underneath the previous one. The tubes were heat-sealed and the gradients were run at the ultracentrifuge (SORVALL® Discovery 90SE). The settings for ultracentrifugation were: speed 68,000 rpm (310,000 g), 1 h 15 min, 18 °C, acceleration “5”, deceleration “0”. After centrifugation the phase containing the pure and concentrated virus solution was removed by inserting the needle connected to a 5 ml syringe slightly underneath the border between 40% and 60% iodixanol gradient and aspirating the 40% gradient solution containing the virus vectors (3-4 ml/tube). Other similar needle was introduced on the top of the tube which allows pressure equilibrium inside the tube. The virus-containing gradient solution was collected in a 50 ml falcon tube can be stored frozen at -20°C or be used directly in the Fast Protein Liquid Chromatography.

### **2.2.2.3. AAV- Fast Protein Liquid Chromatography**

The virus was loaded into a Äkta-FPLC system (Amershan Biosciences) and injected into a HiTrap™ Heparin HP 1 ml column (GE Healthcare) in low salt solution (PBS-MK). The bound AAV was washed in PBS-MK solution until OD at 280 nm was below 0.002 au (arbitrary units) and eluted in high salt solution (40% of PBS-MK 1M NaCl) (Fig. 2.2.5.). The AAV particles were further desalted by dialysis using Slide-A-Lyzer (MWCO = 10,000; PIERCE) in 1 l PBS overnight, with 1 further hour of dialysis in 1 l of fresh PBS for at 4°C. The final virus solution was subjected to real-time PCR (RT-qPCR) quantification of the rAAV-vector genome titre.

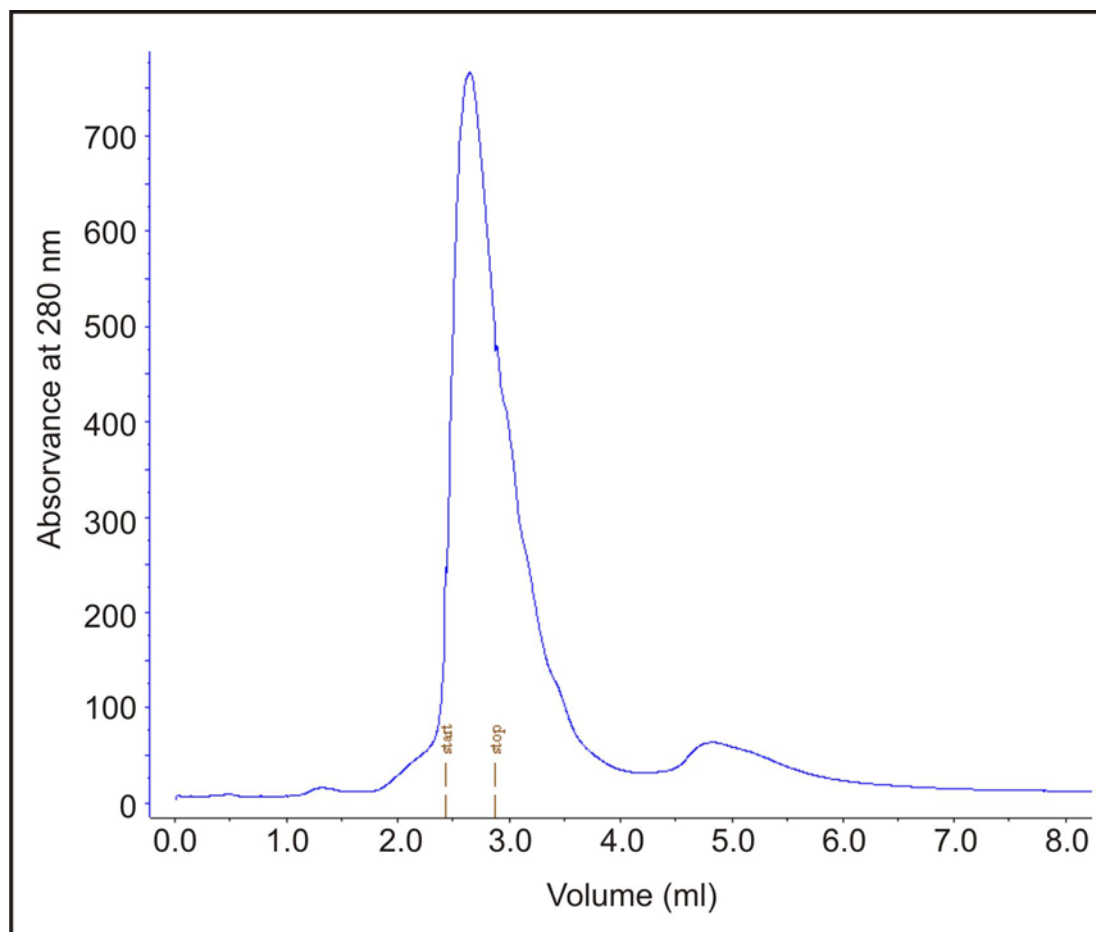


Fig. 2.2.5. Adeno-Associated virus serotype 2 elution peak from Äkta-FPLC system (Amershan Biosciences) loaded into a HiTrap™ Heparin HP 1 ml column (GE Healthcare) in low salt solution (PBS-MK). The bound AAV was washed in PBS-MK solution until no residual protein was recorded at 280 nm and eluted in high salt solution. The Y axis show the absorbance at 280 nm (protein) and the X axis the elution volume.

#### 2.2.2.4. Virus DNA preparation for qPCR:

In brief, 5  $\mu$ l of virus or water (negative control) were subjected to DNase I digestion (NEB) in duplicate in the following solution: 435  $\mu$ l water, 5  $\mu$ l DNase I (units), 50  $\mu$ l 10x DNase I buffer for 1 hour at 37°C water bath. The samples were centrifuged for 1 min at maximum speed and 55  $\mu$ l 10 x Proteinase K buffer was added. The samples were strongly mixed, 5  $\mu$ l Proteinase K (20 mg/ml) was added and samples digested at 37° C for 1 h in water bath. The solutions were then centrifuged at maximum speed for 1 min and phenol/chloroform extracted.

#### 2.2.2.5. Phenol/chloroform extraction:

The phenol/chloroform extraction was performed in the following way: 500  $\mu$ l of phenol equilibrated stabilized at RT was added to each sample. Samples were strongly mixed for 10

seconds and centrifuged at maximum speed at RT for 1 min. The aqueous phase (~500 µl) was transferred into a new e-cup and it was added 250 µl of phenol equilibrated stabilized and 250 µl of chloroform. After a strongly mixture the samples were centrifuged at maximum speed at (RT) for 1 min. The aqueous phase (~500 µl) was transferred into a new e-cup and was added 500 µl of chloroform. The samples were strongly mixed and centrifuged at maximum speed at RT for 1 min. The aqueous solution was transferred into a new e-cup and was added 45 µl of 3M Sodium Acetate (pH 5.0 to 5.3), 1.5 µl of glycogen for molecular biology, and 1 ml of cold 100% ethanol. After mixing the samples were cooled down for 5 min in dry ice and centrifuged at maximum speed at 4° C for 30 min. The extracted DNA pellet was further washed with 1 ml of cool 70% ethanol and centrifuged for further 10 min, the supernatant was removed, the pellet dried and re-dissolved in 200 µl of TE pH 8.0.

#### **2.2.2.6. AAV qPCR**

The amount of PCR product in this type of qPCR is followed in real time by SYBR green incorporation in the dsDNA PCR product. All samples including the negative control were further diluted 1 to 20 before qPCR. The qPCR reaction was set up in 200 µl “thin wall tubes” and contained 10 µl mix (Platinum SYBR<sup>®</sup> Green qPCR SuperMix-UDG), 2 µl primer 1 (4 mM), 2 µl primer 2 (4 mM), 1 µl fluorochrome fluorescein, 4 µl of extracted DNA, standard or positive control, plus 1 µl H<sub>2</sub>O. Each unknown sample was assayed in duplicate and with two primer sets (WPRE and bGH specific primers). qPCR was performed on “icycler” qPCR machine and analysed with keycler software. Amplification started with 15 min incubation at 98°C (to release the antibody bound to the polymerase) followed by 30 cycles of amplification (annealing 15 sec between 60°C and 72°C, elongation for 20 sec/kb at 72°C and separation of DNA strands for 15 sec at 98°C). After amplification a melting curve was performed with 0.5° C increase each 30 seconds until reaching 98° C. The melting curve is an indicator of PCR amplification product specificity. Cyclor was programmed to stay at on hold at 18° C after the melting curve. Concentrations were automatically calculated by a regression curve between the threshold cycle and the known amounts of standards in logarithmic scale. Threshold cycle for unknowns was used to extrapolate the pg of DNA in unknown samples.

#### **2.2.2.7. Calculation of AAV viral genomes**

The correlation between amounts of double stranded DNA used and the qPCR standard (dependent on molecule size) and the single stranded DNA present in the virus genome was

assumed to be 200 pg of ssDNA AAV genome equal to  $5.2 \times 10^7$  genomes ( $0.026 \times 10^7$  genomes/pg of ssDNA).

Titre genome was calculated as follows:

$(\text{value in pg}) \times Z \times Y \times 0.026 \times 10^7 / X / n = \text{genomes}/\mu\text{l}$  (often referred as vg, viral genome).

Where Z corresponds to the ssDNA sample dilution before qPCR (usually 20), Y is the volume where the ssDNA was dissolved after ethanol precipitation, X is volume in  $\mu\text{l}$  of virus used for DNA preparation and n is the volume in  $\mu\text{l}$  applied in the qPCR tube for quantitative determination.

Assuming that only every 30<sup>th</sup> viral genome is infectious, the obtained genomes were divided by 30 to obtain the transduction units values that are used as reference in each *in vitro* transduction or *in vivo* injection.

Finally, the purity of the vectors was determined by SDS-gel electrophoresis followed by coomassie brilliant blue staining. In short, 5  $\mu\text{l}$  of virus were mixed with 6x SDS sample buffer and boiled for 5 min at 95° C. Denaturated virus capsid proteins were loaded in 10 % polyacrylamide/bis-acrylamide gels and were run until the bromophenol blue reached the bottom of the resolving gel. Next coomassie brilliant blue staining was performed using standard protocols (Fig. 2.2.6.). Infectious titres were confirmed by transduction of cultured primary cortical neurons. Aliquots of the AAV vectors were made and stored at -80°C until required. During all procedures dealing with AAV vectors, 0.5% SDS solution in water was used for disinfection.

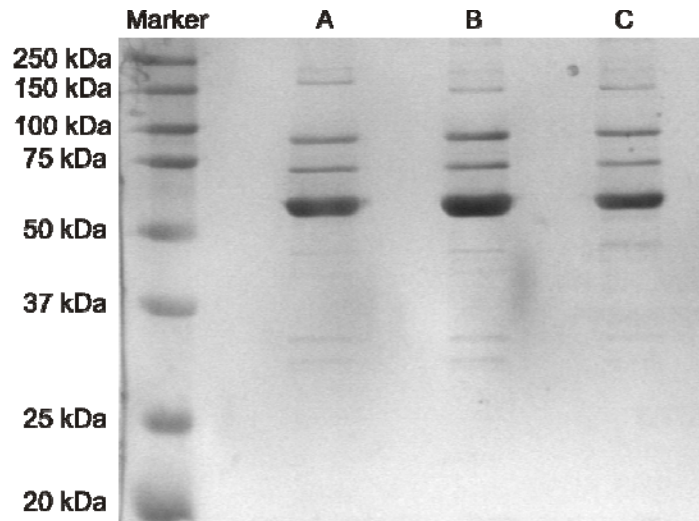


Fig. 2.2.6. Virus purity accessed by SDS-gel electrophoresis followed by coomassie brilliant blue protein staining. The three strongly stained proteins with sizes between 60 and 110 kDa correspond to AAV2 viral vector capsid proteins.

### 2.2.3. Cell culturing

#### 2.2.3.1. Continuous HEK-293 cell culture

HEK-293 (AAV-293) cell culture was performed under sterile conditions. Mammalian HEK-293 were cultured in DMEM supplemented with 10% FCS and 1% PS in 175 cm<sup>2</sup> culture flasks at 37°C, 5% CO<sub>2</sub> and 95 % humidity. After reaching 50 to 60% confluence the cells were split. For this, the medium was removed, cells were washed in 5-8 ml of room temperature PBS and 4 ml of pre-warmed (37° C) 0.05% trypsin/0.02% EDTA solution were added to the culture and left in the incubator at 37° C for 5-8 min until detached from the flask. Trypsin activity was stopped by addition of 7 ml of the cell culture medium to the flask. The mix containing detached cells was carefully transferred to a 50 ml falcon tube and centrifuged at 4,000 g at RT for 5 min. After removing the supernatant a cell pellet was resuspended in 20 ml of fresh medium. Cells were further counted in a hemocytometer and reseeded in 175 cm<sup>2</sup> flasks (~2x10<sup>6</sup> cells) and 12 well plates (3.5x10<sup>5</sup> cells/well).

#### 2.2.3.2. Coating of culture plates for primary cortical cells culture

Culture plates (24-well plates) were coated with different attachment factors creating the physiologically relevant in vitro conditions to support normal cell growth, function, and ensure optimized cell culture conditions. We used poly-D-ornithine (P-ORN), poly-DLysine, (D-isomers are preferred for their resistance to proteases released by cells), and laminin. P-

ORN and poly-D-Lysine are two positively-charged, synthetic polymers which enhance cell attachment to plastic and glass surfaces.

For immunocytochemistry, coverslips (13 mm diameter) were soaked in ethanol, flamed and placed in 24-wells plates. Plates were first incubated for 12 to 24 h at RT with P-ORN (1  $\mu\text{g/ml}$ ) in sterile  $\text{H}_2\text{O}$  (500  $\mu\text{l/well}$ ). After washing twice with 500  $\mu\text{l/well}$  sterile  $\text{H}_2\text{O}$ , plates were incubated with laminin 1:1000 in NBM (1  $\mu\text{g/ml}$ , 500  $\mu\text{l/well}$ ) overnight at  $37^\circ\text{C}$ , 5%  $\text{CO}_2$ , 95% humidity. Before transferring cells into wells, plates were washed twice with sterile NBM (500  $\mu\text{l/well}$ ), then 500  $\mu\text{l}$  of HCN medium (1% PS-N, 0.5 mM L-glutamine, 0.05% Transferrin, 2% B27 supplement in NBM) was added and the plates kept at  $37^\circ\text{C}$ .

### **2.2.3.3. Primary cortical cells culture**

To obtain primary cortical neurons, cortex were dissected from Wistar rat E18 (embryonic day 18) and further processed for establishing dissociated cell cultures as previously described (de Hoop M.J. et al. 1998). All surgical procedures were performed on ice. In brief, cortex tissue pieces were collected in ice-cold CMF medium and centrifuged at 800 rpm for 4 min at  $4^\circ\text{C}$ . The medium was removed and the tissue pellet was incubated in 750  $\mu\text{l}$  trypsin (0.25%, 15 min,  $37^\circ\text{C}$ ). Trypsin activity was then blocked by addition of 700  $\mu\text{l}$  ice-cold FCS and 25  $\mu\text{l}$  DNase was added to dissolve DNA-aggregates released from damaged cells.

The pellet was then mechanically dissociated by gentle move through a fire-polished Pasteur pipette. After centrifugation at 800 rpm for 4 min, the pellet was resuspended in warm HCN culture medium. Cells were seeded in poly-L-ornithine/laminin 24-well culture plates at a density 250,000 cells/well. Cultures were maintained at  $37^\circ\text{C}$  in 5%  $\text{CO}_2$  and 95% humidity in HCN medium and remained in the same medium for the duration of the experiment (up to 14 days).

### **2.2.4. Calcium phosphate transfection of HEK-293 cells**

The procedure is based on slow mixing of calcium chloride, DNA and phosphate buffer producing extremely small precipitates, insoluble particles of calcium phosphate containing condensed DNA (complexes) (Watanabe et al. 1999). Although the mechanism of the calcium phosphate transfection has not been characterized in detail, it is presumed that the calcium phosphate-DNA complexes precipitate into the cell membranes and is internalized by phagocytosis or endocytosis (Loyter et al. 1982). Some factors like cell density, incubation

time of calcium chloride, DNA and phosphate buffer as well as the pH of 2x HBS play a critical role in the complex formation and transfection efficiency.

In brief, 2% FCS DMEM and 2x HBS are equilibrated to 37° C, and small aliquots of 2% FCS DMEM were made. Next H<sub>2</sub>O, 2.5 M CaCl<sub>2</sub> and plasmid DNA for all conditions was aliquoted.

For the luciferase assay system for 3 wells in a 12 well plate the amounts were: 10 µg of pAAV shRNA, 2 µg of pGL3 test sequence, 15 µl of 2.5 M CaCl<sub>2</sub> and H<sub>2</sub>O up to 175 µl. The medium aliquots contained 3.1 ml of 2% FCS DMEM, and were used 175 µl of 2x HBS. 1 ml of medium with DNA complexes was added to each well.

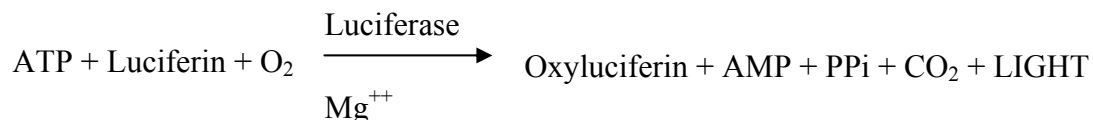
For WB (GCLc and GCLm) for 1 well in a 6 well plate the amounts were: 6 µg of pAAV shRNA, 6 µg of pExpress-1-GCLc or pAAV GCLm, 12.5 µl of 2.5 M CaCl<sub>2</sub> and H<sub>2</sub>O up to 145 µl. The medium aliquots contained 1.7 ml of 2% FCS DMEM, and were used 145 µl of 2x HBS. 2 ml of medium with DNA complexes was added to each well.

Further, the appropriate volume of 2x HBS was added to CaCl<sub>2</sub> DNA mix and was titrated up and down twice. This mixture was incubated for exactly 1 min and the mix of CaCl<sub>2</sub>, HBS and DNA was transferred to the medium aliquot (this mix contains already the calcium phosphate complexes and when added to the medium the complex formation is stopped). Cells culture medium was then removed and 2% FCS DMEM with complexes was mixed and distributed in the wells containing cells. The transfection mixture was kept in cells at 37°C in 5% CO<sub>2</sub> and 95% humidity incubator for 8 up to 16 hours and the medium was replaced by 10% FCS 1% PS DMEM.

### **2.2.5. Luciferase assay**

In 1947 McElroy (Mcelroy 1947) isolated and purified the heat-stable luciferin and the labile enzyme "Luciferase" that were responsible for light production by firefly tails, and showed that adenosine triphosphate (ATP) was also required for the process. He did isolate at that time two important components of most widely used genetic reporter in studies on gene expression/regulation. The assay is simple and due to the high sensitivity, dynamic range and natural absence from mammalian cells is very versatile.

The luciferase assay kit is based on the bioluminescent measurement of firefly luciferase activity. These enzyme catalyses the formation of light from ATP and luciferin according to the following reaction:



Intensity of light emission is directly correlated with the amount of luciferase and was measured using a luminometer. We used the luciferase assay from BD Pharmingen as recommended by the manufacturer, except that 5  $\mu\text{l}$  of sample and 50  $\mu\text{l}$  of solution A and B were used. The overall reaction proceeded as follows: the reagents were equilibrated to room temperature, the cells were washed twice with phosphate buffered saline and incubated at room temperature for 15-20 minutes with 100  $\mu\text{l}$  of cell lysis buffer (supplied in the kit). Cells were then displaced by scraping and transferred to microcentrifuge tube and centrifuged at maximum speed for 1 min to remove cellular debris. Five  $\mu\text{l}$  of cell extract was added to a 96 well plate and 50  $\mu\text{l}$  of solution A was added. Measurement started immediately after addition of 50  $\mu\text{l}$  of solution B. Luminescence was measured with a liquid scintillation and luminescence counter and data were evaluated with the MicroBeta Windows Workstation program.

## 2.2.6. Primary culture treatment

### 2.2.6.1. AAV transduction

On DIV 2 after preparation, cells seeded in 24 well plate (250,000 cells/well) were transduced by addition of 10  $\mu\text{l}$ /well of solution containing the desired amount of AAV diluted in PBS in 300  $\mu\text{l}$  of HCN (normally a total of  $1.5 \times 10^8$  tu/well). Cells were kept at 37°C in 5% CO<sub>2</sub> and 95% humidity between 8 and 16 h and afterwards 500  $\mu\text{l}$  of HCN was added back to each well.

For cells seeded in 96 well plates, usually in 100  $\mu\text{l}$  of HCN (50,000 cells/well) the medium was reduced to approximately 50  $\mu\text{l}$  and 5  $\mu\text{l}$  of solution containing a total of  $3 \times 10^7$  t.u was added. Between 8 and 16 h after transduction, 50  $\mu\text{l}$  of fresh HCN was added per well.



### 2.2.6.2. Ara-C treatment:

Ara-C (cytosine arabinoside) is a mitotic inhibitor and was added to the culture at DIV3, at the same time that the medium was added back in the AAV transduced or PBS only treated wells. Usually the cells were incubated in a final concentration of 0.5  $\mu\text{M}$  of Ara-C diluted in the medium added back to cells after transduction.

### 2.2.7. WST-1 assay

Cell viability was assessed after viral transduction in 96 well plates using the WST-1 proliferation reagent. The assay is based on the cleavage of the tetrazolium salt WST-1 by succinate-tetrazolium reductase producing soluble formazan. The enzyme is part of the respiratory chain in mitochondria. This conversion only occurs in viable cells. Cells were incubated with 50  $\mu\text{l}$  of medium containing WST-1 for 2 hours. The formed formazan dye was quantified via measurement of the absorbance (optical density) at 450 nm using a microplate reader (Tecan RainBow). The absorbance is proportional to the number of metabolically active cells. Blank was subtracted and results are presented as percentage of control.

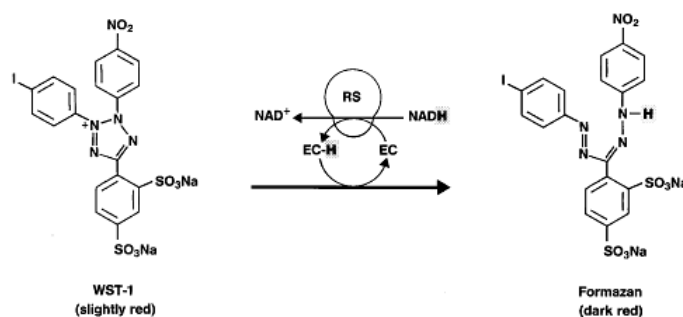


Fig. 2.2.7. conversion of tetrazolium salt WST-1 (4-[3-(4-Iodophenyl)-2-(4-nitrophenyl)-2H-5-tetrazolio]-1,3-benzene disulfonate) to formazan. (copied from: <https://www.roche-applied-science.com/servlet/RCCConfigureUser?URL=StoreFramesetView&storeId=10305&catalogId=10304&langId=-1&countryId=uk>)

### 2.2.8. Glutathione assay

The Glutathione quantity assay is based on the 96 well microplate assay previously reported Baker and collaborators (Baker et al. 1990) as an adaptation from the original enzymatic recycling method first described by Owens (Owens and Belcher 1965). This assay is specific for GSH and/or GSSG, sensitive and enables high throughput measurements. Enzymatic recycling assay is based on the reduction of DTNB (5,5'-Dithio-bis(2-nitrobenzoic acid)),

known as Ellman's Reagent, by glutathione (GSH). DTNB and glutathione (GSH) react to generate 2-nitro-5-thiobenzoic acid (TNB) and glutathione disulfide (GSSG). Since 2-nitro-5-thiobenzoic acid is a yellow colored product, GSH concentration in a sample solution can be determined by the measurement at 412 nm absorbance. GSH is generated from GSSG by glutathione reductase, and reacts with DTNB again to produce 2-nitro-5-thiobenzoic acid. Therefore, this recycling reaction increases the sensitivity of total glutathione detection (Fig. 2.2.8.).

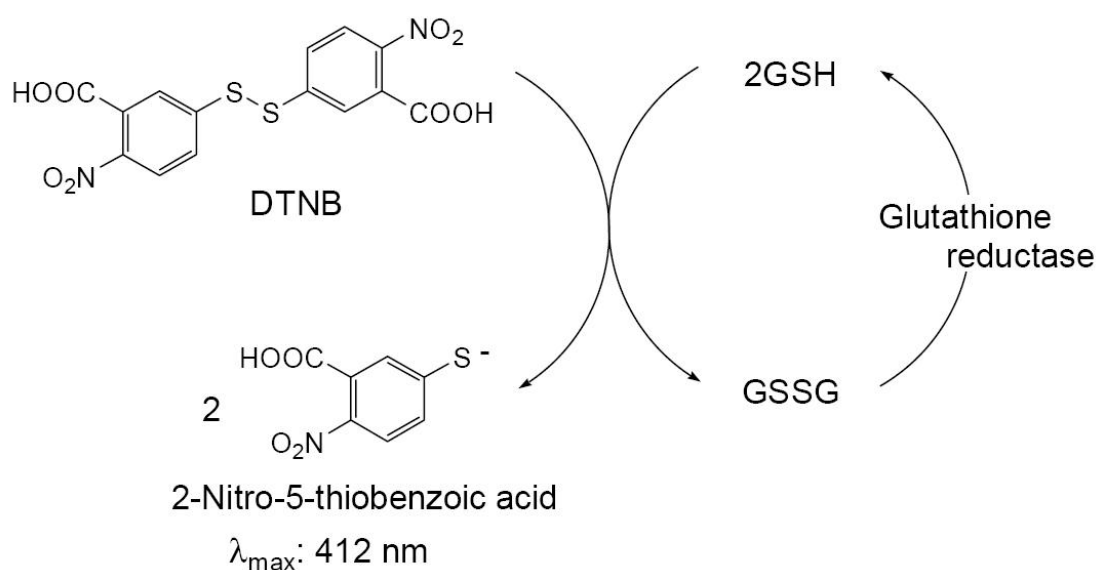


Fig. 2.2.8. Principle of Total Glutathione Quantification (copied from: <http://www.dojindo.com/newimages/TGQKTechnicalInformation.pdf>)

In brief, total glutathione was measured using the following procedure. At selected time points after AAV2 transduction, cells were washed 2 times with ice-cold PBS, and 150  $\mu\text{l}$  of ice-cold 1 % SSA in  $\text{H}_2\text{O}$  was added to each well. Plates were kept on ice for 10 min and the 1% SSA extract was transferred in to ice-cold 1.5 ml e-cup. The 1% SSA extract was centrifuged at  $4^\circ\text{C}$  for 15 min at maximum speed and the supernatant transferred to a new cold e-cup. In a 96 well plate with 90  $\mu\text{l}$  of  $\text{H}_2\text{O}$  in each well, 10  $\mu\text{l}$  of unknown or standard (1.5, 3, 6, 8, 10, 15  $\text{pmol}/\mu\text{l}$ ) solution was added in duplicate. For preparation of standards for both the total glutathione assay (GSx: GSH+GSSG) or the GSSG only assays, the same stock solution of 15  $\mu\text{M}$  GSSG in 1% SSA was used. All other standards were diluted in 1% SSA and kept at  $4^\circ\text{C}$ . The reaction mix was freshly prepared and mixed at room temperature, it contains 93  $\mu\text{l}$  0.1 M phosphate buffer with 1 mM EDTA, pH 7.5; 4  $\mu\text{l}$  of 10 mM NADPH in 0.1 M phosphate buffer with 1 mM EDTA, pH 7.5; 3  $\mu\text{l}$  10 mM DTNB in 0.1 M phosphate buffer with 1 mM EDTA, pH 7.5 and 0.1 unit of GSR (Glutathione Reductase). The final

concentrations of reagent were 0.15 mM DTNB, 0.2 mM NADPH, and 1.0 U GSH reductase/ml.

The reaction was started with the addition of 100  $\mu$ l of reaction mix and absorbance at 412 nm was immediately recorded and followed for 8 min in a 30 seconds measurement interval with plate shake before each measurement (TECAN Rainbow microplate reader, Magellan V3.11 software). The increase in absorbance at 412 nm is direct proportional to the reaction time and higher amount of GSx leads to a higher slope (plotted absorbance at 412 nm versus the time). Total glutathione concentration was determined by correlation between slopes of the standard curve plotted versus the glutathione known amounts. Unknown samples quantities were extrapolated using the measured slopes of the unknown samples. The data was analysed with the Microsoft Office 2003 Excel software.

For the measurement of oxidized glutathione (GSSG) the same method was applied. GSSG produces the identical rate of DTNB reduction as does GSH. Thus, GSSG can be measured only by removal of GSH. GSH was conjugated with 2-vinylpyridine before assay of residual GSSG. For each 65  $\mu$ l of sample or standard were added 25  $\mu$ l of 0.2 M Tris-HCl plus 2.5  $\mu$ l of 2-vinylpyridine (0.25 M final concentration of 2VP). The mix was derivated for 1 hour at room temperature. Samples were mixed and 10  $\mu$ l of sample or standard was measured using the same procedure as for total glutathione measurement.

The cell remnants were scraped from the plate (50  $\mu$ l of 0.1N NaOH/well) using a pipette tip. The collected cells were boiled for 6 min at 98°C. The cell extract was mixed and centrifuged at maximum speed for 15 min at 4 °C. Samples were measured in duplicate, using a BSA standard curve (range from 0.06 and 2 mg/ml) diluted in lysis buffer. Solutions A and B of bicinchoninic acid assay (BCA) were mixed 1:50 and 200  $\mu$ l of the obtained solution were added to 10  $\mu$ l of protein samples diluted in 20  $\mu$ l of PBS. Absorbance was measured in a 96 well plate and protein concentration was determined by correlation between sample absorbance and the standard curve slope using the Microsoft Office 2003 Excel software.

### **2.2.9. Protein analysis, overview:**

The detection the relative amounts of the protein of interest present in different samples was done by western blotting also called immunoblotting, with a specific primary antibody recognizing specifically the protein of interest (Towbin et al. 1979; Burnette 1981). The

separation of large range of proteins with various molecular weights and charges was done under the influence of the electrical field within the polyacrylamide gel. Briefly, the samples are prepared from cells that are homogenized in a buffer that extracts and protects the pool of cellular proteins from degradation. Proteins are denatured by heat and a reducing agent (SDS). Proteins are concentrated into the stacking gel and are separated within the resolving gel upon their molecular weight, the biggest ones being slowed down most by the gel matrix. This matrix is constituted of polyacrylamide/bis-acrylamide (Rotiphorese), the cross-linking is catalysed by free radicals produced by addition of ammonium peroxide and TEMED. Next, the sample proteins are transferred to a nitrocellulose membrane for detection. Then the membrane is incubated with a generic protein (blocking protein e.g. milk proteins) to bind to the remaining sticky places on the membrane in an unspecific manner. A primary antibody is then added to the solution which is able to bind specifically, with high affinity, the protein. Finally a secondary antibody-enzyme conjugate, which recognizes the primary antibody, is added to find locations where the primary antibody is bound.

### **2.2.9.1. Lysis for western blotting**

After removing the medium the cells were washed twice with cold PBS, 20µl/well of the lysis buffer was added, cells were scraped from the plate using a pipette tip and transferred to a 1.5 ml eppendorf tube. Samples were sonicated for 5 to 10 seconds at 30% power and centrifuged 45 min at maximal speed at 4° C in a microcentrifuge. The supernatant was collected and aliquots were frozen at -20°C.

### **2.2.9.2. SDS polyacrylamide gel electrophoresis (SDS-PAGE)**

Polyacrylamide gel with two-phases were used for collection and separation of the proteins according to their molecular weight. Usually, 12% resolving gel and 5% stacking gel were used to separate the proteins of interest. To define a molecular weight of loaded proteins the molecular weight marker (Precision Plus Protein<sup>TM</sup> standards) was loaded and separated in parallel. Equal amounts of total protein samples and 6 x SDS-loading buffer were mixed, subjected to heating at 95°C for 5 min, chilled at RT and loaded in the gel combs. SDS-PAGE was run at 4° C in ice-cold electrophoresis buffer (Mini-PROTEAN 3 cell). The current was 7 mA/gel with a maximum electric field of 90 V was applied for 15 min to allow samples to enter the gel and collect without a smearing. For the protein run in the resolving gel, the current was 15mA/gel with a maximum electric field of 150 V was used until the

bromophenol blue reached the bottom of the resolving gel. Depending on the size of the protein of interest, the run was sometimes continued until the kaleidoscope 25 kDa protein band reached the gel bottom.

### 2.2.9.3. Immunoblotting

For the protein transfer from the polyacrylamide gel to the nitrocellulose membrane the Mini Trans-Blot Cell setup was used. Protein samples are transferred from a SDS-resolving gel to a nitrocellulose membrane by application of an electric current. After electrophoresis the polyacrylamide gel was placed between two sheets of Whatman filter paper and a nitrocellulose membrane which were all preliminary soaked in transfer buffer. Two additional fibber pads were placed on the top on the membrane and the “sandwich” was placed in the Mini Tans-Blot Cell. A current of 360 mA or a maximum voltage of 160 V was applied for 70 min at 4°C.

After the completion of the transfer the membrane was treated with blocking solution for 1 h at room temperature to avoid unspecific binding of the antibody. The membranes were subsequently incubated with unlabeled primary antibody specific for the target protein in 5% non fat Milk TBS-T solution overnight at 4°C or 1 hour at RT. Respective dilutions of the antibodies used in this study are listed in the table 2.1.5. The membranes were washed 3 x 15 min with TBS-T and incubated with secondary immunological reagents (e.g. anti-immunoglobulin) coupled to Horseradish peroxidase (HRP) in 5% non fat Milk TBS-T (usually diluted 1:3000). The membranes were washed 3 x 15 min with TBS-T and equal volumes of ECL-1 and ECL-2 reagents were mixed and applied into the membrane. Chemiluminescence was visualized and quantified at Fluor-S<sup>TM</sup>-Max Gel Imager and Quantity One software (version 4.2.1).

Table 2.1.5. Dilutions of antibodies used for western blotting.

<b>Antigen</b>	<b>Source</b>	<b>Working dilution</b>
GCLc	Rabbit	1:500
GCLm	Rabbit	1:500
GSR	Rabbit	1:1000
Tubulin	Mouse	1:4000
cleaved caspase 3	Rabbit	1:750
hDJ1	Goat	1:1000
α-synuclein	Mouse	1:750

All Antibodies were diluted in 5% milk powder according to the manufacturer’s instructions.

#### **2.2.9.4. Protein concentration determination**

Protein concentration was determined by Lowry assay. In basic conditions, proteins have the ability to reduce  $\text{Cu}^{2+}$  into  $\text{Cu}^+$ . These ions form complexes with 2 molecules of bicinchoninic acid (BCA) and produce a violet compound (maximum absorbance at 562 nm). Absorbance is proportional to the amount of complexes created, therefore to protein amount. Solutions A and B of BCA were mixed 1:50 and 200  $\mu\text{l}$  of the obtained solution were added to 5  $\mu\text{l}$  of protein samples diluted in 35  $\mu\text{l}$  of PBS to quantify in a 96-well plate. All samples were tested in duplicate, and in a dilution series. Simultaneously, a protein standard curve was prepared with BSA diluted in PBS in a concentration range between 0.06 and 2 mg/ml. The plate was then incubated 40 min at 37° C and absorbance was measured at a wavelength of 562 nm using a TECAN Rainbow plate reader and Magellan software (V3.11). Protein concentration was determined by correlation between sample absorbance and the standard curve slope using the Microsoft Office 2003 Excel software.

#### **2.2.10. Immunofluorescence**

##### **2.2.10.1. Immunofluorescence on primary neurons**

Immunocytochemistry (ICC) was used to investigate expression or localisation of proteins of interest within the cells. At selected time points after AAV2 transduction, the cultured neurons were subjected to ICC. The coverslips with primary cortical neurons were rinsed 2 times with ice cold PBS and fixed by incubation in 4% formaldehyde for 8 to 10 min at room temperature. After washing 2 times for 5 min with PBS coverslips were placed on parafilm support and cells were blocked with 10% new-born goat serum (NGS) in PBS with 0.3% Triton X-100 for 30 min at RT to avoid any unspecific binding of the antibodies. Primary antibodies were applied at respective dilutions (Table 2.1.6.) at 4°C overnight or for 90 min at 37° C. Following 2 x PBS washes, appropriate fluorescently-labelled secondary antibodies were then applied for 1 hour at RT (Cy2, Cy3 and Cy5 conjugated diluted 1:250). After 2 x PBS washes, cells were nuclear counterstained with 4', 6-diamidino-2-phenylindole (DAPI), washed with PBS and  $\text{H}_2\text{O}$ . Next coverslips were mounted on glass slides embedded in Moviol mounting medium (16 % Moviol in 30 % Glycerol in PBS, 0.02 % sodium azide) to protect immunofluorescence from bleaching. Fluorescence of samples was observed and recorded on a Zeiss Axioplan 2 microscope equipped with a CCD camera and AxioVision Rel. 4.6 software. When specified a Zeiss Apotome™ device was used.

Table 2.1.6.: Working dilutions of the primary antibodies used for ICC and IHC

Antigen	Species	Dilution
Anti-AU1	mouse monoclonal	1 :300
Anti-cleaved caspase-3 (Asp175)	rabbit polyclonal	1:100
Anti- Cleaved caspase-9	rabbit polyclonal	1:100
Anti-CD11b	mouse monoclonal	1:250
Anti-GCLc	rabbit polyclonal	1:400
Anti-GCLm	rabbit polyclonal	1:300
Anti-GFAP	rabbit polyclonal	1:750
Anti-Glutathione-protein complexes	mouse monoclonal	1:100
Anti-Glutathione Reductase	rabbit polyclonal	1:400
Anti-MAP LC3	goat polyclonal	1:75
Anti-NeuN	mouse monoclonal	1:300
Anti-NT	mouse monoclonal	1:200
Anti-TH	mouse monoclonal	1:500
Anti-TH	rabbit polyclonal	1:700
Anti-VMAT2	rabbit polyclonal	1:1000

All Antibodies were diluted in 2% NGS, 0.3% Triton X-100 in PBS.

### 2.2.10.2. Immunofluorescence on brain slices

For immunohistochemistry (IHC), specimens were dried at 37°C for 1 h, rehydrated in PBS for 45 min and subjected to antigen retrieval in TBS (pH 9.0) for 4 to 6 h in a water bath at 60°C. The antigen retrieval procedure keeps EGFP fluorescence intact. The slides were shortly washed with PBS, and in the perimeter of each section a liquid blocker (SUPER PAP PEN) was applied. Sections were incubated in a blocking solution (10% NGS, 0.3% Triton X-100 in PBS) for 30 min at room temperature to avoid unspecific binding of the antibodies. Incubation with primary antibody was performed overnight at 4°C in 2% NGS, 0.3% Triton X-100 in PBS (for antibody dilutions see Table 2.1.6.:). After washing 3 x 10 min with PBS the secondary antibodies in 2% NGS in PBS (Cy2, Cy3 and Cy5 conjugated diluted 1:250) was applied for 1 h at room temperature. The secondary antibody was washed 3x 10 min with PBS and nuclear counter-stained with DAPI was performed. Specimens were embedded in Moviol, coated by coverslips (SuperFrost<sup>®</sup>Plus microscope slide) and kept at 4°C until microscopy.

### 2.2.11. Animal procedures

All animal experiments were carried out according to the regulations of the local animal research council, legislation of the State of Lower Saxony (Braunschweig) and the European

Community Council Directive of 24<sup>th</sup> November 1986 (86/609/EEC). Adult female Wistar rats (University Hospital Animal Facility, Göttingen) of 250-280g of weight were housed at 12h/12h of light/dark cycle, provided with food and water *ad libitum*. Animals were deeply anaesthetised by 7% chloral hydrate intraperitoneally (340mg/kg body weight) before the surgery. All animals were sacrificed by CO<sub>2</sub> inhalation.

#### **2.2.11.1. Stereotaxic injection into the rat brain**

The head of the rat was fixed by ear bars and a jaw holder in a stereotaxic frame (“Kopf” Instruments) after the 7% chloral hydrate intraperitoneally anaesthesia. A skin covering the skull was longitudinally cut from the imaginary line connecting the eyes in front till the imaginary line connecting the auditory channels in the back. Remaining connective tissue was carefully removed aside by scalpel in order to achieve appropriate visualisation of the skull sutures and visualize the bregma under the operating microscope. Bregma is the crossing point of parasagittal with coronal sutures on the surface of the skull and was defined as “zero” or “start” point. After achieving flat positioning of the skull, the coordinates for the injection were calculated relatively to bregma. For the injection into the left hemisphere SNpc, the following coordinates were used: antero-posterior (AP): -0.53; medio-lateral (ML): +0.22; dorso-ventral (DV): -0.77 accordingly with the rat brain atlas (Paxinos and Watson 1986). Glass capillaries filled with mineral oil and the solution for the injection were attached to the Nanoliter2000 injector. The injector was connected to a microprocessor-based controller, Micro4 smart controller which allows for setting the operating parameters, such as the volume and the speed (nl/min) of the injection. Two µl of AAV-vectors in PBS were injected into SNpc at a speed of 500 nl/min.

#### **2.2.11.2. Transcardial perfusion and brain tissue processing**

Transcardial perfusion under terminal anaesthesia is a commonly used method for tissue fixation in immunohistochemical protocols. This method takes advantage of the animal’s circulatory system to deliver the fixative solution evenly throughout the body tissues, with optimal penetration of the brain. Fixation ensures preservation of the tissue ultra-structure, stabilizes protein and peptide conformation so that antibodies can bind to antigen sites. We used 4% paraformaldehyde (PFA) in phosphate buffer solution (PBS, pH 7.4) as a fixative. This fixative is optimal for fluorescent protein visualization or protein visualization using fluorescent dyes. After a deep anaesthesia with 7% chloral hydrate (800 mg/ml) or CO<sub>2</sub>



inhalation the rat was fixed on rack, the abdominal cavity was opened, and the diaphragm was cut to provide access to the thorax. With large scissors, blunt side down, ribs were bilaterally cut and the rib cage was open to allow heart access. While holding heart steady, the left ventricle was cut and the catheter blunt-ended needle connected to a catheter was inserted through the ventricle and atrium into aorta. Needle position was secured in position by clamping. The liver was cut then to allow a large part of blood volume to leave the body and the nose as was well to control the procedure efficiency and progress. After approximately 50 ml perfusion with ice-cold PBS, the abdominal aorta was clamped to restrict perfusion to the upper part of the body. Thus, if fluid was flowing freely from the cut nose the needle was considered to be appropriately positioned. The pump was operated with a speed of 15–20 ml/min with ice-cold PBS. When blood has been cleared from body (ca. 200 ml of PBS), PBS was replaced with ice-cold 4% PFA solution (200 ml). The rat was decapitated and the brain carefully removed from the skull and placed into 4% PFA overnight at 4°C for post-fixation. The brain was cryoprotected by dehydration in 30% sucrose solution in PBS usually for 3 days, until the brain sinks in the solution, dried in tissue paper and frozen at -80° C until further processing. The brains were embedded in cryomatrix, and coronary sections (18 µm thickness) of the SNpc region were prepared using a Leica cryostat (Leica CM 3050 S) and collected on SuperFrost<sup>®</sup>Plus microscope slide (Menzel-Glaser, Germany).

#### **2.2.12. Microscopy and image analysis**

Fluorescence from tissue sections and fixed cultured cells was recorded on a fluorescence microscope (Zeiss-Axioplan) equipped with a 16 bit greyscale CCD camera (Zeiss). Narrow band filter sets specific for EGFP, Cy3 and Cy5 fluorescence were used. In all recorded images the exposure time was constant between the different sample groups which allowed for direct comparison. Pseudo-colouring of images, generation of overlays and quantification of channels co-localization was performed with AxioVision Rel. 4.6 software. Some pictures were taken with Apotome<sup>™</sup> device which allows the recording of “confocal-like” images by subtracting the fluorescence of nearby layers.

#### **2.2.13. Quantification of neurodegeneration in shRNA rat model of PD**

Brains were processed to 18 µm slices, and immunofluorescent visualization of dopaminergic neurons in SNpc was performed with primary rabbit antibody against tyrosine hydroxylase (anti-TH, 1:600; overnight at 4°C) or anti-vesicular monoamine transporter 2 (anti-VMAT2,

overnight at 4°C) followed by 1h incubation at RT with secondary Cy3-conjugated goat anti-rabbit antibody. Images of brain sections were recorded as described above. TH-immunoreactive (TH-IR) or VMAT2-IR cells were counted in every 8<sup>th</sup> brain section in the region anatomically correspondent to SNpc. TH-IR and VMAT2-IR cells of the ventral tegmental area (VTA) area were excluded from counting. To obtain the corresponding total DA cell numbers the counted values were multiplied by 8, assuming that the average diameter of the adult rat DA-neuron is 16-18µm (Juraska et al. 1977).

#### **2.2.14. EGFP in live cortical neurons**

Primary cortical neurons expressing sufficient EGFP reporter gene (DIV6-7) were incubated in a microscope climate chamber for live cell imaging (37°C, 5% CO<sub>2</sub>) on a fluorescence inverted microscope (Zeiss-Axiovert) equipped with CCD camera and AxioVision Rel. 4.6 software (Zeiss). Contrast phase and EGFP fluorescence photographs of at least 4 random visual fields per culture well were taken.

#### **2.2.15. Statistics**

Luciferase, all data are expressed as mean ± SD. Each group analysed consisted of three independent samples, and all experiments were repeated at least three times. WST-1, all data are expressed as mean % of control ± SD. Each group analysed consisted of 3 to 6 independent samples, and all experiments were repeated at least three times. GSx, all data are expressed as mean % of control ± SD. Each group analysed consisted of at least 3 independent samples, and all experiments were repeated at least three times. TH-IR and VMAT2-IR cell counts are presented as means ± standard deviations. For TH-IR cells and VMAT2 of SNpc region at least 13 sections were counted per animal. Experiments were performed at least in triplicate. One-way ANOVA with Bonferroni's multiple comparison test was performed using GraphPad Prism (version 4.00 for Windows, GraphPad Software, San Diego California USA). Differences between groups were considered statistically significant if  $p < 0.05$ . Significances are indicated with \*  $p < 0.05$ , \*\*  $p < 0.01$ , \*\*\*  $p < 0.001$ .

### 3. Results

#### 3.1. Downregulation of GSH production in cultured primary neurons

These experiments describe the thorough characterization of RNA-interference mediated by viral vectors which was performed before their application into the rat brain. These studies revealed that the estimation of shRNA specificity and efficacy may vary drastically in different situations, depending e.g. on the context of the targeted sequence, the mode of introducing genetic information into the test system, and the cell type under study.

In addition, disruption of GSH production in cultured primary neurons demonstrated that this approach is suitable to induce neurodegeneration. Comparison with results obtained in the living animal (see section 3.2.) revealed that the physiology of cultured neurons derived from embryonic rat brain and the physiology of neurons in the adult brain differ in relevant aspects.

Brief conclusions drawn from individual experiments are outlined in a grey shading.

##### 3.1.1 Characterization of RNAi efficiency

###### 3.1.1.1 Development of a test system for determination of RNAi efficacy

“Protein silencing” has become a promising tool to answer biological questions and raise a window of opportunities for therapeutic intervention in various diseases. RNA-interference is now applied routinely at screening level for protein function characterization in various models, from *in vitro* cell culture applications to yeast, *Caenorhabditis elegans*, drosophila and mouse models. This technique depends on the RNAi targeting efficiency, and thus it is necessary to achieve both specificity and appropriate silencing levels. In an attempt to develop an easy-to-handle universal test system for the evaluation of efficacy of a given shRNA molecule we designed a reporter-gene based strategy depending on the fusion of the target sequence for this shRNA to the cDNA of luciferase firefly (Fig.3.1.1.) (Malik et al. 2006).

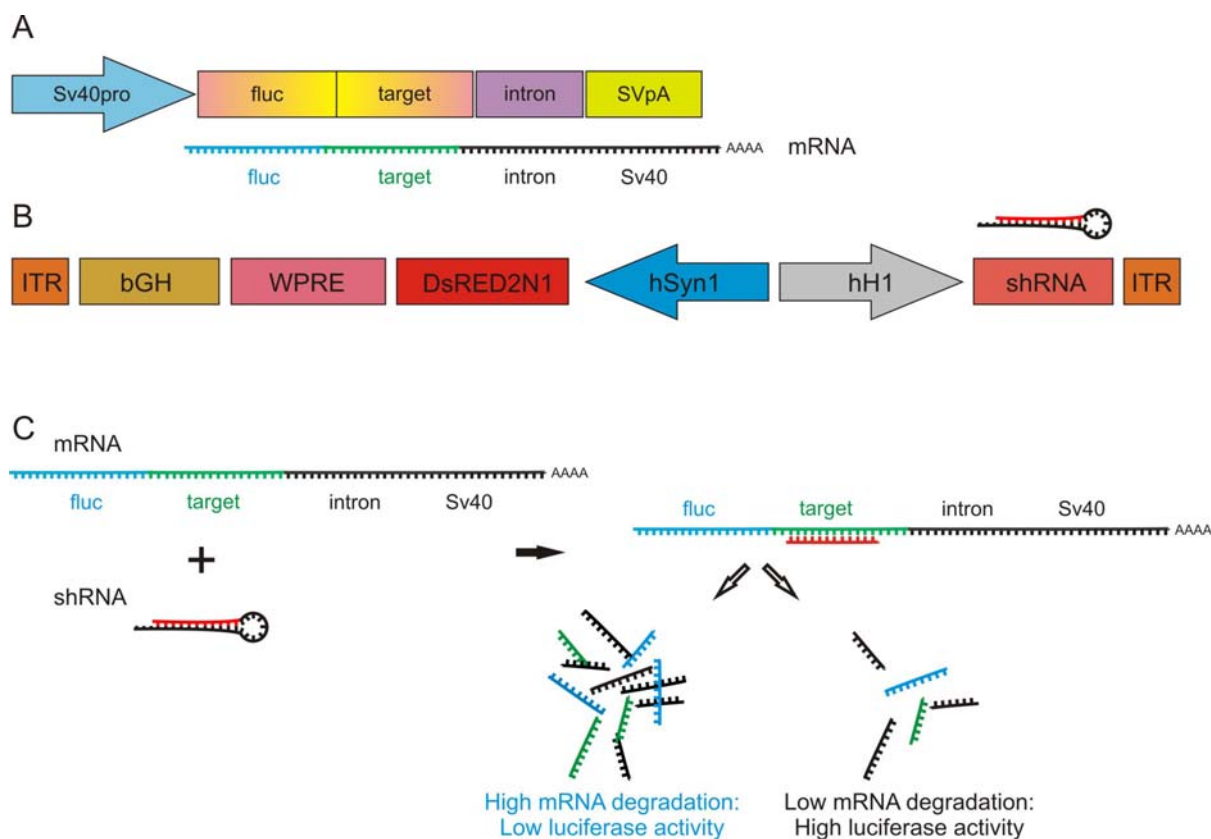


Fig.3.1.1. Schematic outline of the test system vectors. (A) vector expressing the luciferase firefly gene fused to partial cDNA of the target protein. (B) shRNA expressing vectors and (C) the test principle. The test vector (A) contained the simian virus40 promoter (Sv40pro), a reporter protein luciferase firefly (fluc) fused with the target sequence, the chimeric intron (intron from the pCI-Neo vector, Promega) and the polyadenylation site from simian virus-40 (SVpA). (B) the shRNA-expressing vectors, expression of shRNA driven by the human H1 polymerase III promoter. This vector contained the human synapsin 1 gene promoter (hSyn1), a reporter protein (red fluorescent protein, DsRed2N1), the woodchuck hepatitis virus posttranscriptional control element (WPRE), the bovine growth hormone gene polyadenylation site (bGH) and two AAV serotype 2 inverted terminal repeats (ITR). (C) the test is based on the degradation of the firefly luciferase mRNA fused to a partial target mRNA sequence. High level of degradation of fusion mRNA leads to low luciferase activity and means high shRNA sequence efficacy, and low degradation of fusion mRNA leads to high luciferase activity and means low shRNA sequence efficacy.

We first investigated silencing properties in HEK293 cells in culture. In order to achieve quantitative assessment of shRNA efficacy, cells were transfected 24 hours after seeding with the test vector and the shRNA-expressing vector at 1 to 3 molar ratio. The transfection efficiency for each condition at each time point and condition was evaluated by DsRED fluorescence reaching up to 90 % at 48 hours after transfection. The luciferase activity was recorded 24, 48 and 96 hours after transfection. For GCLc (catalytic subunit of Glutamate Cysteine Ligase) a partial cDNA sequence, here named shortGCLc test sequence, consisted of a 737 bp fragment (base pair 255-991 from accession number NM\_012815). A negative control shRNA (EGFP-shRNA expressing vector) or a positive control (fluc-shRNA#1 expressing vector) were also co-transfected for comparison purposes. As shown in Fig.3.1.2.A

all three different shRNAs targeting GCLc significantly down-regulated the expression of luciferase at the three studied time points. The GCLc-shRNA#2 and GCLc-shRNA#3 had the strongest effects which were comparable to the down-regulation of luciferase expression by the luciferase specific shRNA (fluc-shRNA#1).

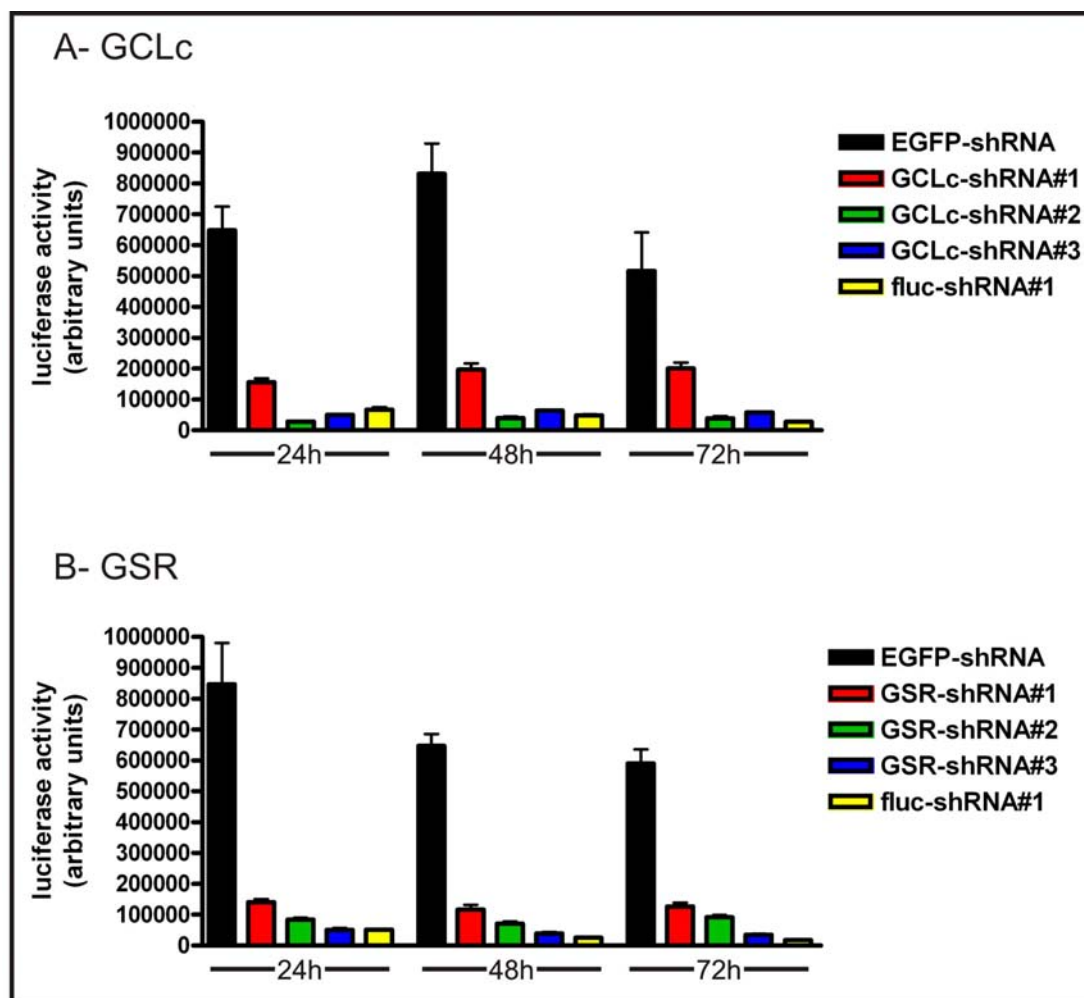


Fig.3.1.2. Silencing of luciferase expression by GCLc-specific shRNAs in **A** and GSR-shRNAs in **B**. In **A**, HEK293 cells were transfected with a plasmid expressing luciferase firefly as a reporter and GCLc-specific target sequence (pGL3-SV40-fluc-shortGCLc-test1) together with a plasmid expressing a control shRNA (EGFP-shRNA, black columns), one of three different GCLc-specific shRNAs (GCLc-shRNA#1, red columns; GCLc-shRNA#2, green columns; GCLc-shRNA#3, blue columns), or the luciferase specific shRNA (fluc-shRNA#1, yellow columns). In **B**, HEK293 cells were transfected with a plasmid expressing luciferase firefly as a reporter and GSR-specific target sequence (pGL3-SV40-fluc-shortGSR-test1) together with a plasmid expressing a control shRNA (EGFP-shRNA, black columns), one of three different GSR-specific shRNAs (GSR-shRNA#1, red columns; GSR-shRNA#2, green columns; GSR-shRNA#3, blue columns), or the luciferase specific shRNA (fluc-shRNA#1, yellow columns). Luciferase expression is shown on the Y axis in mean arbitrary units  $\pm$  SD from 3 replicates. Three independent experiments were performed in triplicate and this is one representative experiment. Measurements were done 24, 48, and 72 h after transfection.

For GSR (Glutathione Reductase) the test sequence consisted of a 594 bp fragment (base pair 286 to 880 from accession number NM\_053906). A negative control shRNA (EGFP-shRNA

expressing vector) or a positive control (fluc-shRNA#1 expressing vector) were also co-transfected. As shown in Fig. 3.1.2.B all three different shRNAs targeting GCLc significantly down-regulated the expression of luciferase at all three time points studied. The GSR-shRNA#2 and GSR-shRNA#3 had the strongest effects with GSR-shRNA#3 having comparable down-regulation as the luciferase specific shRNA (fluc-shRNA#1).

These results based on the luciferase based test system suggested that the GCLc-shRNA#2 and the GSR-shRNA#3 are the most efficient shRNAs to target the GCLc or GSR mRNAs respectively.

### **3.1.1.2. Quantification of protein down-regulation by shRNAs**

#### **3.1.1.2.1. Evaluation of GCLc shRNAs efficiency by western blot in HEK293 cells**

In order to confirm efficacy of the shRNAs in protein silencing, HEK293 cells were co-transfected with one plasmid expressing the rat GCLc and one other expressing the respective shRNA. These results confirmed in general the luciferase system based results for RNAi efficacy as described above. All shRNAs resulted in a decrease/silencing of GCLc protein levels, with the GCLc-shRNA#1 being the least effective in contradiction with the results obtained by the luciferase based test system. The GCLc-shRNA#2 and GCLc-shRNA#3 produced the strongest down-regulation in GCLc expression (Fig.3.1.3.A), recapitulating the efficacy demonstrated in the luciferase based test system (Fig.3.1.2.A).

These results demonstrate that GCLc-shRNA#2 and GCLc-shRNA#3 are the most efficient shRNAs in GCLc protein silencing in HEK293 cells co-transfection experiments.

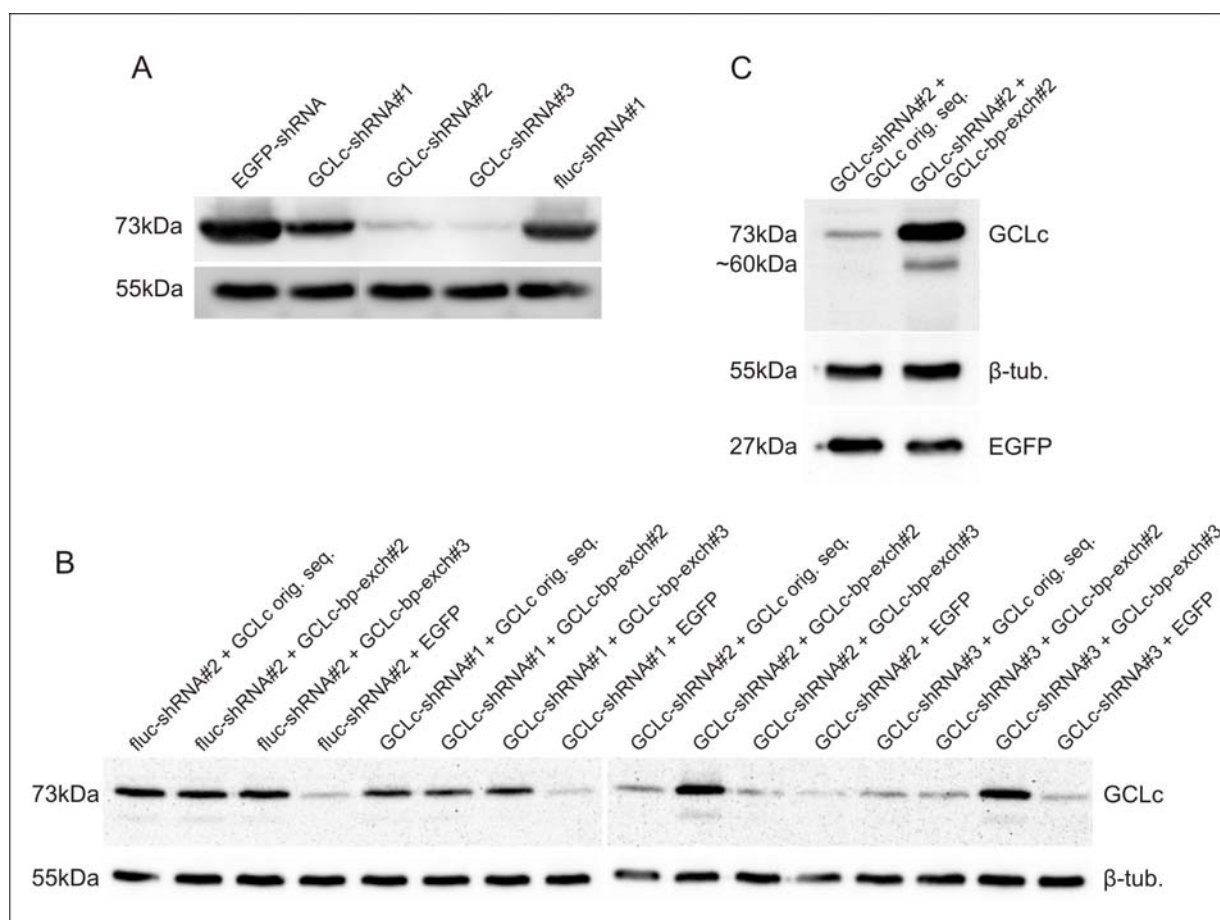


Fig.3.1.3. Western blot protein down regulation analysis by GCLc-specific shRNAs in HEK293 cells. **(A)** HEK293 cells co-transfected with pExpress-1-GCLc and one plasmid expressing a control shRNA (EGFP-shRNA), plasmids expressing different GCLc-specific shRNAs (GCLc-shRNA#1, GCLc-shRNA#2 and GCLc-shRNA#3), or fluc-shRNA#1. **(B)** HEK293 cells co-transfected with 2 plasmids, one expressing the shRNAs, either the control fluc-shRNA#2, or the GCLc specific shRNAs (GCLc-shRNA#1, GCLc-shRNA#2 and GCLc-shRNA#3) in combination with one plasmid expressing either the GCLc original sequence, the GCLc-bp-exch#2, the GCLc-bp-exch#3 or EGFP. **(C)** HEK293 cells co-transfected with one plasmid expressing EGFP and a second plasmid co-expressing GCLc-shRNA#2 plus GCLc original sequence or GCLc-shRNA#2 plus GCLc-bp-exch#2. Membranes were consecutively probed with anti GCLc rat specific antibody, anti-tubulin antibody for loading control and anti-EGFP antibody for transfection control. Cells were harvested 48 hours after transfection. Size standards are shown in the left.

### 3.1.1.2.2. Non targeted GCLc design for “rescue experiments”

In order to rule out that the effects of the expressed shRNAs could result from “off-target” silencing of unrelated transcripts, we intended to prove specificity of the respective shRNA by a so-called “rescue experiment”. In this condition a protein is co-expressed with the specific shRNA which consists of the same amino-acid sequence as the target protein, but contains nucleotides exchanges within its cDNA. Thus, this protein can not be targeted by the shRNA targeting the endogenous protein and its expression should reverse the effect caused by the down-regulation of the endogenous protein. These “new” coding sequences are referred as

GCLc-bp-exch#2 or GCLc-bp-exch#3 (change in the GCLc-shRNA#2 or GCLc-shRNA#3 binding sequences respectively, Fig.3.1.4.).

This strategy is based on the genetic code redundancy, that is, there are various codons coding for the same amino acid. We did 8 nucleotides change in GCLc-bp-exch#2 and 6 nucleotides change in GCLc-bp-exch#3 (Fig.3.1.4.).

Next we tested the resistance of the GCLc-bp-exch#2 expression to GCLc-shRNA#2 and the resistance of GCLc-bp-exch#3 expression to GCLc-shRNA#3. Figure.3.1.3.B shows that both GCLc-bp-exch#2 and GCLc-bp-exch#3 are resistant to GCLc-shRNA#2 or GCLc-shRNA#3, respectively. All sequences were designed to target the rat GCLc mRNA, the GCLc-shRNA#1 and GCLc-shRNA#3 have one non pairing nucleotide with the human sequence. The GCLc-shRNA#2 has 100% pairing complementarity with the GCLc human mRNA sequence, resulting in partial silencing of the endogenous levels of human GCLc in HEK293 cells, Fig. 3.1.3.B.

In Fig. 3.1.3.C, one plasmid expressing the GCLc-shRNA#2 and the GCLc native sequence (original sequence) or the GCLc-shRNA#2 and the GCLc-bp-exch#2 (schematic description Fig. 2.2.4. H) were co-transfected with a plasmid expressing EGFP as transfection control. This transfection was used to validate the expression of GCLc from the same vector that co-expresses the shRNA. This vector had the disadvantage of losing the genetic coded reporter protein (EGFP) that allows for the labelling of all transfected cells. On the other hand it had the advantage of ensuring that all cells expressing the shRNA also express the rescue construct or vice-versa. As can be observed in Fig. 3.1.3.C, there is substantially more GCLc in the condition where the resistant GCLc-bp-exch#2 were transfected as compared with the GCLc original sequence. Transfection efficiency and total protein loaded into the gel was equivalent as assessed with EGFP and  $\beta$ -tubulin immunoblot. One unexpected band appeared at the size of approximately 60 kDa. This band has been reported by others as a result of caspase-3 dependent cleavage of the GCLc (Franklin et al. 2002), indicating that cells react to high levels of GCLc, degrading it in a caspase-3 dependent manner. This same band was also observed with comparable intensity in the GCLc-bp-exch#2 and GCLc-bp-exch#3 expression by a different plasmid in the same cells (Fig. 3.1.3.B).



This experiment showed the high efficiency in GCLc silencing of GCLc-shRNA#2 and GCLc-shRNA#3. The experiment also validated that GCLc-bp-exch#2 and GCLc-bp-exch#3 constructs are resistance to silencing by the respective shRNAs.

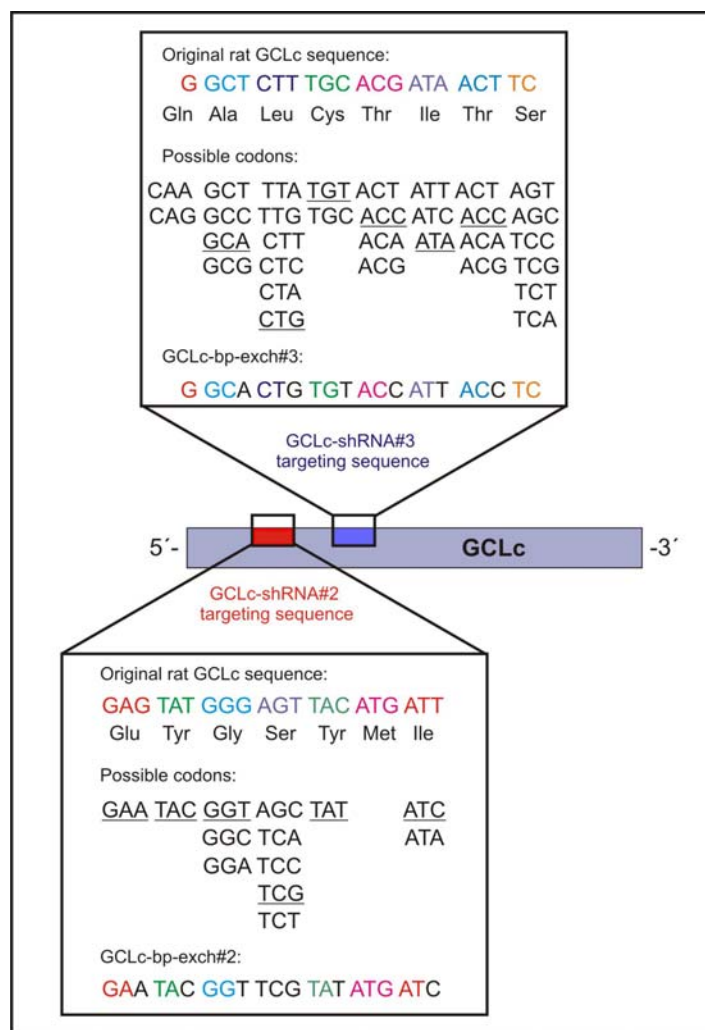


Fig.3.1.4. Schematic description of the original and changed nucleotides coding for GCLc non-targetable mRNAs. The GCLc-shRNA#2 (red rectangle, GCLc mRNA position 286 to 306) and GCLc-shRNA#3 (blue rectangle, GCLc mRNA position 417 to 437) targeting sequences. They encode for the mentioned amino acids that can be replaced by all mentioned possible codons. The underlined codons were chosen, and the final sequence is shown, with the black characters representing the final changes.

### 3.1.1.2.3. Evaluation of GCLm shRNAs efficiency by western blot in HEK293 cells

The activity of the GCL heterodimer depends on the presence of the GCL modulatory subunit (GCLm). Therefore we also designed and constructed shRNAs targeting the GCLm subunit.

In this experiment the designed shRNAs targeting GCLM were evaluated by western blot for their efficacy in rat GCLM silencing. In addition, we evaluated if human GCLM, which differs in sequence from the rat GCLM, could serve as a rescue construct. HEK293 cells were co-transfected with one plasmid expressing either EGFP, or the rat GCLM, or the human GCLM and other plasmid expressing control shRNAs or GCLM specific shRNAs.

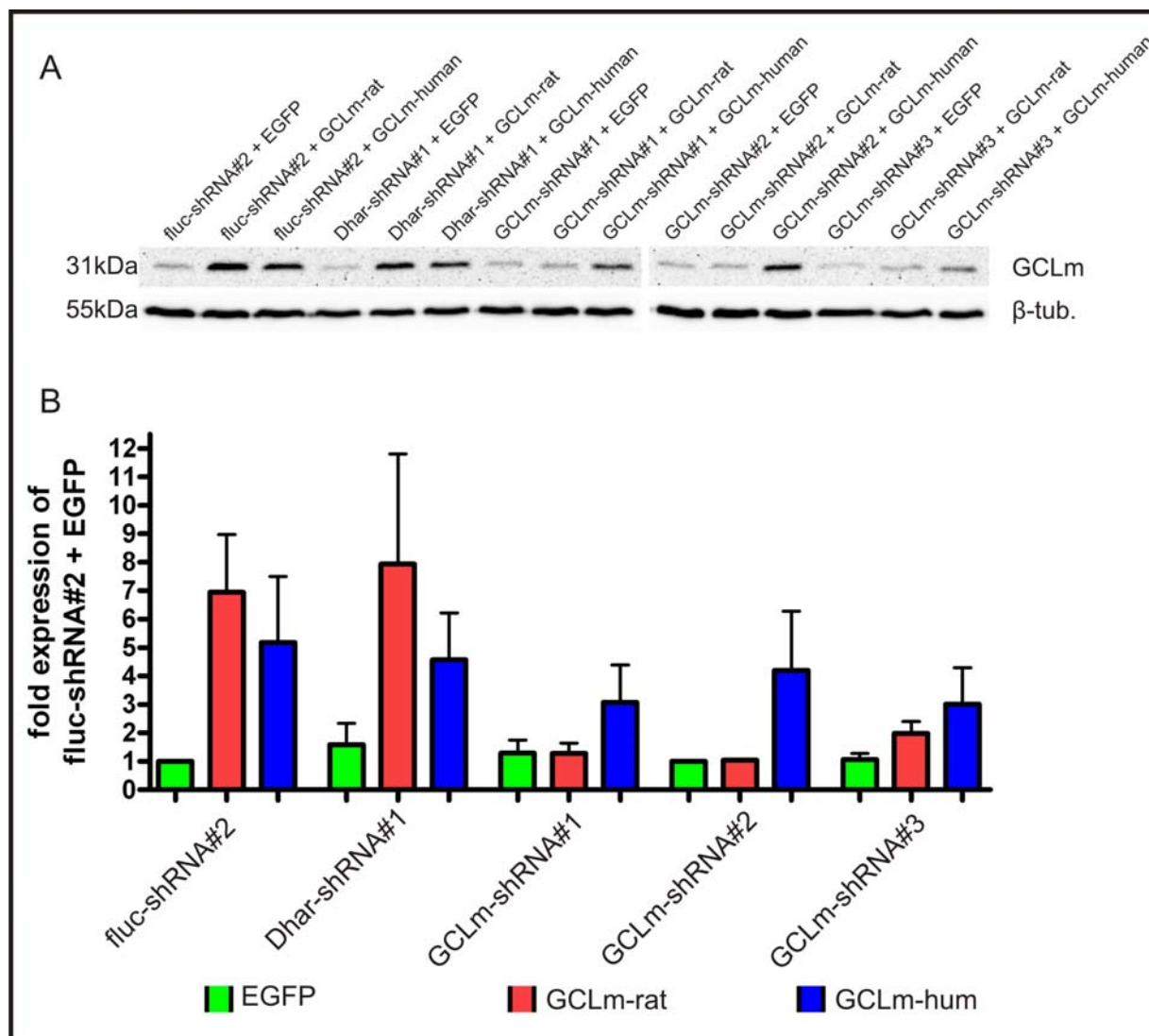


Fig.3.1.5. Analysis by western blot of protein down-regulation by GCLM-specific shRNAs in HEK293 cells. Cells were co-transfected with 2 plasmid DNAs per condition in the 1 to 1 ratio. (A) representative western blot. One plasmid expressing the shRNA combined with one other plasmid expressing EGFP, rat GCLM or human GCLM. Two shRNA control plasmids (fluc-shRNA#2 or Dhar-shRNA#1) were transfected or one of three GCLM shRNAs (GCLM-shRNA#1, GCLM-shRNA#2, or GCLM-shRNA#3). Cells were lysed 48 hours after transfection. Membranes were consecutively probed with anti GCLM rat specific antibody and anti-tubulin antibody for loading control. Size standards are shown in the left. (B) densitometry graph of 3 independent replicates, same conditions as in A, green columns represent EGFP expressing vector, red columns represent GCLM-rat and blue columns represent GCLM-human. The GCLM band densitometry was normalized with the densitometry of the  $\beta$  tubulin band. GCLM content is shown on the Y axis in mean percentage of fluc-shRNA#2 plus EGFP  $\pm$  SD or percentage of GCLM-shRNA#2 plus EGFP  $\pm$  SD.

When rat GCLM was co-transfected in the presence of control shRNAs, there was 5 to 10 fold increase in GCLM protein levels (Fig.3.1.5. A and B). The co-transfection of GCLM and the specific GCLM-shRNA#1 or GCLM-shRNA#2 resulted in complete suppression of GCLM rat protein to endogenous levels (note: HEK cells are human derived). The expression of GCLM-human protein was approximately 3-4 fold of the endogenous levels (Fig.3.1.5.A and B). GCLM-shRNA#3 did not show significant silencing of the GCLM-rat when compared with the GCLM-human expression.

GCLM-shRNA#1 and GCLM-shRNA#2 were selected as the more efficient shRNAs to silence the expression of rat GCLM. They did not target the GCLM human protein, allowing to use human GCLM as a rescue construct. These shRNAs were further used for both *in vitro* and *in vivo* experiments.

### 3.1.2. Construction of AAV vectors for transduction of primary cortical neurons

AAV vectors are excellent tools for gene transfer into neurons in cell culture and long term gene transfer into the mammalian brain. AAV vector genomes with a single (Fig. 3.1.6.A) or bi-cistronic (Fig.3.1.6.B) expression cassette were produced. Due to limited genome capacity of AAV small transcriptional regulatory elements have been used.

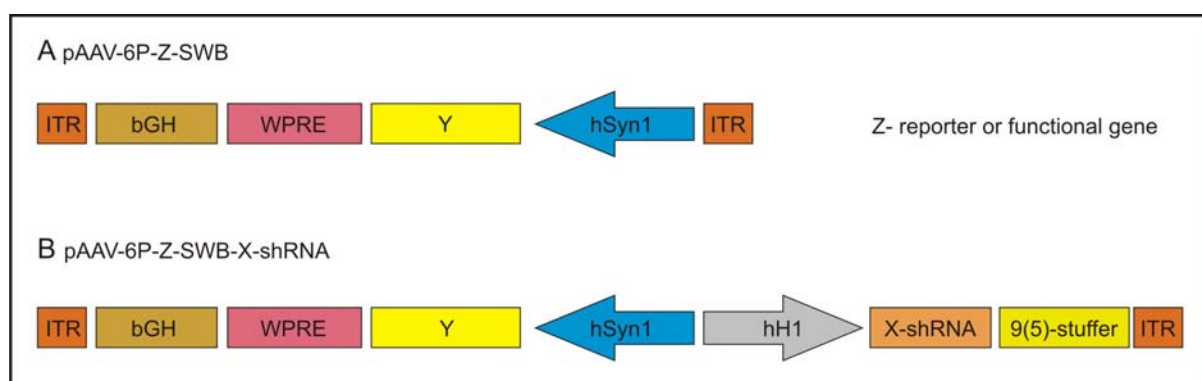


Fig. 3.1.6. Schematic representation of the single (A) and bi-cistronic (B) expression vectors used in this study. (B) Vectors used for the expression of the shRNAs carry a second, independent expression cassette for the expression of a reporter gene or a functional gene (Z) e.g. GCLc, GCLM, or hDJ1. bGH - bovine growth hormone derived polyadenylation site; hH1- human polymerase III H1 RNA promoter; hSyn1- human synapsin 1 gene promoter; ITR-inverted terminal repeats of AAV2; WPRE- woodchuck hepatitis virus posttranscriptional regulatory element; 9(5)-stuffer-untranscribed 2281 bp fragment of the porcine gene UM 9(5)p; X-shRNA- shRNAs sequence; reporter EGFP (enhanced green fluorescent protein) or DsRED2N1 (red fluorescent protein); functional transgene GCLc (glutamate cysteine ligase catalytic subunit), GCLM (glutamate cysteine ligase modulatory subunit), hDJ1(human wild type DJ1), $\alpha$ -synA53T ( $\alpha$ -synucleinA53T)

The expression of a fluorescent reporter gene (Z, e.g. EGFP, DsRED2N1) or a functional transgene (Z, e.g. GCLc, GCLm, hDJ1) was promoted by a short neuron-specific hSyn1 gene promoter. The expression of the shRNA molecule was promoted by a RNA polymerase III promoter, the human H1 promoter (hH1).

### **3.1.2.1. Targeting GCLc protein in primary cortical neuron culture**

Following the construction of recombinant AAV vectors, we first investigated their transduction properties in primary cortical neurons. The transgene expression levels were evaluated by the expression of the EGFP reporter gene in cortical neuron culture. This culture is initially mainly constituted of neurons, but with time the amount of astrocytes increases due to their mitotic properties. Viral transduction was performed at DIV 2 with approximately  $1 \times 10^8$  transducing vector units. The transduction with this amount of virus allows the genetic manipulation of up to 70 % of primary cortical neurons in culture. The onset of transgene expression after AAV vector transduction is often claimed to be “slow”, supposedly due to the necessity of conversion of the single stranded genome into double-stranded DNA, especially in non-dividing cells. Accordingly, when primary cortical cultures were infected by AAV2 EGFP vectors at DIV 2, readily detectable transgene expression emerged in neurons at DIV 6-7, reaching close to 70 % transduction efficacy at DIV 11 (Fig. 3.1.8.A, E). Transgene expression was completely restricted to neurons as identified by anti-NeuN staining (Fig.3.1.7.A).

AAV2 vectors were constructed to express EGFP driven by the GFAP promoter (glial fibrillary acidic protein promoter, an astrocyte specific promoter). The AAV2 serotype transduced and expressed significant EGFP driven by the GFAP promoter in astrocytes (Fig.3.1.7.B). When we immunostained these cultures with GCLc antibody (glutamate cysteine ligase catalytic subunit), we observed that this subunit is strongly expressed in astrocytes when compared to neurons (Fig. 3.1.7.E). As the expression of the shRNAs in all respective vectors is driven by the ubiquitously active H1 promoter, this may result in astrocytic silencing of GSH synthesis. As we intended to evaluate the effects of GSH silencing specifically in neurons, astrocytes were depleted from primary cultures by Ara-C application. Ara-C is a potent anti-mitotic drug used to avoid astrocyte replication (Ahlemeyer et al. 2003). Treatment of the culture with 0.5  $\mu$ M Ara-C reduced significantly the percentage of astrocytes (Fig. 3.1.7.C and D).

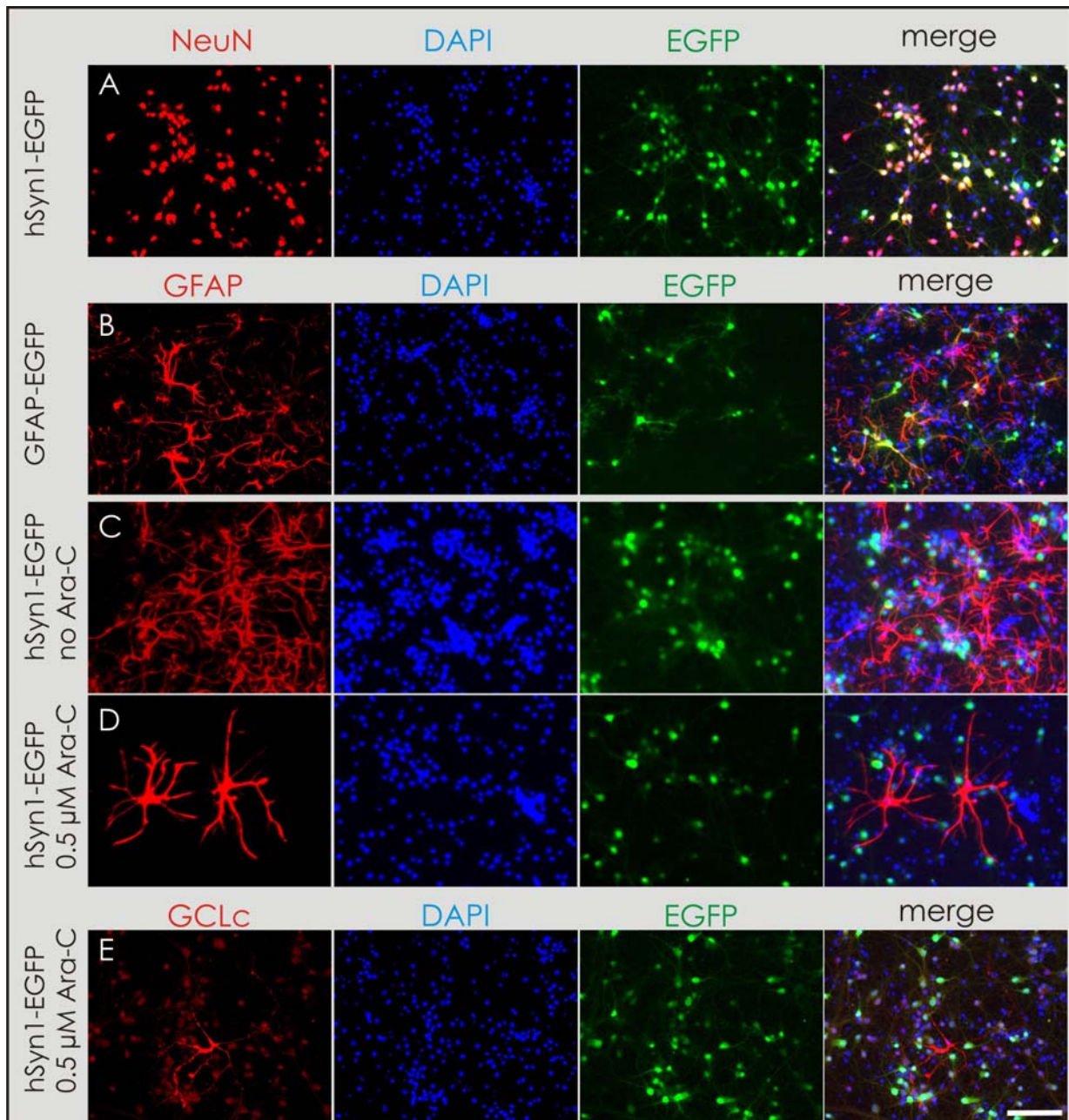


Fig.3.1.7. Primary cortical culture. A, C, D, E- cells transduced with AAV2 hSyn1-EGFP viral vector results in specific neuronal EGFP expression as observed by NeuN staining in A. B- cells transduced with AAV2 GFAP-EGFP viral vector results in specific EGFP expression in astrocytes as observed by GFAP staining. C- without Ara-C treatment and D with 0.5  $\mu$ M Ara-C treatment resulting in neuronal enrichment. E, levels of GCLc in neurons and astrocytes. Cells were transduced with  $1.0 \times 10^8$  tu/well in 24 well plates (250 000 cells/well) of AAV2 vector expressing EGFP at DIV 2. In A cells were stained with NeuN (neuron specific nuclear protein). B-D with GFAP antibody (glial fibrillary acidic protein), in E with GCLc antibody (Glutamate Cysteine Ligase catalytic subunit) In E and E cells were treated with 0.5  $\mu$ M of ARA-C at DIV 3. (Scale bar: 100  $\mu$ m.)

AAV2 vectors transduced both neurons and astrocytes in culture. Treatment of the cultured cells with Ara-C significantly reduced the percentage of astrocytes.

We investigated the efficacy of the AAV2 vectors expressing the GCLc-shRNA#2 in silencing of the endogenous levels of GCLc in primary cortical neuron culture. We also investigated the respective rescue constructs and the effects of  $\alpha$ -synuclein in combination with GCLc-shRNA#2 on cell viability. Figure 3.1.8. show representative pictures from transduced cells.

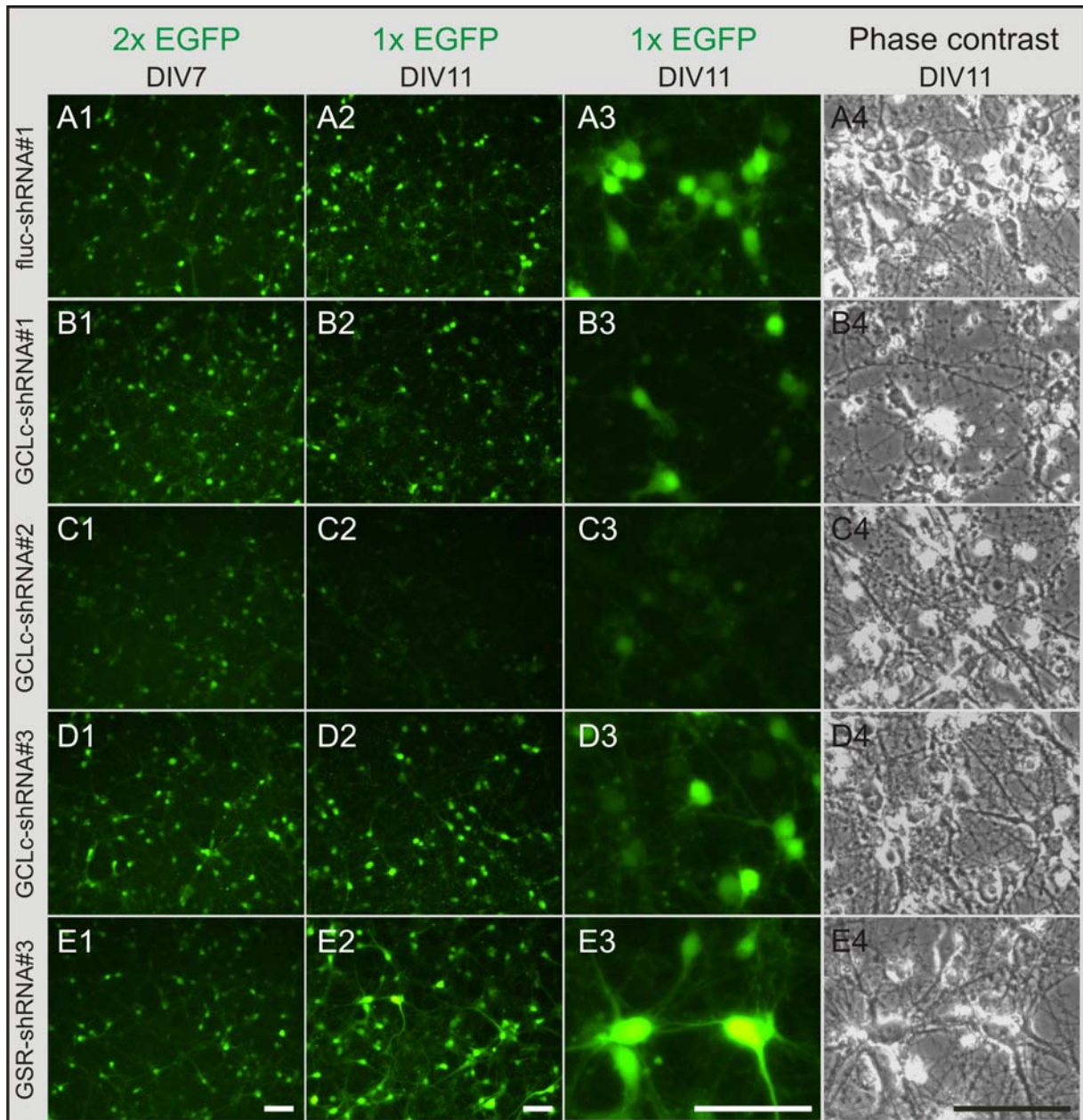


Fig. 3.1.8. EGFP expression in primary cortical neurons transduced with rAAV-shRNAs. Cells (250 000 cells/well) were transduced with  $1 \times 10^8$  t.u./well of AAV2 fluc-shRNA#1 (row A), GCLc-shRNA#1 (row B), GCLc-shRNA#2 (row C), GCLc-shRNA#3 (row D), and GSR-shRNA#3 (row E). Low power magnification photomicrographs in column 1 and 3 or high power magnifications photomicrographs in column 2 and 4 representing EGFP expression (left 2 columns) or phase contrast cells (right two columns) were recorded at DIV11. (Scale bar: 50  $\mu$ m.)

Detectable levels of EGFP fluorescence were observed at DIV7, and at this time point no difference in EGFP expression level was detectable between conditions except for GCLc-shRNA#2 which already at DIV7 showed lower EGFP expression. Note that at DIV7 double EGFP acquisition time was used when compared with DIV11. Between DIV7 and DIV11 in GCLc-shRNA#1 and GCLc-shRNA#2 treated cells the EGFP fluorescence stopped to increase over time. Changes in cell morphology were observed indicating a decrease in cell viability as it can be observed in the phase contrast high magnification photos (Fig.3.1.8 B4, C4). GCLc-shRNA#2 was shown to be effective in GCLc protein silencing (Fig.3.1.3.). GCLc-shRNA#1 which was the least effective in protein silencing in co-transfected HEK293 cells, also induced morphological cellular changes and decreased cell viability. The GCLc-shRNA#3 which effectively silenced GCLc in co-transfection experiments did not induce any apparent change in cell morphology. These results suggested that prediction of efficacy of a given shRNA is difficult if not impossible in heterologous reporter gene systems. Next, cell lysates were made from the primary cortical culture at DIV 10 to verify the silencing properties of GCLc-shRNA#2. We confirmed the capacity of GCLc-shRNA#2 in silencing GCLc when compared with control virus transduced cells (Fig. 3.1.9.).

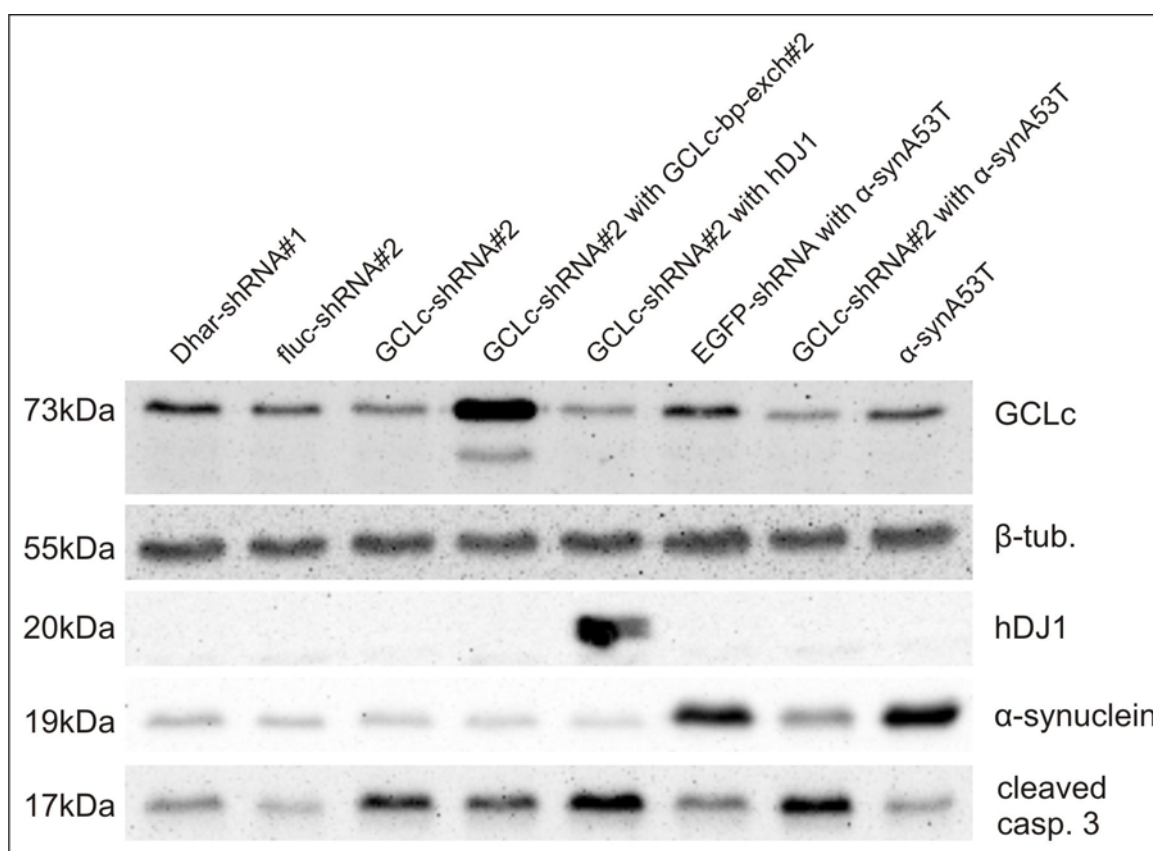


Fig.3.1.9. Western blot analysis of cortical neurons transduced with  $1.0 \times 10^8$  tu/well in 24 well plates using different AAV2 vectors. Cells were transduced with AAV2 expressing Dhar-shRNA#1, fluc-

shRNA#2, GCLc-shRNA#2, GCLc-shRNA#2-with-GCLc-bp-exch#2, GCLc-shRNA#2-with-hDJ1, EGFP-shRNA with  $\alpha$ -synA53T, GCLc-shRNA#2 with  $\alpha$ -synA53T and  $\alpha$ -synA53T. Cells were harvested at DIV10. Membranes were consecutively probed with anti GCLc rat specific antibody, anti-tubulin antibody for loading control, anti-cleaved caspase-3, anti- $\alpha$ -synuclein and anti-hDJ1. Size standards are shown in the left.

High levels of GCLc protein were detected when GCLc-bp-exch#2 was co-expressed with GCLc-shRNA#2. As observed in HEK293 cells the expression of GCLc-bp-exch#2 results in the appearance of a 60 kDa protein recognized by the GCLc antibody that has been reported to be the result of active caspase-3 dependent cleavage of GCLc. Another attempt to rescue the effect of GCLc silencing was performed based on the observation that human wild type DJ1 (hDJ1) induces 2.5 fold increase in GCLc mRNA in cells and by this means increases GCLc activity (Zhou and Freed 2005). Expression of hDJ1 in the presence of GCLc-shRNA#2 did not result in a net increase in the GCLc protein level (Fig.3.1.9.). Thus it may be that DJ1 does induce the up-regulation of GCLc mRNA but because the mRNA is targeted for degradation by the specific GCLc-shRNA#2 there is no net increase in GCLc protein. Figure 3.1.9. also shows the EGFP control shRNA expression together with a genetic mutant of  $\alpha$ -synuclein ( $\alpha$ -synuclein A53T). When the GCLc-shRNA#2 was co-expressed with the  $\alpha$ -synuclein, there was a reduction of GCLc protein levels (Fig.3.1.9.), this effect was not present when EGFP-shRNA was expressed with  $\alpha$ -synuclein A53T or with  $\alpha$ -synuclein A53T expression only. The down-regulation of GCLc by the shRNA#2 was shown in three independent constructs/virus in comparison with the respective controls. Expression of  $\alpha$ -synuclein A53T is shown at the corresponding size of 19 kDa.

In summary, GCLc-shRNA#2 is effective in GCLc silencing in cortical neurons, the GCLc-bp-exch#2 is resistant to degradation and the hDJ1 does not induce an increase in cellular GCLc protein in primary cortical neurons.

### **3.1.2.2. GCLc silencing induced cell viability loss in primary cortical culture**

Cellular change in morphology and fragmentation of neurites observed in phase contrast microscopy together with the weak EGFP expression was suggestive for decreased cell viability. In order to quantify cell viability the WST-1 assay was used. This test is based on the measurement of the activity of mitochondrial succinate dehydrogenase in living cells.



Figure 3.1.10. shows in A the cell viability at DIV 9 and in B at DIV12 after viral transduction.

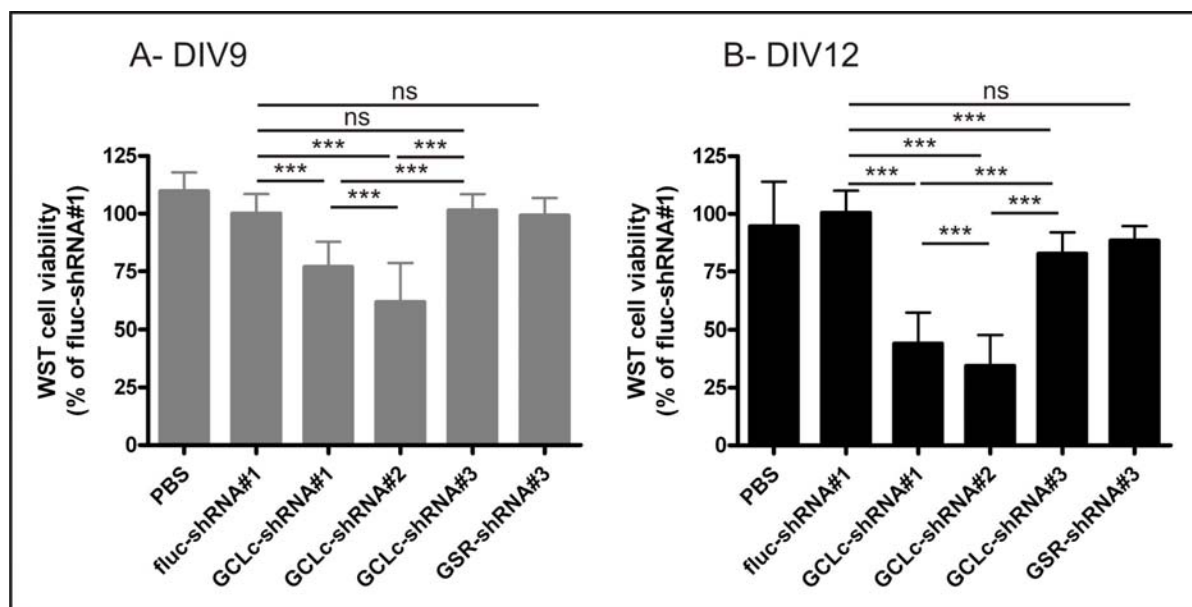


Fig.3.1.10. Cell viability assay of cortical neurons in culture at DIV9 (A) and DIV12 (B). Cells were treated with PBS or transduced with virus expressing a control shRNA (fluc-shRNA#1), one of three different GCLc-specific shRNAs (GCLc-shRNA#1; GCLc-shRNA#2; and GCLc-shRNA#3), or the GSR specific shRNA (GSR-shRNA#3). Cells (250 000 cells/well) were treated at DIV 2 with  $1.0 \times 10^8$  tu/well of the described virus. Cell viability is shown on the Y axis in mean percentage of control  $\pm$  SD (fluc-shRNA#1) from at three independent experiments performed at least in triplicate. (\*\*\*) $p < 0.001$ , (\*\*) $p < 0.01$ , (\*) $p < 0.05$  and ns  $p > 0.05$  (non-significant))

The GCLc-shRNA#1, and GCLc-shRNA#2 induced significant cell death both at DIV9 and DIV12. These results were in accordance with the microscope observations, and have shown for the GCLc-shRNA#2 a direct correlation between silencing efficiency and cell death. GCLc-shRNA#3 did not induce significant cell death at DIV 9 but showing milder cell death at DIV12. The GCLc-shRNA#1 considered to be the least effective shRNA in HEK293 cells showed high levels of cell death both at DIV9 and DIV12.

These experiments demonstrated the increase of neurodegenerative processes due to the targeting of GCLc in primary neurons.

### 3.1.2.3. GCLc cell loss mechanism in primary cortical culture

Other groups have reported that glutathione depletion results in apoptotic cell death (Nicole et al. 1998;Wullner et al. 1999). We addressed the levels of cleaved caspase-3, the key executioner of apoptosis using a specific antibody recognizing the large fragment (17/19 kDa) of activated caspase-3. We did observe endogenous levels of active caspase-3, indicating neuronal degeneration that can be attributed to some cell death which cortical neurons exhibit in culture. The other possible reason for this endogenous levels of cleaved caspase-3 is the application of Ara-C, reported to induce cell death in a caspase-3 dependent way in astrocytes and neurons (Courtney and Coffey 1999;Geller et al. 2001). Cortical neurons treated with GCLc-shRNA#2 exhibited higher cleaved caspase-3 levels in all studied vector combinations in comparison with the respective controls ( Fig.3.1.9.). The increase in cleaved caspase-3 was also investigated at the cellular level by ICC in cells transduced with AAV vectors. There was an increase in cleaved caspase-3 staining in conditions where GCLc-shRNA#2 was used (data not shown).

These results indicate that caspase-3 is involved in cell death induced by GCLc-shRNA#2 expression, suggesting cell death to be at least partially apoptotic.

### 3.1.2.4. Glutathione quantification upon GCLc silencing in primary cortical culture

To ensure that the described effects in cell death are due to GSH depletion, the total cellular glutathione content (GSx) was measured after AAV2 mediated shRNA expression. The assay used allows for determination of both GSx and oxidized glutathione (GSSG) using two distinct procedures. Although the levels of GSx were found to be reduced, there was no increased levels of the oxidized form of glutathione (GSSG), which were always very small (at the method's detection limit) and equivalent in all conditions. For this reasons we consider the GSx levels to truly reflect the GSH cellular content. The measured GSx content was normalized to protein level of each lysate. This procedure ensures that GSx was measured independently from potentially ongoing neurodegeneration on a “per cell basis”. These experiments demonstrated that there was not a reduction of GSx as a consequence to cell

death but that GSx was reduced per cell. As predicted, GCLc-shRNA#1 and GCLc-shRNA#2 produced a significant decrease in the GSx levels when compared with control fluc-shRNA#1 both at DIV 9 and DIV 12. (Fig. 3.1.11.).

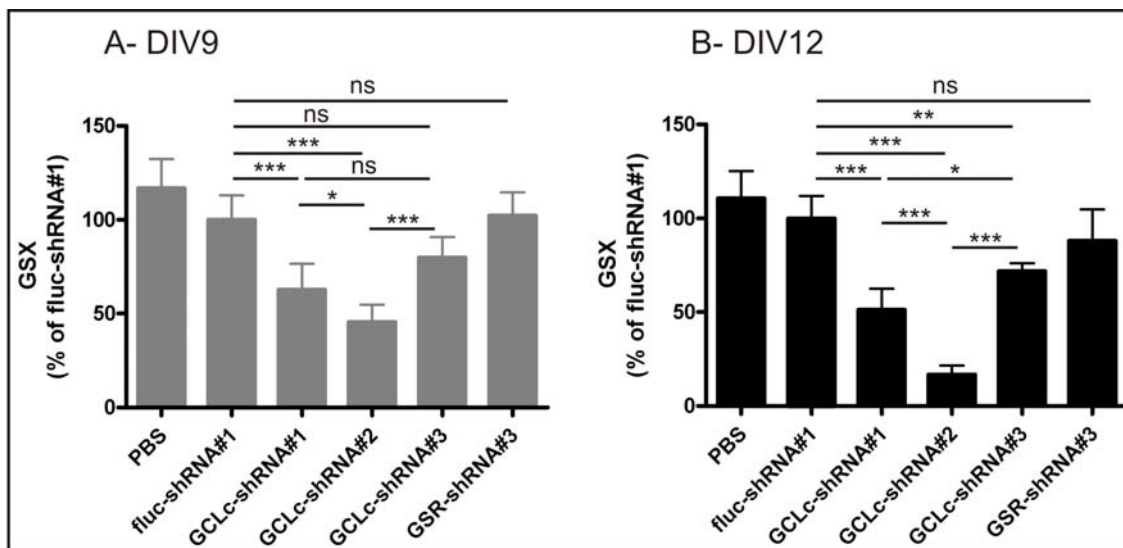


Fig. 3.1.11. Total glutathione measurement of cortical neurons in culture at DIV9 (A) or DIV12 (B). Cells were treated with PBS, or transduced with a virus expressing a control shRNA (fluc-shRNA#1), one of three different GCLc-specific shRNAs (GCLc-shRNA#1, GCLc-shRNA#2, and GCLc-shRNA#3), or the GSR specific shRNA (GSR-shRNA#3). Cells (250 000 cells/well) were treated at DIV 2 with  $1.0 \times 10^8$  tu/well of the described virus. GSx content was normalized to protein level of each lysate. Total glutathione content is shown on the Y axis in mean percentage of control  $\pm$  SD (fluc-shRNA#1) from at least three independent experiments performed at least in triplicate. (\*\*\*) $p < 0.001$ , (\*\*) $p < 0.01$ , (\*) $p < 0.05$  and ns  $p > 0.05$  (non-significant)).

The decrease in GSx content is directly correlated with the verified loss in cell viability, i.e. the GCLc-shRNA#1 and GCLc-shRNA#2 induced higher GSx decrease and high cell death. GCLc-shRNA#3 expression resulted in a small decrease in cell death and GSx levels only significant at DIV12.

In summary, this experiment shows that there is a reduction in cellular glutathione with the silencing of GCLc. The extent of GSx reduction is directly correlated with the decrease in cell viability.

### 3.1.2.5. Influence of GCLc-shRNA#2 and $\alpha$ -synucleinA53T expression on reduction of GSH levels in primary cortical culture

We attempted to combine and possibly enhance the toxicity driven by GCLc silencing with the overexpression of a PD associated mutant form of  $\alpha$ -synuclein ( $\alpha$ -synuclein A53T). For this purpose, the control EGFP-shRNA or the GCLc-shRNA#2 was co-expressed with  $\alpha$ -synucleinA53T. Expression of  $\alpha$ -synucleinA53T failed to induce reduction in cell viability when compared with the PBS treated cells (Fig.3.1.12.). Without significance, rather there was a small tendency of an increase in cell viability when  $\alpha$ -synucleinA53T expression was compared with control shRNAs only. We could not observe an increase in cell toxicity provoked by  $\alpha$ -synuclein A53T in combination with GCLc-shRNA#2, rather there was a significant improvement in cell viability at DIV 9 and 12 when compared with GCLc-shRNA#2 expression only (Fig.3.1.12.). The  $\alpha$ -synuclein A53T expression was confirmed by ICC (data not shown) and by western blot (Fig.3.1.9.).

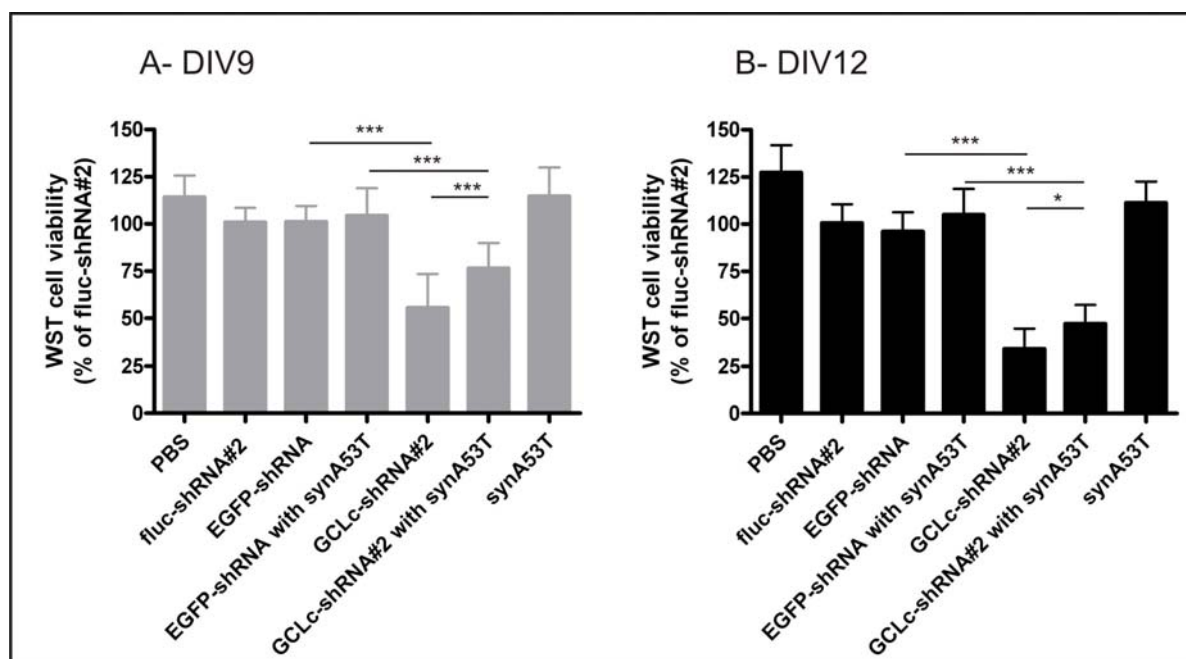


Fig.3.1.12. Cell viability assay of cortical neurons in culture at DIV9 (A) and DIV12 (B). Cells were treated with PBS or transduced with a virus expressing a control shRNA (fluc-shRNA#2) or a second control shRNA (EGFP-shRNA), one control shRNA plus the mutant  $\alpha$ -synucleinA53T (EGFP-shRNA with synA53T), the best GCLc-specific shRNA (GCLc-shRNA#2), the GCLc-shRNA#2 plus the mutant  $\alpha$ -synucleinA53T (GCLc-shRNA#2 with synA53T) or the mutant  $\alpha$ -synucleinA53T only (synA53T). Cells (250 000 cells/well) were treated at DIV 2 with  $1.0 \times 10^8$  tu/well of the described virus. Cell viability is shown on the Y axis in mean percentage of control  $\pm$  SD (fluc-shRNA#2) from at least three independent experiments performed at least in triplicate. (\*\*\*) $p < 0.001$ , (\*\*) $p < 0.01$ , (\*) $p < 0.05$  and ns  $p > 0.05$  (non-significant)).

Expression of  $\alpha$ -synuclein A53T does not increase neurotoxicity of GCLc targeting, but rather demonstrated a minor but significant rescue effect.

### 3.1.2.6. No prevention of neurotoxicity of GCLc targeting effects by expression of rescue constructs!

In addition, we tested the prevention of GCLc-shRNA#2 induced cell death with the expression of two rescue constructs. Prevention by the expression of GCLc-bp-exch#2 or hDJ1 would also prove the specificity of the shRNA approach. In this expression vectors the shRNA is expressed in the same vector as the rescue construct, ensuring that all cells expressing the shRNA also express the rescue gene (Fig.3.1.6.B). At DIV9 and DIV12 the GCLc-bp-exch#2 did not significantly rescue GCLc-shRNA#2 induced cell viability loss. The overexpression of hDJ1 showed significant cell viability rescue at DIV9 without a significant effect at DIV12 (Fig.3.1.13.).

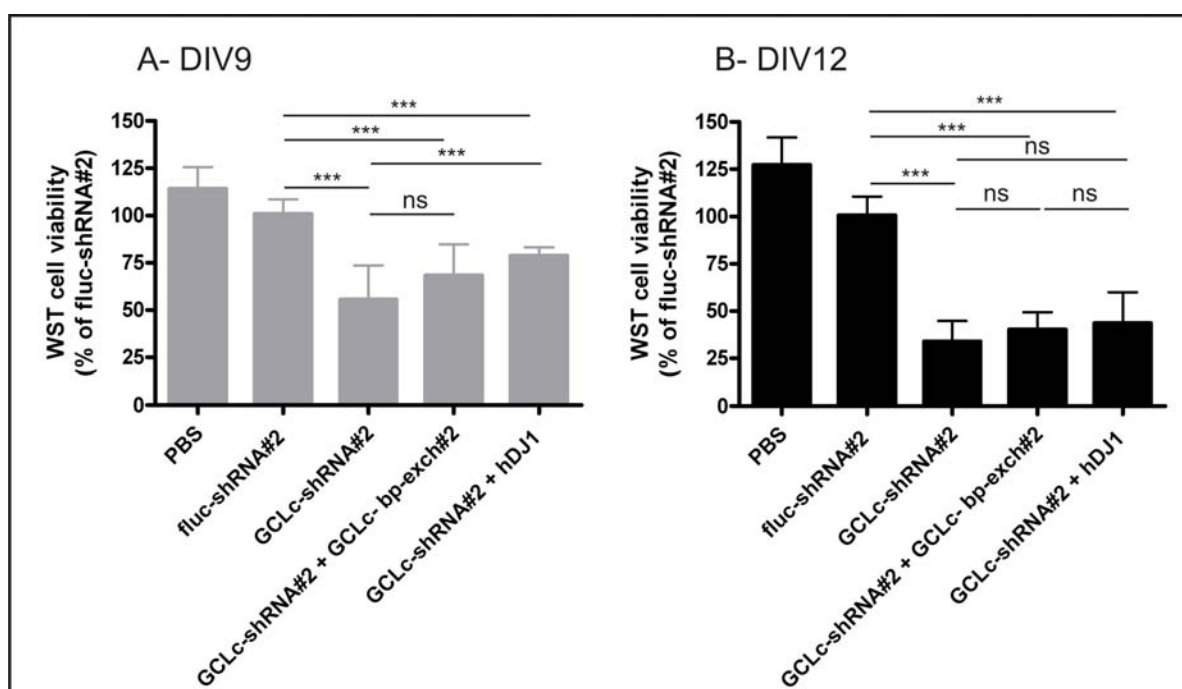


Fig.3.1.13. Cell viability assay of cortical neurons in culture at DIV9 (A) or DIV12 (B). Cells were treated with PBS, transduced with a virus expressing a control shRNA (fluc-shRNA#2), the GCLc-shRNA#2, the rescue construct expressing a resistant form of GCLc (GCLc-shRNA#2 + GCLc-bp-exch#2) or other rescue construct GCLc-shRNA#2 + hDJ1. Cells (250 000 cells/well) were treated at DIV 2 with  $1.0 \times 10^8$  tu/well of the described virus. Cell viability is shown on the Y axis in mean percentage of control  $\pm$  SD (fluc-shRNA#2) from at least three independent experiments performed in triplicate. (\*\*\*) $p < 0.001$ , (\*\*) $p < 0.01$ , (\*) $p < 0.05$  and ns  $p > 0.05$  (non-significant)).

The general failure in the prevention of neurotoxicity was not due to failure in the rescue protein's expression. As shown in figure 3.1.9., substantial expression of GCLc-bp-exch#2 and hDJ1 was achieved. GCLc expression was also evaluated by ICC using a GCLc specific antibody. A reduction in GCLc levels in cells expressing GCLc-shRNA#2 and an increase in staining in cells co-expressing GCLc-shRNA#2 and GCLc-bp-exch#2 was observed (data not shown).

For the GCLc-shRNA#3, we created the GCLc-bp-exch#3 which is non-targeted by this shRNA. Here we employed two viruses, one virus expressing the GCLc-shRNA#3 plus the EGFP reporter, and a second virus expressing GCLc-bp-exch#3. Both at DIV9 and DIV13 the expression of GCLc-bp-exch#3 did not prevent the GCLc-shRNA#3 induced effects (Fig. 3.1.14.).

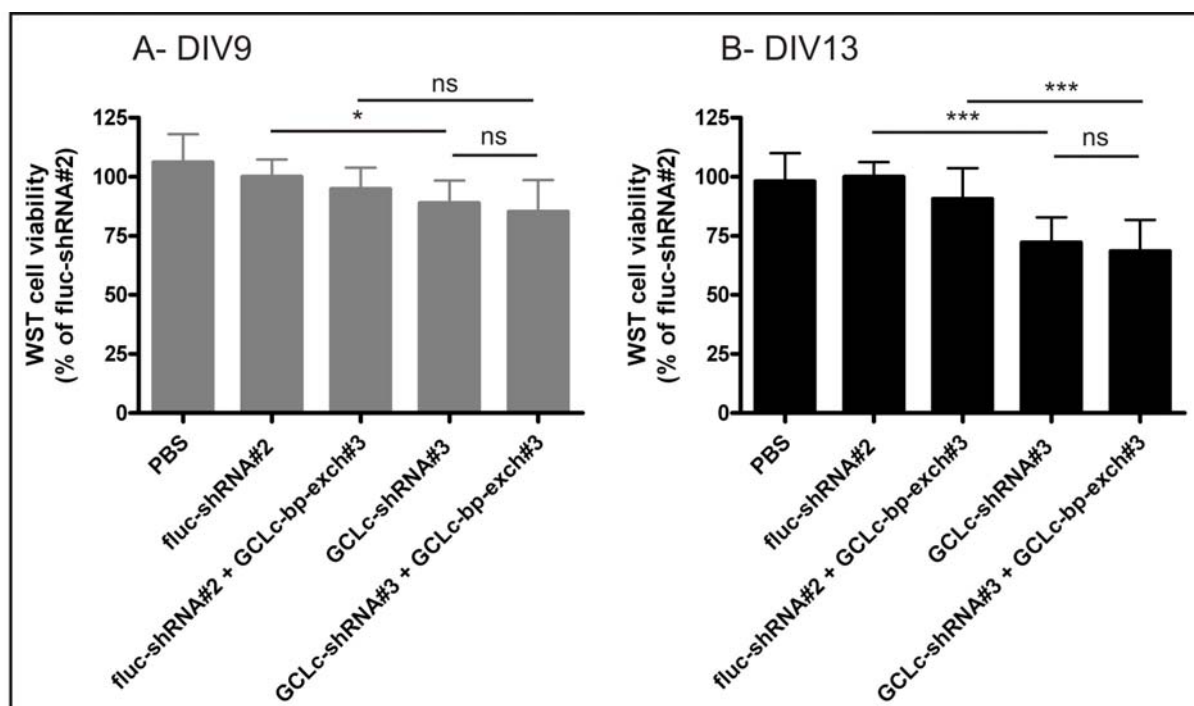


Fig. 3.1.14. Cell viability assay of cortical neurons in culture at DIV9 (A) and DIV13 (B). Cells were treated with PBS, or transduced with a virus expressing a control shRNA (fluc-shRNA#2), the control fluc-shRNA#2 plus the GCLc-shRNA#3 rescue construct (GCLc-bp-exch#3), one GCLc-specific shRNA (GCLc-shRNA#3) and the GCLc-shRNA#3 plus GCLc-bp-exch#3. Cells (250 000 cells/well) were treated at DIV 2 with a total of  $1.5 \times 10^8$  tu/well of the described virus ( $0.75 \times 10^8$  tu/well each virus, one virus without promoter/transgene expression was used to achieve the same total amount of virus/well). Cell viability is shown on the Y axis in mean percentage of control  $\pm$  SD (fluc-shRNA#2) from at least three independent experiments performed at least in triplicate. (\*\*\*) $p < 0.001$ , (\*\*) $p < 0.01$ , (\*) $p < 0.05$  and ns  $p > 0.05$  (non-significant)).

Next, we analysed the expression of GCLc-bp-exch#3 both by immunoblot (data not shown) and ICC. Using both techniques, we observed strong expression of GCLc-bp-exch#3, note that the recording time in cells expressing GCLc-bp-exch#3 was 3 times lower (Fig. 3.1.15.)

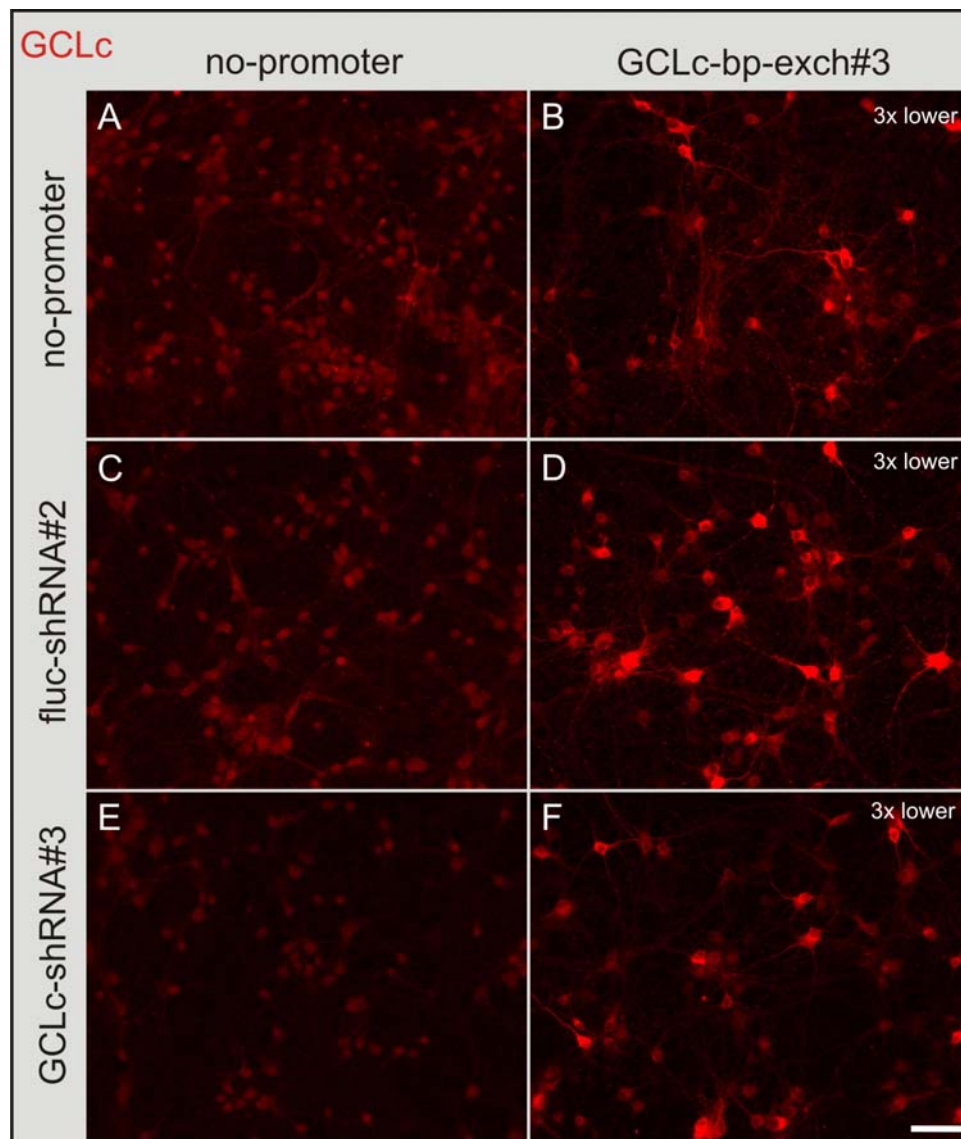


Fig. 3.1.15. GCLc expression levels in primary cortical neurons transduced with rAAV-shRNAs. Cells (250 000 cells/well) were treated with PBS (row A) or transduced with  $1.5 \times 10^8$  t.u./well of AAV2 ( $0.75 \times 10^8$  t.u. of each virus/well, 2 virus/well). (B) fluc-shRNA#2 plus no-prom; (C) fluc-shRNA#2 plus GCLc-bp-exch#3; (D) GCLc-shRNA#3 plus no-prom; (E) GCLc-shRNA#3 plus GCLc-bp-exch#3; (F) GCLm-hum plus no-prom; (G) GCLc-bp-exch#3 plus no-prom. In conditions B, D and F the GCLc exposition time is 3 times lower (3x lower). GCLc fluorescence photomicrographs representing GCLc levels. Cells were recorded at DIV11. (Scale bar: 50  $\mu$ m.)

The failure in cell loss reversion could theoretically be attributed to expression of an inactive or dominant negative GCLc enzyme, although this possibility was very unlikely, as the rescue construct hold the same aminoacid composition as the endogenous protein. To address this question, we measured total glutathione in cells expressing GCLc-bp-exch#2 and GCLc-bp-

exch#3. Expression in primary cortical neurons of non-targetable GCLc's resulted in approximately 1.5 to 2.5 fold GSx level increase in cells co-expressing control or GCLc specific shRNAs (Fig. 3.1.16.).The co-expression of hDJ1 and GCLc-shRNA#2 did not result in increased GSx levels at both studied time points.

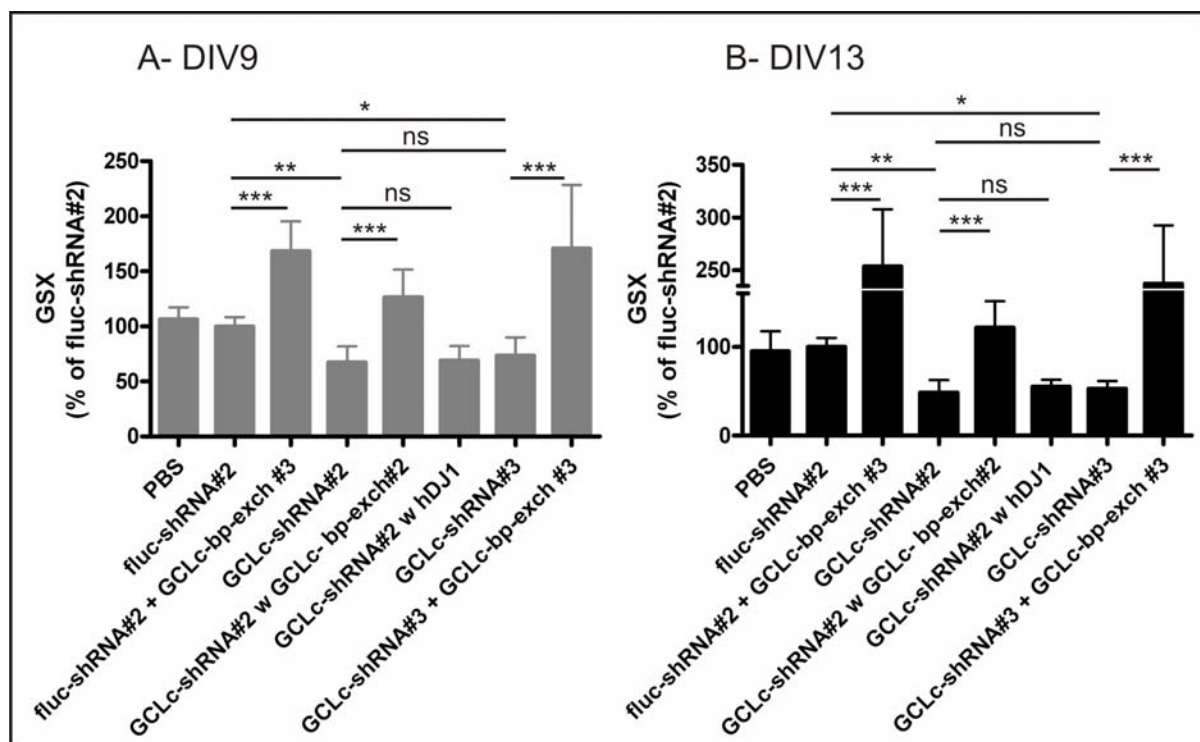


Fig. 3.1.16. Total glutathione measurement of cortical neurons in culture at DIV9 (A) and DIV13 (B). Cells were treated with PBS, or transduced with virus expressing a control shRNA (fluc-shRNA#2 plus no-prom); the control fluc-shRNA#2 plus GCLc-bp-exch#3; GCLc-shRNA#2 plus no-prom; GCLc-shRNA#3 plus no-prom; GCLc-shRNA#2 with GCLc-bp-exch#2 plus no-prom; GCLc-shRNA#2 with hDJ1 plus no-prom; and GCLc-shRNA#3 plus GCLc-bp-exch#3. Cells were transduced at DIV2 with a total of  $1.5 \times 10^8$  tu/well of the described virus ( $0.75 \times 10^8$  tu/well each virus). Total glutathione is shown on the Y axis in mean percentage of control  $\pm$  SD (fluc-shRNA#2) from at least two independent experiments performed at least in triplicate. (\*\*\*) $p < 0.001$ , (\*\*) $p < 0.01$ , (\*) $p < 0.05$  and ns  $p > 0.05$  (non-significant)).0

In summary, for GCLc-shRNA#2 at DIV9 there is a small tendency towards cell death rescue by GCLc-bp-exch#2 and significant rescue by hDJ1. At DIV12 both approaches failed to prevent cell death. For GCLc-shRNA#3 at both time points expression of GCLc-bp-exch#3 failed to prevent cell death. Both GCLc-shRNA#2 and GCLc-shRNA#3 expression resulted in a active protein which significantly increased GSx production. These results challenged the assumed specificity of the shRNAs used for the targeting of GCLc!



### 3.1.3. Targeting the modulatory subunit of the GCL holoenzyme

Results obtained so far by targeting the catalytic subunit of glutamate cysteine ligase (GCLc) demonstrated a pronounced reduction of GSx, cell viability and integrity or neurite morphology. Three different shRNAs resulted in different levels of neurodegeneration, while two control shRNAs demonstrated only a minor impact on neuronal integrity. The impact of control shRNAs on neuronal physiology can not be neglected, but the fact that three different specific shRNAs resulted in gradual induction of neurodegeneration through glutathione depletion suggested that this effect was indeed specific and depends on the level of GCLc downregulation.

However it has not been possible to significantly “rescue” the shRNA mediated silencing of GSH production by co-expression of a non-targetable GCLc. Thus, it could not be ruled out formally that degeneration of cultured cortical neurons was not due to reduction of GSH but due to “off-target” effects of the three “specific” shRNAs, although it is difficult to explain how three different shRNAs should generate the same “off-target” effect.

Levels of GSH production also depend on the presence of the modulatory subunit of GCL, GCLm, which forms a heterodimer with GCLc to generate a highly active enzyme. Thus, we decided to target GCLm in order to confirm that another set of shRNAs targeting a distinct mRNA coding for a necessary component of the holoenzyme would result in the same phenotype of neurodegeneration though depletion of GSH synthesis.

While experiments targeting GCLc were performed by using one viral vector for each condition (i.e. one vector expressing both the shRNA and the EGFP reporter or the rescue construct) we decided for higher flexibility in the experiments targeting GCLm. Here, we employed two viruses per transduction, e.g. one virus expressing the shRNA plus the EGFP reporter, and a second virus expressing the rescue construct. In the case that only one functional construct was intended to be expressed, the second virus was an “empty” vector which lacked a promoter (termed no-promoter) and thus expressed only very low levels of EGFP.

### **3.1.3.1. Targeting GCLM protein in primary cortical neuron culture**

All viruses co-expressing the shRNAs and EGFP were tested in cortical neurons. At DIV7 the cells transduced with the GCLM-shRNA#1 showed lower EGFP fluorescence, although EGFP fluorescence in cells expressing GCLM-shRNA#2 was not different from control. The difference in EGFP fluorescence increased over time and at DIV13 there was evident cell loss and low EGFP expression in cells expressing GCLM-shRNA#1 with or without GCLM-human expression (data not shown). Both shRNAs specific for rat GCLM do not target the expression of GCLM human protein which was used as rescue construct. High power magnification phase contrast micrographs showed that cells transduced with GCLM-shRNA#1 with or without GCLM-human expression looked less viable, with more round shape detached cells and fragmented projections, recapitulating the effect observed upon GCLC-shRNA#2 expression (Fig. 3.1.17.).

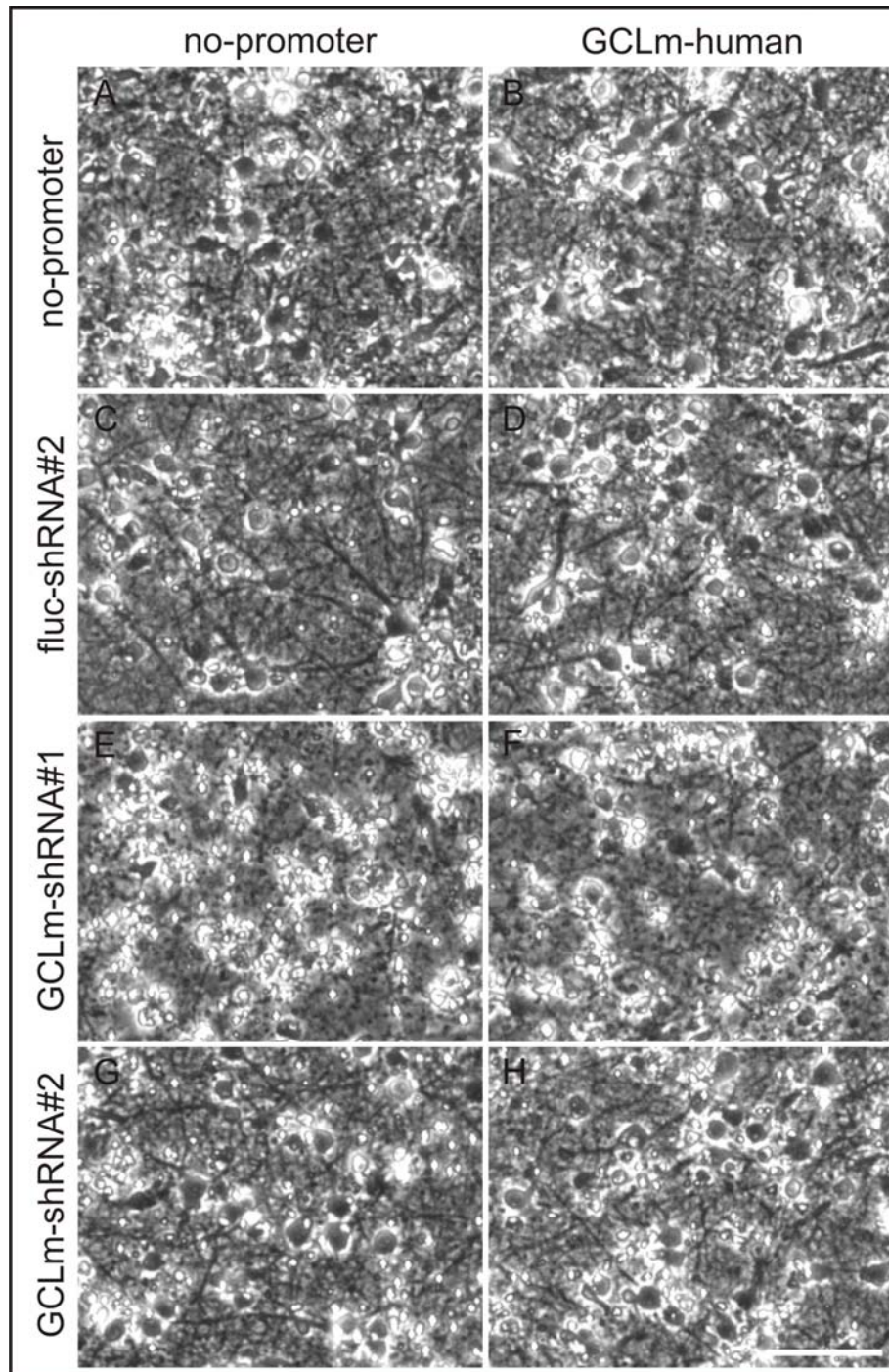


Fig. 3.1.17. Phase contrast photomicrographs of primary cortical neurons, at DIV13, transduced with AAV2 viral vectors. Cells were transduced with two AAV2 virus ( $0.75 \times 10^8$  t.u. of each virus/well). Transduced with A- no-promoter; B- GCLm-human plus no-prom; C- fluc-shRNA#2 plus no-prom; D- fluc-shRNA#2 plus GCLm-human; E- GCLm-shRNA#1 plus no-prom; F- GCLm-shRNA#1 plus GCLm-human; G- GCLm-shRNA#2 plus no-prom; H- GCLm-shRNA#2 plus GCLm-human. (Scale bar: 50  $\mu$ m.)

Further the silencing of the modulatory subunit of glutamate cysteine ligase (GCLm) in cortical neurons in culture with two shRNAs was analysed (Fig.3.1.5.). Endogenous GCLm is difficult to detect by western blot in cortical primary neurons, nevertheless GCLm-shRNA#1

showed a decrease of GCLm levels in cortical neurons (Fig.3.1.18.). The GCLm-shRNA#2 showed higher silencing efficiency, abolishing almost completely the endogenous expression of GCLm (Fig.3.1.18.).

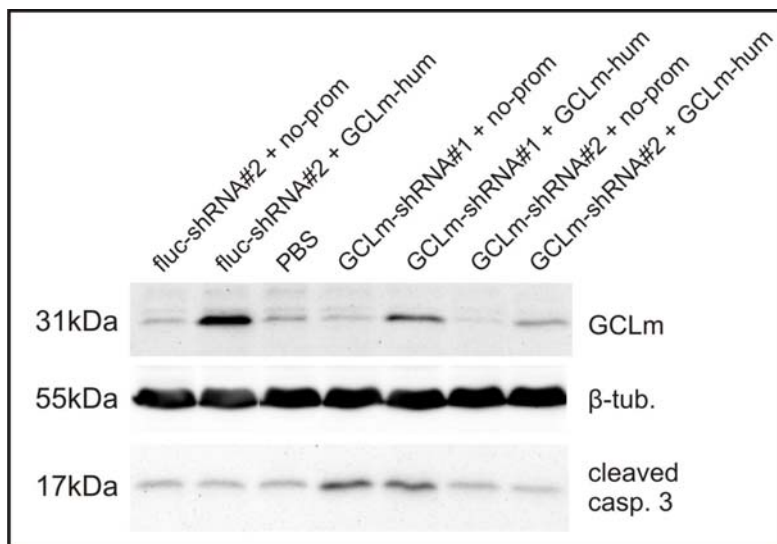


Fig.3.1.18. Western blot analysis of cortical neurons transduced with two different virus per condition in a total of  $1.5 \times 10^8$  tu/well ( $0.75 \times 10^8$  tu/well each virus). Cells were transduced with fluc-shRNA#2 plus no-prom, fluc-shRNA#2 plus GCLm-hum, treated with PBS, GCLm-shRNA#1 plus no-prom, GCLm-shRNA#1 plus GCLm-hum, GCLm-shRNA#2 plus no-prom, GCLm-shRNA#2 plus GCLm-hum. Cells were harvested 7 days after transduction. Membranes were consecutively probed with anti GCLm specific antibody, anti-tubulin antibody for loading control and anti-cleaved caspase 3. Size standards are shown in the left.

The expression of GCLm-human was consistently lower in combination with the GCLm-shRNAs #1 and #2 when compared with the GCLm-human co-expressed with control shRNA (Fig.3.1.18.). Although GCLm-shRNA#1 and GCLm-shRNA#2 contain 5 and 2 mismatches with the sequence of GCLm-human, respectively.

For qualitative comparison of silencing efficiency of shRNAs, neurons in culture were grown on coverslips, transduced with AAV vectors and stained with a GCLm specific antibody. GCLm-shRNA#1 and GCLm-shRNA#2 expression resulted in reduced intensity of GCLm immunostaining, thus indicating effective GCLm silencing (Fig. 3.1.19. E and G). GCLm-shRNA#1 or GCLm-shRNA#2 co-expressed with the GCLm-human resulted in increased GCLm staining. Nevertheless, in these conditions the number of cells overexpressing GCLm and the staining intensity was reduced when compared with the co-expression of control shRNA and GCLm-human or GCLm-human expression only (Fig. 3.1.19. B and D).

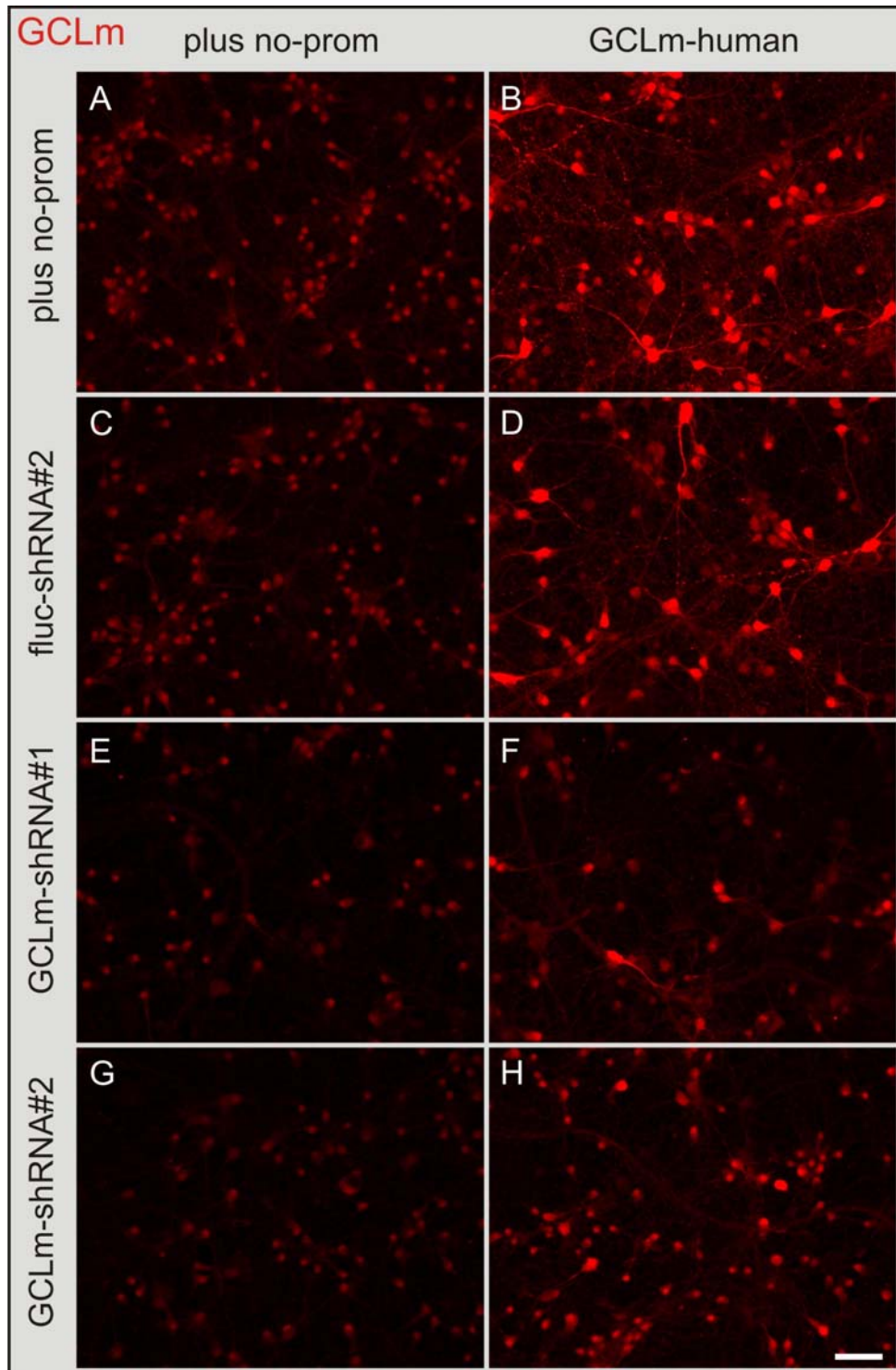


Fig. 3.1.19. GCLm expression levels in primary cortical neurons transduced with AAV shRNAs. Cells were transduced with AAV vectors coding in A- no-promoter; B- GCLm-hum plus no-prom; C- fluc-shRNA#2 plus no-prom; D- fluc-shRNA#2 plus GCLm-hum; E- GCLm-shRNA#1 plus no-prom; F- GCLm-shRNA#1 plus GCLm-hum; G- GCLm-shRNA#2 plus no-prom; H- GCLm-shRNA#2 plus GCLm-hum. GCLm fluorescence photomicrographs. Cells were fixed at DIV12. (Scale bar: 50  $\mu$ m.) Cells over-expressing GCLc-bp-exch#3 were immunostained with GCLm antibody, in order to verify a possible up-regulation of GCLm upon GCLc expression. We did not find any increase in GCLm levels both by immunoblot and immunohistochemistry (data not shown).

In summary, GCLm-shRNA#1 and GCLm-shRNA #2 result in silencing of endogenous GCLm. Unexpectedly both shRNAs partially reduced the expression of GCLm-human. GCLm-shRNA#1 expression produced neurite fragmentation indicating that targeting of GCLm was also neurotoxic.

### 3.1.3.2. GCLm silencing results in cell viability loss in a primary cortical culture

The cellular morphological change, the fragmentation of neurites and the lower EGFP fluorescence upon GCLm-shRNA#1 expression indicated a decrease in cell viability. Cell viability was quantified using the WST-1 cell assay. GCLm-shRNA#1 or GCLm-shRNA#2 expression induced significant cell death both at DIV9 and DIV13. The co-expression of GCLm-shRNA#1 and GCLm-human or GCLm-shRNA#1 and GCLm-human did not prevent the cell death induced by GCLm-shRNA#1 or GCLm-shRNA#2 at both time points (Fig. 3.1.20.).

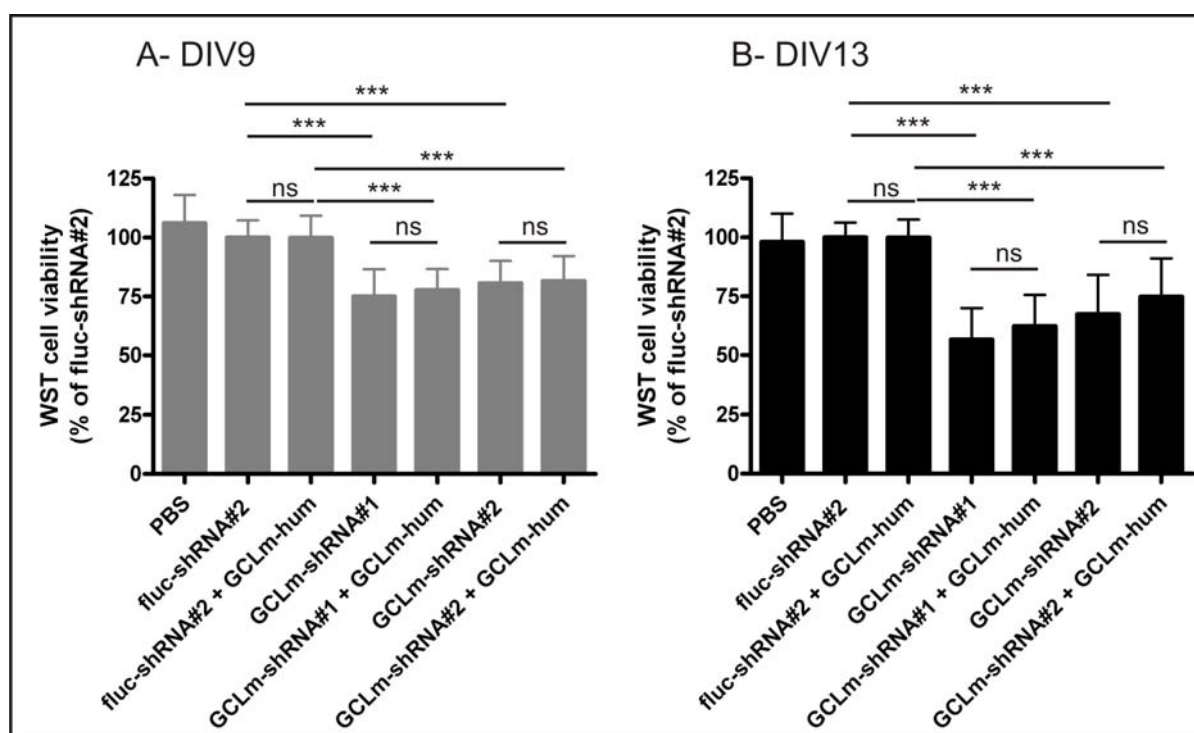


Fig. 3.1.20. Cell viability assay of cortical neurons in culture at DIV9 (A) and DIV13 (B). Cells were treated with PBS, or transduced with a virus expressing a control shRNA (fluc-shRNA#2), the control fluc-shRNA#2 plus the GCLm rescue construct (GCLm-hum), one of two different GCLm-specific shRNAs (GCLm-shRNA#1 and GCLm-shRNA#2), and the GCLm-shRNA#1 or GCLm-shRNA#2 plus the GCLm-hum. Cell viability is shown on the Y axis in mean percentage of control  $\pm$  SD (fluc-shRNA#2) from at least three independent experiments performed at least in triplicate. (\*\*\*) $p < 0.001$ , (\*\*) $p < 0.01$ , (\*) $p < 0.05$  and ns  $p > 0.05$  (non-significant)).

Expression of both GCLm-shRNA#1 and GCLm-shRNA#2 induces a significant decrease in cell viability. This effect was not prevented by the expression of GCLm-human, although a small tendency of cell viability rescue was observed at DIV13.

### 3.1.3.3. Glutathione levels upon GCLm silencing in primary cortical culture

We measured the levels of total glutathione (GSx) in cells expressing the GCLm-shRNA#1 or GCLm-shRNA#2, and evaluated the contribution of GCLm-human expression to GSx levels. Expression of GCLm-shRNA#1 or GCLm-shRNA#2 resulted in a significant decrease in the levels of total glutathione in cells both at DIV9 and DIV13 (Fig. 3.1.21.). The expression of GCLm-human did not increase significantly the levels of GSx in cells transduced with GCLm-shRNA#1 at DIV9 and DIV13.

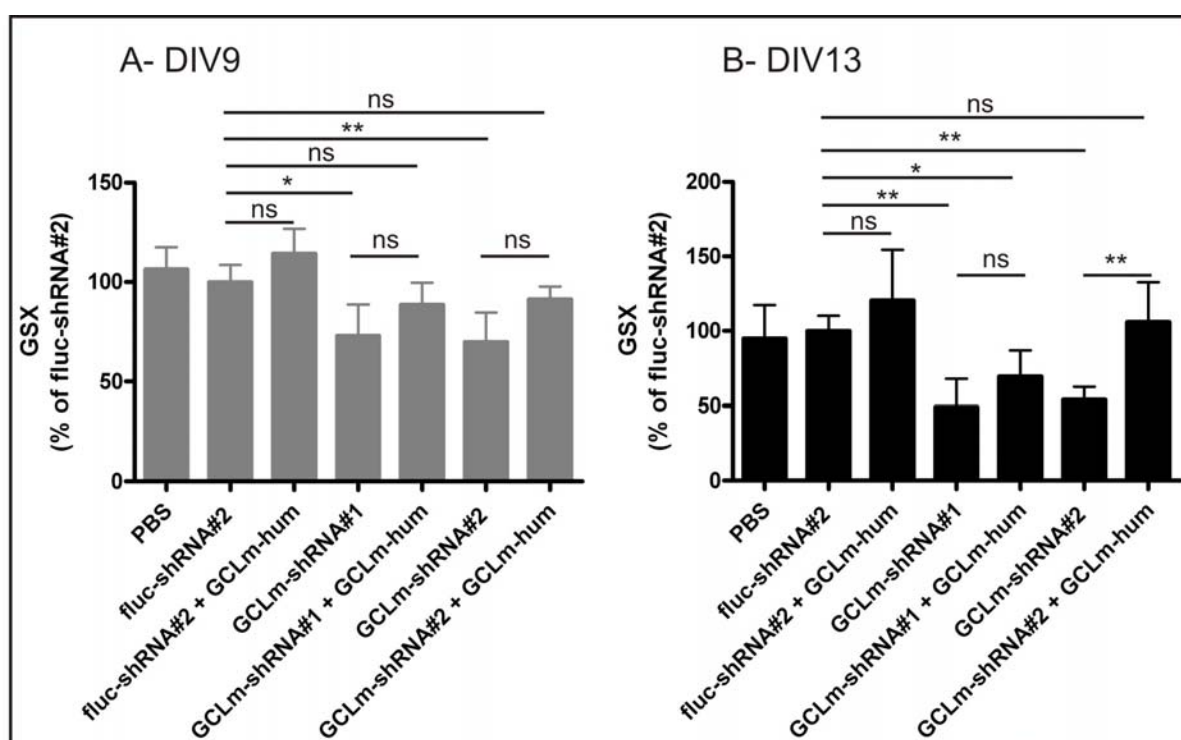


Fig. 3.1.21. Total glutathione measurement of cortical neurons in culture at DIV9 (A) and DIV13 (B). Cells were treated with PBS, or transduced with a virus expressing a control shRNA (fluc-shRNA#2), the control fluc-shRNA#2 plus the GCLm rescue construct (GCLm-hum), one of two different GCLm-specific shRNAs (GCLm-shRNA#1 and GCLm-shRNA#2), the GCLm-shRNA#1 or GCLm-shRNA#2 plus the GCLm-hum. Total glutathione is shown on the Y axis in mean percentage of control  $\pm$  SD (fluc-shRNA#2) from at least three independent experiments performed at least in triplicate. (\*\*\*) $p < 0.001$ , (\*\*) $p < 0.01$ , (\*) $p < 0.05$  and ns  $p > 0.05$  (non-significant)).

Cells co-expressing GCLm-shRNA#2 and GCLm-human the GSx content did not increased significantly at DIV9, nevertheless at DIV13 GSx content was significant increased (approximately 110% of the control shRNA). It should be mentioned that upon GCLm-shRNA#2 expression at DIV13 the number of surviving cells is approximately the same with and without GCLm-human expression indicating that the increased GSx content results from higher GSx load per cell. At the studied time points, co-expression of GCLm-human and control shRNA showed a tendency towards an increase in GSx content.

In summary, both GCLm-shRNA#1 and #2 induced a significant decrease in GSx at both studied time points. Overall there was a tendency for higher GSx levels with GCLm-human expression, the increase in GSx was only statistically significant in combination with GCLm-shRNA#2 at DIV13.

#### **3.1.3.4. Mechanism of cell loss in primary cortical culture upon GCLm silencing**

As described in section 3.1.2.4., the expression of GCLc-shRNA#2 resulted in decreased GSx levels and apoptotic cell death dependent on active cleaved caspase-3. We used cell lysates from cortical neurons in which GCLm-shRNAs were expressed for immunoblot using a specific antibody for cleaved caspase-3. Figure 3.1.18. shows that expression of GCLm-shRNA#1 with and without GCLm-human provoked the increase in the levels of active caspase-3. For the GCLm-shRNA#2 such increase in cleaved caspase-3 levels was not observed. Next, transduced cells grown on coverslips were stained with cleaved caspase-3 antibody, confirming at the cellular level the increase in cleaved caspase-3 in cells expressing GCLm-shRNA#1. Cells expressing the control shRNA or GCLm-shRNA#2 did not show an increase for active caspase-3 staining both by western blot and by immunohistochemistry (Fig. 3.1.22.).

Expression of GCLm-shRNA#1 results in increased levels of cleaved caspase-3 in cultured neurons, thus indicating that a decrease in GSx content may induce apoptotic cell death.



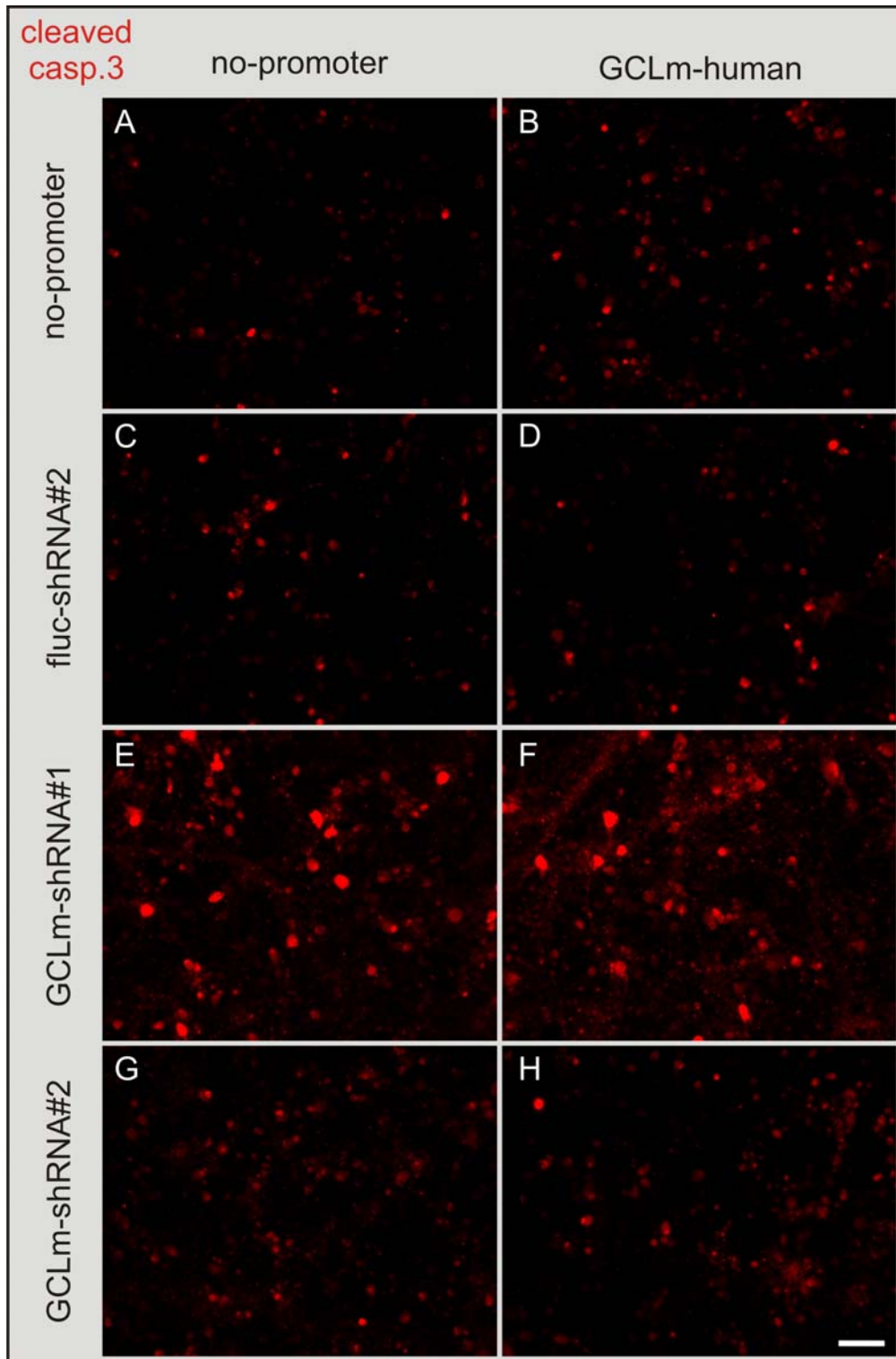


Fig. 3.1.22. Cleaved caspase-3 staining in primary cortical neurons. Cells were transduced with AAV2 vectors coding in A- no-promoter or expressing in B- GCLM-human plus no prom; C- fluc-shRNA#2 plus no-prom; D- fluc-shRNA#2 plus GCLM-human; E- GCLM-shRNA#1 plus no-prom; F- GCLM-shRNA#1 plus GCLM-human; G- GCLM-shRNA#2 plus no-prom; H- GCLM-shRNA#2 plus GCLM-hum. Cells were fixed 9 days after transduction. (Scale bar: 50  $\mu$ m.)

### 3.1.4. GCLc or GCLm over-expression in primary cortical culture is not neurotoxic

We tested the activity and the effects of the expression of each GCL subunit alone or in combination. The high capacity of GCLc to increase GSx content verified in combination with the GCLc-shRNAs may result in un-physiologic and perhaps toxic GSx concentrations. Expression of GCLm did not increase significantly the GSx content at both studied time points, however a tendency towards high GSx content was observed at DIV13 (Fig. 3.1.23.).

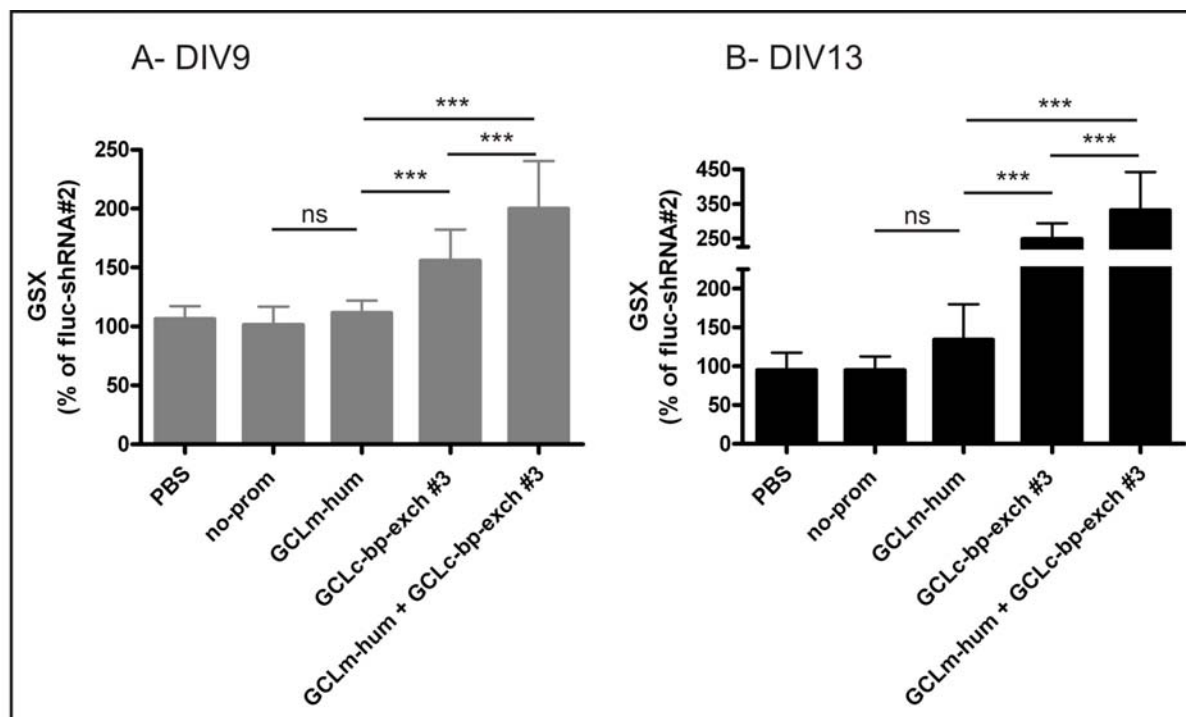


Fig. 3.1.23. Total glutathione measurement of cortical neurons in culture at DIV9 (A) and DIV13 (B). Cells were treated with PBS, or transduced with a control virus where the promoter was deleted (no-prom), expressing GCLm-hum, GCLc-bp-exch#3 or both GCLm-hum plus GCLc-bp-exch#3. Total glutathione is shown on the Y axis in mean percentage of control  $\pm$  SD (fluc-shRNA#2) from two independent experiments performed at least in triplicate. (\*\* $p < 0.001$ , \*\* $p < 0.01$ , \* $p < 0.05$  and ns  $p > 0.05$  (non-significant)).

In contrast, expression of GCLc resulted in a significant increase in cell GSx content both at DIV9 and DIV13 (approximately 1.5 and 2.5 fold of control respectively). Co-expression of GCLc and GCLm further increased significantly the GSx levels to approximately 2 fold at DIV9 and 3.5 fold of control at DIV13.

Next, the effect of high levels of GSx on cell viability was tested. Expression of GCLc, GCLm or co-expression of both did not induce a significant decrease in cell viability, although a small tendency for a decrease in cell viability in cells co-expressing both GCLc and GCLm at DIV13 (Fig. 3.1.24.B).

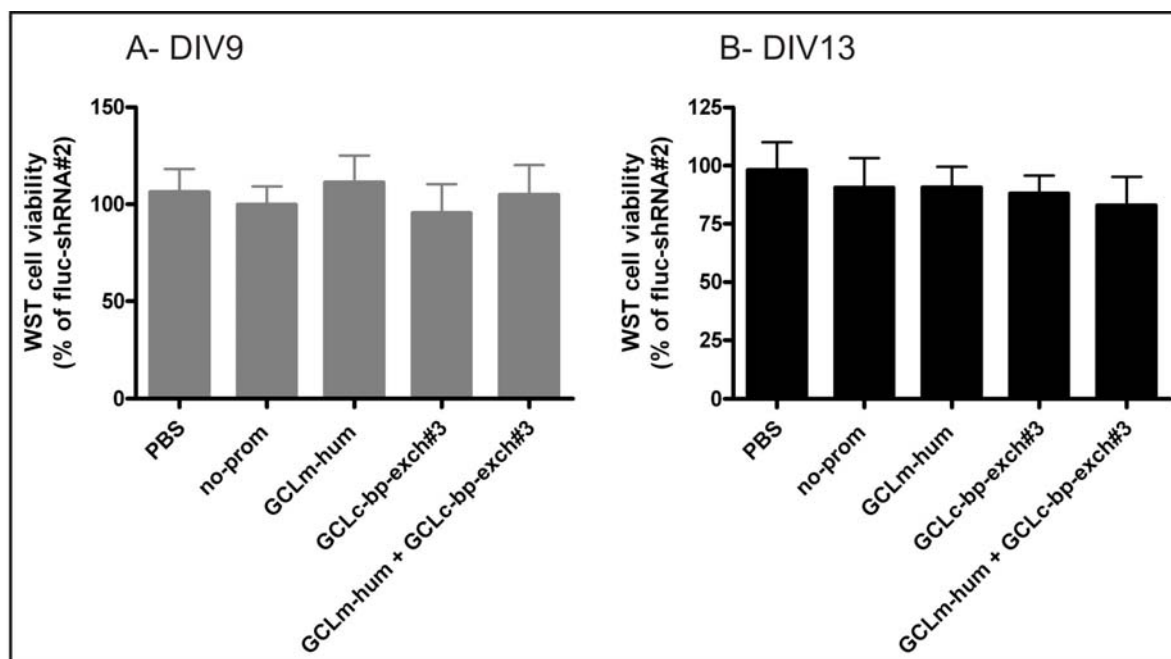


Fig. 3.1.24. Cell viability assay of cortical neurons in culture treated for 7 and 11 days (graph A and B respectively) with PBS, or transduced with a control virus where the promoter was deleted (no-prom), expressing the GCL modulatory subunit (GCLm-hum), the GCL catalytic subunit exchanged to become resistant to GCLc-shRNA#3 (GCLc-bp-exch#3) or both GCL subunits together (GCLm-hum + GCLc-bp-exch#3). Cells (250 000 cells/well) were treated at DIV 2 with a total of  $1.5 \times 10^8$  tu/well of the described virus ( $0.75 \times 10^8$  tu/well each virus, one virus without promoter/transgene expression was used to achieve the same total amount of virus/well). Cell viability is shown on the Y axis in mean percentage of control  $\pm$  SD (fluc-shRNA#2) from at least two independent experiments performed at least in triplicate. (\*\*\*) $p < 0.001$ , (\*\*) $p < 0.01$ , (\*) $p < 0.05$  and ns $> 0.05$  (non-significant)).

In brief, at the studied time points the expression of GCLm alone did not significantly increase GSx levels. Expression of GCLc increases the GSx contents at both time points and the expression of both GCLc and GCLm further increases the cellular GSx load. The increase in GSx does not result in decreased cell viability at the studied time points.

### 3.1.5. Summary of *in vitro* results

Estimation of specificity and efficacy of a given shRNA molecule may vary drastically depending of the assays system used (i.e. GCLc-shRNA#1 had low silencing efficacy both in the luciferase based test system and in western blot from co-transfected HEK293 cells, nevertheless it severely impaired cell viability and GSx levels in primary cortical neurons), see table 3.1.1.. No major differences in cell morphology were observed with GCLc-shRNAs expression at DIV7, while at DIV11 GCLc-shRNA#1 and GCLc-shRNA#2 induced neurite destructions, thus indicating progressive cell impairment. At DIV9 and DIV12 clear reduction in cell viability was measured, meaning either less surviving cells or more cellular impairment upon GCLc disruption. Cell reduction in cell viability followed the reduction in GSx content, thus indicating for a specific effect of GCLc silencing. The expression of non-targetable GCLc protein or hDJ1 failed to prevent cell death induced by GCLc-shRNAs expression, while expression of  $\alpha$ -synucleinA53T had a small but significant rescue effect, indicating a protective role of  $\alpha$ -synuclein in this oxidative stress paradigm. Not less important, a minor influence on both neurites morphology and cell viability by control shRNAs expression was observed when compared with cells expressing EGFP only.

Targeting of GCLm protein was effectively achieved by the expression of two specific shRNAs, resulting in lower cell viability and GSx contents, such effects were not detected by the expression of control shRNAs. The achieved effects were moderate and delayed in comparison with the results of targeting GCLc. Cell viability loss was not prevented by the expression of GCLm human, only a minor tendency was observed at the later time point. Nevertheless, the GSx content showed a trend towards an increase with GCLm-human expression, although this increase was only significant at DIV13 for the GCLm-shRNA#2 expressing cells. Expression of GCLm-human showed a tendency towards higher GSx levels, although no cytotoxicity was measured using the WST-1 assay.

Table 3.1.1. Comparison of shRNAs effects *in vitro*.

	Luciferase test system/co-transfection HEK293 cells (partial sequence)	Western Blot/co-transfection HEK293 cells (full sequence)	neurite morphology (cortical neurons)	cell viability assay (cortical neurons)	GSx (cortical neurons)
GCLc-shRNA#1	(++)	(+)	(+++)	(++++)	(+++)
GCLc-shRNA#2	(+++++)	(+++++)	(+++++)	(++++)	(+++++)
GCLc-shRNA#3	(+++)	(+++++)	(-)	(+)	(++)
GCLm-shRNA#1	nd	(+++++)	(+++++)	(+++)	(+++)
GCLm-shRNA#2	nd	(+++++)	(++)	(++)	(+++)
GCLm-shRNA#3	nd	(+++)	nd	nd	nd
GSR-shRNA#1	(++)	nd	nd	nd	nd
GSR-shRNA#2	(+++)	nd	nd	nd	nd
GSR-shRNA#3	(+++++)	nd	(-)	(-)	(-)

Estimation of specificity and efficacy of the shRNAs in the different used assay systems demonstrated large variances of efficacy of respective shRNAs depending on the assay system used. Maximum (+++++), no detectable effect (-). nd, non-determined.

### 3.2. Targeting GSH metabolism in the SNpc *in vivo*

#### 3.2.1 Transduction of SNpc by stereotaxic injection of AAV2 vector

Expression of 5 different shRNAs targeting GSH production in cultured primary neuron's derived from embryonic rat brain resulted in a gradual decline in total glutathione levels which were tightly correlated to impairments in neuronal physiology and neurite integrity. Expression of 3 different control shRNAs did not impair neuronal physiology to a significant extent. However, specificity of the approach could not be demonstrated unequivocally since the phenotype could not be prevented by co-expression of non-targetable GCLs.

We none the less aimed for investigating effects of GSH depletion in dopaminergic neurons of the adult rat *in vivo*, since these neurons are more relevant to PD. DA neurons of adult rat SNpc are terminally differentiated in a complete different microenvironment which is impossible to reproduce *in vitro*, and may react differently to oxidative stress than neurons derived from embryonic brain.

##### 3.2.1.1 Efficiency of AAV2 vectors injection in SNpc

The use of a fluorescent reporter made possible the tracing of the transduced cell populations and the quantification the targeting efficiency. After stereotaxic injection of  $1.2 \times 10^8$  transducing units (t.u.) of AAV2 EGFP into the substantia nigra, we detected efficient

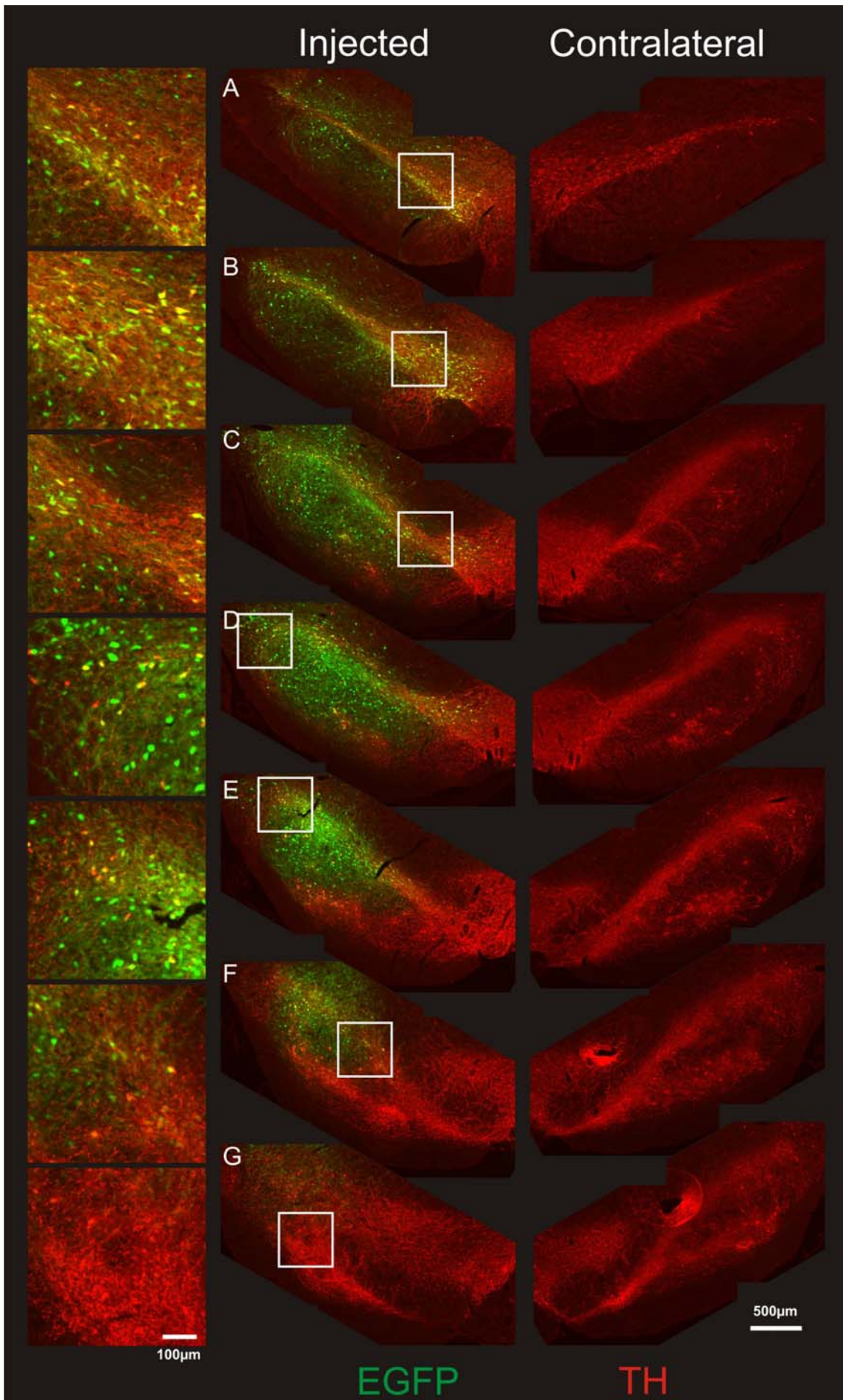


Fig.3.2.1. Transduction of rat brain by AAV2 vectors. Representative transduction of SNpc dopaminergic neurons after  $1.2 \times 10^8$  t.u. of AAV2 expressing fluc-shRNA#2 and EGFP. Dopaminergic neurons are visualized by TH immunoreactivity (red) and virus transduction by EGFP expression (green). High magnification represent the square indicated areas. Scale bar 500  $\mu\text{m}$  in low magnification pictures and 100  $\mu\text{m}$  in high power magnification pictures.

transduction of dopaminergic neurons. The transduction was limited to the anterior part of the SNpc (Fig.3.2.1.A-E). The most posterior part of SNpc was in generally not transduced, resulting in transgene expression in approximately 70% of DA neurons. Transduction was completely not restricted to DA neurons, other populations within the SNpc region are also transduced, especially in the vicinity of the injection needle track.

### 3.2.1.2 AAV2 allowed for neuron specific transduction

Tropism of AAV2 vectors for neurons has been reported to be very high (Kaplitt et al. 1994; Mccown et al. 1996; During et al. 1998; Mandel et al. 1998). Expression of proteins can be restricted to neurons with the use of neuronal specific promoter like hSyn1 promoter, but the shRNA expression is driven by the polymerase III H1-RNA gene promoter. The H1-RNA promoter is active in all cell types including astrocytes where it could promote shRNA production and thus induce RNAi (Li et al. 2006). In order to investigate the potential influence of astrocyte transduction on our study, we injected  $1 \times 10^8$  t.u. of AAV2 vector expressing EGFP controlled by the GFAP promoter (astrocyte specific promoter) into rat SNpc. The number of astrocytes expressing EGFP at 3 weeks after injection was very low, confirming the low tropism of AAV2 vectors towards astrocytes (Fig.3.2.2.). Unexpectedly, some cells expressing EGFP were negative for GFAP staining (Fig.3.2.2.A), but positive for NeuN (not shown) and for TH (Fig.3.2.2.D), further demonstrating the “restricted” tropism of AAV2 vectors for neurons.

These results demonstrated that AAV2 viral vectors have an almost neuron specific tropism allowing to restrict effects of GSH downregulation solely to neurons.

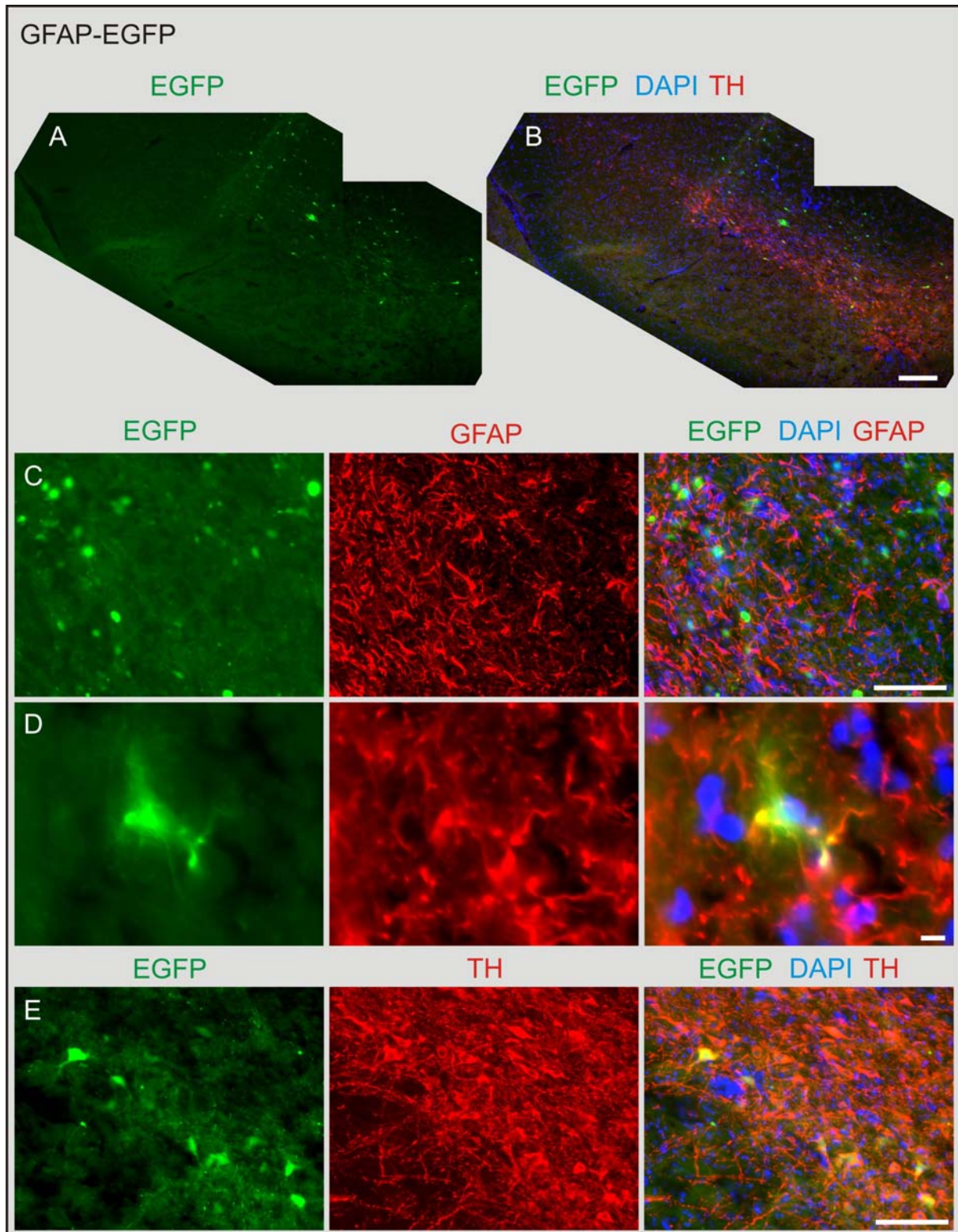


Fig.3.2.2. Expression of EGFP in the SNpc at 3 weeks after injection of AAV2 GFAP EGFP vector. A and B representing the overall EGFP expression in the SNpc driven by the GFAP promoter. The majority of EGFP expressing cells do not co-localize with GFAP staining (C), while a small minority are positive for GFAP marker (D). In E, some cells expressing EGFP are TH positive. (Scale bar: 200  $\mu$ m in A and B, and 100  $\mu$ m in C, D, and E)



### 3.2.2.1 *In vivo* neurotoxicity of control shRNAs

We expressed four different control shRNAs in rat SNpc in order to control for the possible side effects of shRNAs expression in the DA system. Two control shRNAs were sequences specific to the luciferase firefly gene (fluc-shRNA#1 and fluc-shRNA#2), one specific for EGFP (EGFP-shRNA) and the other with at least 4 mismatches with all known human, rat and mouse genes (Dhar-shRNA#1). Vectors expressing control shRNAs were injected into rat SNpc ( $1.2 \times 10^8$  t.u. in a 2  $\mu$ l injection volume) and the number of DA neurons was quantified at 3, 6 and 9 weeks after vector injection (both TH and VMAT2 markers were used). The reduction in TH immunostaining resulting from the control shRNA application was obvious when compared to the contralateral non injected side. Part of this reduction results from the stereotactic injection procedure as the injection of a vector expressing EGFP or coding EGFP but lacking promoter (not expressing) produced similar effects (Fig. 3.2.3.).

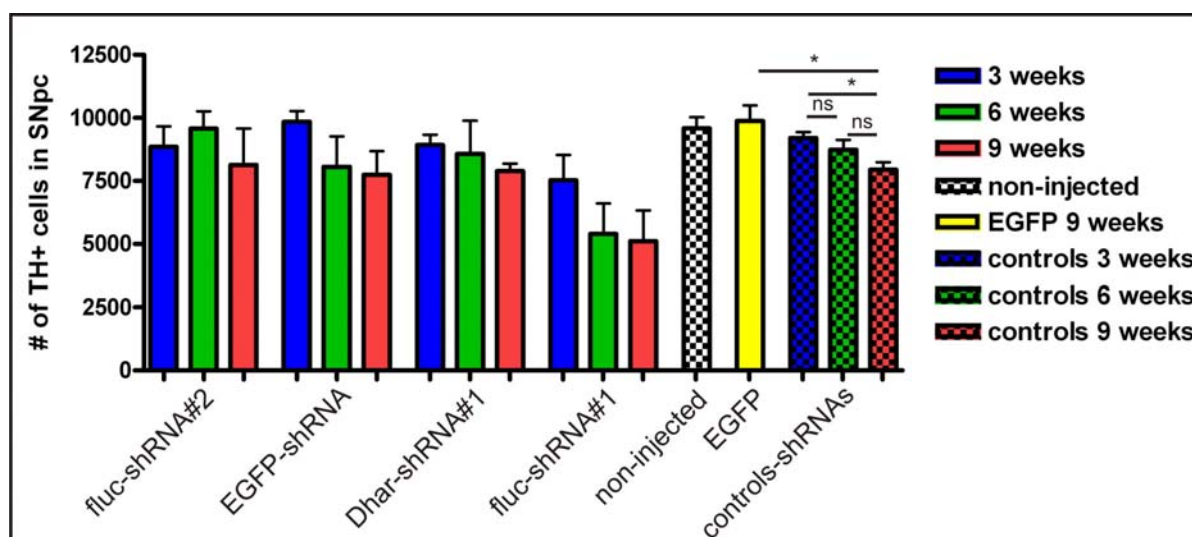


Fig. 3.2.3. Quantification of DA-neuron survival after AAV2 vectors were injected into rat SNpc. The number of surviving TH<sup>+</sup> neurons was determined after injection of 4 different shRNA control vectors or a vector expressing EGFP into the SNpc. Blue columns, green columns and red columns represent the mean values of surviving TH<sup>+</sup> neurons in SNpc respectively at 3, 6 and 9 weeks after vector injection. White chequered column represents the number of TH positive neurons in control non-injected SNpc. Yellow column represent the mean values of surviving TH<sup>+</sup> neurons in SNpc 9 weeks after injection of AAV2 EGFP control virus. Blue chequered columns, green chequered columns and red chequered columns represent the mean of three controls (fluc-shRNA#2, EGFP-shRNA and Dhar-shRNA#1) mean values  $\pm$  SD of surviving TH<sup>+</sup> neurons in SNpc respectively at 3, 6 and 9 weeks after the vector injection. A total dosage of  $1.2 \times 10^8$  t.u. of recombinant AAV2 vectors were injected in the rat SNpc. Columns represent mean values  $\pm$  standard deviation (\*\* $p < 0.001$ , \* $p < 0.01$ ,  $p < 0.05$  and ns  $p > 0.05$  (non-significant)).

Number of TH<sup>+</sup> cells in rat SNpc after expression of three control shRNAs was equivalent at each time point (3, 6 and 9 weeks). The number of surviving TH<sup>+</sup> cells from fluc-shRNA#2,

EGFP-shRNA and Dhar-shRNA#1 expression groups were combined for each time point (controls 3 weeks, controls 6 weeks and controls 9 weeks). At 9 weeks after co-expression of EGFP plus shRNAs the number of TH<sup>+</sup> cells was statistically reduced when compared with EGFP expression only (Fig. 3.2.3.). These results indicate an inherent neurotoxic effect resulting from the shRNAs expression; this effect is slowly progressive reaching statistical significance when TH<sup>+</sup> cells at 3 weeks were compared with those at 9 weeks. One control shRNA targeting luciferase firefly gene (fluc-shRNA#1) induced remarkable cell loss *in vivo* at all studied time points. Both at 6 and 9 weeks the reduction in TH positive cells in SNpc was statistically different from the other shRNAs individually or the combination of them (Fig. 3.2.3. and Table 3.2.1.). Thus, the fluc-shRNA#1 control was not used for further experiments due to the observed “off-target/unspecific” effect in the survival of DA neurons.

This experiment showed that expression of control shRNAs with no predicted target can result in moderate cell death, suggesting that shRNA expression per se can induce low level of neurodegeneration. One control shRNA targeting the firefly luciferase induced significant cell death.

Table 3.2.1. Number of surviving TH positive neurons in rat SNpc at 3, 6 and 9 weeks after viral injection

Condition	TH <sup>+</sup> cells at 3 weeks		TH <sup>+</sup> cells at 6 weeks		TH <sup>+</sup> cells at 9 weeks	
	Mean ± SD	N	Mean ± SD	N	Mean ± SD	N
fluc-shRNA#2	8853 ± 812	3	9581 ± 682	3	8128 ± 1446	4
EGFP-shRNA	9845 ± 431	3	8061 ± 1205	3	7749 ± 936	3
Dhar-shRNA#1	8923 ± 414	3	8576 ± 1319	3	7891 ± 304	3
fluc-shRNA#1	7531 ± 1003	6	5403 ± 1203	7	5107 ± 1224	5
all controls	9207 ± 696	9	8740 ± 1167	9	7943 ± 970	10
GSR-shRNA#3	8152 ± 273	3	7581 ± 780	3	7355 ± 593	5
GCLc-shRNA#2	7389 ± 490	5	5726 ± 1201	8	3458 ± 562	7
GCLc-shRNA#2 w GCLc- bp-exch#2	8278 ± 1236	8	6234 ± 1319	4	4854 ± 708	5
GCLc-shRNA#2 w hDJ1	7632 ± 380	4	4550 ± 724	4	3376 ± 657	5
GCLc-shRNA#3	8619 ± 900	3	6893 ± 612	3	5912 ± 454	4
GCLc-shRNA#2 w a-synA53T					5258 ± 636	4
EGFP-shRNA w a-synA53T					8504 ± 585	4
EGFP					9877 ± 619	3

TH surviving neurons in the rat SNpc after AAV2 mediated shRNA expression. A total dosage of 1.2x10<sup>8</sup> t.u. of recombinant AAV2 vectors were injected in the rat SNpc and the number of TH positive neurons were accessed 3, 6 and 9 weeks after injection. Numbers represent means ± SD from N independent injected SNpc.

### 3.2.2.2. DA neuron degeneration mediated by targeting the catalytic subunit of GCL

In order to confirm that knock-down of GSH synthesizing enzymes directly resulted in neurodegeneration as suggested by the in vitro studies, several groups of AAV vector injected rats were analysed at 3, 6, and 9 weeks after vector application. DA neuron numbers were counted within the whole SNpc by immunostaining for TH and VMAT2.

The following groups were analysed, a) controls: shRNAs specific for EGFP, luciferase or with at least 4 mismatches with all known human, rat and mouse genes were expressed in at least 3 animals per shRNA and time point. As further control an shRNA targeting glutathione reductase (GSR) was expressed, which has been demonstrated to be efficient on the mRNA level but did not result in Downregulation of GSR protein levels; b) shRNAs targeting GCLc: GCLc specific shRNA#2 demonstrated the most pronounced Downregulation of GCLc protein and glutathione synthesis in cultured neurons, while shRNA#3 has demonstrated more moderate effects on both parameters; c) rescue constructs: these vectors expressed GCLc specific shRNA#2 together with either a non-targetable version of GCLc (GCLc-bp-exch#2) or with hDJ1

Figure 3.2.3. and Table 3.2.1. show DA neuron numbers as quantified at 3, 6 and 9 weeks after vector injections. As outlined in section 3.2.1.2. expression of control shRNAs resulted in low level loss of DA neurons as compared to the non-injected or EGFP expressing cells in SNpc. Injection of GSR-shRNA#3 did not induce a significant decrease in TH<sup>+</sup> cells, further validating it as a control shRNA.

Expression of GCLc-shRNA#2 resulted in a progressive degeneration of DA neurons, leading to 20% loss at 3 weeks, 35% loss at 6 weeks and 60% loss at 9 weeks compared to control shRNAs. Figure 3.2.5. shows representative pictures of control shRNA or GCLc-shRNA#2 injected SNpc at 3, 6 and 9 weeks after injection. Expression of GCLc-shRNA#3 resulted in a much slower but significant degeneration of DA neurons at 9 weeks after injection (10% loss at 3 weeks, 20% loss at 6 weeks and 26% loss at 9 weeks) (Fig. 3.2.4. and Table 3.2.1.).

Co-expression of hDJ1 together with GCLc-shRNA#2 had no neuroprotective effect at all time points investigated. Co-expression of a non-targetable GCLc protein together with GCLc-shRNA#2 showed a non-significant tendency for neuroprotection at 3 and 6 weeks

after vector injection, however at 9 weeks after injection a significant rescue was verified (Fig. 3.2.4.).

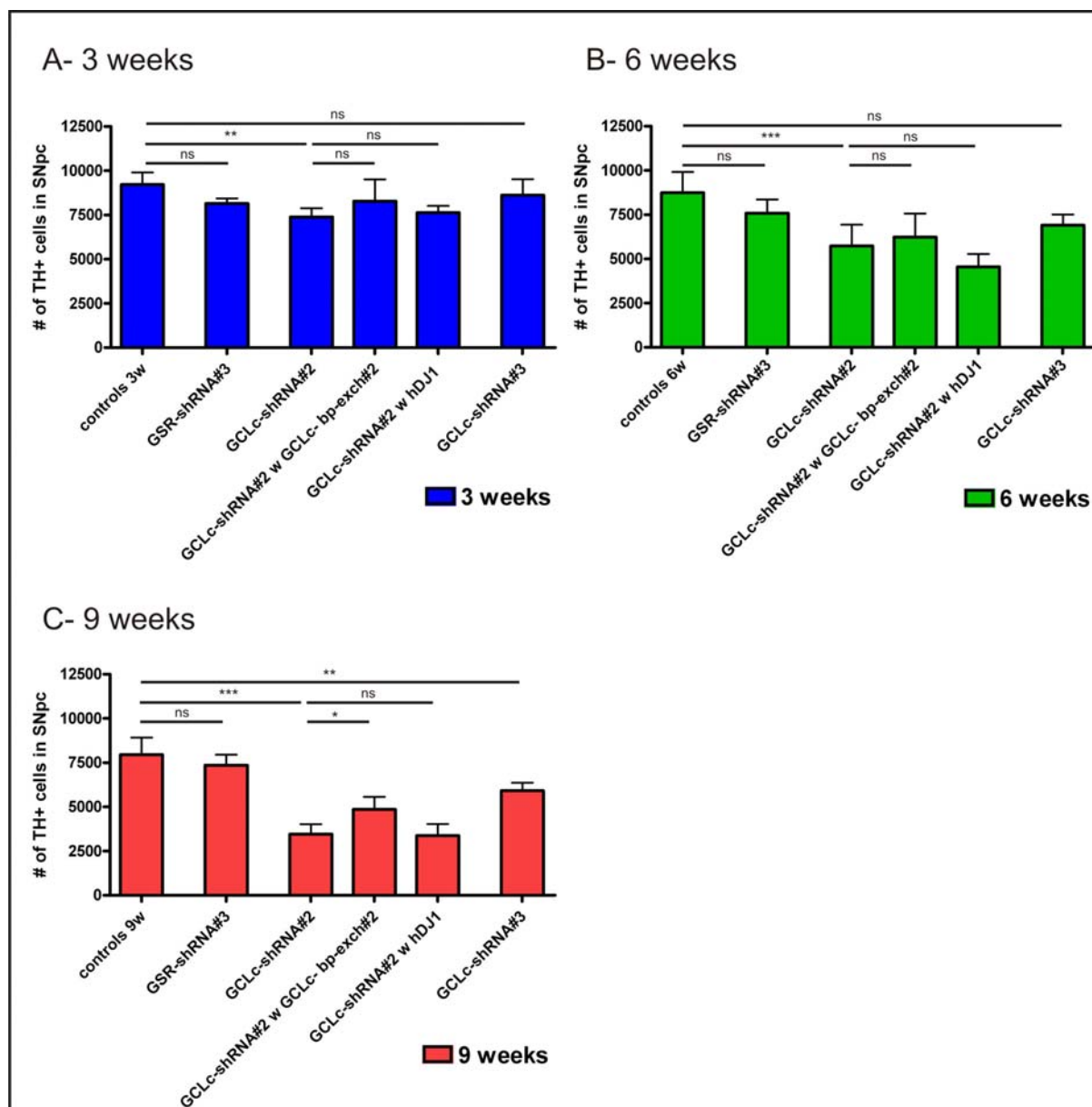


Fig. 3.2.4. Quantification of DA-neuron survival after specific AAV2 expressing shRNAs were injected into rat SNpc. The number of surviving TH<sup>+</sup> neurons was determined 3 weeks (A-blue columns), 6 weeks (B-green columns) and 9 weeks (C-red columns) after shRNAs injection. AAV2 vectors expressing control shRNAs, GSR-shRNA#3, GCLc-shRNA#2, GCLc-shRNA#3 or co-expressing GCLc-shRNA#2 plus GCLc-bp-exch#2 or GCLc-shRNA#2 plus hDJ1 were injected. A total dosage of  $1.2 \times 10^8$  t.u. of recombinant AAV2 vectors were injected in the rat SNpc. Columns represent mean values  $\pm$  standard deviation ( $***p < 0.001$ ,  $**p < 0.01$ ,  $*p < 0.05$  and ns  $p > 0.05$  (non-significant)).

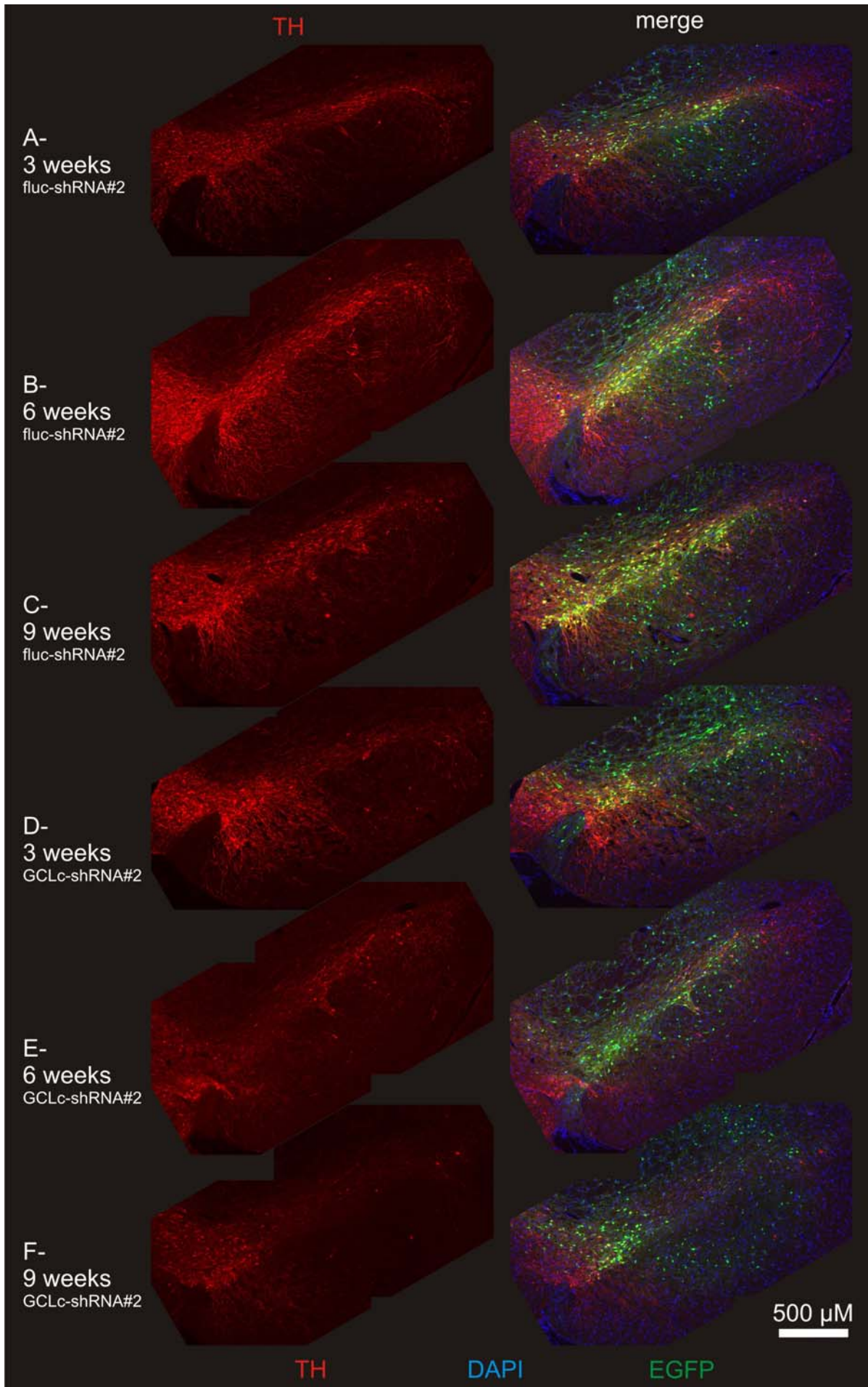


Fig.3.2.5. Representative pictures from rat SNpc were AAV expressing control fluc-shRNA#2 or GCLc-shRNA #2 were injected. A, B and C representative photomicrographs of AAV2 fluc-shRNA#2 injection at 3, 6 and 9 weeks post injection. D, E, and F are representative photomicrographs of AAV2 GCLc-shRNA #2 injection into rat SNpc at 3, 6 and 9 weeks post injection. A total dosage of  $1.2 \times 10^8$  t.u. of AAV2 were injected into rat SNpc in a 2  $\mu$ l volume. DA neurons in the SNpc were stained for TH in red, green shows the EGFP expressing cells and blue represents nuclear DNA staining (DAPI). (Scale bar: 500  $\mu$ m)

Importantly, it was demonstrated in this set of experiments that at least a minor rescue effect was achieved after longer investigation time when co-expressing a GCLc which could not be targeted for degradation by GCLc-shRNA#2. In order to confirm this result with independent data a second set of experiments was conducted. In this experiment the fluc-shRNA#2 served as control, GCLc-shRNA#3 was used to target and down-regulate GCLc, and GCLc-bp-exch#3 (non-targetable) was used for co-expression. Due to the slower kinetics of GCLc-shRNA#3 in induction of neurodegeneration these brains were analysed only at 9 weeks after vector injections. In contradiction to results obtained with GCLc-shRNA#2 we did not detect any rescue effect under these conditions, rather we detected a significant amplification of DA neuron loss by co-expression of non-targetable GCLc (~20% reduction with GCLc-shRNA#3 and 40% reduction with co-expression of GCLc-shRNA#3 and GCLc-bp-exch#3) (Fig. 3.2.6. and Table 3.2.2.). These results were the first hint that overexpression of GSH synthesizing enzymes *per se* could result in induction of neurodegeneration.

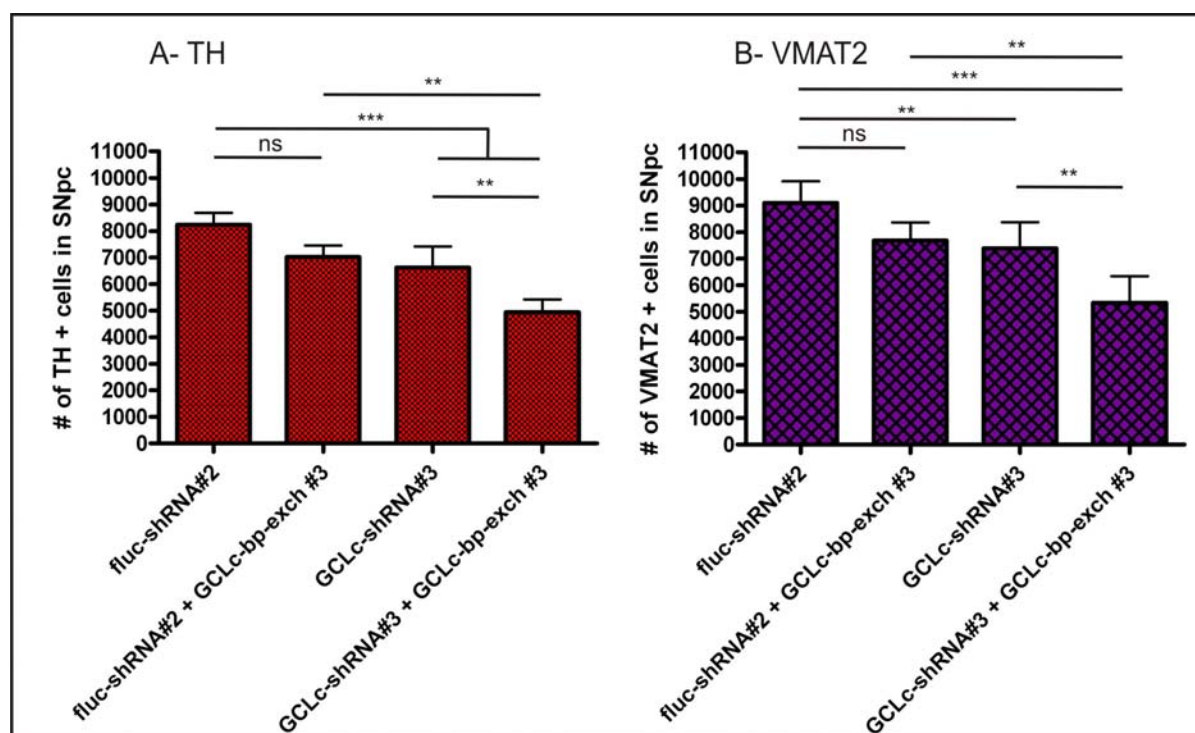


Fig. 3.2.6. Quantification of DA-neuron survival after injection of AAV2 encoding specific shRNAs into rat SNpc. The number of surviving TH<sup>+</sup> neurons (A) or VMAT2<sup>+</sup> neurons (B) was determined 9

## Results

weeks after one control shRNA (fluc-shRNA#2) or one shRNA targeting the catalytic subunit of glutamate cysteine ligase (GCLc-shRNA#3) were injected. The rescue construct for the GCLc-shRNA#3 was also co-injected with the control fluc-shRNA or the GCLc-shRNA#3. One AAV2 encoding EGFP but lacking the promoter (no-prom) was used as “empty vector” to fill up the virus amount (normally  $0.6 \times 10^8$  t.u. was used of each virus, total  $1.2 \times 10^8$  t.u.). Columns represent mean values  $\pm$  standard deviation (\*\* $p < 0.001$ , \* $p < 0.01$  and ns  $p > 0.05$  (non-significant)).

Table 3.2.2. Number of surviving TH<sup>+</sup> or VMAT2<sup>+</sup> neurons in rat SNpc 9 weeks after viral injection.

Condition	TH <sup>+</sup> cells			VMAT2 <sup>+</sup> cells		
	Mean	$\pm$ SD	N	Mean	$\pm$ SD	N
fluc-shRNA#2 + no-prom	8232	$\pm$ 454	10	9102	$\pm$ 815	10
fluc-shRNA#2 + GCLc-bp-exch#3	7026	$\pm$ 428	4	7682	$\pm$ 687	4
GCLc-shRNA#3 + no-prom	6623	$\pm$ 793	6	7393	$\pm$ 981	6
GCLc-shRNA#3 + GCLc-bp-exch#3	4948	$\pm$ 472	4	5342	$\pm$ 998	4

TH or VMAT2 surviving neurons in the rat SNpc after AAV2 mediated shRNA expression. In the rat SNpc a total dosage of  $1.2 \times 10^8$  t.u. of recombinant AAV2 vectors were co-injected. One virus encoding EGFP but lacking the promoter (no-prom) was used as “empty vector” to fill up the total virus particles (normally  $0.6 \times 10^8$  t.u. was used of each virus). Number of TH and VMAT2 positive neurons were accessed 9 weeks after injection. Numbers represent means  $\pm$  SD from N independent injected SNpc.

Expression of GCLc-bp-exch#3 was confirmed by immunohistochemistry (Fig.3.2.7. D).

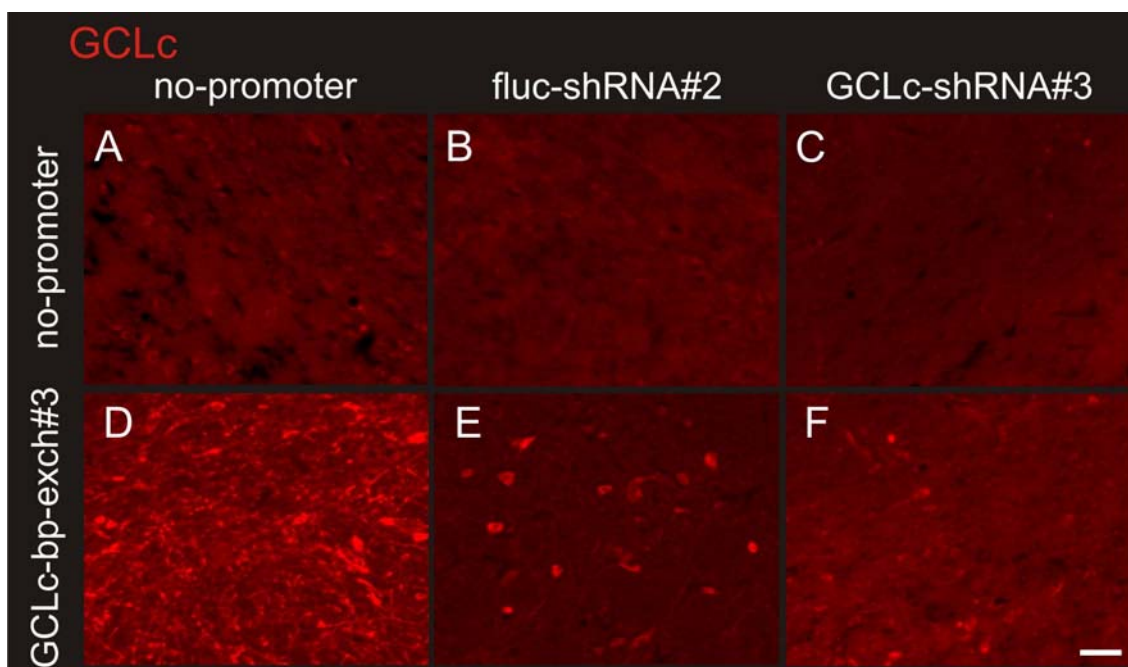


Fig.3.2.7. GCLc staining pictures after AAV2 vector injection into SNpc, expressing in A no-promoter (empty vector); B control fluc-shRNA#2 co-injected with no-promoter; C GCLc-shRNA#3 vector co-injected with no-promoter; D no-promoter co-injected with GCLc-bp-exch#3; E control fluc-shRNA#2 co-injected with GCLc-bp-exch#3; F GCLc-shRNA#3 vector co-injected with GCLc-bp-exch#3. A total dosage of  $1.2 \times 10^8$  t.u. of AAV2 vectors ( $0.6 \times 10^8$  t.u. each AAV) was used. Rats were perfused 9 weeks after injection. (Scale bar: 50  $\mu$ m)

The endogenous levels of GCLc were hardly detectable in SNpc or control shRNA injected brains by the available antibodies (Fig.3.2.7. A and B). Co-expression of control shRNA (fluc-shRNA#2) and GCLc-bp-exch#3 resulted in increased GCLc protein levels (Fig.3.2.7. E), although the expression of GCLc is lower when compared with GCLc expression only (Fig.3.2.7. D). When GCLc-shRNA#3 was co-expressed with the non-targetable GCLc, cells expressing GCLc over the endogenous levels were observed, although the number of cells and the staining intensity was reduced as compared to GCLc-bp-exch#3 expression only.

This experiment demonstrated *in vivo* that GCLc down-regulation results in death of DA neurons. AAV mediated expression of GCLc-shRNA#2 induced relatively fast progressive and robust DA cell loss. GCLc-shRNA#3 expression resulted in a slowly progressive degeneration. The expression of a GCLc-shRNA#2 non-targetable GCLc prevented death of DA neurons significantly in SNpc at the 9 weeks time point, however the co-expression of GCLc-bp-exch#3 and GCLc-shRNA#3 further decreased the number of surviving neurons, thus indicating for the first time that overexpression of GSH synthesizing enzymes *per se* can induce cytotoxic effects.

### **3.2.2.3. $\alpha$ -synucleinA53T partially rescues DA neurons from degeneration induced by GCLc knock-down**

We attempted to combine and possibly enhance the toxicity driven by GCLc silencing with the over-expression of one PD associated mutant form of  $\alpha$ -synuclein ( $\alpha$ -synuclein A53T). Figure 3.2.8. shows the number of DA neuron survival at 9 weeks after vector injection. Injection of AAV2 EGFP control shRNA or EGFP control shRNA plus the  $\alpha$ -synucleinA53T did not induce changes in the number of DA neurons. The combination of GCLc-shRNA#2 plus  $\alpha$ -synucleinA53T increased the number of surviving neurons when compared with the expression of GCLc-shRNA#2 alone. Confirming *in vitro* studies a small but statistical significant neuroprotection was observed.



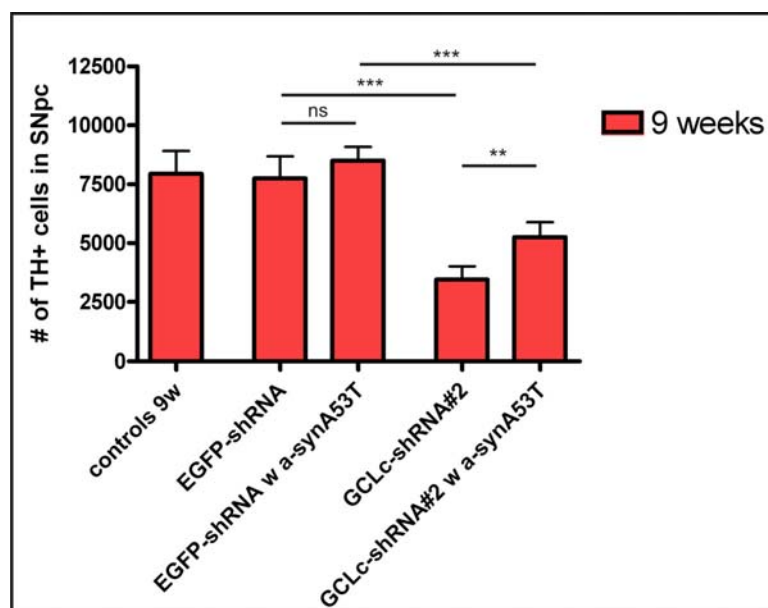


Fig. 3.2.8. Quantification of DA neuron survival after control or GCLC-shRNA#2 plus  $\alpha$ -synuclein A53T expression mediated by AAV2 injection into rat SNpc. The number of surviving TH<sup>+</sup> neurons was determined 9 weeks after injection of AAV2 expressing EGFP control shRNA (EGFP-shRNA), one vector co-expressing EGFP-shRNA and  $\alpha$ -synucleinA53T, one vector expressing GCLC-shRNA#2 or on vector co-expressing GCLC-shRNA#2 and  $\alpha$ -synucleinA53T. A total dosage of  $1.2 \times 10^8$  t.u. of recombinant AAV2 vectors were injected in the rat SNpc. Columns represent mean values  $\pm$  standard deviation (\*\* $p < 0.01$ , \*\*\* $p < 0.001$  and ns  $p > 0.05$  (non-significant)).

These results demonstrated that as in cultured primary neurons  $\alpha$ -synuclein overexpression (at least at the level obtained under our experimental conditions) could partially prevent neurodegeneration induced by decreasing the neuron's capability to counter-act oxidative stress.

#### 3.2.2.4. FluoroJade C staining for degenerating neurons

FluoroJade C is a marker for degenerating neurons regardless of the mechanism inducing the degeneration. Figure 3.2.9. A shows staining in rat cortex tissue at 48 hours after brain ischemia as a control resulting in clear staining of neuronal cell bodies of degenerating neurons. EGFP or control shRNAs expression in the SNpc resulted in a staining composed of some small dots and some fibrous like structures. With expression of GCLC-shRNA#2 the number of those stained small dots and protrusions increased and larger structures surrounding DAPI stained nuclei were observed, apparently cell bodies of neuronal cells. In figure 3.2.9. D one cell body like structures is shown.

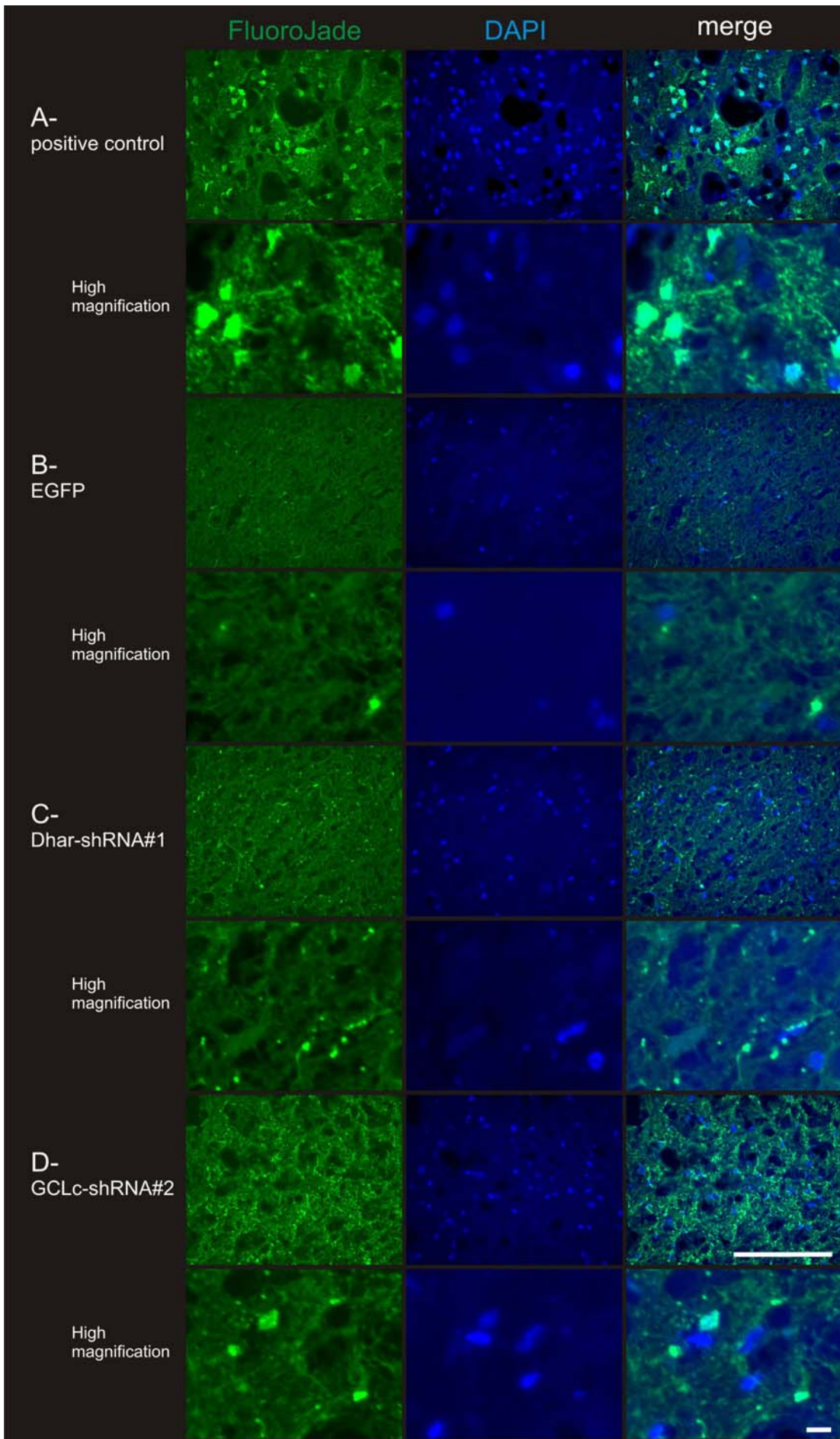


Fig.3.2.9. FluoroJade C staining for degenerating neurons. A is a positive control of rat tissue subjected to transient ischemia. The degenerating cells in A are from a area in the cortex where degenerating neurons could be observed. In B, C and D  $1.2 \times 10^8$  t.u. of recombinant virus expressing EGFP only, Dhar-shRNA#1 or GCLc-shRNA#2 respectively was injected into the rat SNpc. The pictures in B, C and D are from the SNpc region of rats perfused 9 weeks after viral application. Green is the FluoroJade C staining and in blue the DAPI nuclear DNA staining. (Scale bar: 100  $\mu$ m)

Knockdown of GCLc in the SNpc resulted in increased FluoroJade C staining of cell protrusions, but not well defined cell bodies as in control ischemic tissue.

### 3.2.2.5. shRNAs targeting the modulatory subunit of GCL in DA neurons

GCL is a heterodimer constituted by a modulatory (GCLm) and a catalytic subunit (GCLc). The GCLm has no catalytic activity, but regulates the GCLc activity. We investigated DA neurons cell survival upon GCLm down-regulation.

In this section of the study one AAV vector co-expressing the control or GCLm-shRNAs and a reporter gene (e.g. EGFP) was co-injected with another vector having no significant expression of EGFP (“no-promoter”) or expressing GCLm-human as a rescue construct. The “no-promoter” vector was used to fill up the total amount of virus to be injected, excluding potential artefacts resulting from injection of different vector dosages. Normally  $0.6 \times 10^8$  t.u. of each virus was used, making a total of  $1.2 \times 10^8$  t.u. in each SNpc injection in a 2  $\mu$ l volume. The number of DA neurons was quantified by staining the SNpc with two independent markers, TH and VMAT2 (vesicular monoamine transporter 2) at 9 weeks after injection.

At 9 weeks after AAV2 mediated GCLm-shRNA#1 or GCLm-shRNA#2 expression in SNpc, the number of DA neurons was statistically reduced when compared with control fluc-shRNA#2 expression (approximately 35% and 20% reduction respectively, Fig. 3.2.10. and Table 3.2.3.). Co-injection of GCLm-human with the GCLm-shRNA#1 or GCLm-shRNA#2 did not prevent DA neurons degeneration in SNpc (Fig. 3.2.10.). Fig.3.2.11. shows representative TH immunostained pictures of SNpc in red and in green the EGFP expression levels, showing the viral targeted cells.

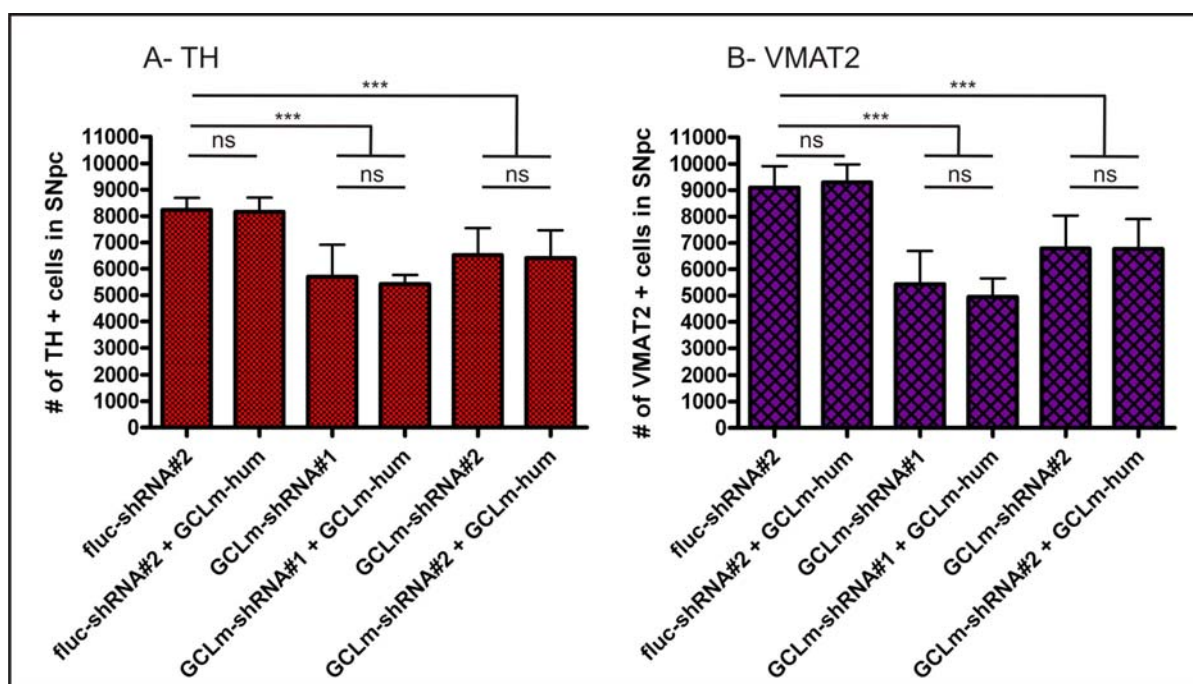
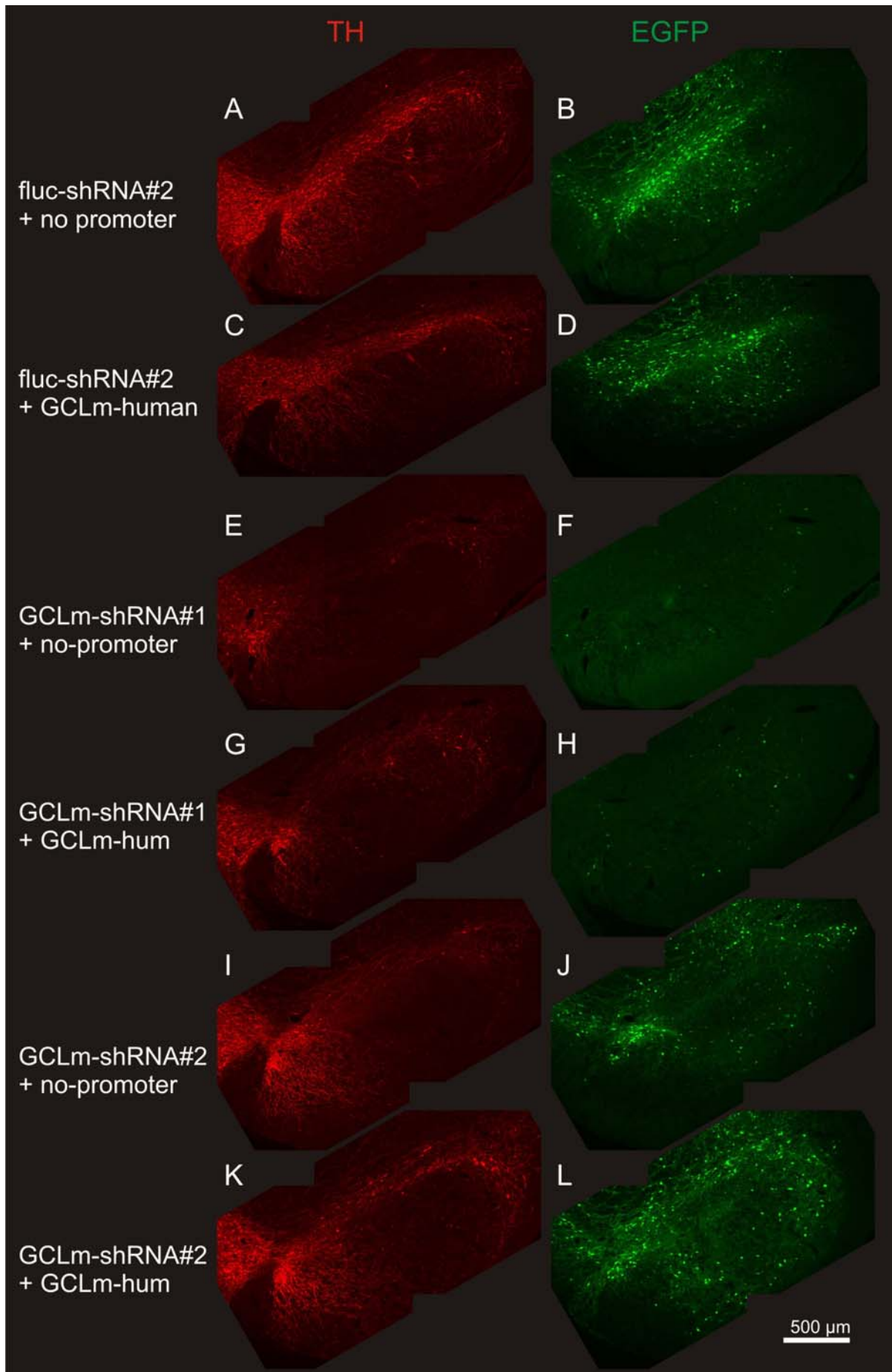


Fig. 3.2.10. Quantification of DA-neuron survival after injection of AAV2 encoding GCLM specific shRNAs into rat SNpc. The number of surviving TH<sup>+</sup> neurons (A) or VMAT2<sup>+</sup> neurons (B) was determined 9 weeks after one control shRNA (fluc-shRNA#2) or two shRNAs targeting the modulatory subunit of glutamate cysteine ligase (GCLm-shRNA#1 or GCLm-shRNA#2) were co-injected with no-promoter or a vector expressing GCLm-human. A total dosage of  $1.2 \times 10^8$  t.u. of recombinant AAV2 vectors were injected in the rat SNpc. A virus encoding EGFP but lacking the promoter (no-prom) was used as “empty vector” to fill up the virus amount (normally  $0.6 \times 10^8$  t.u. was used of each virus). Columns represent mean values  $\pm$  standard deviation (\*\* $p < 0.001$  and ns  $p > 0.05$  (non-significant)).

Table 3.2.3. Number of surviving TH<sup>+</sup> or VMAT2<sup>+</sup> neurons in rat SNpc 9 weeks after viral injection.

Condition	TH <sup>+</sup> cells			VMAT2 <sup>+</sup> cells		
	Mean	$\pm$ SD	N	Mean	$\pm$ SD	N
fluc-shRNA#2 + no-prom	8232	$\pm$ 454	10	9102	$\pm$ 815	10
fluc-shRNA#2 + GCLm-hum	8161	$\pm$ 536	6	9289	$\pm$ 685	6
GCLm-shRNA#1 + no-prom	5699	$\pm$ 1213	6	5435	$\pm$ 1252	6
GCLm-shRNA#1 + GCLm-hum	5420	$\pm$ 344	6	4947	$\pm$ 701	6
GCLm-shRNA#2 + no-prom	6524	$\pm$ 1018	6	6787	$\pm$ 1244	6
GCLm-shRNA#2 + GCLm-hum	6405	$\pm$ 1047	6	6772	$\pm$ 1137	6

TH or VMAT2 surviving neurons in the rat SNpc after AAV2 mediated shRNA expression. In the rat SNpc a total dosage of  $1.2 \times 10^8$  t.u. of recombinant AAV2 vectors were co-injected. One virus encoding EGFP but lacking the promoter (no-prom) was used as “empty vector” to fill up the total virus particles (normally  $0.6 \times 10^8$  t.u. was used of each virus). Number of TH and VMAT2 positive neurons were accessed 9 weeks after injection. Numbers represent means  $\pm$  SD from N independent injected SNpc.



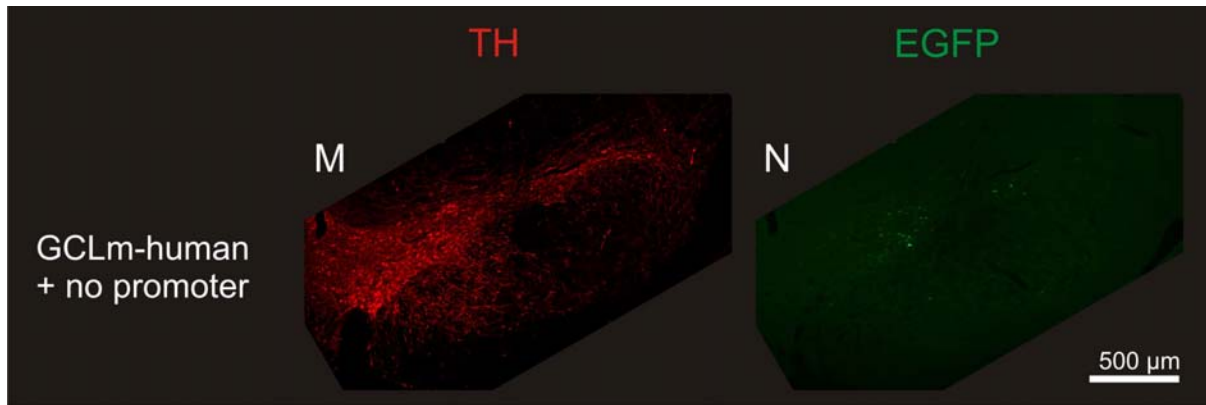


Fig.3.2.11. TH surviving DA neurons in the SNpc after AAV2 vectors co-injection. EGFP is expressed from the shRNA containing vector. A and B control fluc-shRNA#2 co-injected with no-promoter; C and D control fluc-shRNA#2 co-injected with GCLm-human; E and F GCLm-shRNA#1 vector co-injected with no-promoter; G and H GCLm-shRNA#1 vector co-injected with GCLm-human; I and J GCLm-shRNA#2 vector co-injected with no-promoter; K and L GCLm-shRNA#2 vector co-injected with GCLm-human; M and N GCLm-human co-injected with no-promoter. TH in red and EGFP in green. A total dosage of  $1.2 \times 10^8$  t.u. of AAV2 vectors ( $0.6 \times 10^8$  t.u. each AAV) was used. Rats were perfused 9 weeks after injection. (Scale bar: 500  $\mu$ m)

Using immunohistochemistry we looked for the expression of GCLm in the SNpc. In figure 3.2.12., the E, F, G and H show photomicrographs of brains where GCLm-human was co-injected with “no-promoter”, control fluc-shRNA#2, GCLm-shRNA#1, or GCLm-shRNA#2, respectively.

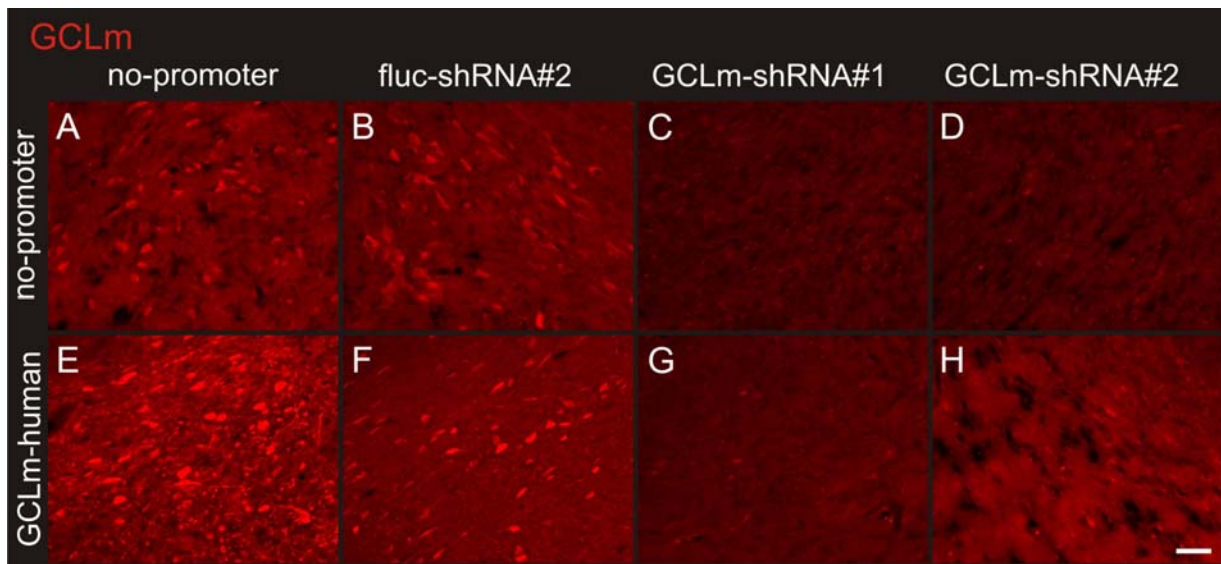


Fig.3.2.12. GCLm staining pictures after AAV2 vector injection into SNpc, expressing in A no-promoter (empty vector); B control fluc-shRNA#2 co-injected with no-promoter; C GCLm-shRNA#1 vector co-injected with no-promoter; D GCLm-shRNA#2 vector co-injected with no-promoter; E GCLm-human co-injected with no-promoter; F control fluc-shRNA#2 co-injected with GCLm-human; G GCLm-shRNA#1 vector co-injected with GCLm-human; H GCLm-shRNA#2 vector co-injected with GCLm-human. A total dosage of  $1.2 \times 10^8$  t.u. of AAV2 vectors ( $0.6 \times 10^8$  t.u. each AAV) was used. Rats were perfused 9 weeks after injection. (Scale bar: 50  $\mu$ m)

It was not possible to detect an increase in the GCLm immunostaining when GCLm-human was co-expressed with control or GCLm specific shRNAs (Fig. 3.2.12.). Increased GCL-human immunostaining was observed *in vivo* when GCL-human was co-injected with “no-promoter” virus, thus showing the virus capacity to express GCLm-human (Fig. 3.2.12. E).

These results showed that GCLm down-regulation by expression of specific shRNAs induces DA neurons cell death. Expression of a non-targetable construct failed to prevent the shRNA expression mediated effects, however no obvious GCLm-human overexpression was detected. In conditions where GCLm was co-expressed a few dystrophic dendrites were observed by TH staining, thus indicating that GCLm may be expressed in some DA cells and may be responsible for the dendrite abnormalities.

### **3.2.2.6. Overexpression of both subunits of GCL provoked degeneration of DA neurons**

The failure of “rescue” experiments under most experimental conditions used in this study suggested that either all “specific” shRNAs would induce off-target effects, or that overexpression of GCLc and / or GCLm themselves could lead to neurodegeneration, although in the *in vitro* studies do not corroborate this hypothesis. To investigate this issue we co-injected GCLm human or the GCLc-bp-exch#3 plus the “no-promoter” vector into rat SNpc. We observed a approximately 30% reduction in DA neurons when GCLm human or the GCLc-bp-exch#3 expression was compared with control “no-promoter” injection at 9 weeks after injection. There was no difference between injection of GCLm human or the GCLc-bp-exch#3 (Fig. 3.2.13. and Table 3.2.4.).

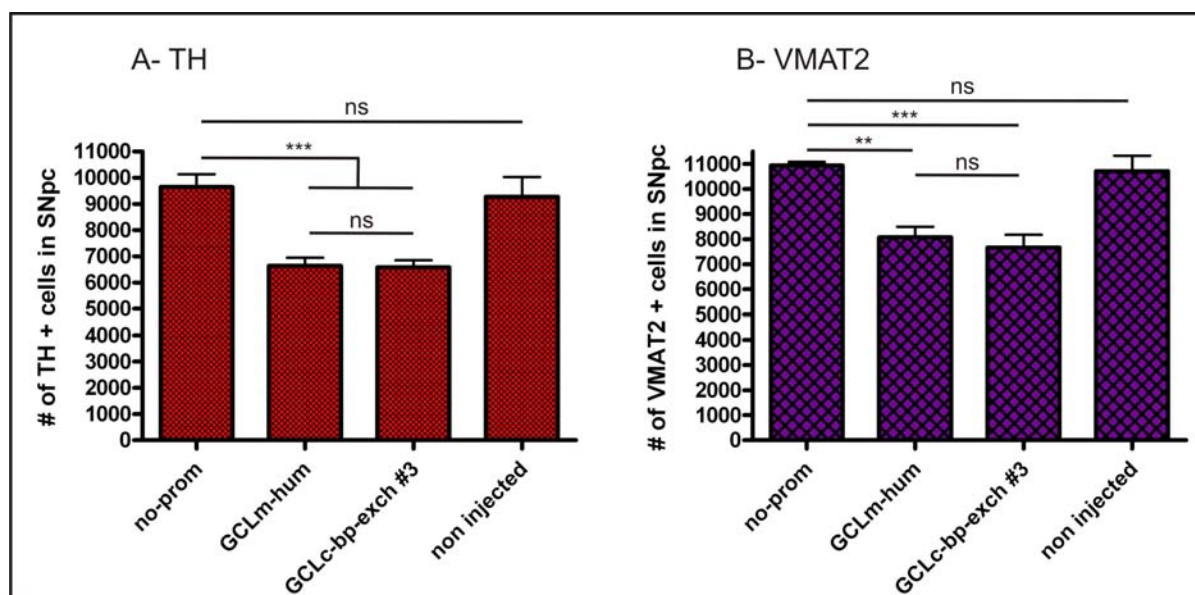


Fig. 3.2.13. Quantification of DA-neuron survival after rescue constructs coding rAAV2 injection into rat SNpc. The number of surviving TH<sup>+</sup> neurons (A) or VMAT2<sup>+</sup> neurons (B) was determined 9 weeks after one control non expressing vector (no-prom), the human modulatory subunit of glutamate cysteine ligase (GCLm-hum) or the catalytic subunit of glutamate cysteine ligase (GCLc-bp-exch#3) vector injection into rat SNpc. Total number DA neurons in non injected SNpc was also determined. A total dosage of  $1.2 \times 10^8$  t.u. of recombinant AAV2 vectors were injected in the rat SNpc. A virus coding EGFP but lacking the promoter (no-prom) was used as “empty vector” to fill up the virus amount in the case just one effective virus was desirable (normally  $0.6 \times 10^8$  t.u. was used of each virus). Columns represent mean values  $\pm$  standard deviation (\*\*\* $p < 0.001$ , \*\* $p < 0.01$  and ns  $p > 0.05$  (non-significant)).

Table 3.2.4. Number of surviving TH<sup>+</sup> or VMAT2<sup>+</sup> neurons in rat SNpc 9 weeks after viral injection.

Condition	TH <sup>+</sup> cells			VMAT2 <sup>+</sup> cells		
	Mean	$\pm$ SD	N	Mean	$\pm$ SD	N
no-prom + no-prom	9652	$\pm$ 481	3	10944	$\pm$ 136	3
GCLm-hum + no-prom	6636	$\pm$ 305	8	8075	$\pm$ 417	8
GCLc-bp-exch #3 + no-prom	6573	$\pm$ 267	8	7663	$\pm$ 515	8
non injected	9270	$\pm$ 756	8	10709	$\pm$ 620	8

TH or VMAT2 surviving neurons in the rat SNpc after AAV2 mediated transfer of no-promoter, ex. In the rat SNpc a total dosage of  $1.2 \times 10^8$  t.u. of recombinant AAV2 vectors were co-injected. One virus encoding EGFP but lacking the promoter (no-prom) was used as “empty vector” to fill up the total virus particles (normally  $0.6 \times 10^8$  t.u. was used of each virus). Number of TH and VMAT2 positive neurons were accessed 9 weeks after injection. Numbers represent means  $\pm$  SD from N independent injected SNpc.

The over-expression of both GCLc and GCLm induced swellings of the DA neuron’s dendrites revealed by TH immunostaining (Fig.3.2.14 .B and C). We also observed that those dystrophic neuritis were positive for GCLm, indicating that cellular overload with glutathione producing enzymes was responsible for this effect (Fig.3.2.14 .E and F). We hypothesized that these dystrophic dendrites would be a consequence of too much glutathione production in



the DA neurons. An antibody specific for glutathione-protein complexes was used in immunohistochemistry to test the presence of these complexes in the cells.

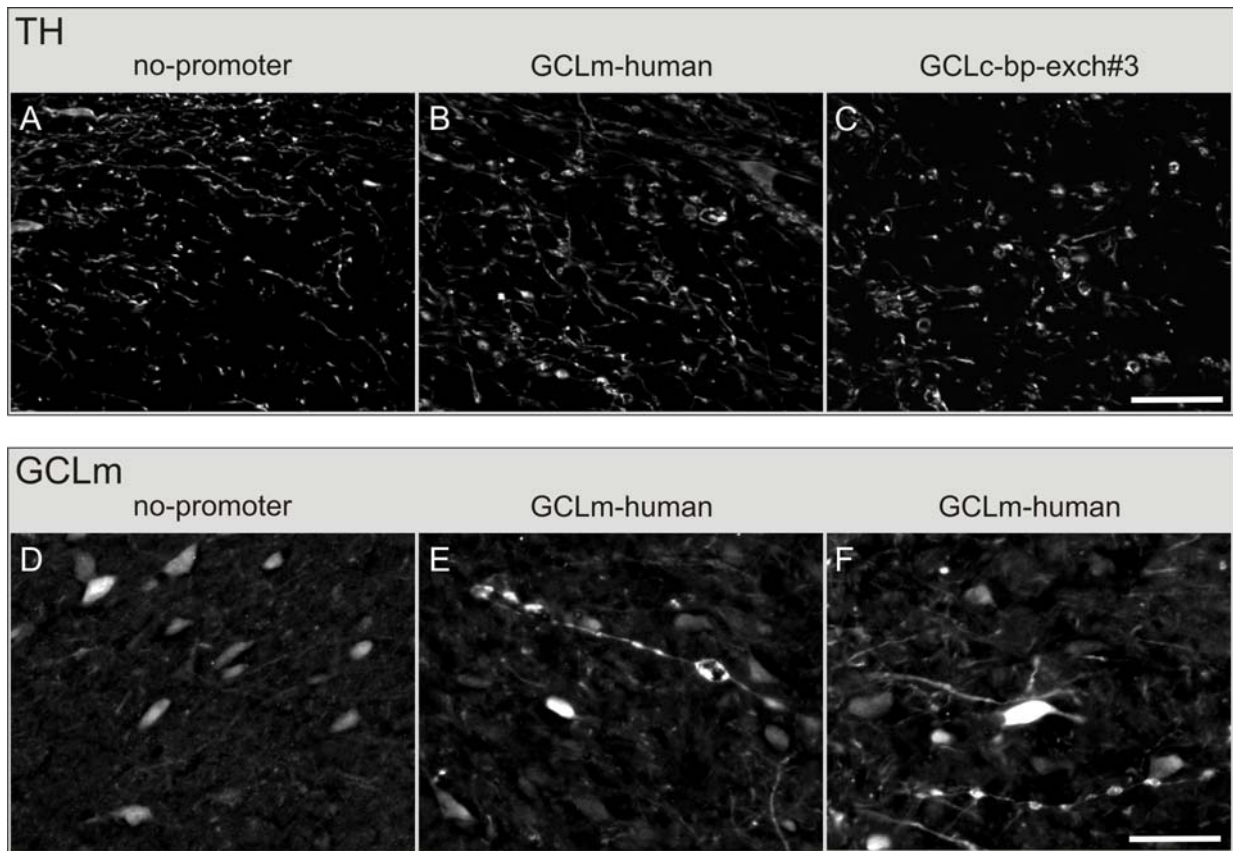


Fig.3.2.14. Representative pictures from rat SNpc where AAV2 were injected expressing in A and D no-promoter (empty vector); in B, E and F GCLm-human plus no-promoter and in C GCLc-bp-exch#3 plus no-promoter. A, B and C shows SNpc cells and dendrites stained with TH antibody. In D, E and F shows SNpc cells and dendrites stained with GCLm antibody. Pictures were taken at 9 weeks post injection. (Scale bar: 50  $\mu$ m)

Figure 3.2.15. A and D shows normal morphology of dendrites after “no-promoter” injection into SNpc. DA neurons in B and E where subjected to GCLm-human overexpression and demonstrate prominent swellings in dendrite which in some cases are as voluminous as the DA neurons cell bodies (Fig. 3.2.15. B and E). The expression of GCLc-bp-exch#3 induced similar alterations in dendrite morphology (Fig. 3.2.15. C and F). Confocal like high power magnification pictures were acquired and showed co-localization of TH (green) and GSH protein complexes (red) stained structures in the DA neurons swellings but not in not no-promoter transduced cells (Fig.3.2.15.).

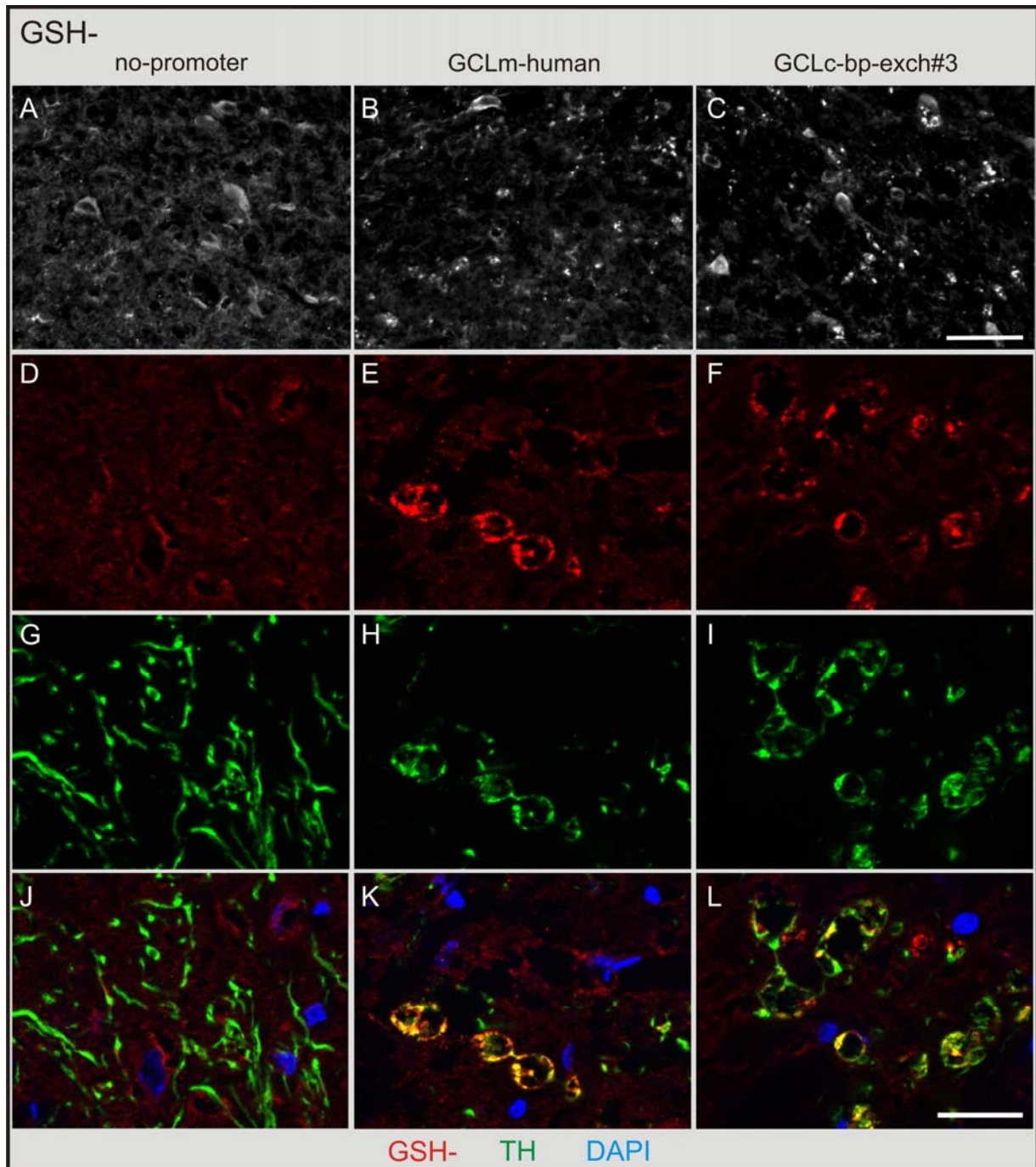


Fig.3.2.15. Representative pictures from rat SNpc injected with AAV2 vector expressing no-promoter (A, D, G and J), GCLM-human plus no-promoter (B, E, H and K) or GCLc-bp-exch#3 plus no-promoter (C, F, I and L). A-F were immunostained with a GSH protein complexes antibody. G-I were stained for tyrosine hydroxylase. From J-L red represents in red GSH protein complexes staining, green the TH staining, and blue DAPI staining of nuclear DNA. A total dosage of  $1.2 \times 10^8$  t.u. of virus was injected in a 2  $\mu$ l volume. (Scale bar: 50  $\mu$ m in A-C; or 20  $\mu$ m in D-L).

Expression of GCLc or GCLm induces significant death DA neurons *in vivo* at 9 weeks after expression. Dystrophic and swollen dendrites were observed after overexpression of GCLc and GCLm. In swollen dendrites, GSH protein complexes were recognized by a specific antibody, thus indicating that GSH over-production may induce detrimental effects in DA neurons.

### **3.2.2.7. NeuN loss in the SNpc upon GCLm or GCLc shRNAs expression.**

During the last years it was demonstrated that in some cases in DA neurons TH expression can be down-regulated or post-translationally modified in a way that pan antibodies may not detect it any more. For this reason we also used the VMAT2 marker as another DA neuron's specific marker, to evaluate the number of DA neurons. No significant difference was found between the number of TH positive neurons and the number of VMAT2 positive DA neurons. In order to confirm neuronal loss using an independent marker, we used NeuN to assess the effects of shRNAs expression in DA neurons and in other neuronal populations. Figure 3.2.16. show representative pictures of SNpc sections immunostained with NeuN antibody at 9 weeks after injection. After expressing GCLc-shRNA#2, GCLc-shRNA#3 and GCLm-shRNA#2 we confirmed a loss of NeuN neurons in the SNpc region. GCLm-shRNA#1 expression resulted in neuronal loss in other cell populations apart from the DA neurons. Normally, in the needle tract some cells are transduced and express the reporter gene. In brains where GCLm-shRNA#1 was expressed the number of EGFP expressing cells (cells also expressing GCLm-shRNA#1) was very low, thus indicating that all cells receiving the GCLm-shRNA#1 died. This effect may result from high GCLm knock-down efficacy.

Staining the brain sections with NeuN specific antibody further confirmed the neuronal cell loss resulting from shRNAs targeting GCLc and GCLm expression. GCLm-shRNA#1 expression induced cell death in the DA neurons and other cell populations in the vicinity of the injection tract.

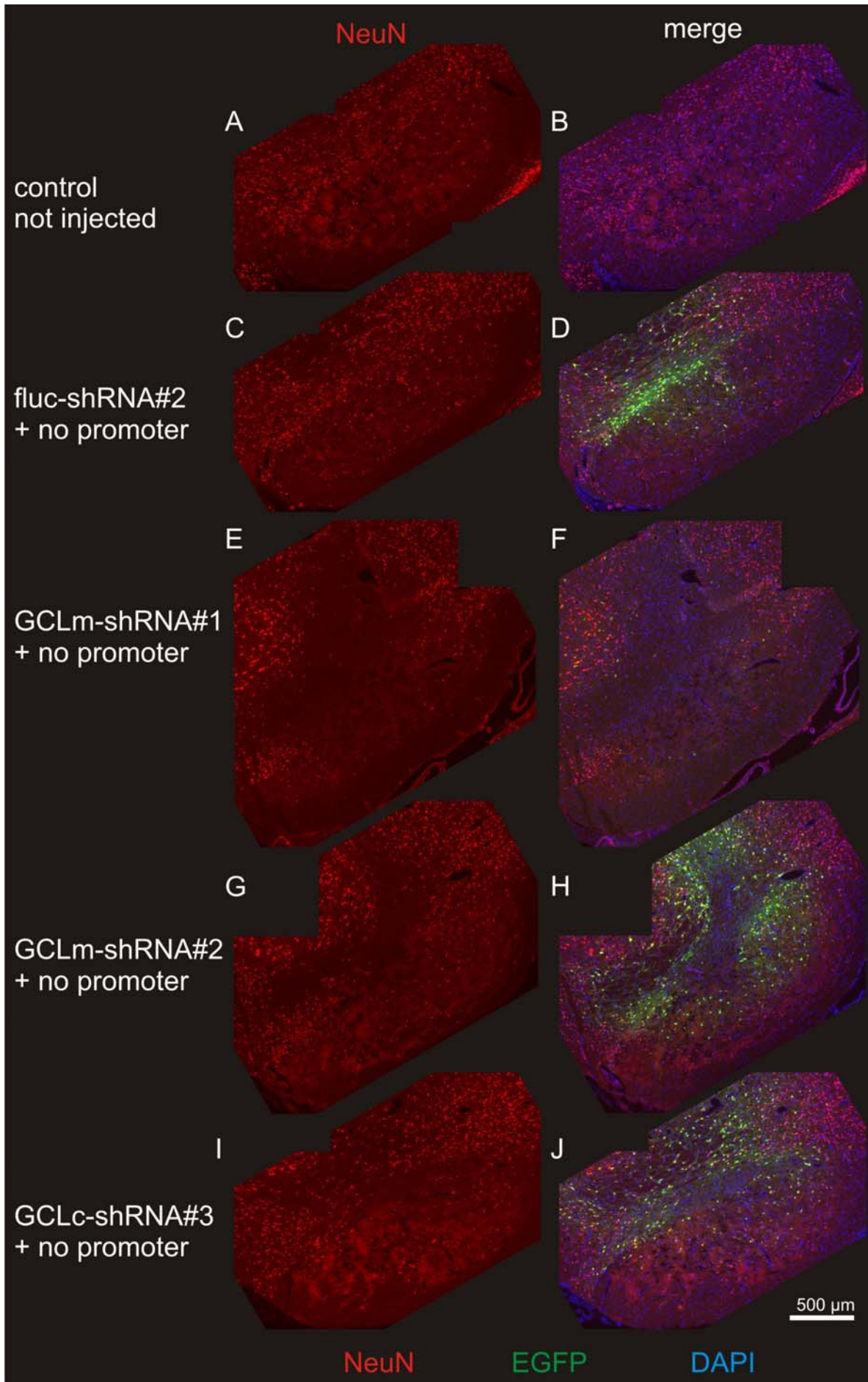


Fig.3.2.16. Representative NeuN pictures from rat SNpc. Representative pictures of SNpc in a non injected specimen (A and B), control injected SNpc (C and D), GCLm-shRNA#1 (E and F), GCLm-shRNA#2 (G and H) and GCLc-shRNA#3 (I and J). Red corresponds to NeuN staining, green to EGFP expression and blue to DAPI nuclear DNA staining. A total dosage of  $1.2 \times 10^8$  t.u. of virus was injected in a 2  $\mu$ l volume in the SNpc. Brains were perfused 9 weeks after virus application. (Scale bar: 500  $\mu$ m).



## 4. Discussion

In post mortem analysis of PD brains the GSH levels were specifically reduced in substantia nigra (Sofic et al. 1992; Sian et al. 1994a). This effect appears to be specific for PD, since patients suffering from multiple-system atrophy, and progressive supranuclear palsy that also exhibit nigral cell loss did not show a reduction in GSH (Sian et al. 1994a). Therefore the altered GSH/GSSG ratio in the substantia nigra in Parkinson's disease suggested that oxidative stress may be a major component in the pathogenesis of dopaminergic neuron degeneration. Several studies have been conducted to investigate the effects of glutathione depletion in DA neurons using a pharmacological approach. Infusion of L-buthionine (S,R) sulphoximine (L-BSO), a irreversible inhibitor of GCLc, into the left lateral ventricle or locally to the SNpc of adult rats failed to induce DA neuron degeneration (Wullner et al. 1996; Toffa et al. 1997). However, combination of nigral injections of L-BSO with intra-striatal injections of MPP<sup>+</sup> in adult rats potentiated DA neurons cell death (Wullner et al. 1996). These studies suggested that GSH depletion *per se* is not an inducer of neuron degeneration, but these studies did not deplete GSH specifically in DA neurons.

We aimed for the reduction of GSH contents specifically in SNpc neurons of adult rats, in order to readdress the role of GSH depletion in PD. For this purpose, viral vector based RNA-interference was used to down-regulate or overexpress key enzymes of GSH synthesis *in vivo*, specifically in DA neurons, by AAV vector mediated gene transfer.

We show that knock-down of either the catalytic or modulatory subunits of glutamate cysteine ligase (GCL), the rate limiting enzyme in GSH synthesis, elicits spontaneous neurodegeneration both in primary cortical neurons *in vitro* and in DA neurons *in vivo*. By knock-down of either the catalytic or the modulatory GCL subunit we created a new animal model of PD, thus corroborating the important role of GSH in the maintenance of neuronal survival.

### 4.1. AAV2 as a gene transfer vehicle

We aimed to investigate the consequences of depleting neurons from their major antioxidant defence *in vivo*. Neurons rely on astrocytes which supply precursors for GSH *de novo* synthesis, e.g. astrocytes release the glutamate precursor glutamine, and GSH which is processed in the extracellular space providing cysteine and glycine (for review see Dringen

and Hirrlinger 2003). Thus, interference with astrocytic GSH synthesis could indirectly result in increased neuronal vulnerability for cell death *in vivo*. For this reason AAV2 serotype viral vector was used as a tool for gene transfer, because it preferentially transduces neurons in culture and in the CNS (Mandel et al. 1998; Xu et al. 2001; Shevtsova et al. 2005), has especially high affinity to DA neurons of SNpc (Paterna et al. 2004; Shevtsova et al. 2006) and results in long-lasting transgene expression *in vivo*.

*In vitro* AAV2 vectors transduce mainly neurons but also astrocytes to some extent. For this reason, and because the polymerase III H1 RNA promoter driving expression of the respective shRNAs is a ubiquitous promoter (Myslinski et al. 2001), we treated the primary neuronal culture with Ara-C to inhibit astrocyte proliferation. In the achieved neuronal enriched culture we have studied the effect of GSH reduction principally in neurons.

*In vivo* AAV2 vectors exhibited a very low tropism towards astrocytes in the SNpc region. The number of transduced astrocytes expressing EGFP driven by the GFAP promoter was neglectable. Weak EGFP expression, driven by the GFAP promoter, was found in TH positive cells. These observations further supported the concept of higher AAV2 tropism towards neurons in general and DA neurons in particular. With a single injection of AAV2 viral vector into the SNpc we achieved high transduction efficiency (up to 75% of total SNpc DA neurons). This targeting efficiency was sufficient and reliable to evaluate the effects of knock-down or overexpression of either the catalytic or modulatory GCL subunits.

#### **4.2. shRNA silencing efficacy**

The RNAi test system used in this work for the screening of siRNAs/shRNAs targeted towards the genes of interest has previously been published (Malik et al. 2006). This test system is easy-to-handle, allows for the sequence analysis in a reasonable time, the reporter protein is easy to measure, and the dynamic range of regulation is good allowing for discrimination of knock-down efficacies. Nevertheless, this test system as well as co-transfection experiments performed in cell lines are based on the downregulation of an extrinsic mRNA which is not in the same context as the endogenous mRNA to be silenced. Flanking sequences, secondary and tertiary mRNA structures and the regulation of endogenous mRNAs will finally dictate the success of a silencing experiment. In addition, these experiments are normally carried out for short time periods in easy to handle, fast dividing and resistant cells, where off-target effects are difficult to quantify. Our results



clearly demonstrate that such “easy going” test systems do not reliably predict the silencing efficacy of a given shRNA molecule. Nevertheless they are necessary in the screening of various shRNA molecules.

#### **4.3. *In vitro* experiments as proof of concept**

Our data demonstrated that the knock-down of the catalytic or the modulatory GCL subunits is sufficient to cause decreased glutathione concentrations and induce cell death *in vitro*: We used efficient tools to transduce and manipulate gene expression significantly in cultured neurons. In the manipulated neurons the total glutathione (GSx) levels were measured. The used assay system allowed for independent GSSG (glutathione disulfide) and GSx (total glutathione) measurement, but not of GSH determination directly. GSH can be calculated as the result of GSx minus GSSG concentration. As GSSG measurements revealed very low levels when compared with total glutathione concentrations, we considered GSx to directly reflect the GSH content. GSx content was normalized to protein levels of each lysate, thus excluding GSx decrease as result of cell death and showing that GSx levels were reduced per cell.

The targeting of the subunits of GCL holoenzyme with several different shRNAs resulted in cell death and glutathione depletion. Expression of these different shRNAs induced different degrees of cell impairment and GSx depletion which strongly suggests a specific effect. The expression of control shRNAs *in vitro* had a minor and insignificant impact on these parameters. Importantly, we verified that targeting of the subunits of GCL holoenzyme resulted in decreased GSx levels, which was absolutely necessary to be demonstrated *in vitro* since GSH content can not be measured within individual neurons *in vivo*. However, these results were challenged by the fact that it was not possible to “rescue” the effects of different shRNAs by co-expression of non-targetable GCLc and GCLm. GCLc rescue protein resulted in elevated GSx levels and thus proved to be functional, and both GCLc and GCLm “rescue” constructs did not show neurotoxicity. Thus at present we can not explain this *in vitro* result.

#### **4.4. *In vivo* targeting of GSH metabolism**

It has been a matter of debate for many years whether an impairment of GSH production could directly lead to neurodegeneration *in vivo*. We aimed at depleting levels of GCLc and GCLm specifically in neurons by neuron specific gene transfer, and this approach

demonstrated for the first time under *in vivo* conditions that neurodegeneration occurs as a direct consequence of GCLc or GCLm downregulation. However, as a determination of actual GSH levels on a per neuron basis is impossible in fixed tissue specimen we can not give a quantitative assessment of the extent of GSH depletion resulting from GCLc or GCLm downregulation. None the less, results obtained in this study strongly suggest a direct correlation of the extent of depletion of neuronal GSx levels with severity of neurodegeneration. This is exemplified by the fact that shRNAs demonstrating higher levels of GSH depletion *in vitro* result in higher levels of DA neuron loss *in vivo*.

We observed that knock-down of the catalytic or the modulatory GCL subunit is sufficient to induce cell death *in vivo*. These results are in agreement with previous reported genetic models in which complete disruption of the GCLc subunit gene in mice was lethal after embryonic day 8, while heterozygote appear to have a normal phenotype (Dalton et al. 2000; Shi et al. 2000). Contradicting data resulted from pharmacological studies in which L-BSO infusion into the left lateral ventricle of adult rats resulting in reduced GSH concentrations in the substantia nigra and in the striatum. Toffa and colleagues have reported that a 65% GSH reduction upon L-BSO infusion in the substantia nigra did not induce DA neuron cell loss (Toffa et al. 1997). In this study the levels of glutathione were estimated not in DA neurons but in the overall tissue surrounding the nigra region (including astrocytes and other glial cells), thus failing to demonstrate the specific reduction of GSH in DA neurons. The discrepancy between our results and L-BSO infusion model may be explained by the fact that we use RNAi approach to impair enzymes expression specifically in DA neurons. Our shRNA is continuously expressed and not self limiting in SNpc DA neurons over a long period of time.

In contrast to our results, no apparent deficits were found in GCLm KO mice which demonstrated GSH levels of approximately 20% of the control littermates (McConnachie et al. 2007). Again, in this experimental condition the estimation of brain GSH did not discriminate between neuronal and total tissue GSH thus, thus not showing a specific reduction of GSH in neurons. However, the overall “viability” of the GCLm KO mice does not exclude ongoing degeneration in brain cell populations more vulnerable to oxidative stress, e.g. the SNpc. Nevertheless, under “non stress” conditions glutathione levels 20% of normal might be sufficient for cell survival.

The reproducibility of the *in vitro* results *in vivo*, and the different levels of cell death which reflected the GSH depletion *in vitro*, indicated for a specific shRNA mediated downregulation of the target proteins *in vivo*. Nevertheless during the course of *in vivo* experiments we experienced that all control shRNAs induced significant and not neglectable cell toxicity which increased over time. One control shRNA directed against the luciferase firefly gene (fluc-shRNA#1) induced remarkable cell death *in vivo*, however the same shRNA *in vitro* did not induce significant toxic effects. The difference between *in vitro* and *in vivo* might have resulted from the different expression times. Aiming to rule out the reasons for the cell loss induced by the control shRNA we performed a comparison of free Gibbs energy for each shRNA sequence using a web server for nucleic acid folding (mfold). The analysis revealed that fluc-shRNA#1 has a higher folding energy (-45,9 kcal/mol) when compared with all other shRNAs (~ -32 kcal/mol) (Mathews et al. 1999;Zuker 2003). The difference in free Gibbs energy may indicate the need of more energy for dsRNA strands unwinding; which may potentially lead to an increase in the dsRNA stability and to the accumulation of these molecules in the cell. Recently RNAi induced toxicities had been uncovered and the inducing mechanisms include saturation of endogenous RNAi machinery, stimulation of cellular responses to dsRNA, unbiased loading of the RISC complex, sequence specific off targeting due to partial complementarity and accumulation of antisense RNA sequences (Bridge et al. 2003;Sledz and Williams 2004;Yi et al. 2005;Hornung et al. 2005;Grimm et al. 2006;Birmingham et al. 2006;Castanotto et al. 2007;Stewart et al. 2008;Denovan-Wright et al. 2008;McBride et al. 2008). Detection of these off target effects may require systematic analyses of cellular transcriptional activity, either at the RNA level or at protein level. The next generation of algorithms for RNAi design will have to consider rules to avoid side effects while at present times empirical testing of the RNAi sequences may be required for each target and in each experimental condition (Boudreau et al. 2008).

In our experiments we prevented shRNA induced cell death *in vivo* by co-expression of non-targetable GCLc and the GCLc specific shRNA in the same vector at the 9 weeks time point. This result strongly demonstrated the specificity of the approach. Nevertheless at 3 and 6 weeks no more than a tendency for protection was observed. Interestingly, expression of  $\alpha$ -synuclein from the same vector as GCLc shRNA partially prevented DA neuron cell death. This indicated that under certain conditions  $\alpha$ -synuclein A53T can exert neuroprotective effects. The contribution of  $\alpha$ -synuclein to the pathogenesis of PD is still enigmatic with some authors attributing to  $\alpha$ -synuclein a protective role, while other consider it to induce toxicity

(Tanaka et al. 2004;Albani et al. 2004;for review see Tofaris and Spillantini 2005;Colapinto et al. 2006). The expression of hDJ1 induced 2.5 fold increased levels of GCLc mRNA in cultured cells and by this means increased GCLc activity (Zhou and Freed 2005). In our experiments hDJ1 expression failed to prevent cell death, this result may be explained by GCLc specific shRNA#2 mediated targeting of endogenous upregulated GCLc mRNA.

In contradiction, the expression of non-targetable GCLc and a specific GCLc shRNA from different vectors did not prevent DA neurons death in SNpc. Rather expression of non-targetable GCLc increased cell death significantly. This result suggested that high levels of GCLc may result in DA neurons cell death. This unexpected induction of neurodegeneration resulting from GCLc expression stimulated us to investigate the effects of GCLc and GCLm overexpression *in vivo*. Over 9 weeks the expression of GCLc or GCLm in the SNpc resulted in approximately 30% reduction of DA neurons. In addition to cell death, we observed swellings of the remaining TH positive dendrites located ventrally to SNpc. This observation of swollen dendrites suggested that too much of GSH producing enzymes may result in unphysiological GSH concentration in the cells which resulted in cell death. In addition they suggested that at least in DA neurons a fine tuned regulation of GSH levels is necessary for cell maintenance. There are various lines of evidence which support the existence of redox signalling and redox regulation as mediators of physiological cellular function. Meanwhile it is accepted that the concept of considering oxidative stress (ROS) only as “bad” and antioxidants only as “good” can not be drawn anymore (Ghezzi et al. 2005). The ratio between GSH/GSSG regulates several enzymes of glycolysis and gluconeogenesis (Gilbert 1984) by protein modifications which include glutathionylation, carbonylation, nitrotyrosilation and disulfide bond formation. Moreover, it has been demonstrated that GSH participates in cellular signal transduction pathways in which ionotropic receptor function was modulated (Gozlan and Benari 1995;Bains and Shaw 1997;Mayer et al. 1998;Janaky et al. 1999;Grima et al. 2003). In addition reactive oxygen species (ROS), e.g. hydrogen peroxide (H<sub>2</sub>O<sub>2</sub>) and nitric oxide (NO), have physiological roles as signalling molecules (Veal et al. 2007;Giorgio et al. 2007). Together, our data unambiguously supported the cellular redox state as one important modulator of DA neuron maintenance.

Although we were not able to measure GSH content in DA neurons, the dystrophic and swollen dendrites in addition with cell loss appears to be attributed to a higher GSH content. Overexpression of GSH producing enzymes can result in excess GSH concentration which may impair the proteins structure and functionality. An antibody specific for complexes of

glutathione and protein residues recognized the presence of GSH protein complexes within the dendrite swellings. We also observed the localization of the GCLm protein within the dendrite swellings. These results suggested that overexpression of GSH producing enzymes may result in GSH overproduction and therefore may imbalance the essential cellular redox equilibrium.

#### **4.5. Cell death mechanism**

It has been shown that GSH depletion can result in complex I inhibition (Merad-Boudia et al. 1998;Merad-Saidoune et al. 1999;Hsu et al. 2005;Bharath and Andersen 2005;Chinta and Andersen 2006). Complex I inhibition following acute glutathione depletion appears to take place via an NO-mediated event (Hsu et al. 2005;Chinta and Andersen 2006). These results suggested that the early glutathione depletions observed in the Parkinsonian SNpc (Jenner et al. 1992;Sian et al. 1994a) could be responsible for subsequent complex I inhibition, mitochondrial dysfunction, and neuronal cell loss (Schapira et al. 1990;Jenner et al. 1992;Mann et al. 1994;Gu et al. 1998). We have used Fluorojade C staining as general marker for neurodegeneration. Fluorojade C labels degenerating neurons resulting from diverse insults (e.g. kainic acid, domoic acid, 3-nitropropionic acid, and 1-methyl-4-phenyl-1,2,3,6-tetrahydropyridine (MPTP)). Fluorojade C demonstrated neuronal staining in ischemic rat brain tissue used as positive control. In the SNpc mainly “fibrous” stained material was observed in GCLc depleted nigra. These processes most likely represent neuronal dendrites or axons, although they can also be derived from activated astrocytes (Colombo and Puissant 2002;Schmued et al. 2005). Few cell body like structures were identified which could not be assigned unequivocally to degenerating neurons. We therefore used cleaved caspase-3 and cleaved caspase-9 specific antibodies to further evaluate the presence of these mediators of apoptotic cell death in DA neurons in the SNpc. *In vitro* cleaved caspase-3 staining suggested a contribution of apoptotic process to neurodegeneration. We did not achieve *in vivo* a specific and therefore unambiguous staining signal for these apoptotic cell death markers. In addition the presence of fragmented picnotic nucleus in the SNpc of injecting animals was never observed, which argues against a prominent contribution of apoptosis to DA neuron degeneration in this model. In PD neuronal cell death appears to occur by apoptosis rather than necrosis, although there is controversy over the extent to which this occurs.(Mochizuki et al. 1996;Anglade et al. 1997;Kosel et al. 1997;Banati et al. 1998;Kingsbury et al. 1998;Tatton et al. 1998;Tatton 2000). Knowing about the possible involvement of autophagy in cell death mediated by oxidative stress as the result of inhibition of mitochondrial complex I or complex

II *in vitro* (Chen et al. 2007b), we have used a specific antibody for MAP light chain 3 (MAP LC3) protein. MAP LC3 is essential for autophagy and becomes associated with the autophagosome membranes after processing. Within the SNpc we did not find a specific increased signal for increased autophagy in transduced DA neurons.

Overall we could not identify the cell death mechanism induced by knockdown of GSH producing enzymes *in vivo*. We can not exclude apoptosis or autophagy as mediators of cell death in our model, due to the lack of positive control material to show that the antibodies actually work with sufficient sensitivity. We found a low number of degenerating cells with Fluorojade C staining indicating that the number of degenerating cells at certain time point may be very low, thus this may be the reason why we did not find apoptotic or autophagy specific staining at a given time point .

#### **4.6. Perspectives**

We have created a rat model with slow and progressive DA neuron degeneration by decreasing levels of the cells principal oxidative defence. Although we achieved DA neurons degeneration the mechanism promoting cell death remains elusive. We will produce positive control tissue in order to re-evaluate the contribution of both autophagy and apoptosis in mediating cell death in this model. Furthermore rat and human wild type or mutant forms of  $\alpha$ -synuclein will be expressed in order to compare and re-evaluate the role of  $\alpha$ -synuclein in protection against oxidative stress in our model. We will further evaluate the long term effects of GSH producing enzymes overexpression or knock-down both in DA neurons and astrocytes. High levels of GSH (~196%) and reduced levels of GSSG (60%) were shown in the globus pallidus of patients dying with multiple-system atrophy disease, thus indicating that aberrantly high levels of GSH may have relevance in human neurodegenerative diseases (Sian et al. 1994a). Although shRNA mediated silencing is a powerful and efficient technique to silence the proteins of interest, recent reports and our data have revealed that caution should be taken with their application. Therefore we will create a GCLc dominant negative protein, which will form a dimer with GCLm and create a non-functional holoenzyme. By this means cells will be deprived from a functional enzyme capable of *de novo* GSH synthesis. Using cell specific promoters and viral vectors with high tropism either for neurons or astrocytes we will further evaluate in neurons and for the first time in astrocytes redox equilibrium contribution to the pathogenesis of PD.

## 5. Summary

Parkinson's disease (PD) is characterized by a progressive degeneration of the nigrostriatal system. Only in few patients genetic mutations have been identified to cause disease onset, while the vast majority of cases remains idiopathic. The oxidative stress hypothesis claims that generation of neurotoxic oxidant species is crucially involved in disease onset and progression. In concordance with this hypothesis reduced levels of glutathione (GSH), the cell's most effective antioxidant, have been detected in the substantia nigra (SN) of PD patients. In an attempt to generate an animal model of PD closely resembling the human idiopathic situation, viral vector based RNA interference was used to down-regulate key enzymes of GSH synthesis in dopaminergic (DA) neurons of the rat SN *in vivo*. *In vitro* we developed experiments for the characterization of shRNA molecules efficacy. In primary neurons targeting the catalytic subunit (GCLc) or modulatory subunit (GCLm) of glutamate cysteine ligase (GCL) resulted in decreased glutathione levels which were correlated with neuronal impairment. *In vivo* we observed slowly progressive neurodegeneration which depended on the shRNA efficacy. The most effective shRNA targeting GCLc (GCLc-shRNA#2) induced 20% loss at 3 weeks, 35% loss at 6 weeks and 60% loss at 9 weeks compared with respective control shRNAs. The effect induced by GCLc-shRNA#2 was partially prevented by the expression of a non-targetable GCLc construct, thus demonstrating a specific knock-down mediated effect. We furthermore demonstrated that overexpression of GCLc and GCLm which may increase GSH production has neurodegenerative effects. Expression of these proteins resulted in dystrophic dendrites and induced approximately 30% DA neuron cell loss, thus indicating that a delicate balance of neuronal redox potential is essential for neuronal integrity. Our work demonstrated for the first time *in vivo* a direct evidence that the reduction of the DA neuron's antioxidative defence directly impairs neuronal survival. Moreover overexpression of each subunit of glutamate cysteine ligase in neurons by neuron-specific gene transfer into the SNpc resulted in DA neuron cell death.

Taken together these results substantially corroborate the oxidative stress hypothesis of neurodegeneration in PD and strongly suggested that changes in the fine-tuned regulation of glutathione homeostasis may result in detrimental changes of cellular equilibriums.





## 6. References

- Adams R. N., Blank L., KAROLCZA.M, Murrill E., and McCreery R. (1972) 6-Hydroxydopamine, A New Oxidation Mechanism. *European Journal of Pharmacology* **17**, 287-&.
- Ahlemeyer B., Kolker S., Zhu Y., Hoffmann G. F., and Krieglstein J. (2003) Cytosine arabinofuranoside-induced activation of astrocytes increases the susceptibility of neurons to glutamate due to the release of soluble factors. *Neurochemistry International* **42**, 567-581.
- Albani D., Peverelli E., Rametta R., Batelli S., Veschini L., Negro A., and Forloni G. (2004) Protective effect of TAT-delivered alpha-synuclein: relevance of the C-terminal domain and involvement of HSP70. *Faseb Journal* **18**, 1713-+.
- Anderson J. P., Walker D. E., Goldstein J. M., de Laat R., Banducci K., Caccavello R. J., Barbour R., Huang J. P., Kling K., Lee M., Diep L., Keim P. S., Shen X. F., Chataway T., Schlossmacher M. G., Seubert P., Schenk D., Sinha S., Gai W. P., and Chilcote T. J. (2006) Phosphorylation of Ser-129 is the dominant pathological modification of alpha-synuclein in familial and sporadic Lewy body disease. *Journal of Biological Chemistry* **281**, 29739-29752.
- Anglade P., Vyas S., JavoyAgid F., Herrero M. T., Michel P. P., Marquez J., MouattPrigent A., Ruberg M., Hirsch E. C., and Agid Y. (1997) Apoptosis and autophagy in nigral neurons of patients with Parkinson's disease. *Histology and Histopathology* **12**, 25-31.
- Ascherio A., Chen H. P., Weisskopf M. G., O'Reilly E., McCullough M. L., Calle E. E., Schwarzschild M. A., and Thun M. J. (2006) Pesticide exposure and risk for Parkinson's disease. *Annals of Neurology* **60**, 197-203.
- Atchison R. W., Casto B. C., and Hammon W. M. (1965) Adenovirus-Associated Defective Virus Particles. *Science* **149**, 754-&.
- Auricchio A., Kobinger G., Anand V., Hildinger M., O'Connor E., Maguire A. M., Wilson J. M., and Bennett J. (2001) Exchange of surface proteins impacts on viral vector cellular specificity and transduction characteristics: the retina as a model. *Human Molecular Genetics* **10**, 3075-3081.
- Bains J. S. and Shaw C. A. (1997) Neurodegenerative disorders in humans: the role of glutathione in oxidative stress-mediated neuronal death. *Brain Research Reviews* **25**, 335-358.
- Baker M. A., Cerniglia G. J., and Zaman A. (1990) Microtiter plate assay for the measurement of glutathione and glutathione disulfide in large numbers of biological samples. *Analytical Biochemistry* **190**, 360-365.
- Balaban R. S., Nemoto S., and Finkel T. (2005) Mitochondria, oxidants, and aging. *Cell* **120**, 483-495.
- Banati R. B., Daniel S. E., and Blunt S. B. (1998) Glial pathology but absence of apoptotic nigral neurons in long-standing Parkinson's disease. *Movement Disorders* **13**, 221-227.
- Bankiewicz K. S., Forsayeth J., Eberling J. L., Sanchez-Pernaute R., Pivrotto P., Bringas J., Herscovitch P., Carson R. E., Eckelman W., Reutter B., and Cunningham J. (2006) Long-term clinical

- improvement in MPTP-lesioned primates after gene therapy with AAV-hAADC. *Molecular Therapy* **14**, 564-570.
- Bantel-Schaal U., Delius H., Schmidt R., and zur Hausen H. (1999) Human adeno-associated virus type 5 is only distantly related to other known primate helper-dependent parvoviruses. *Journal of Virology* **73**, 939-947.
- Barton G. M. and Medzhitov R. (2002) Retroviral delivery of small interfering RNA into primary cells. *Proceedings of the National Academy of Sciences of the United States of America* **99**, 14943-14945.
- Beilina A., Van Der Brug M., Ahmad R., Kesavapany S., Miller D. W., Petsko G. A., and Cookson M. R. (2005) Mutations in PTEN-induced putative kinase 1 associated with recessive parkinsonism have differential effects on protein stability. *Proceedings of the National Academy of Sciences of the United States of America* **102**, 5703-5708.
- Bennett M. C. (2005) The role of alpha-synuclein in neurodegenerative diseases. *Pharmacology & Therapeutics* **105**, 311-331.
- Benshachar D., Zuk R., and Glinka Y. (1995) Dopamine Neurotoxicity - Inhibition of Mitochondrial Respiration. *Journal of Neurochemistry* **64**, 718-723.
- Bernstein E., Caudy A. A., Hammond S. M., and Hannon G. J. (2001) Role for a bidentate ribonuclease in the initiation step of RNA interference. *Nature* **409**, 363-366.
- Bernstein E., Kim S. Y., Carmell M. A., Murchison E. P., Alcorn H., Li M. Z., Mills A. A., Elledge S. J., Anderson K. V., and Hannon G. J. (2003) Dicer is essential for mouse development. *Nature Genetics* **35**, 215-217.
- Betarbet R., Sherer T. B., MacKenzie G., Garcia-Osuna M., Panov A. V., and Greenamyre J. T. (2000) Chronic systemic pesticide exposure reproduces features of Parkinson's disease. *Nature Neuroscience* **3**, 1301-1306.
- Bharath S. and Andersen J. K. (2005) Glutathione depletion in a midbrain-derived immortalized dopaminergic cell line results in limited tyrosine nitration of mitochondrial complex I subunits: Implications for Parkinson's disease. *Antioxidants & Redox Signaling* **7**, 900-910.
- Billy E., Brondani V., Zhang H. D., Muller U., and Filipowicz W. (2001) Specific interference with gene expression induced by long, double-stranded RNA in mouse embryonal teratocarcinoma cell lines. *Proceedings of the National Academy of Sciences of the United States of America* **98**, 14428-14433.
- Birmingham A., Anderson E. M., Reynolds A., Ilsley-Tyree D., Leake D., Fedorov Y., Baskerville S., Maksimova E., Robinson K., Karpilow J., Marshall W. S., and Khvorova A. (2006) 3' UTR seed matches, but not overall identity, are associated with RNAi off-targets. *Nat Meth* **3**, 199-204.
- Bjorklund A., Rosenblad C., Winkler C., and Kirik D. (1997) Studies on neuroprotective and regenerative effects of GDNF in a partial lesion model of Parkinson's disease. *Neurobiology of Disease* **4**, 186-200.
- Blaszczyk J., Tropea J. E., Bubunencko M., Routzahn K. M., Waugh D. S., Court D. L., and Ji X. H. (2001) Crystallographic and modeling studies of RNase III suggest a mechanism for double-stranded RNA cleavage. *Structure* **9**, 1225-1236.
- Bodiswollner I. (1990) Visual Deficits Related to Dopamine Deficiency in Experimental-Animals and Parkinsons-Disease Patients. *Trends in Neurosciences* **13**, 296-302.

## References

---

- Bonifati V., Rizzu P., van Baren M. J., Schaap O., Breedveld G. J., Krieger E., Dekker M. C. J., Squitieri F., Ibanez P., Joosse M., van Dongen J. W., Vanacore N., van Swieten J. C., Brice A., Meco G., van Duijn C. M., Oostra B. A., and Heutink P. (2003) Mutations in the DJ-1 gene associated with autosomal recessive early-onset parkinsonism. *Science* **299**, 256-259.
- Boudreau R. L., Monteys A. M., and Davidson B. L. (2008) Minimizing variables among hairpin-based RNAi vectors reveals the potency of shRNAs. *Rna-A Publication of the Rna Society* **14**, 1834-1844.
- Braak H. and Braak E. (2000) Pathoanatomy of Parkinson's disease. *Journal of Neurology* **247**, 3-10.
- Braak H., De Vos R. A. I., Bohl J., and Del Tredici K. (2006a) Gastric alpha-synuclein immunoreactive inclusions in Meissner's and Auerbach's plexuses in cases staged for Parkinson's disease-related brain pathology. *Neuroscience Letters* **396**, 67-72.
- Braak H., Del Tredici K., Rub U., De Vos R. A. I., Steur E. N. H. J., and Braak E. (2003) Staging of brain pathology related to sporadic Parkinson's disease. *Neurobiology of Aging* **24**, 197-211.
- Braak H., Muller C. M., Rub U., Ackermann H., Bratzke H., De Vos R. A. I., and Del Tredici K. (2006b) Pathology associated with sporadic Parkinson's disease - where does it end? *Journal of Neural Transmission-Supplement* 89-97.
- Breese G. R. and Traylor T. D. (1971) Depletion of Brain Noradrenaline and Dopamine by 6-Hydroxydopamine. *British Journal of Pharmacology* **42**, 88-&.
- Brice A. (2005) How much does dardarin contribute to Parkinson's disease? *Lancet* **365**, 363-364.
- Bridge A. J., Pebernard S., Ducraux A., Nicoulaz A. L., and Iggo R. (2003) Induction of an interferon response by RNAi vectors in mammalian cells. *Nature Genetics* **34**, 263-264.
- Brummelkamp T. R., Bernards R., and Agami R. (2002a) A system for stable expression of short interfering RNAs in mammalian cells. *Science* **296**, 550-553.
- Brummelkamp T. R., Bernards R., and Agami R. (2002b) Stable suppression of tumorigenicity by virus-mediated RNA interference  
BRUMMELKAMP2002. *Cancer Cell* **2**, 243-247.
- Brummelkamp T. R., Bernards R., and Agami R. (2002c) A System for Stable Expression of Short Interfering RNAs in Mammalian Cells. *Science* **296**, 550-553.
- Buller R. M. L., Janik J. E., Sebring E. D., and Rose J. A. (1981) Herpes-Simplex Virus Type-1 and Type-2 Completely Help Adenovirus-Associated Virus-Replication. *Journal of Virology* **40**, 241-247.
- Burnette W. N. (1981) Western Blotting - Electrophoretic Transfer of Proteins from Sodium Dodecyl Sulfate-Polyacrylamide Gels to Unmodified Nitrocellulose and Radiographic Detection with Antibody and Radioiodinated Protein-A. *Analytical Biochemistry* **112**, 195-203.
- Cabreravaldivia F., Jimenezjimenez F. J., Molina J. A., Fernandezcalle P., Vazquez A., Canizaresliebana F., Larumbelobalde S., Ayusoperalta L., Rabasa M., and Codoceo R. (1994) Peripheral Iron-Metabolism in Patients with Parkinsons-Disease. *Journal of the Neurological Sciences* **125**, 82-86.
- Canet-Aviles R. M., Wilson M. A., Miller D. W., Ahmad R., McLendon C., Bandyopadhyay S., Baptista M. J., Ringe D., Petsko G. A., and Cookson M. R. (2004) The Parkinson's disease protein DJ-1 is neuroprotective due to cysteine-sulfinic acid-driven mitochondrial localization. *Proceedings of the National Academy of Sciences of the United States of America* **101**, 9103-9108.

## References

---

- Castanotto D., Sakurai K., Lingeman R., Li H. T., Shively L., Aagaard L., Soifer H., Gatignol A., Riggs A., and Rossi J. J. (2007) Combinatorial delivery of small interfering RNAs reduces RNAi efficacy by selective incorporation into RISC. *Nucleic Acids Research* **35**, 5154-5164.
- Cearley C. N., Vandenberghe L. H., Parente M. K., Carnish E. R., Wilson J. M., and Wolfe J. H. (2008) Expanded repertoire of AAV vector serotypes mediate unique patterns of transduction in mouse brain. *Molecular Therapy* **16**, 1710-1718.
- Cearley C. N. and Wolfe J. H. (2006) Transduction characteristics of adeno-associated virus vectors expressing cap serotypes 7, 8, 9, and Rh10 in the mouse brain. *Molecular Therapy* **13**, 528-537.
- Chao H. J., Liu Y. B., Rabinowitz J., Li C. W., Samulski R. J., and Walsh C. E. (2000) Several log increase in therapeutic transgene delivery by distinct adeno-associated viral serotype vectors. *Molecular Therapy* **2**, 619-623.
- Chen Y., Shertzer H. G., Schneider S. N., Nebert D. W., and Dalton T. P. (2005) Glutamate cysteine ligase catalysis - Dependence on ATP and modifier subunit for regulation of tissue glutathione levels. *J Biol Chem* **280**, 33766-33774.
- Chen Y. C., Lin M. C., Yao H., Wang H., Zhang A. Q., Yu J., Hui C. K., Lau G. K., He M. L., Sung J., and Kung H. F. (2007a) Lentivirus-mediated RNA interference targeting enhancer of zeste homolog 2 inhibits hepatocellular carcinoma growth through down-regulation of stathmin. *Hepatology* **46**, 200-208.
- Chen Y. Q., McMillan-Ward E., Kong J. M., Israels S. J., and Gibson S. B. (2007b) Mitochondrial electron-transport-chain inhibitors of complexes I and II induce autophagic cell death mediated by reactive oxygen species  
CHEN2007. *Journal of Cell Science* **120**, 4155-4166.
- Chinta S. J. and Andersen J. K. (2006) Reversible inhibition of mitochondrial complex I activity following chronic dopaminergic glutathione depletion in vitro: Implications for Parkinson's disease. *Free Radical Biology and Medicine* **41**, 1442-1448.
- Choi J., Liu R. M., Kundu R. K., Sangiorgi F., Wu W. C., Maxson R., and Forman H. J. (2000) Molecular mechanism of decreased glutathione content in human immunodeficiency virus type 1 Tat-transgenic mice. *Journal of Biological Chemistry* **275**, 3693-3698.
- Chung K. K. K., Zhang Y., Lim K. L., Tanaka Y., Huang H., Gao J., Ross C. A., Dawson V. L., and Dawson T. M. (2001) Parkin ubiquitinates the alpha-synuclein-interacting protein, synphilin-1: implications for Lewy-body formation in Parkinson disease. *Nature Medicine* **7**, 1144-1150.
- Circu M. L. and Aw T. Y. (2008) Glutathione and apoptosis. *Free Radical Research* **42**, 689-706.
- Clarke D. D. and Sokoloff L. (1999) Circulation and energy metabolism of the brain. In: *Basic Neurochemistry: Molecular, Cellular, and Medical Aspects*, G.J. Sigel, B.W. Agranoff, R.W. Albers, S.K. Fisher, and M.D.Uhler, pp. 637-669. Edition: Lippincott-Raven (Philadelphia, USA).
- Cohen G. and Heikkila R. E. (1974) Generation of Hydrogen-Peroxide, Superoxide Radical, and Hydroxyl Radical by 6-Hydroxydopamine, Dialuric Acid, and Related Cytotoxic Agents. *Journal of Biological Chemistry* **249**, 2447-2452.
- Colapinto M., Mila S., Giraudo S., Stefanazzi P., Molteni M., Rossetti C., Bergamasco B., Lopiano L., and Fasano M. (2006) alpha-synuclein protects SH-SY5Y cells from dopamine toxicity. *Biochemical and Biophysical Research Communications* **349**, 1294-1300.
- Colombo J. A. and Puissant V. I. (2002) Fluoro Jade stains early and reactive astroglia in the primate cerebral cortex. *Journal of Histochemistry & Cytochemistry* **50**, 1135-1137.

## References

---

- Connor J. R., Snyder B. S., Arosio P., Loeffler D. A., and Lewitt P. (1995) A Quantitative-Analysis of Isoferritins in Select Regions of Aged, Parkinsonian, And, Alzheimers Diseased Brains. *Journal of Neurochemistry* **65**, 717-724.
- Cooper J. M. and Schapira A. H. V. (1997) Mitochondrial dysfunction in neurodegeneration. *Journal of Bioenergetics and Biomembranes* **29**, 175-183.
- Courtney M. J. and Coffey E. T. (1999) The mechanism of Ara-C-induced apoptosis of differentiating cerebellar granule neurons. *European Journal of Neuroscience* **11**, 1073-1084.
- Dalton T. P., Dieter M. Z., Yang Y., Shertzer H. G., and Nebert D. W. (2000) Knockout of the mouse glutamate cysteine ligase catalytic subunit (Gclc) gene: Embryonic lethal when homozygous, and proposed model for moderate glutathione deficiency when heterozygous. *Biochemical and Biophysical Research Communications* **279**, 324-329.
- Damier P., Hirsch E. C., Zhang P., Agid Y., and JavoyAgid F. (1993) Glutathione-Peroxidase, Glial-Cells and Parkinsons-Disease. *Neuroscience* **52**, 1-6.
- Dauer W. and Przedborski S. (2003) Parkinson's disease: Mechanisms and models. *Neuron* **39**, 889-909.
- Davis G. C., Williams A. C., Markey S. P., Ebert M. H., Caine E. D., Reichert C. M., and Kopin I. J. (1979) Chronic Parkinsonism Secondary to Intravenous-Injection of Meperidine Analogs. *Psychiatry Research* **1**, 249-254.
- Dawson T. M. and Dawson V. L. (2003) Molecular pathways of neurodegeneration in Parkinson's disease. *Science* **302**, 819-822.
- de Hoop M.J., Meyn L., and otti C. G. (1998) *Culturing hippocampal neurons and astrocytes from fetal rodent brain.*, San Diego: Academic Press..
- Denovan-Wright E. M., Rodriguez-Lebron E., Lewin A. S., and Mandel R. J. (2008) Unexpected off-targeting effects of anti-huntingtin ribozymes and siRNA in vivo. *Neurobiology of Disease* **29**, 446-455.
- deRijk M. C., Tzourio C., Breteler M. M. B., Dartigues J. F., Amaducci L., LopezPousa S., ManubensBertran J. M., Alperovitch A., and Rocca W. A. (1997) Prevalence of parkinsonism and Parkinson's disease in Europe: The EUROPARKINSON collaborative study. *Journal of Neurology Neurosurgery and Psychiatry* **62**, 10-15.
- Deumens R., Blokland A., and Prickaerts J. (2002) Modeling Parkinsn's disease in rats: An evaluation of 6-OHDA lesions of the nigrostriatal pathway. *Experimental Neurology* **175**, 303-317.
- Dexter D. T., Carayon A., Vidailhet M., Ruberg M., Agid F., Agid Y., Lees A. J., Wells F. R., Jenner P., and Marsden C. D. (1990) Decreased Ferritin Levels in Brain in Parkinsons-Disease. *Journal of Neurochemistry* **55**, 16-20.
- Dexter D. T., Carter C. J., Wells F. R., JavoyAgid F., Agid Y., Lees A., Jenner P., and Marsden C. D. (1989a) Basal Lipid-Peroxidation in Substantia Nigra Is Increased in Parkinsons-Disease DEXTER1989. *Journal of Neurochemistry* **52**, 381-389.
- Dexter D. T., Wells F. R., Lees A. J., Agid F., Agid Y., Jenner P., and Marsden C. D. (1989b) Increased Nigral Iron Content and Alterations in Other Metal-Ions Occurring in Brain in Parkinsons-Disease. *Journal of Neurochemistry* **52**, 1830-1836.
- Diaz-Hernandez J. I., Almeida A., Delgado-Esteban M., Fernandez E., and Bolanos J. P. (2005) Knockdown of Glutamate-Cysteine Ligase by Small Hairpin RNA Reveals That Both Catalytic and

- Modulatory Subunits Are Essential for the Survival of Primary Neurons. *J Biol Chem* **280**, 38992-39001.
- Dick F. D., De Palma G., Ahmadi A., Scott N. W., Prescott G. J., Bennett J., Semple S., Dick S., Counsell C., Mozzoni P., Haites N., Wettinger S. B., Mutti A., Otelea M., Seaton A., Soederkvist P., and Felice A. (2007) Environmental risk factors for Parkinson's disease and parkinsonism: the Geoparkinson study. *Occupational and Environmental Medicine* **64**, 666-672.
- Dickinson D. A. and Forman H. J. (2002a) Cellular glutathione and thiols metabolism. *Biochemical Pharmacology* **64**, 1019-1026.
- Dickinson D. A. and Forman H. J. (2002b) Glutathione in defense and signaling - Lessons from a small thiol. *Cell Signaling, Transcription, and Translation As Therapeutic Targets* **973**, 488-504.
- Dong J. Y., Fan P. D., and Frizzell R. A. (1996) Quantitative analysis of the packaging capacity of recombinant adeno-associated virus. *Human Gene Therapy* **7**, 2101-2112.
- Dringen R., Gutterer J. M., and Hirrlinger J. (2000) Glutathione metabolism in brain - Metabolic interaction between astrocytes and neurons in the defense against reactive oxygen species. *European Journal of Biochemistry* **267**, 4912-4916.
- Dringen R. and Hirrlinger J. (2003) Glutathione pathways in the brain. *Biological Chemistry* **384**, 505-516.
- Duan D. S., Sharma P., Yang J. S., Yue Y. P., Dudus L., Zhang Y. L., Fisher K. J., and Engelhardt J. F. (1998) Circular intermediates of recombinant adeno-associated virus have defined structural characteristics responsible for long-term episomal persistence in muscle tissue. *Journal of Virology* **72**, 8568-8577.
- Duan D. S., Yue Y. P., and Engelhardt J. F. (2001) Expanding AAV packaging capacity with trans-splicing or overlapping vectors: A quantitative comparison. *Molecular Therapy* **4**, 383-391.
- During M. J., Samulski R. J., Elsworth J. D., Kaplitt M. G., Leone P., Xiao X., Li J., Freese A., Taylor J. R., Roth R. H., Sladek J. R., O'Malley K. L., and Redmond D. E. (1998) In vivo expression of therapeutic human genes for dopamine production in the caudates of MPTP-treated monkeys using an AAV vector. *Gene Therapy* **5**, 820-827.
- Elbashir S. M., Lendeckel W., and Tuschl T. (2001a) RNA interference is mediated by 21- and 22-nucleotide RNAs. *Genes & Development* **15**, 188-200.
- Elbashir S. M., Martinez J., Patkaniowska A., Lendeckel W., and Tuschl T. (2001b) Functional anatomy of siRNAs for mediating efficient RNAi in *Drosophila melanogaster* embryo lysate ELBASHIR2001. *Embo Journal* **20**, 6877-6888.
- Elston T., Wang H. Y., and Oster G. (1998) Energy transduction in ATP synthase. *Nature* **391**, 510-513.
- Estrela J. M., Ortega A., and Obrador E. (2006) Glutathione in cancer biology and therapy. *Critical Reviews in Clinical Laboratory Sciences* **43**, 143-181.
- Fahn S. (1997) Levodopa-induced neurotoxicity - Does it represent a problem for the treatment of Parkinson's disease? *Cns Drugs* **8**, 376-393.
- Fahn S. (2003) Description of Parkinson's disease as a clinical syndrome. *Parkinson'S Disease: the Life Cycle of the Dopamine Neuron* **991**, 1-14.

## References

---

- Fahn S. and Cohen G. (1992) The Oxidant Stress Hypothesis in Parkinsons-Disease - Evidence Supporting It. *Annals of Neurology* **32**, 804-812.
- Fearnley J. M. and Lees A. J. (1991) Aging and Parkinsons-Disease - Substantia-Nigra Regional Selectivity. *Brain* **114**, 2283-2301.
- Fechner H., Sipo I., Westermann D., Pinkert S., Wang X. M., Suckau L., Kurreck J., Zeichhardt H., Muller O., Vetter R., Erdmann V., Tschöpe C., and Poller W. (2008) Cardiac-targeted RNA interference mediated by an AAV9 vector improves cardiac function in coxsackievirus B3 cardiomyopathy. *Journal of Molecular Medicine-Jmm* **86**, 987-997.
- Feigin A., Kaplitt M. G., Tang C., Lin T., Mattis P., Dhawan V., During M. J., and Eidelberg D. (2007) Modulation of metabolic brain networks after subthalamic gene therapy for Parkinson's disease. *Proceedings of the National Academy of Sciences of the United States of America* **104**, 19559-19564.
- Fire A., Xu S. Q., Montgomery M. K., Kostas S. A., Driver S. E., and Mello C. C. (1998) Potent and specific genetic interference by double-stranded RNA in *Caenorhabditis elegans*. *Nature* **391**, 806-811.
- Fitzmaurice P. S., Ang L., Guttman M., Rajput A. H., Furukawa Y., and Kish S. J. (2003) Nigral glutathione deficiency is not specific for idiopathic Parkinson's disease. *Movement Disorders* **18**, 969-976.
- Fleming S. M., Zhu C. N., Fernagut P. O., Mehta A., DiCarlo C. D., Seaman R. L., and Chesselet M. F. (2004) Behavioral and immunohistochemical effects of chronic intravenous and subcutaneous infusions of varying doses of rotenone. *Experimental Neurology* **187**, 418-429.
- Floor E. and Wetzel M. G. (1998) Increased protein oxidation in human substantia nigra pars compacta in comparison with basal ganglia and prefrontal cortex measured with an improved dinitrophenylhydrazine assay. *Journal of Neurochemistry* **70**, 268-275.
- Flotte T. R., Afione S. A., and Zeitlin P. L. (1994) Adenoassociated Virus Vector Gene-Expression Occurs in Nondividing Cells in the Absence of Vector Dna Integration. *American Journal of Respiratory Cell and Molecular Biology* **11**, 517-521.
- Flotte T. R., Solow R., Owens R. A., Afione S., Zeitlin P. L., and Carter B. J. (1992) Gene-Expression from Adenoassociated Virus Vectors in Airway Epithelial-Cells. *American Journal of Respiratory Cell and Molecular Biology* **7**, 349-356.
- Fornai F., Vaglini F., Maggio R., Bonuccelli U., and Corsini G. U. (1997) Species differences in the role of excitatory amino acids in experimental parkinsonism. *Neuroscience and Biobehavioral Reviews* **21**, 401-415.
- Forno L. S. (1996) Neuropathology of Parkinson's disease. *Journal of Neuropathology and Experimental Neurology* **55**, 259-272.
- Franco R., Schoneveld O. J., Pappa A., and Panayiotidis M. I. (2007) The central role of glutathione in the pathophysiology of human diseases. *Archives Of Physiology And Biochemistry* **113**, 234-258.
- Franich N. R., Fitzsimons H. L., Fong D. M., Klugmann M., During M. J., and Young D. (2008) AAV vector-mediated RNAi of mutant huntingtin expression is neuroprotective in a novel genetic rat model of Huntington's disease. *Molecular Therapy* **16**, 947-956.
- Franklin C. C., Krejsa C. M., Pierce R. H., White C. C., Fausto N., and Kavanagh T. J. (2002) Caspase-3-dependent cleavage of the glutamate-L-cysteine ligase catalytic subunit during apoptotic cell death. *American Journal of Pathology* **160**, 1887-1894.

## References

---

- Fukuchi K., Tahara K., Kim H. D., Maxwell J. A., Lewis T. L., Accavitti-Loper M. A., Kim H., Ponnazhagan S., and Lalonde R. (2006) Anti-A beta single-chain antibody delivery via adeno-associated virus for treatment of Alzheimer's disease. *Neurobiology of Disease* **23**, 502-511.
- Fukui H. and Moraes C. T. (2008) The mitochondrial impairment, oxidative stress and neurodegeneration connection: reality or just an attractive hypothesis? *Trends in Neurosciences* **31**, 251-256.
- Gao G. P., Vandenberghe L. H., and Wilson J. M. (2005) New recombinant serotypes of AAV vectors. *Current Gene Therapy* **5**, 285-297.
- Garza J. C., Kim C. S., Liu J., Zhang W., and Lu X. Y. (2008) Adeno-associated virus-mediated knockdown of melanocortin-4 receptor in the paraventricular nucleus of the hypothalamus promotes high-fat diet-induced hyperphagia and obesity. *Journal of Endocrinology* **197**, 471-482.
- Geller H. M., Cheng K. Y., Goldsmith N. K., Romero A. A., Zhang A. L., Morris E. J., and Grandison L. (2001) Oxidative stress mediates neuronal DNA damage and apoptosis in response to cytosine arabinoside. *Journal of Neurochemistry* **78**, 265-275.
- Ghezzi P., Bonetto V., and Fratelli M. (2005) Thiol-disulfide balance: From the concept of oxidative stress to that of redox regulation. *Antioxidants & Redox Signaling* **7**, 964-972.
- Gilbert H. F. (1984) Redox Control of Enzyme-Activities by Thiol Disulfide Exchange. *Methods in Enzymology* **107**, 330-351.
- Giorgio M., Trinei M., Migliaccio E., and Pelicci P. G. (2007) Hydrogen peroxide: a metabolic by-product or a common mediator of ageing signals? *Nature Reviews Molecular Cell Biology* **8**, 722A-7728.
- Goldberg M. S. and Lansbury P. T. (2000) Is there a cause-and-effect relationship between alpha-synuclein fibrillization and Parkinson's disease? *Nature Cell Biology* **2**, E115-E119.
- Golden T. A., Schauer S. E., Lang J. D., Pien S., Mushegian A. R., Grossniklaus U., Meinke D. W., and Ray A. (2002) Short Integuments1/Suspensor1/Carpel Factory, A Dicer Homolog, Is A Maternal Effect Gene Required for Embryo Development in Arabidopsis. *Plant Physiology* **130**, 808-822.
- Goldman J. E., Yen S. H., Chiu F. C., and Peress N. S. (1983) Lewy Bodies of Parkinsons-Disease Contain Neurofilament Antigens. *Science* **221**, 1082-1084.
- Gorbatyuk O. S., Li S., Sullivan L. F., Chen W., Kondrikova G., Manfredsson F. P., Mandel R. J., and Muzyczka N. (2008) The phosphorylation state of Ser-129 in human alpha-synuclein determines neurodegeneration in a rat model of Parkinson disease. *Proceedings of the National Academy of Sciences of the United States of America* **105**, 763-768.
- Gotz M. E., Dirr A., Burger R., Janetzky B., Weinmuller M., Chan W. W., Chen S. C., Reichmann H., Rausch W. D., and Riederer P. (1994) Effect of Lipoic Acid on Redox State of Coenzyme-Q in Mice Treated with 1-Methyl-4-Phenyl-1,2,3,6-Tetrahydropyridine and Diethyldithiocarbamate. *European Journal of Pharmacology-Molecular Pharmacology Section* **266**, 291-300.
- Gozlan H. and Benari Y. (1995) Nmda Receptor Redox Sites - Are They Targets for Selective Neuronal Protection. *Trends in Pharmacological Sciences* **16**, 368-374.
- Graham D. G., Tiffany S. M., Bell W. R., and Gutknecht W. F. (1978) Autoxidation Versus Covalent Binding of Quinones As Mechanism of Toxicity of Dopamine, 6-Hydroxydopamine, and Related Compounds Toward C1300-Neuroblastoma Cells Invitro. *Molecular Pharmacology* **14**, 644-653.



- Griffith O. W. (1999) Biologic and pharmacologic regulation of mammalian glutathione synthesis. *Free Radical Biology and Medicine* **27**, 922-935.
- Grima G., Benz B., Parpura V., Cuenod M., and Do K. Q. (2003) Dopamine-induced oxidative stress in neurons with glutathione deficit: implication for schizophrenia. *Schizophrenia Research* **62**, 213-224.
- Grimm D., Kern A., Rittner K., and Kleinschmidt J. A. (1998) Novel tools for production and purification of recombinant adenoassociated virus vectors. *Human Gene Therapy* **9**, 2745-2760.
- Grimm D., Streetz K. L., Jopling C. L., Storm T. A., Pandey K., Davis C. R., Marion P., Salazar F., and Kay M. A. (2006) Fatality in mice due to oversaturation of cellular microRNA/short hairpin RNA pathways. *Nature* **441**, 537-541.
- Gu M., Owen A. D., Toffa S. E. K., Cooper J. M., Dexter D. T., Jenner P., Marsden C. D., and Schapira A. H. V. (1998) Mitochondrial function, GSH and iron in neurodegeneration and Lewy body diseases. *Journal of the Neurological Sciences* **158**, 24-29.
- Hammond S. M., Bernstein E., Beach D., and Hannon G. J. (2000) An RNA-directed nuclease mediates post-transcriptional gene silencing in *Drosophila* cells. *Nature* **404**, 293-296.
- Hannon G. J. (2002) RNA interference. *Nature* **418**, 244-251.
- Hauck B., Chen L., and Xiao W. D. (2003) Generation and characterization of chimeric recombinant AAV vectors. *Molecular Therapy* **7**, 419-425.
- Healy D. G., Falchi M., O'Sullivan S. S., Bonifati V., Durr A., Bressman S., Brice A., Aasly J., Zabetian C. P., Goldwurm S., Ferreira J. J., Tolosa E., Kay D. M., Klein C., Williams D. R., Marras C., Lang A. E., KWSzolek Z., Berciano J., Schapira A. H. V., Lynch T., Bhatia K. P., Gasser T., Lees A. J., and Wood N. W. (2008) Phenotype, genotype, and worldwide genetic penetrance of LRRK2-associated Parkinson's disease: a case-control study. *Lancet Neurology* **7**, 583-590.
- Hegde R., Srinivasula S. M., Zhang Z. J., Wassell R., Mukattash R., Cilenti L., DuBois G., Lazebnik Y., Zervos A. S., Fernandes-Alnemri T., and Alnemri E. S. (2002) Identification of Omi/HtrA-2 as a mitochondrial apoptotic serine protease that disrupts inhibitor of apoptosis protein-caspase interaction. *Journal of Biological Chemistry* **277**, 432-438.
- Herting B., Bietenbeck S., Scholz K., Haehner A., Hummel T., and Reichmann H. (2008) Olfactory dysfunction in Parkinson's disease. Its role as a new cardinal sign in early and differential diagnosis. *Nervenarzt* **79**, 175-+.
- Hildinger M., Auricchio A., Gao G., Wang L., Chirmule N., and Wilson J. M. (2001) Hybrid vectors based on adeno-associated virus serotypes 2 and 5 for muscle-directed gene transfer. *Journal of Virology* **75**, 6199-6203.
- Hirsch E. C., Brandel J. P., Galle P., JavoyAgid F., and Agid Y. (1991) Iron and Aluminum Increase in the Substantia-Nigra of Patients with Parkinsons-Disease - An X-Ray-Microanalysis. *Journal of Neurochemistry* **56**, 446-451.
- Hoglinger G. U., Feger J., Prigent A., Michel P. P., Parain K., Champy P., Ruberg M., Oertel W. H., and Hirsch E. C. (2003) Chronic systemic complex I inhibition induces a hypokinetic multisystem degeneration in rats. *Journal of Neurochemistry* **84**, 491-502.
- Hornung V., Guenther-Biller M., Bourquin C., Ablasser A., Schlee M., Uematsu S., Noronha A., Manoharan M., Akira S., de Fougerolles A., Endres S., and Hartmann G. (2005) Sequence-specific potent induction of IFN-alpha by short interfering RNA in plasmacytoid dendritic cells through TLR7. *Nature Medicine* **11**, 263-270.

- Hsu M., Srinivas B., Kumar J., Subramanian R., and Andersen J. (2005) Glutathione depletion resulting in selective mitochondrial complex I inhibition in dopaminergic cells is via an NO-mediated pathway not involving peroxynitrite: implications for Parkinson's disease. *Journal of Neurochemistry* **92**, 1091-1103.
- Huang C. S., Chang L. S., Anderson M. E., and Meister A. (1993) Catalytic and Regulatory Properties of the Heavy Subunit of Rat-Kidney Gamma-Glutamylcysteine Synthetase. *J Biol Chem* **268**, 19675-19680.
- Huang Z. Z., Yang H. P., Chen C. J., Zeng Z. H., and Lu S. C. (2000) Inducers of gamma-glutamylcysteine synthetase and their effects on glutathione synthetase expression. *Biochimica et Biophysica Acta-Gene Structure and Expression* **1493**, 48-55.
- Hughes A. J., Ben Shlomo Y., Daniel S. E., and Lees A. J. (2001) What features improve the accuracy of clinical diagnosis in Parkinson's disease: A clinicopathologic study. *Neurology* **57**, S34-S38.
- Ibanez P., Lesage S., Lohmann E., Thobois S., De Michele G., Borg M., Agid Y., Durr A., and Brice A. (2006) Mutational analysis of the PINK1 gene in early-onset parkinsonism in Europe and North Africa. *Brain* **129**, 686-694.
- Janaky R., Ogita K., Pasqualotto B. A., Bains J. S., Oja S. S., Yoneda Y., and Shaw C. A. (1999) Glutathione and signal transduction in the mammalian CNS. *Journal of Neurochemistry* **73**, 889-902.
- Janaky R., Varga V., Saransaari P., and Oja S. S. (1993) Glutathione Modulates the N-Methyl-D-Aspartate Receptor-Activated Calcium Influx Into Cultured Rat Cerebellar Granule Cells. *Neuroscience Letters* **156**, 153-157.
- Javoy F., Sotelo C., Herbet A., and Agid Y. (1976) Specificity of Dopaminergic Neuronal Degeneration Induced by Intracerebral Injection of 6-Hydroxydopamine in Nigrostriatal Dopamine System. *Brain Research* **102**, 201-215.
- Jefferies H., Coster J., Khalil A., Bot J., McCauley R. D., and Hall J. C. (2003) Glutathione. *Anz Journal of Surgery* **73**, 517-522.
- Jellinger K., Paulus W., Grundkeiqbal I., Riederer P., and Youdim M. B. H. (1990) Brain Iron and Ferritin in Parkinsons and Alzheimers Diseases. *Journal of Neural Transmission-Parkinsons Disease and Dementia Section* **2**, 327-340.
- Jenner P. (2003) Oxidative stress in Parkinson's disease. *Annals of Neurology* **53**, S26-S36.
- Jenner P., Schapira A. H. V., and Marsden C. D. (1992) New Insights Into the Cause of Parkinsons-Disease. *Neurology* **42**, 2241-2250.
- Jeon B. S., Jacksonlewis V., and Burke R. E. (1995) 6-Hydroxydopamine Lesion of the Rat Substantia-Nigra - Time-Course and Morphology of Cell-Death. *Neurodegeneration* **4**, 131-137.
- Jia P. L., Shi T. L., Cai Y. D., and Li Y. X. (2006) Demonstration of two novel methods for predicting functional siRNA efficiency. *Bmc Bioinformatics* **7**.
- Johannsen P., Velander G., Mai J., Thorling E. B., and Dupont E. (1991) Glutathione-Peroxidase in Early and Advanced Parkinsons-Disease. *Journal of Neurology Neurosurgery and Psychiatry* **54**, 679-682.
- Jonsson G. (1980) Chemical Neurotoxins As Denervation Tools in Neurobiology. *Annual Review of Neuroscience* **3**, 169-187.

## References

---

- Juraska J. M., Wilson C. J., and Groves P. M. (1977) Substantia Nigra of Rat - Golgi Study. *Journal of Comparative Neurology* **172**, 585-600.
- Kahle P. J., Neumann M., Ozmen L., Muller V., Jacobsen H., Schindzielorz A., Okochi M., Leimer U., van der Putten H., Probst A., Kremmer E., Kretschmar H. A., and Haass C. (2000) Subcellular localization of wild-type and Parkinson's disease-associated mutant alpha-synuclein in human and transgenic mouse brain. *Journal of Neuroscience* **20**, 6365-6373.
- Kaplitt M. G., Feigin A., Tang C., Fitzsimons H. L., Mattis P., Lawlor P. A., Bland R. J., Young D., Strybing K., Eidelberg D., and During M. J. (2007) Safety and tolerability of gene therapy with an adeno-associated virus (AAV) borne GAD gene for Parkinson's disease: an open label, phase I trial. *Lancet* **369**, 2097-2105.
- Kaplitt M. G., Leone P., Samulski R. J., Xiao X., Pfaff D. W., Omalley K. L., and During M. J. (1994) Long-Term Gene-Expression and Phenotypic Correction Using Adenoassociated Virus Vectors in the Mammalian Brain. *Nature Genetics* **8**, 148-154.
- Karunakaran S., Diwakar L., Saeed U., Agarwal V., Ramakrishnan S., Iyengar S., and Ravindranath V. (2007) Activation of apoptosis signal regulating kinase 1 (ASK1) and translocation of death-associated protein, Daxx, in substantia nigra pars compacta in a mouse model of Parkinson's disease: protection by alpha-lipoic acid. *Faseb Journal* **21**, 2226-2236.
- Kim Y. J., Ahn J., Jeung S. Y., Kim D. S., Na H. N., Cho Y. J., Yun S. H., Jee Y., Jeon E. S., Lee H., and Nam J. H. (2008) Recombinant lentivirus-delivered short hairpin RNAs targeted to conserved coxsackievirus sequences protect against viral myocarditis and improve survival rate in an animal model. *Virus Genes* **36**, 141-146.
- Kingsbury A. E., Mardsen C. D., and Foster O. J. F. (1998) DNA fragmentation in human substantia nigra: Apoptosis or perimortem effect? *Movement Disorders* **13**, 877-884.
- Kirik D., Annett L. E., Burger C., Muzyczka N., Mandel R. J., and Bjorklund A. (2003) Nigrostriatal alpha-synucleinopathy induced by viral vector-mediated overexpression of human alpha-synuclein: A new primate model of Parkinson's disease. *Proceedings of the National Academy of Sciences of the United States of America* **100**, 2884-2889.
- Kirik D., Rosenblad C., Burer C., Lundberg C., Johansen T. E., Muzyczka N., Mandel R. J., and Bjorklund A. (2002) Parkinson-like neurodegeneration induced by targeted overexpression of alpha-synuclein in the nigrostriatal system. *Journal of Neuroscience* **22**, 2780-2791.
- Kish S. J., Morito C., and Hornykiewicz O. (1985) Glutathione-Peroxidase Activity in Parkinsons-Disease Brain. *Neuroscience Letters* **58**, 343-346.
- Kitada T., Asakawa S., Hattori N., Matsumine H., Yamamura Y., Minoshima S., Yokochi M., Mizuno Y., and Shimizu N. (1998) Mutations in the parkin gene cause autosomal recessive juvenile parkinsonism. *Nature* **392**, 605-608.
- Knight S. W. and Bass B. L. (2001) A role for the RNase III enzyme DCR-1 in RNA interference and germ line development in *Caenorhabditis elegans*. *Science* **293**, 2269-2271.
- Kosel S., Egensperger R., vonEitzen U., Mehraein P., and Graeber M. B. (1997) On the question of apoptosis in the parkinsonian substantia nigra. *Acta Neuropathologica* **93**, 105-108.
- Kozak M. (1984) Point Mutations Close to the Aug Initiator Codon Affect the Efficiency of Translation of Rat Preproinsulin In vivo. *Nature* **308**, 241-246.
- Kozak M. (1986) Point Mutations Define A Sequence Flanking the Aug Initiator Codon That Modulates Translation by Eukaryotic Ribosomes. *Cell* **44**, 283-292.

## References

---

- Kozak M. (1987) An Analysis of 5'-Noncoding Sequences from 699 Vertebrate Messenger-Rnas. *Nucleic Acids Research* **15**, 8125-8148.
- Kruger R., Eberhardt O., Riess O., and Schulz J. B. (2002) Parkinson's disease: one biochemical pathway to fit all genes? *Trends in Molecular Medicine* **8**, 236-240.
- Kruger R., Kuhn W., Muller T., Woitalla D., Graeber M., Kosel S., Przuntek H., Epplen J. T., Schols L., and Riess O. (1998) Ala30Pro mutation in the gene encoding alpha-synuclein in Parkinson's disease. *Nature Genetics* **18**, 106-108.
- Kugler S., Hahnwald R., Garrido M., and Reiss J. (2007) Long-term rescue of a lethal inherited disease by adeno-associated virus-mediated gene transfer in a mouse model of molybdenum-cofactor deficiency. *American Journal of Human Genetics* **80**, 291-297.
- Kügler S., Lingor P., Schöll U., Zolotukhin S., and Bähr M. (2003) Differential transgene expression in brain cells in vivo and in vitro from AAV-2 vectors with small transcriptional control units. *Virology* **311**, 89-95.
- Kuiper M. A., Mulder C., Vankamp G. J., Scheltens P., and Wolters E. C. (1994) Cerebrospinal-Fluid Ferritin Levels of Patients with Parkinsons-Disease, Alzheimers-Disease, and Multiple System Atrophy. *Journal of Neural Transmission-Parkinsons Disease and Dementia Section* **7**, 109-114.
- Kuzuhara S., Mori H., Izumiyama N., Yoshimura M., and Ihara Y. (1988) Lewy Bodies Are Ubiquitinated - A Light and Electron-Microscopic Immunocytochemical Study. *Acta Neuropathologica* **75**, 345-353.
- Lane E. and Dunnett S. (2008) Animal models of Parkinson's disease and L-dopa induced dyskinesia: How close are we to the clinic? *Psychopharmacology* **199**, 303-312.
- Langston J. W., Ballard P., Tetrud J. W., and Irwin I. (1983) Chronic Parkinsonism in Humans Due to A Product of Meperidine-Analog Synthesis. *Science* **219**, 979-980.
- Lau Y. S., Trobough K. L., Crampton J. M., and Wilson J. A. (1990) Effects of Probenecid on Striatal Dopamine Depletion in Acute and Long-Term 1-Methyl-4-Phenyl-1,2,3,6-Tetrahydropyridine (Mptp)-Treated Mice. *General Pharmacology* **21**, 181-187.
- Leaver S. G., Cui Q., Bernard O., and Harvey A. R. (2006) Cooperative effects of bcl-2 and AAV-mediated expression of CNTF on retinal ganglion cell survival and axonal regeneration in adult transgenic mice. *European Journal of Neuroscience* **24**, 3323-3332.
- Lee M. K., Stirling W., Xu Y. Q., Xu X. Y., Qui D., Mandir A. S., Dawson T. M., Copeland N. G., Jenkins N. A., and Price D. L. (2002) Human alpha-synuclein-harboring familial Parkinson's disease-linked Ala-53 -> Thr mutation causes neurodegenerative disease with alpha-synuclein aggregation in transgenic mice. *Proceedings of the National Academy of Sciences of the United States of America* **99**, 8968-8973.
- Lee T. D., Yang H. P., Whang J., and Lu S. C. (2005) Cloning and characterization of the human glutathione synthetase 5'-flanking region. *Biochemical Journal* **390**, 521-528.
- Leroy E., Boyer R., Auburger G., Leube B., Ulm G., Mezey E., Harta G., Brownstein M. J., Jonnalagada S., Chernova T., Dehejia A., Lavedan C., Gasser T., Steinbach P. J., Wilkinson K. D., and Polymeropoulos M. H. (1998) The ubiquitin pathway in Parkinson's disease. *Nature* **395**, 451-452.
- Lesage S., Durr A., Tazir M., Lohmann E., Leutenegger A. L., Janin S., Pollak P., and Brice A. (2006) LRRK2 G2019S as a cause of Parkinson's disease in North African Arabs. *New England Journal of Medicine* **354**, 422-423.

## References

---

- Li S. T., Wang L. Y., Berman M. A., Zhang Y., and Dorf M. E. (2006) RNAi screen in mouse astrocytes identifies phosphatases that regulate NF-kappa B signaling. *Molecular Cell* **24**, 497-509.
- Li W. and Cha L. (2007) Predicting siRNA efficiency. *Cellular and Molecular Life Sciences* **64**, 1785-1792.
- Lo Bianco C., Schneider B. L., Bauer M., Sajadi A., Brice A., Iwatsubo T., and Aebischer P. (2004) Lentiviral vector delivery of parkin prevents dopaminergic degeneration in an alpha-synuclein rat model of Parkinson's disease. *Proceedings of the National Academy of Sciences of the United States of America* **101**, 17510-17515.
- Logroscino G., Marder K., Graziano J., Freyer G., Slavkovich V., LoIacono N., Cote L., and Mayeux R. (1997) Altered systemic iron metabolism in Parkinson's disease. *Neurology* **49**, 714-717.
- Lotharius J. and Brundin P. (2002a) Impaired dopamine storage resulting from alpha-synuclein mutations may contribute to the pathogenesis of Parkinson's disease. *Human Molecular Genetics* **11**, 2395-2407.
- Lotharius J. and Brundin P. (2002b) Pathogenesis of Parkinson's disease: Dopamine, vesicles and alpha-synuclein. *Nature Reviews Neuroscience* **3**, 932-942.
- Loyter A., Scangos G. A., and Ruddle F. H. (1982) Mechanisms of Dna Uptake by Mammalian-Cells - Fate of Exogenously Added Dna Monitored by the Use of Fluorescent Dyes. *Proceedings of the National Academy of Sciences of the United States of America-Biological Sciences* **79**, 422-426.
- MacLeod D., Dowman J., Hammond R., Leete T., Inoue K., and Abeliovich A. (2006) The familial parkinsonism gene LRRK2 regulates neurite process morphology. *Neuron* **52**, 587-593.
- Malik I., Garrido M., Bahr M., Kugler S., and Michel U. (2006) Comparison of test systems for RNAinterference. *Biochemical and Biophysical Research Communications* **341**, 245-253.
- Mandel R. J. and Burger C. (2004) Clinical trials in neurological disorders using AAV vectors: Promises and challenges. *Current Opinion in Molecular Therapeutics* **6**, 482-490.
- Mandel R. J., Rendahl K. G., Spratt S. K., Snyder R. O., Cohen L. K., and Leff S. E. (1998) Characterization of intrastriatal recombinant adeno-associated virus-mediated gene transfer of human tyrosine hydroxylase and human GTP-cyclohydrolase I in a rat model of Parkinson's disease. *Journal of Neuroscience* **18**, 4271-4284.
- Mann V. M., Cooper J. M., Daniel S. E., Srai K., Jenner P., Marsden C. D., and Schapira A. H. V. (1994) Complex-I, Iron, and Ferritin in Parkinsons-Disease Substantia-Nigra. *Annals of Neurology* **36**, 876-881.
- Marklund S. L., Westman N. G., Lundgren E., and Roos G. (1982) Copper-Containing and Zinc-Containing Superoxide-Dismutase, Manganese-Containing Superoxide-Dismutase, Catalase, and Glutathione-Peroxidase in Normal and Neoplastic Human Cell-Lines and Normal Human-Tissues. *Cancer Research* **42**, 1955-1961.
- Martinez J., Patkaniowska A., Urlaub H., Luhrmann R., and Tuschl T. (2002) Single-stranded antisense siRNAs guide target RNA cleavage in RNAi. *Cell* **110**, 563-574.
- Martins L. M., Iaccarino I., Tenev T., Gschmeissner S., Totty N. F., Lemoine N. R., Savopoulos J., Gray C. W., Creasy C. L., Dingwall C., and Downward J. (2002) The serine protease Omi/HtrA2 regulates apoptosis by binding XIAP through a reaper-like motif. *Journal of Biological Chemistry* **277**, 439-444.

## References

---

- Marttila R. J., Lorentz H., and Rinne U. K. (1988) Oxygen-Toxicity Protecting Enzymes in Parkinsons-Disease - Increase of Superoxide Dismutase-Like Activity in the Substantia Nigra and Basal Nucleus. *Journal of the Neurological Sciences* **86**, 321-331.
- Marx F. P., Holzmann C., Strauss K. M., Li L., Eberhardt O., Gerhardt E., Cookson M. R., Hernandez D., Farrer M. J., Kachergus J., Engelender S., Ross C. A., Berger K., Schols L., Schulz J. B., Riess O., and Kruger R. (2003) Identification and functional characterization of a novel R621C mutation in the synphilin-1 gene in Parkinson's disease. *Human Molecular Genetics* **12**, 1223-1231.
- Maslah E., Rockenstein E., Veinbergs I., Mallory M., Hashimoto M., Takeda A., Sagara Y., Sisk A., and Mucke L. (2000) Dopaminergic loss and inclusion body formation in alpha-synuclein mice: Implications for neurodegenerative disorders. *Science* **287**, 1265-1269.
- Mastakov M. Y., Baer K., Symes C. W., Leichtlein C. B., Kotin R. M., and During M. J. (2002) Immunological aspects of recombinant adeno-associated virus delivery to the mammalian brain. *Journal of Virology* **76**, 8446-8454.
- Mathews D. H., Sabina J., Zuker M., and Turner D. H. (1999) Expanded sequence dependence of thermodynamic parameters improves prediction of RNA secondary structure. *Journal of Molecular Biology* **288**, 911-940.
- Mayer B., Pfeiffer S., Schrammel A., Koesling D., Schmidt K., and Brunner F. (1998) A new pathway of nitric oxide cyclic GMP signaling involving S-nitrosoglutathione. *Journal of Biological Chemistry* **273**, 3264-3270.
- Mayer R. A., Kindt M. V., and Heikkila R. E. (1986) Prevention of the Nigrostriatal Toxicity of 1-Methyl-4-Phenyl-1,2,3,6-Tetrahydropyridine by Inhibitors of 3,4-Dihydroxyphenylethylamine Transport. *Journal of Neurochemistry* **47**, 1073-1079.
- McBride J. L., Boudreau R. L., Harper S. Q., Staber P. D., Monteys A. M., Martins I., Gilmore B. L., Burstein H., Peluso R. W., Polisky B., Carter B. J., and Davidson B. L. (2008) Artificial miRNAs mitigate shRNA-mediated toxicity in the brain: Implications for the therapeutic development of RNAi. *Proceedings of the National Academy of Sciences of the United States of America* **105**, 5868-5873.
- McBride J. L., During M. J., Wu J., Chen E. Y., Leurgans S. E., and Kordower J. H. (2003) Structural and functional neuroprotection in a rat model of Huntington's disease by viral gene transfer of GDNF. *Experimental Neurology* **181**, 213-223.
- McConnachie L. A., Mohar I., Hudson F. N., Ware C. B., Ladiges W. C., Fernandez C., Chatterton-Kirchmeier S., White C. C., Pierce R. H., and Kavanagh T. J. (2007) Glutamate Cysteine Ligase Modifier Subunit Deficiency and Gender as Determinants of Acetaminophen-Induced Hepatotoxicity in Mice. *Toxicol Sci* **99**, 628-636.
- Mccown T. J., Xiao X., Li J., Breese G. R., and Samulski R. J. (1996) Differential and persistent expression patterns of CNS gene transfer by an adeno-associated virus (AAV) vector. *Brain Research* **713**, 99-107.
- Mcelroy W. D. (1947) The Energy Source for Bioluminescence in An Isolated System. *Proceedings of the National Academy of Sciences of the United States of America* **33**, 342-345.
- McNaught K. S. P. and Jenner P. (2001) Proteasomal function is impaired in substantia nigra in Parkinson's disease. *Neuroscience Letters* **297**, 191-194.
- McNaught K. S. P., Olanow C. W., Halliwell B., Isacson O., and Jenner P. (2001) Failure of the ubiquitin-proteasome system in Parkinson's disease MCNAUGHT2001. *Nature Reviews Neuroscience* **2**, 589-594.

## References

---

- Meister A. and Anderson M. E. (1983) Glutathione. *Annual Review of Biochemistry* **52**, 711-760.
- Mello C. C. and Conte D. (2004) Revealing the world of RNA interference. *Nature* **431**, 338-342.
- Melov S. (2004) Modeling mitochondrial function in aging neurons. *Trends in Neurosciences* **27**, 601-606.
- Merad-Boudia M., Nicole A., Santiard-Baron D., Saille C., and Ceballos-Picot I. (1998) Mitochondrial impairment as an early event in the process of apoptosis induced by glutathione depletion in neuronal cells: Relevance to Parkinson's disease. *Biochemical Pharmacology* **56**, 645-655.
- Merad-Saidoune M., Boitier E., Nicole A., Marsac C., Martinou J. C., Sola B., Sinet P. M., and Ceballos-Picot I. (1999) Overproduction of Cu/Zn-superoxide dismutase or Bcl-2 prevents the brain mitochondrial respiratory dysfunction induced by glutathione depletion. *Experimental Neurology* **158**, 428-436.
- Meredith G. E., Halliday G. M., and Totterdell S. (2004) A critical review of the development and importance of proteinaceous aggregates in animal models of Parkinson's disease: new insights into Lewy body formation. *Parkinsonism & Related Disorders* **10**, 191-202.
- Meredith G. E., Sonsalla P. K., and Chesselet M. F. (2008) Animal models of Parkinson's disease progression. *Acta Neuropathologica* **115**, 385-398.
- Meredith G. E., Totterdell S., Petroske E., Cruz K. S., Callison R. C., and Lau Y. S. (2002) Lysosomal malfunction accompanies alpha-synuclein aggregation in a progressive mouse model of Parkinson's disease. *Brain Research* **956**, 156-165.
- Meyer A. J. (2008) The integration of glutathione homeostasis and redox signaling. *Journal of Plant Physiology* **165**, 1390-1403.
- Michel U., Malik I., Ebert S., Bahr M., and Kugler S. (2005) Long-term in vivo and in vitro AAV-2-mediated RNA interference in rat retinal ganglion cells and cultured primary neurons. *Biochemical and Biophysical Research Communications* **326**, 307-312.
- Miller D. W., Ahmad R., Hague S., Baptista M. J., Canet-Aviles R., McLendon C., Carter D. M., Zhu P. P., Stadler J., Chandran J., Klinefelter G. R., Blackstone C., and Cookson M. R. (2003) L166P mutant DJ-1, causative for recessive Parkinson's disease, is degraded through the ubiquitin-proteasome system. *Journal of Biological Chemistry* **278**, 36588-36595.
- Miyagishi M. and Taira K. (2002) U6 promoter-driven siRNAs with four uridine 3' overhangs efficiently suppress targeted gene expression in mammalian cells. *Nature Biotechnology* **20**, 497-500.
- Mizuno Y., Ohta S., Tanaka M., Takamiya S., Suzuki K., Sato T., Oya H., Ozawa T., and Kagawa Y. (1989) Deficiencies in Complex-I Subunits of the Respiratory-Chain in Parkinsons-Disease. *Biochemical and Biophysical Research Communications* **163**, 1450-1455.
- Mochizuki H., Goto K., Mori H., and Mizuno Y. (1996) Histochemical detection of apoptosis in Parkinson's disease. *Journal of the Neurological Sciences* **137**, 120-123.
- Moore D. J., West A. B., Dawson V. L., and Dawson T. M. (2005a) Molecular pathophysiology of Parkinson's disease. *Annual Review of Neuroscience* **28**, 57-87.
- Moore M. D., McGarvey M. J., Russell R. A., Cullen B. R., and McClure M. O. (2005b) Stable inhibition of hepatitis B virus proteins by small interfering RNA expressed from viral vectors. *Journal of Gene Medicine* **7**, 918-925.

## References

---

- Muramatsu S. I., Fujimoto K. I., Ikeguchi K., Shizuma N., Kawasaki K., Ono F., Shen Y., Wang L. J., Mizukami H., Kume A., Matsumura M., Nagatsu I., Urano F., Ichinose H., Nagatsu T., Terao K., Nakano I., and Ozawa K. (2002) Behavioral recovery in a primate model of Parkinson's disease by triple transduction of striatal cells with adeno-associated viral vectors expressing dopamine-synthesizing enzymes. *Human Gene Therapy* **13**, 345-354.
- Myslinski E., Ame J. C., Krol A., and Carbon P. (2001) An unusually compact external promoter for RNA polymerase III transcription of the human H1RNA gene. *Nucleic Acids Research* **29**, 2502-2509.
- Nakajima A., Kataoka K., Hong M., Sakaguchi M., and Huh N. (2003) BRPK, a novel protein kinase showing increased expression in mouse cancer cell lines with higher metastatic potential. *Cancer Letters* **201**, 195-201.
- Neumann M., Kahle P. J., Giasson B. I., Ozmen L., Borroni E., Spooeren W., Muller V., Odoy S., Fujiwara H., Hasegawa M., Iwatsubo T., Trojanowski J. Q., Kretschmar H. A., and Haass C. (2002) Misfolded proteinase K-resistant hyperphosphorylated alpha-synuclein in aged transgenic mice with locomotor deterioration and in human alpha-synucleinopathies. *Journal of Clinical Investigation* **110**, 1429-1439.
- Newmeyer D. D. and Ferguson-Miller S. (2003) Mitochondria: Releasing power for life and unleashing the machineries of death. *Cell* **112**, 481-490.
- Nicole A., Santiard-Baron D., and Ceballos-Picot I. (1998) Direct evidence for glutathione as mediator of apoptosis in neuronal cells. *Biomedicine & Pharmacotherapy* **52**, 349-355.
- Nykanen A., Haley B., and Zamore P. D. (2001) ATP requirements and small interfering RNA structure in the RNA interference pathway. *Cell* **107**, 309-321.
- Ochi T. (1995) Hydrogen peroxide increases the activity of gamma-glutamylcysteine synthetase in cultured Chinese hamster V79 cells. *Archives of Toxicology* **70**, 96-103.
- Okochi M., Walter J., Koyama A., Nakajo S., Baba M., Iwatsubo T., Meijer L., Kahle P. J., and Haass C. (2000) Constitutive phosphorylation of the Parkinson's disease associated alpha-synuclein. *Journal of Biological Chemistry* **275**, 390-397.
- Olzmann M. (2004) Preface. *Zeitschrift fur Physikalische Chemie-International Journal of Research in Physical Chemistry & Chemical Physics* **218**, 373-376.
- Owens C. W. I. and Belcher R. V. (1965) A Colorimetric Micro-Method for Determination of Glutathione. *Biochemical Journal* **94**, 705-&.
- Ozelius L. J., Senthil G., Saunders-Pullman R., Ohmann E., Deligtisch A., Tagliati M., Hunt A. L., Klein C., Henick B., Hailpern S. M., Lipton R. B., Soto-Valencia J., Risch N., and Bressman S. B. (2006) LRRK2 G2019S as a cause of Parkinson's disease in Ashkenazi Jews. *New England Journal of Medicine* **354**, 424-425.
- Paddison P. J., Caudy A. A., Bernstein E., Hannon G. J., and Conklin D. S. (2002a) Short hairpin RNAs (shRNAs) induce sequence-specific silencing in mammalian cells. *Genes & Development* **16**, 948-958.
- Paddison P. J., Caudy A. A., and Hannon G. J. (2002b) Stable suppression of gene expression by RNAi in mammalian cells  
PADDISON2002. *Proceedings of the National Academy of Sciences of the United States of America* **99**, 1443-1448.
- Paisan-Ruiz C., Jain S., Evans E. W., Gilks W. P., Simon J., Van Der Brug M., de Munain A. L., Aparicio S., Gil A. M., Khan N., Johnson J., Martinez J. R., Nicholl D., Carrera I. M., Pena A. S., de



## References

---

- Silva R., Lees A., Marti-Masso J. F., Perez-Tur J., Wood N. W., and Singleton A. B. (2004) Cloning of the gene containing mutations that cause PARK8-linked Parkinson's disease. *Neuron* **44**, 595-600.
- Paolicchi A., Dominici S., Pieri L., Maellaro E., and Pompella A. (2002) Glutathione catabolism as a signaling mechanism. *Biochemical Pharmacology* **64**, 1027-1035.
- Park W., Li J. J., Song R. T., Messing J., and Chen X. M. (2002) CARPEL FACTORY, a Dicer homolog, and HEN1, a novel protein, act in microRNA metabolism in *Arabidopsis thaliana*. *Current Biology* **12**, 1484-1495.
- Parkinson J. (2002) An essay on the shaking palsy (Reprinted). *Journal of Neuropsychiatry and Clinical Neurosciences* **14**, 223-236.
- Paskowitz D. M., Greenberg K. P., Yasumura D., Grimm D., Yang H., Duncan J. L., Kay M. A., Lavail M. M., Flannery J. G., and Vollrath D. (2007) Rapid and stable knockdown of an endogenous gene in retinal pigment epithelium. *Human Gene Therapy* **18**, 871-880.
- Paterna J. C., Feldon J., and Bueler H. (2004) Transduction profiles of recombinant adeno-associated virus vectors derived from serotypes 2 and 5 in the nigrostriatal system of rats. *Journal of Virology* **78**, 6808-6817.
- Paul C. P., Good P. D., Winer I., and Engelke D. R. (2002) Effective expression of small interfering RNA in human cells. *Nature Biotechnology* **20**, 505-508.
- Paule M. R. and White R. J. (2000) Transcription by RNA polymerases I and III. *Nucleic Acids Research* **28**, 1283-1298.
- Paxinos G. and Watson C. (1986) *The rat brain in stereotactic coordinates*, Academic Press, San Diego, USA.
- Pelicano H., Carney D., and Huang P. (2004) ROS stress in cancer cells and therapeutic implications. *Drug Resistance Updates* **7**, 97-110.
- Perry T. L., Godin D. V., and Hansen S. (1982) Parkinsons-Disease - A Disorder Due to Nigral Glutathione Deficiency. *Neuroscience Letters* **33**, 305-310.
- Petroske E., Meredith G. E., Callen S., Totterdell S., and Lau Y. S. (2001) Mouse model of Parkinsonism: A comparison between subacute MPTP and chronic MPTP/probenecid treatment. *Neuroscience* **106**, 589-601.
- Plun-Favreau H., Klupsch K., Moiso N., Gandhi S., Kjaer S., Frith D., Harvey K., Deas E., Harvey R. J., McDonald N., Wood N. W., Martins L. M., and Downward J. (2007) The mitochondrial protease HtrA2 is regulated by Parkinson's disease-associated kinase PINK1. *Nature Cell Biology* **9**, 1243-1U63.
- Polymeropoulos M. H., Lavedan C., Leroy E., Ide S. E., Dehejia A., Dutra A., Pike B., Root H., Rubenstein J., Boyer R., Stenroos E. S., Chandrasekharappa S., Athanassiadou A., Papapetropoulos T., Johnson W. G., Lazzarini A. M., Duvoisin R. C., DiIorio G., Golbe L. I., and Nussbaum R. L. (1997) Mutation in the alpha-synuclein gene identified in families with Parkinson's disease. *Science* **276**, 2045-2047.
- Provost P., Dishart D., Doucet J., Fren Dewey D., Samuelsson B., and Radmark O. (2002) Ribonuclease activity and RNA binding of recombinant human Dicer. *Embo Journal* **21**, 5864-5874.
- Rabinowitz J. E., Bowles D. E., Faust S. M., Ledford J. G., Cunningham S. E., and Samulski R. J. (2004) Cross-dressing the virion: the transcapsidation of adeno-associated virus serotypes functionally defines subgroups. *Journal of Virology* **78**, 4421-4432.

## References

---

- Radil T., Roth J., Ruzicka E., Tichy J., and Wysocki C. J. (1995) Olfactory dysfunction: A symptom of Parkinson's disease? *Ceska A Slovenska Neurologie A Neurochirurgie* **58**, 286-289.
- Ransom B. R., Kunis D. M., Irwin I., and Langston J. W. (1987) Astrocytes Convert the Parkinsonism Inducing Neurotoxin, Mptp, to Its Active Metabolite, Mpp+. *Neuroscience Letters* **75**, 323-328.
- Rauschhuber C., Xu H., Salazar F. H., Marion P. L., and Ehrhardt A. (2008) Exploring gene-deleted adenoviral vectors for delivery of short hairpin RNAs and reduction of hepatitis B virus infection in mice. *Journal of Gene Medicine* **10**, 878-889.
- Riederer P., Sofic E., Rausch W. D., Schmidt B., Reynolds G. P., Jellinger K., and Youdim M. B. H. (1989) Transition-Metals, Ferritin, Glutathione, and Ascorbic-Acid in Parkinsonian Brains. *Journal of Neurochemistry* **52**, 515-520.
- Riederer P. and Wuketich S. (1976) Time Course of Nigrostriatal Degeneration in Parkinsons-Disease - Detailed Study of Influential Factors in Human-Brain Amine Analysis. *Journal of Neural Transmission* **38**, 277-301.
- Rizzuto R., Pinton P., Brini M., Chiesa A., Filippin L., and Pozzan T. (1999) Mitochondria as biosensors of calcium microdomains. *Cell Calcium* **26**, 193-199.
- Rossetti Z. L., Sotgiu A., Sharp D. E., Hadjiconstantinou M., and Neff N. H. (1988) 1-Methyl-4-Phenyl-1,2,3,6-Tetrahydropyridine (Mptp) and Free-Radicals Invitro. *Biochemical Pharmacology* **37**, 4573-4574.
- Rubinson D. A., Dillon C. P., Kwiatkowski A. V., Sievers C., Yang L. L., Kopinja J., Zhang M. D., McManus M. T., Gertler F. B., Scott M. L., and Van Parijs L. (2003) A lentivirus-based system to functionally silence genes in primary mammalian cells, stem cells and transgenic mice by RNA interference. *Nature Genetics* **33**, 401-406.
- Saggu H., Cooksey J., Dexter D., Wells F. R., Lees A., Jenner P., and Marsden C. D. (1989) A Selective Increase in Particulate Superoxide-Dismutase Activity in Parkinsonian Substantia Nigra. *Journal of Neurochemistry* **53**, 692-697.
- Sakamoto N., Tanabe Y., Yokota T., Satoh K., Sekine-Osajima Y., Nakagawa M., Itsui Y., Tasaka M., Sakurai Y., Cheng-Hsin C., Yano M., Ohkoshi S., Aoyagi Y., Maekawa S., Enomoto N., Kohara M., and Watanabe M. (2008) Inhibition of hepatitis C virus infection and expression in vitro and in vivo by recombinant adenovirus expressing short hairpin RNA. *Journal of Gastroenterology and Hepatology* **23**, 1437-1447.
- Sambrook J., Fritsch E.F., and Maniatis T. (1989) *Molecular Cloning: A Laboratory Manual*, Cold Spring Harbor Laboratory Press, Cold Spring Harbor.
- Samulski R. J., Chang L. S., and Shenk T. (1989) Helper-Free Stocks of Recombinant Adeno-Associated Viruses - Normal Integration Does Not Require Viral Gene-Expression. *Journal of Virology* **63**, 3822-3828.
- Saner A. and Thoenen H. (1971) Model Experiments on Molecular Mechanism of Action of 6-Hydroxydopamine. *Molecular Pharmacology* **7**, 147-&.
- Schapira A. H. V. (1994) Evidence for Mitochondrial Dysfunction in Parkinsons-Disease - A Critical-Appraisal. *Movement Disorders* **9**, 125-138.
- Schapira A. H. V., Cooper J. M., Dexter D., Clark J. B., Jenner P., and Marsden C. D. (1990) Mitochondrial Complex I Deficiency in Parkinsons-Disease. *Journal of Neurochemistry* **54**, 823-827.

## References

---

- Schmued L. C., Stowers C. C., Scallet A. C., and Xu L. L. (2005) Fluoro-Jade C results in ultra high resolution and contrast labeling of degenerating neurons. *Brain Research* **1035**, 24-31.
- Schwarz D. S., Hutvagner G., Haley B., and Zamore P. D. (2002) Evidence that siRNAs function as guides, not primers, in the Drosophila and human RNAi pathways. *Molecular Cell* **10**, 537-548.
- Seelig G. F. and Meister A. (1985) Glutathione Biosynthesis - Gamma-Glutamylcysteine Synthetase from Rat-Kidney. *Methods in Enzymology* **113**, 379-390.
- Shen F. X., Su H., Fan Y. F., Chen Y. M., Zhu Y. Q., Liu W. Z., Young W. L., and Yang G. Y. (2006) Adeno-associated viral vector-mediated hypoxia-inducible vascular endothelial growth factor gene expression attenuates ischemic brain injury after focal cerebral ischemia in mice. *Stroke* **37**, 2601-2606.
- Shendelman S., Jonason A., Martinat C., Leete T., and Abeliovich A. (2004) DJ-1 is a redox-dependent molecular chaperone that inhibits alpha-synuclein aggregate formation. *Plos Biology* **2**, 1764-1773.
- Sherer T. B., Kim J. H., Betarbet R., and Greenamyre J. T. (2003) Subcutaneous rotenone exposure causes highly selective dopaminergic degeneration and alpha-synuclein aggregation. *Experimental Neurology* **179**, 9-16.
- Shevtsova Z., Malik I., Garrido M., Scholl U., Buhr M., and Kugler S. (2006) Potentiation of in vivo neuroprotection by BclX(L) and GDNF co-expression depends on post-lesion time in deafferented CNS neurons. *Gene Therapy* **13**, 1569-1578.
- Shevtsova Z., Malik J. M. I., Michel U., Bahr M., and Kugler S. (2005) Promoters and serotypes: targeting of adeno-associated virus vectors for gene transfer in the rat central nervous system in vitro and in vivo. *Experimental Physiology* **90**, 53-59.
- Shi Z. Z., Osei-Frimpong J., Kala G., Kala S. V., Barrios R. J., Habib G. M., Lukin D. J., Danney C. M., Matzuk M. M., and Lieberman M. W. (2000) Glutathione synthesis is essential for mouse development but not for cell growth in culture. *Proceedings of the National Academy of Sciences of the United States of America* **97**, 5101-5106.
- Shimura H., Hattori N., Kubo S., Mizuno Y., Asakawa S., Minoshima S., Shimizu N., Iwai K., Chiba T., Tanaka K., and Suzuki T. (2000) Familial Parkinson disease gene product, parkin, is a ubiquitin-protein ligase. *Nature Genetics* **25**, 302-305.
- Shulman L. M. (2000) Levodopa toxicity in Parkinson disease: Reality or myth? Reality - Practice patients should change. *Archives of Neurology* **57**, 406-407.
- Sian J., Dexter D. T., Lees A. J., Daniel S., Agid Y., Javoyagid F., Jenner P., and Marsden C. D. (1994a) Alterations in Glutathione Levels in Parkinsons-Disease and Other Neurodegenerative Disorders Affecting Basal Ganglia. *Annals of Neurology* **36**, 348-355.
- Sian J., Dexter D. T., Lees A. J., Daniel S., Jenner P., and Marsden C. D. (1994b) Glutathione-Related Enzymes in Brain in Parkinsons-Disease. *Annals of Neurology* **36**, 356-361.
- Sies H. (1999) Glutathione and its role in cellular functions. *Free Radical Biology and Medicine* **27**, 916-921.
- Singleton A. B., Farrer M., Johnson J., Singleton A., Hague S., Kachergus J., Hulihan M., Peuralinna T., Dutra A., Nussbaum R., Lincoln S., Crawley A., Hanson M., Maraganore D., Adler C., Cookson M. R., Muentner M., Baptista M., Miller D., Blancato J., Hardy J., and Gwinn-Hardy K. (2003) alpha-synuclein locus triplication causes Parkinson's disease. *Science* **302**, 841.

## References

---

- Sledz C. A. and Williams B. R. G. (2004) RNA interference and double-stranded-RNA-activated pathways. *Biochemical Society Transactions* **32**, 952-956.
- Sofic E., Lange K. W., Jellinger K., and Riederer P. (1992) Reduced and Oxidized Glutathione in the Substantia-Nigra of Patients with Parkinsons-Disease. *Neuroscience Letters* **142**, 128-130.
- Sofic E., Riederer P., Heinsen H., Beckmann H., Reynolds G. P., Hebenstreit G., and Youdim M. B. H. (1988) Increased Iron(Iii) and Total Iron Content in Post-Mortem Substantia Nigra of Parkinsonian Brain. *Journal of Neural Transmission* **74**, 199-205.
- Spillantini M. G., Crowther R. A., Jakes R., Hasegawa M., and Goedert M. (1998) alpha-synuclein in filamentous inclusions of Lewy bodies from Parkinson's disease and dementia with Lewy bodies. *Proceedings of the National Academy of Sciences of the United States of America* **95**, 6469-6473.
- Spillantini M. G., Schmidt M. L., Lee V. M. Y., Trojanowski J. Q., Jakes R., and Goedert M. (1997) alpha-synuclein in Lewy bodies. *Nature* **388**, 839-840.
- Spina M. B. and Cohen G. (1988) Exposure of School Synaptosomes to L-Dopa Increases Levels of Oxidized Glutathione. *Journal of Pharmacology and Experimental Therapeutics* **247**, 502-507.
- Srivastava A., Lusby E. W., and Berns K. I. (1983) Nucleotide-Sequence and Organization of the Adeno-Associated Virus-2 Genome. *Journal of Virology* **45**, 555-564.
- Staniek K., Gille L., Kozlov A. V., and Nohl H. (2002) Mitochondrial superoxide radical formation is controlled by electron bifurcation to the high and low potential pathways. *Free Radical Research* **36**, 381-387.
- Stewart C. K., Li J., and Golovan S. P. (2008) Adverse effects induced by short hairpin RNA expression in porcine fetal fibroblasts. *Biochemical and Biophysical Research Communications* **370**, 113-117.
- Stichel C. C., Zhu X. R., Bader V., Linnartz B., Schmidt S., and Lubbert H. (2007) Mono- and double-mutant mouse models of Parkinson's disease display severe mitochondrial damage. *Human Molecular Genetics* **16**, 2377-2393.
- Stokes A. H., Hastings T. G., and Vrana K. E. (1999) Cytotoxic and genotoxic potential of dopamine. *Journal of Neuroscience Research* **55**, 659-665.
- Strauss K. M., Martins L. M., Plun-Favreau H., Marx F. P., Kautzmann S., Berg D., Gasser T., Wszolek Z., Muller T., Bornemann A., Wolburg H., Downward J., Riess O., Schulz J. B., and Kruger R. (2005) Loss of function mutations in the gene encoding Omi/HtrA2 in Parkinson's disease. *Human Molecular Genetics* **14**, 2099-2111.
- Sulzer D., Bogulavsky J., Larsen K. E., Behr G., Karatekin E., Kleinman M. H., Turro N., Krantz D., Edwards R. H., Greene L. A., and Zecca L. (2000) Neuromelanin biosynthesis is driven by excess cytosolic catecholamines not accumulated by synaptic vesicles. *Proceedings of the National Academy of Sciences of the United States of America* **97**, 11869-11874.
- Sun W. M., Huang Z. Z., and Lu S. C. (1996) Regulation of gamma-glutamylcysteine synthetase by protein phosphorylation. *Biochemical Journal* **320**, 321-328.
- Taira T., Saito Y., Niki T., Iguchi-Ariga S. M. M., Takahashi K., and Ariga H. (2004) DJ-1 has a role in antioxidative stress to prevent cell death. *Embo Reports* **5**, 213-218.
- Tanaka M., Kim Y. M., Lee G., Junn E., Iwatsubo T., and Mouradian M. M. (2004) Aggresomes formed by alpha-synuclein and synphilin-1 are cytoprotective. *J Biol Chem* **279**, 4625-4631.

## References

---

- Tatton N. A. (2000) Increased caspase 3 and Bax immunoreactivity accompany nuclear GAPDH translocation and neuronal apoptosis in Parkinson's disease. *Experimental Neurology* **166**, 29-43.
- Tatton N. A., Maclean-Fraser A., Tatton W. G., Perl D. P., and Olanow C. W. (1998) A fluorescent double-labeling method to detect and confirm apoptotic nuclei in Parkinson's disease. *Annals of Neurology* **44**, S142-S148.
- Taysi S., Polat F., Gul M., Sari R. A., and Bakan E. (2002) Lipid peroxidation, some extracellular antioxidants, and antioxidant enzymes in serum of patients with rheumatoid arthritis. *Rheumatology International* **21**, 200-204.
- Thomas B. and Beal M. F. (2007) Parkinson's disease. *Human Molecular Genetics* **16**, R183-R194.
- Thress K., Kornbluth S., and Smith J. J. (1999) Mitochondria at the crossroad of apoptotic cell death. *Journal of Bioenergetics and Biomembranes* **31**, 321-326.
- Timmons L. and Fire A. (1998) Specific interference by ingested dsRNA. *Nature* **395**, 854.
- Tipton K. F. and Singer T. P. (1993) Advances in Our Understanding of the Mechanisms of the Neurotoxicity of Mptp and Related-Compounds. *Journal of Neurochemistry* **61**, 1191-1206.
- Tofaris G. K. and Spillantini M. G. (2005) Alpha-Synuclein dysfunction in Lewy body diseases. *Movement Disorders* **20**, S37-S44.
- Toffa S., Kunikowska G. M., Zeng B. Y., Jenner P., and Marsden C. D. (1997) Glutathione depletion in rat brain does not cause nigrostriatal pathway degeneration. *Journal of Neural Transmission* **104**, 67-75.
- Towbin H., Staehelin T., and Gordon J. (1979) Electrophoretic Transfer of Proteins from Polyacrylamide Gels to Nitrocellulose Sheets - Procedure and Some Applications. *Proceedings of the National Academy of Sciences of the United States of America* **76**, 4350-4354.
- Tu Z. H. and Anders M. W. (1998) Expression and characterization of human glutamate-cysteine ligase. *Archives of Biochemistry and Biophysics* **354**, 247-254.
- Tuschl T., Zamore P. D., Lehmann R., Bartel D. P., and Sharp P. A. (1999) Targeted mRNA degradation by double-stranded RNA in vitro. *Genes & Development* **13**, 3191-3197.
- Unoki M. and Nakamura Y. (2001) Growth-suppressive effects of BPOZ and EGR2, two genes involved in the PTEN signaling pathway. *Oncogene* **20**, 4457-4465.
- Valente E. M., Abou-Sleiman P. M., Caputo V., Muqit M. M. K., Harvey K., Gispert S., Ali Z., Del Turco D., Bentivoglio A. R., Healy D. G., Albanese A., Nussbaum R., Gonzalez-Maldonado R., Deller T., Salvi S., Cortelli P., Gilks W. P., Latchman D. S., Harvey R. J., Dallapiccola B., Auburger G., and Wood N. W. (2004) Hereditary early-onset Parkinson's disease caused by mutations in PINK1. *Science* **304**, 1158-1160.
- Van Den Eeden S. K., Tanner C. M., Bernstein A. L., Fross R. D., Leimpeter A., Bloch D. A., and Nelson L. M. (2003) Incidence of Parkinson's disease: Variation by age, gender, and Race/Ethnicity. *American Journal of Epidemiology* **157**, 1015-1022.
- van der Putten H., Wiederhold K. H., Probst A., Barbieri S., Mistl C., Danner S., Kauffmann S., Hofe K., Spooren W. P. J. M., Ruegg M. A., Lin S., Caroni P., Sommer B., Tolnay M., and Bilbe G. (2000) Neuropathology in mice expressing human alpha-synuclein. *Journal of Neuroscience* **20**, 6021-6029.

## References

---

- Veal E. A., Day A. M., and Morgan B. A. (2007) Hydrogen peroxide sensing and signaling. *Molecular Cell* **26**, 1-14.
- Volpe T. A., Kidner C., Hall I. M., Teng G., Grewal S. I. S., and Martienssen R. A. (2002) Regulation of heterochromatic silencing and histone H3 lysine-9 methylation by RNAi. *Science* **297**, 1833-1837.
- Wallace D. C. (2005) A mitochondrial paradigm of metabolic and degenerative diseases, aging, and cancer: A dawn for evolutionary medicine. *Annual Review of Genetics* **39**, 359-407.
- Wang H. Y., Baxter C. F., and Schulz H. (1991) Regulation of Fatty-Acid Beta-Oxidation in Rat-Heart Mitochondria. *Archives of Biochemistry and Biophysics* **289**, 274-280.
- Wang H. Y. and Oster G. (1998) Energy transduction in the F-1 motor of ATP synthase. *Nature* **396**, 279-282.
- Watanabe S. Y., Albsoul-Younes A. M., Kawano T., Itoh H., Kaziro Y., Nakajima S., and Nakajima Y. (1999) Calcium phosphate-mediated transfection of primary cultured brain neurons using GFP expression as a marker: application for single neuron electrophysiology. *Neuroscience Research* **33**, 71-78.
- West A. B., Moore D. J., Choi C., Andrabi S. A., Li X. J., Dikeman D., Biskup S., Zhang Z., Lim K. L., Dawson V. L., and Dawson T. M. (2007) Parkinson's disease-associated mutations in LRRK2 link enhanced GTP-binding and kinase activities to neuronal toxicity. *Human Molecular Genetics* **16**, 223-232.
- Witting S. R., Brown M., Saxena R., Nabinger S., and Morral N. (2008) Helper-dependent adenovirus-mediated short hairpin RNA expression in the liver activates the interferon response. *Journal of Biological Chemistry* **283**, 2120-2128.
- Wu G. Y., Fang Y. Z., Yang S., Lupton J. R., and Turner N. D. (2004) Glutathione metabolism and its implications for health. *Journal of Nutrition* **134**, 489-492.
- Wullner U., Loschmann P. A., Schulz J. B., Schmid A., Dringen R., Eblen F., Turski L., and Klockgether T. (1996) Glutathione depletion potentiates MPTP and MPP(+) toxicity in nigral dopaminergic neurones. *Neuroreport* **7**, 921-923.
- Wullner U., Seyfried J., Groscurth P., Beinroth S., Winter S., Gleichmann M., Heneka M., Loschmann P. A., Schulz J. B., Weller M., and Klockgether T. (1999) Glutathione depletion and neuronal cell death: the role of reactive oxygen intermediates and mitochondrial function. *Brain Research* **826**, 53-62.
- Xu R., Janson C. G., Mastakov M., Lawlor P., Young D., Mouravlev A., Fitzsimons H., Choi K. L., Ma H., Dragunow M., Leone P., Chen Q., Dicker B., and Doring M. J. (2001) Quantitative comparison of expression with adeno-associated virus (AAV-2) brain-specific gene cassettes. *Gene Therapy* **8**, 1323-1332.
- Xu Z., Cawthon D., McCastlain K. A., Slikker W., and Ali S. F. (2005) Selective alterations of gene expression in mice induced by MPTP. *Synapse* **55**, 45-51.
- Yamamoto T., Miyoshi H., Yamamoto N., Yamamoto N., Inoue J. I., and Tsunetsugu-Yokota Y. (2006) Lentivirus vectors expressing short hairpin RNAs against the U3-overlapping region of HIV nef inhibit HIV replication and infectivity in primary macrophages. *Blood* **108**, 3305-3312.
- Yang H. P., Zeng Y., Lee T. D., Yang Y., Ou X. P., Chen L. X., Haque M., Rippe R., and Lu S. C. (2002) Role of AP-1 in the coordinate induction of rat glutamate-cysteine ligase and glutathione synthetase by tert-butylhydroquinone. *Journal of Biological Chemistry* **277**, 35232-35239.

## References

---

- Yi R., Doehle B. P., Qin Y., Macara I. G., and Cullen B. R. (2005) Overexpression of Exportin 5 enhances RNA interference mediated by short hairpin RNAs and microRNAs. *Rna-A Publication of the Rna Society* **11**, 220-226.
- Yoo J. Y., Kim J. H., Kim J., Huang J. H., Zhang S. N., Kang Y. A., Kim H., and Yun C. O. (2008) Short hairpin RNA-expressing oncolytic adenovirus-mediated inhibition of IL-8: effects on antiangiogenesis and tumor growth inhibition. *Gene Therapy* **15**, 635-651.
- Zahm D. S. (1991) Compartments in Rat Dorsal and Ventral Striatum Revealed Following Injection of 6-Hydroxydopamine Into the Ventral Mesencephalon. *Brain Research* **552**, 164-169.
- Zamore P. D., Tuschl T., Sharp P. A., and Bartel D. P. (2000) RNAi: Double-stranded RNA directs the ATP-dependent cleavage of mRNA at 21 to 23 nucleotide intervals. *Cell* **101**, 25-33.
- Zarranz J. J., Alegre J., Gomez-Esteban J. C., Lezcano E., Ros R., Ampuero I., Vidal L., Hoenicka J., Rodriguez O., Atares B., Llorens V., Tortosa E. G., del Ser T., Munoz D. G., and de Yebenes J. G. (2004) The new mutation, E46K, of alpha-synuclein causes Parkinson and Lewy body dementia. *Annals of Neurology* **55**, 164-173.
- Zhang H. D., Kolb F. A., Brondani V., Billy E., and Filipowicz W. (2002) Human Dicer preferentially cleaves dsRNAs at their termini without a requirement for ATP. *Embo Journal* **21**, 5875-5885.
- Zhang J., Perry G., Smith M. A., Robertson D., Olson S. J., Graham D. G., and Montine T. J. (1999) Parkinson's disease is associated with oxidative damage to cytoplasmic DNA and RNA in substantia nigra neurons. *American Journal of Pathology* **154**, 1423-1429.
- Zhang L., Shimoji M., Thomas B., Moore D. J., Yu S. W., Marupudi N. I., Torp R., Torgner I. A., Ottersen O. P., Dawson T. M., and Dawson V. L. (2005) Mitochondrial localization of the Parkinson's disease related protein DJ-1: implications for pathogenesis. *Human Molecular Genetics* **14**, 2063-2073.
- Zhang Y., Gao J., Chung K. K. K., Huang H., Dawson V. L., and Dawson T. M. (2000) Parkin functions as an E2-dependent ubiquitin-protein ligase and promotes the degradation of the synaptic vesicle-associated protein, CDCrel-1. *Proceedings of the National Academy of Sciences of the United States of America* **97**, 13354-13359.
- Zhou W. B. and Freed C. R. (2005) DJ-1 up-regulates glutathione synthesis during oxidative stress and inhibits A53T alpha-synuclein toxicity. *J Biol Chem* **280**, 43150-43158.
- Zhu H. B., Zhu Y. P., Hu J. Z., Hu W. X., Liao Y. Q., Zhang J., Wang D., Huang X. F., Fang B. L., and He C. (2007) Adenovirus-mediated small hairpin RNA targeting Bcl-XL as therapy for colon cancer. *International Journal of Cancer* **121**, 1366-1372.
- Zimprich A., Biskup S., Leitner P., Lichtner P., Farrer M., Lincoln S., Kachergus J., Hulihan M., Uitti R. J., Calne D. B., Stoessel A. J., Pfeiffer R. F., Patenge N., Carbajal I. C., Vieregge P., Asmus F., Muller-Myhsok B., Dickson D. W., Meitinger T., Strom T. M., Wszolek Z. K., and Gasser T. (2004) Mutations in LRRK2 cause autosomal-dominant Parkinsonism with pleomorphic pathology. *Neuron* **44**, 601-607.
- Zincarelli C., Soltys S., Rengo G., and Rabinowitz J. E. (2008) Analysis of AAV serotypes 1-9 mediated gene expression and tropism in mice after systemic injection. *Molecular Therapy* **16**, 1073-1080.
- Zolotukhin S., Byrne B. J., Mason E., Zolotukhin I., Potter M., Chesnut K., Summerford C., Samulski R. J., and Muzyczka N. (1999) Recombinant adeno-associated virus purification using novel methods improves infectious titer and yield. *Gene Therapy* **6**, 973-985.

## References

---

Zuker M. (2003) Mfold web server for nucleic acid folding and hybridization prediction. *Nucleic Acids Research* **31**, 3406-3415.



## 7. Annexes

### 7.1. Abbreviations

**9(5)-stuffer:** untranscribed 2281 bp fragment of the porcine gene UM 9(5)p

**AAV2:** adeno-associated virus serotype 2

**ADP:** adenosine diphosphate

**AraC:** cytosine arabinoside

**ATP:** adenosine triphosphate

**BB:** back bone (linearized vector genome)

**BCA:** bicinchoninic acid

**bGH:** bovine growth hormone derived polyadenylation site

**bp:** base pairs

**BSA:** bovine serum albumine

**CF:** cell factory

**CNS:** central nervous system

**DA:** dopaminergic

**dATP:** 2' deoxyadenosine 5'-triphosphate

**DAPI:** 4',6-diamidino-2-phenylindole

**dCTP:** 2' deoxycytidine 5'-triphosphate

**dGTP:** 2' deoxyguanosine 5'-triphosphate

**DIV:** day *in vitro*

**DMEM:** Dulbecco's modified Eagle's medium

**DNA:** desoxyribonucleic acid

**dsRNA:** double stranded RNA

**DsRed2N1:** *Discosoma sp.* red fluorescent protein, reporter gene, Clontech

**DTT:** dithiothreitol

**dTTP:** 2' deoxythymidine 5'-triphosphate

**EDTA:** ethylenediaminetetraacetic acid

**e.g.:** for example

**EGFP:** enhanced green fluorescent protein

**FCS:** fetal calf serum

**fluc:** firefly luciferase

**FPLC:** fast protein liquid chromatography

**GCL:** glutamate cysteine ligase

**GCLc:** GCL catalytic subunit  
**GCLm:** GCL modulatory subunit  
**GFAP:** glial fibrillary acidic protein  
**GSH:** glutathione (reduced glutathione)  
**GSR:** glutathione reductase  
**GSSG:** glutathione disulfide (oxidized glutathione)  
**GSx:** total glutathione (GSH + GSSG)  
**HCN:** hippocampus and cortex primary culture medium  
**hDJ1:** human wild type DJ1  
**hH1:** human polymerase III H1 promoter  
**hSyn1:** human synapsin 1 gene promoter  
**HRP:** horse reddish peroxidase  
**ICC:** immunocytochemistry  
**IHC:** immunohistochemistry  
**Intron:** intron from the pCI-Neo vector, Promega  
**L-BSO:** L-buthionine (S,R) sulphoximine  
**MAP LC3:** microtubule-associated protein light chain 3  
**MPP<sup>+</sup>:** 1-methyl-4-phenylpyridinium  
**MPTP:** 1-methyl-4-phenyl-1,2,3,6-tetrahydropyridin  
**mRNA:** messenger RNA  
**NADPH:** nicotinamide adenine dinucleotide phosphate  
**NBM:** neurobasal medium  
**NDD:** neurodegenerative disorders  
**NeuN:** neuron specific nuclear protein  
**NGS:** newborn goat serum  
**nt:** nucleotide  
**NT:** nitrotyrosine  
**ORF:** open reading frame  
**PAGE:** polyacrylamide gel electrophoresis  
**PBS:** phosphate buffered saline  
**PCR:** polymerase chain reaction  
**PD:** Parkinson`s disease  
**PIc:** Protease inhibitor cocktail  
**PFA:** paraformaldehyde

**PS:** penicillin-streptomycin

**PS-N:** penicillin-streptomycin-neomycin

**RNA:** ribonucleic acid

**RNAi:** RNA interference

**ROS:** reactive oxygen species

**rpm:** rotations per minute

**RT:** room temperature

**RT-PCR:** real time polymerase chain reaction

**SDS:** sodium dodecylsulfate

**shRNA:** short hairpin RNA

**SNpc:** substantia nigra pars compacta

**SSA:** 5-sulfosalicylic acid dehydrate

**SV40pro:** simian virus 40 promoter

**SVpA:** simian virus 40 polyadenylation

**TB:** synthetic transcription blocker

**TBS:** tris buffered saline

**TBS-T:** TBS-tween 20

**TEMED:** tetraaminethylendiamine

**TH:** tyrosine hydroxylase

**UTR:** untranslated region

**VMAT2:** vesicular monoamine transporter 2

**VTA:** ventral tegmental area of the midbrain

**WPRES:** woodchuck hepatitis virus posttranscriptional regulatory element

**WB:** western blotting

## 7.2. Acknowledgements

A PhD thesis is never only the work of the PhD candidate, and my thesis is not an exception. It was accomplished through the efforts of many people. Therefore I would like to express my gratitude to all, who contributed in different ways to the completion of my thesis.

I'm very grateful to:

Prof. Dr. Mathias Bähr for providing me with a position to work in his laboratory and for making this work possible.

My direct supervisor Dr. Sebastian Kügler for his strong support, and fruitful discussions which helped me to get an in deep knowledge of the field. Thank you for the deep encouragement in all scientific challenges.

Prof. Dr. Uwe Michel, for his strong and continuous support, for all the fruitful discussions, and for the scientific and non-scientific guidelines.

Prof. Dr. Dr. Gunnar P. H. Dietz, for running the "Doktorandenseminar" where fruitful discussions were raised and knowledge was very efficiently transferred in diferent subjects.

Prof. Dr. Ralf Heinrich for agreeing to be the referee and main examiner of my thesis as well as to Prof. Dr. Frauke Melchior for granting permission to be the co-referee of my Ph.D. thesis.

My dear friend Dr. Sebastian Deeg always there to share wonderful and sad moments. Sebastian, thank you for making my live so much easier in Göttingen.

All my colleagues and friends which accompanied me during the last years, in particular to Dr. Zinayida Shevtsova, Ulrike Schöll, Dr Johannes Schlachetzki, Dr Grit Taschenberger, Dr Ivana Gadjanski, Dr Florian Nagel, Elisabeth Barski, Petranka Krumova, Ligia Ferreira, Monika Zebski and to all others which are not listed here and have make my time in the laboratory and outside full of great memories.

All my friends in Portugal and all-round-the-world for being my friends, those that apart from the distance are always available and will always be there for me.

My sister Sandra and my parents Anibal Emílio and Ana Rosa for continuous support and love in every moment of my life. Thank you for always believed in me...

Last but not least, Dulce Azevedo for her patience, support in so many other things that I cannot list them all here...

### **7.3. Curriculum vitae**

#### **Personal details:**

Name: Manuel Joaquim Marques Garrido

Citizenship: Portuguese

Date of birth: 15th January 1980

Place of birth: Pardilhó, Portugal

#### **Education:**

2005-2008 PhD education, Laboratory of Prof. Dr. Mathias Bähr, Viral vector lab, Department of Neurology, University Hospital of Göttingen, Germany. Awarded a European Commission Marie Curie Actions Fellowship enrolled in a Research Training Network entitled “Nervous System Repair” (NSR) Reference RTN-NSR #504636.

2004-2005 Research Fellowship coordinated by “Bluepharma, Indústria Farmacêutica, S.A.” Coimbra, Portugal. “Biotechnological strategies for the treatment of infectious diseases”, Founded by “Agência de Inovação”, financed by POCTI and sponsored by FEDER.

2002-2003 Internship at the Center for Neuroscience and Cell Biology of Coimbra (CNC), University of Coimbra, Portugal. “Mechanisms of neurodegeneration in diabetic retinopathy: role of glutamate” funded by the Portuguese Foundation for Science and Technology (FCT), Portugal. Final mark very good, with eighteen values (18/20)

1998-2003 “Licenciatura” Degree in Biochemistry, at the Faculty of Science and Technology, University of Coimbra, Portugal. Final mark Good, with fifteen values (15/20)

1995-1998 High school diploma in sciences at the High school of Estarreja, Estarreja, Portugal. Final mark Good, with seventeen values (17/20)

#### 7.4. Publications

Kügler S, Hahnewald R, Garrido M, Reiss J. (2007) Long-term rescue of a lethal inherited disease by adeno-associated virus mediated gene transfer in a mouse model of molybdenum-cofactor deficiency. *American Journal of Human Genetics* 80(2) 291-297.

Shevtsova Z, Malik I, Garrido M, Schöll U, Bähr M, Kügler S. (2006) Potentiation of in vivo neuroprotection by BclX(L) and GDNF co-expression depends on post-lesion time in deafferented CNS neurons. *Gene Therapy* 13(22) 1569-1578.

Malik I\*, Garrido M\*, Bähr M, Kügler S, Michel U. (2006) Comparison of test systems for RNA interference. *Biochemical and Biophysical Research Communications* 341(1) 245-253.

\*equal contribution